MEASUREMENT OF EMISSIONS FROM BRAKE AND TYRE WEAR

Final Report – Phase 1

Report for: Department for Transport

Ref. T0018 - TETI0037

Ricardo ref. ED14775 Issue: 2 24/02/2023

Ricardo Energy & Environment, Gemini Building, Fermi Avenue, Harwell, Oxfordshire, OX11 0QR, UK | +44(0)1235 75 3000 | ee.ricardo.com
Registered company no. 08229264 | VAT no. GB 212 8365 24

Customer:
Department for Transport

Customer reference:
T0018 - TETI0037

Contact:
Louisa Kramer, Gemini Building, Fermi Avenue, Harwell, Didcot, OX11 0QR, UK

T: +44 (0) 1235 753 315
E: louisa.kramer@ricardo.com

Authors:
Jon Andersson, Michael Campbell, Ian Marshall, Louisa Kramer, John Norris (contributors: Simon de Vries, Jason Southgate).

Approved by:
Jason Southgate

Signed

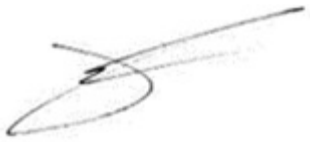

Ricardo reference:
ED 14775

Date:
24th February 2023

Ricardo is certified to ISO9001, ISO14001, ISO27001 and ISO45001.

EXECUTIVE SUMMARY

Ricardo, in collaboration with the Arup AECOM consortium were contracted by the Department for Transport (DfT), to develop a “proof-of-concept” system for measuring non-exhaust emissions (NEE) of particles, under real-world driving conditions.

NEE of particles from road vehicles primarily arise from a combination of brake wear, tyre wear, road surface wear, and the resuspension of dust particles. Emission data from the UK National Atmospheric Emissions Inventory (NAEI) estimate that NEE are now the dominant source of coarse and fine particulate matter (PM_{10} and $PM_{2.5}$) from road transport in the UK. Therefore, it is important to improve knowledge on NEE and address the gaps so it can be used to inform policy and legislation aimed at reducing tyre and brake wear particulate emissions, particularly as the percentage of electric and hybrid vehicles on the roads is increasing.

The project consists of three phases:

- Phase 1: Develop an on-board device to accurately measure brake and tyre wear particles.
- Phase 2: Study parameters affecting emissions from brake and tyre wear.
- Phase 3: Develop recommendations for policy and legislation to control emissions.

This report provides the results and outcomes from Phase 1 of the project. The primary aims of Phase 1 of the study were to design, build, test, and assess a complete system for measuring brake and tyre wear from light duty vehicles under real-world conditions.

A prototype sampling and measurement system-based approach was developed which consisted of:

- A sampling duct for tyre wear, fixed to the wheel hub carrier (to allow movement with steering) to draw samples from behind the tyre-road contact patch into the measurement system.
- Brake enclosures for sampling emissions from the brake pads and discs – three designs were tested with differing interfaces of static and rotating components.
- Sampling probes for background ambient particulate sampling.
- Sampling tunnel, from which the analysers sub-sampled from.
- A pair of Dekati Electrical Low Pressure Impactor (ELPI+) analysers for real-time measurement of particle number and size distribution. One ELPI (cold) was run at ambient temperature to measure total particles, the second ELPI (hot) was heated to 180°C and sampled via a heated line to provide a measurement with volatile particles removed. A Dekati eFilter was used to measure particle mass in real time, along with cumulative gravimetric mass via a glass-fibre filter. During chassis dynamometer testing an external Horiba MEXA-2100SPCS Solid Particle Counting System (SPCS) was also used to measure entirely non-volatile particles.

The entire system was installed to a small light duty van (front wheel) and testing undertaken in a chassis dynamometer facility; on a nearby test-track; and on-road in an urban environment. A brake enclosure was subsequently installed on a passenger car (rear wheel) to assess the transferability of the enclosure and to measure emissions from a different set of pads and discs.

The main conclusions drawn from the results of the tests on the two vehicles are as follows:

- Background particle number concentrations in the chassis dyno facility were up to 10 times lower than roadside backgrounds.
- For brake emissions the samples from the glass-fibre filters indicated that the particles were >95% non-volatile and non-oxidizable.
- Brake particle number emissions measured from the van by the SPCS and hot ELPI during the chassis dynamometer tests were of the order $5x10^9$#/km/brake. Cold ELPI number concentrations were around half of this. Gravimetric particulate mass emissions were approximately 1.6mg/km/brake.
- Gravimetric particle mass emissions were lower during urban driving than on the chassis dynamometer at ~0.9mg/km/brake. However, particle number concentrations were similar (2 to $5x10^9$ #/km/brake from cold and hot ELPI).

- Moderate braking events (from ~50mph) on the test track showed that both particle number and particle mass emissions increased proportionally with kinetic energy supplied to the brakes.
- Emissions increased with extreme braking events. The extreme braking events also resulted in considerably higher pad/disc temperatures (up to ~300°C for the pad and ~400°C for the disc) and indicated that at these temperatures the continuous release of particle emissions can be observed.
- Background particles dominated the tyre samples when measuring on the road, however, in the test facility, tyre wear particles could be measured above the chassis dynamometer background levels.
- Analysis of the filter samples of tyre emissions obtained in the test facility indicated that the material is mainly comprised of non-volatile, non-oxidizable materials (~63%). The remaining components (~35%) included water and volatiles, with around 2% elemental carbon
- Reducing the tyre pressures (from 2.9 to 2.0 bar) resulted in an 8-fold increase in particle number sampled by the cold ELPI. The eFilter observed an increase in mass (by ~2 times). The decreased tyre pressure also resulted in an increase in particles in the nucleation mode (< 20nm), suggesting an increase in volatile / semi-volatile materials under these conditions.
- During moderate braking events on the test track, particle number and particle mass emissions from tyres were not always aligned with every braking event.
- Particle mass emissions from the tyre during the moderate braking events were ~3.2 mg/km/tyre. During urban driving the levels were lower at ~2.5 mg/km/tyre.
- Particle number emissions from the sampled tyre, measured in the chassis dynamometer, were ~$3.3x10^9$ #/km/tyre for the cold ELPI and ~$0.6x10^9$ #/km/tyre for the hot ELPI illustrating a strong emission of volatile particles. Higher emissions were observed on the road, which is likely due to the influence of background particles.
- All three brake enclosures designed and tested showed broadly similar results, indicating that any of these could be used for brake wear sampling
- Measured brake particle mass emissions were lower when sampling the rear wheel on the passenger car compared to the front wheel of the van. In contrast, non-volatile particle number emissions were higher from the rear wheel. The differences may be related to variations in composition of the brake pads and discs.

Based on the results and conclusions from the study a number of recommendations were made regarding measuring real-world particle emissions from brake and tyre wear. In summary these are:

- To measure particle number concentrations from brake and tyre wear a similar approach to that developed by the PMP (i.e. non-volatile particle measurement) would be the best approach. For example a Mobile Particle Emission Counter (MPEC+) with a high temperature volatile particle remover could be used. An additional advantage of this analyser is that it is smaller and requires less power than the ELPI+.
- The results show that the eFilter approach can be used for measuring real-time particle mass. The additional use of a glass-fibre filter enables further analysis, such as chemical composition, to be undertaken. However, specific calibrations for brake and tyre wear measurements should be applied to the eFilter's real-time data
- As a result of high background concentrations on the road, measurements of tyre wear are challenging. With the current system, repeatable results were only possible on the chassis dynamometer. As such it is recommended that the efficiency of the tyre wear sample inlet is further assessed, and if required, a full tyre enclosure should be designed and fabricated, to reduce the effect of sampling background particles on the road.

Phase 2 of the project will incorporate the recommendations above to optimise the sampling system. The new system will then be used to assess the parameters affecting emissions from brake and tyre wear and the impact of regenerative braking on NEE for light-duty vehicles.

Phase 3 will involve assessing the contribution of brake and tyre wear to particulate matter in the UK using current emission factors and incorporating the findings from Phase 2 to provide recommendations on legislation and policy to reduce brake and tyre wear emissions.

CONTENTS

Appendices

GLOSSARY

Term	Meaning/expansion
µm	micrometres (10^{-6}m)
4WD	Four wheel drive
A27	A27, a highway road near Ricardo
A270	A270, an urban road near Ricardo
A283	A283, a rural road near Ricardo
AM	Ante meridiem
APS	Aerodynamic particle sizer
ATOFMS	Aerosol time of flight mass spectrometer
C	Centre-mounted (sample probe)
CAN	Controller Area Network
CAST	Combustion aerosol standard
CFD	Computational fluid dynamics
CoV	Coefficient of variance
CPC	Condensation particle counter
CVS	Constant volume sampler
DfT	Department for Transport
Dp	Particle diameter
EEPS	Engine exhaust particle sizer
ELPI	Electrical low-pressure impactor
FMPS	Fast mobility particle sizer
GC/MS	Gas chromatography / mass spectrometry
GF/A	Whatman glass fibre filter, type A
GPS	Global positioning system
HDS	Highly dispersed silica (tyre composition)
HEPA	High efficiency particulate air (filter)
I/O	Input/output
ID	Internal diameter
ISO	International standards organisation
kph	Kilometres per hour
LACT	Los Angeles Congested Traffic (drive cycle)
Li-ion	Lithium ion
LS	Low steel (brake pads)
MEXA	Motor exhaust (emissions) analyser
mph	Miles per hour
MT	Manual transmission
NAO	Non-asbestos (brake pads)
NEE	Non exhaust emissions
nm	Nanometre (10^{-9}m)
OBD	On-board diagnostics
OD	Outer diameter
OPC	Optical particle counter
PDT	Particle dilution tunnel
PEMS	Portable emissions measurement system
PG-42	~42 minutes duration particle generation cycle

PM	Particulate mass or particulate matter
PM10	PM sampled with an inlet of 50% efficiency at 10µm
PM2.5	PM sampled with an inlet of 50% efficiency at 2.5µm
PMP	Particle measurement programme
PN	Particle number
RL	Upper right (sample probe)
RU	Lower right (sample probe)
S/N	Serial number
SEM	Scanning electron microscopy
slpm	Standard litres per minute
SPCS	Solid particle counting system
STARS-VETS	Chassis dynamometer control & data acquisition suite from Horiba
STC	Shoreham Technical Centre
TEM	Transmission electron microscopy
TEOM	Tapered element oscillating microbalance
TGA	Thermogravimetric analyser
VERC	Vehicle Emissions Research Centre
WLTC	World harmonised light-duty test cycle
WLTP	World harmonised light-duty test procedure

1. INTRODUCTION

Non-exhaust emissions (NEE) are now the primary source of PM_{10} and $PM_{2.5}$ from road transport in the UK. There are, however, still gaps in our understanding of the sources of particulates from NEE and their composition. The Department for Transport (DfT) are aiming to close these gaps on NEE, to inform policy and legislation aiming at reducing tyre and brake wear emissions. This will be achieved through a work order programme comprising three different phases:

1. Develop a robust measuring system and methodology for measuring and characterising particles emitted from brake and tyre wear in real driving conditions.
2. Fill knowledge gaps in the measurement and characterisation of brake and tyre wear emissions from road vehicles.
3. Investigate the effect of the use of regenerative braking on brake and tyre wear emissions.

Ricardo and Arup-AECOM were contracted to deliver Phase 1 of this project, which was addressed over five tasks:

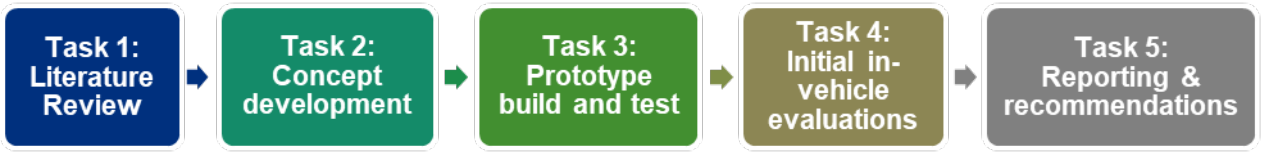

This report describes the overall findings from Phase 1 of the project.

2. BACKGROUND

A high-level literature review on current technologies and activities was undertaken to gather information related to the sampling and measurement of brake and tyre wear particles. The work for this task included: the review of the Particle Measurement Program (PMP - an informal working group within the United Nations Economic Commission for Europe (UNECE) Transport Division) activities and published papers (including laboratory based and on-road studies); stakeholder interviews (see Appendix 1); and discussions with groups undertaking similar research.

This section of the final report contains a synopsis of the information contained in Sections 2-4 of the separate document “Summary of Literature Review and High-Level Specification”. Its structure is:

- Overview of tyre and brake wear particle emissions (2.1)
- Sample inlets (2.2)
- Sample transport (2.3)
- Sample analysis (2.4)
- Summary of implications for this study (2.5)

The aim of the review was to determine the overall feasibility of on-road tyre and brake wear measurements and to assess whether a common sample transfer system and measurement equipment can be used for both brake and tyre wear measurements. This review occurred ahead of the concept development, laboratory evaluation and in-vehicle testing and evaluation.

2.1 OVERVIEW OF TYRE AND BRAKE WEAR PARTICLE EMISSIONS

For brake systems the two key components that generate non-exhaust emissions are:

- Brake disc (rotor)
- Brake pads (inner and outer pads)

Friction between these two components occurs when the brake pedal is pressed, and these two components are squeezed together. This causes the vehicle's kinetic energy to be degraded into heat in both the brake disc and pads, and the vehicle slows down. Particles are generated when the surfaces of the brake disc and pads are in contact. However, studies have shown that particles are also released into the atmosphere on subsequent accelerations, and when the vehicle is cruising.

Tyres are comprised of various components, essential for their safe operation, and they provide the only contact point between the vehicle and the ground. The tread provides traction and cornering grip and has the biggest effect of all components on rolling resistance. Particles are generated at the point of contact between the vehicle and the road by friction between these two, i.e., from the tyre's tread and the road surface. In addition, resuspension of existing "road dust" complicates determining the provenance of the aerosol generated in the vicinity of the tyres. The operational uses and loads for light to medium, and heavy-duty vehicles differ, thus so does their tyre composition. The focus for this project is on light duty vehicles only. Further details on the particles produced by brake systems and tyres are given in Section 2.4 below.

The literature review analysed in some depth seven road studies and nine laboratory studies of brake and tyre wear (Table 2-1 and Table 2-2 below) and these are the primary source for the information that follows.

Table 2-1: Overview of on road studies of brake and tyre wear

Study	Inlet	Transport	Analyser	Measurements	Reference
Brake Wear/Tyre Wear	Brake: fully enclosed system Tyre: sampling funnel mounted behind wheel	Evacuation volume flow	CPC based PN-PEMS (AIP) TSI DustTrak and a DEKATI E-filter ((<10 µm, < 2.5µm and <1µm)	Particle number concentration particle mass concentration	Feißel, et al. (2020) [1]
Brake Wear (RDE)	Fully enclosed system (as above)	anti-static duct, diffuser, and rectilinear smoothing section	CPC based PN-PEMS	Particle number concentration	Augsburg, et al. (2019) [2]
Tyre Wear	5 x SS sampling tubes (0.4 cm diam) inside wheel housing (1 as a background measurement)	Conductive tubing ID 0.8 cm - average length = 6 m 50 l min^{-1} non-isokinetic sampling	TSI EEPS	PN size distributions Particle number concentration	Mathissen, et al. (2011) [3]
Brake Wear	Cone shaped collector covering all wheel rim openings and dust shields	38 mm diam. hose connected to 100 mm diam. hose and tube/blower system	TSI APS 3321 TSI DustTrak 8533 TSI EEPS DustTrak 8533 (PM_{10}) (background)	Particle sizing Particle mass Particle size range	Farwick Zum Hagen, et al. (2019a) [4]
Brake Wear	Two tubes mounted near the outlet of the disc brake and two tubes near front of car	NA	GRIMM OPC DustTrak	Particle size distribution Particle mass concentrations (PM_{10}, $PM_{2.5}$ or PM_1)	Wahlström, et al. (2008) [5]

Study	Inlet	Transport	Analyser	Measurements	Reference
Tyre Wear (Tyre/Wheel Assembly and	Nozzle 220x17.5mm, CVS mixing chamber, ambient air at 5m^3/min	Isokinetic sample at 20l/min to filter	GC/MS analysis of rubber components to determine tyre vs road Tyre/wheel weighing A multi cascade sampler was used as a PM sampler to divide the particle sizes into $PM_{2.5}$and PM_{10}. A quartz filter of 47mmφ and 47mmφ OD × 20mmφ ID were used as a collection filter	Particle mass concentrations (PM_{10} and $PM_{2.5}$)	Tonegawa & Sasaki (2021) [6]
Tyre Wear	2 x metal tube inlets one behind each front tyre (1.9 cm diam. 230 cm long) 21 cm above the ground, 5 cm behind the tyre. 3rd inlet for background measurements	60-cm-long torpedo-shaped manifold, ID= 7.5 cm	Three DustTraks (one for each inlet) GRIMM (front right tyre)	Particle mass concentration Particle size distribution	Hussein, et al. (2008) [7]

Table 2-2: Overview of laboratory studies of brake and tyre wear

Study	Inlet	Transport	Analyser	Measurements	Reference
Brake Wear (chassis dynamometer)	2 x ¼ in. SS pipes positioned close to the brake disc/pad	single conductive silicon tube non-isokinetic sampling	TSI CPC 3775 (0.003 – 3.0 µm) ELPI (0.033 - 10 µm)	Particle number concentration size distribution	Chasapidis, et al. (2018) [8]
Brake Wear (chassis dynamometer)	partly enclosed	flexible, conductive tubing with a blower	TSI CPC 3772 & Airmodus AM20 CPC (detection efficiency 50% at 10 nm) TSI CPC3752 (detection efficiency 50% at 4 nm) 2 x TSI EEPS TSI DustTrak 8530 TSI APS 3321	Particle number concentration PN size distributions Particle mass Particle sizing	Mathissen, et al. (2019) [9]

Study	Inlet	Transport	Analyser	Measurements	Reference
Brake Wear (brake dynamometer, test stand)	2 x Isokinetic probes connected to cyclone (10µm cut-off)	Isokinetic sampling duct	ELPI + ELPI + (thermodenuder) HT ELPI+ (heater sampling line)	Particle size distribution	Perricone, et al. (2019) [10]
Brake Wear (brake dynamometer)	Electro-polished steel enclosure around brake - cooled air flow (20C)	900 m^3/h and 1200 m^3/h air flow through ducts ID= 175 mm	Three EN 13284-1/ISO 9096 compliant probes Two straight probes	$PM_{2.5}$, PM_{10} and thermally treated PN PN and real-time size distribution measurements	Mamakos, et al. (2021) [11]
Tyre Wear simulator (Preconditioned type 1 safety walk tape)	Tyre located within controlled-volume chamber (enclosed system)	NA	OPS DustTrak (PM_{total}), PM_{10}, $PM_{2.5}$, and PM_1) Fast Mobility Particle Sizer Sample collection	particle mass size distributions mass concentrations particle number and number size distributions SEM, TEM	Park et al. (2018) [12]
Tyre Wear simulator (Preconditioned type 1 safety walk tape)	Inner drum tire test bench (enclosed system)	NA	EEPS	particle size distribution	Foitzik et al. (2018) [13]
Tyre Wear simulator (flat metal surface)	inlets located 15 cm from the tyre/wheel interface	1 m long 1/4-inch, conductive plastic tubing	ATOFMS APS 2 x SMPS	Mass spectra of individual particles aerosol size distributions	Dall'Osto et al. (2014) [14]
Tyre Wear (VTI road simulator and pavement ring)	No details	No details	TEOM (gravimetric PM_{10}) DustTrak (PM_{10}) DustTrak ($PM_{2.5}$) TSI APS 3321 TSI SMPS	Particle mass concentrations Particle size distribution Number distribution	Grigoratos, et al. (2018) [15]
Tyre Wear (VTI road simulator and pavement ring)	No details	No details	TEOM DustTrak TSI APS 3321 TSI SMPS	Particle mass concentrations Particle size distribution Number distribution	Sjödin et al. (2010) [16]

2.2 SAMPLE INLETS

2.2.1 Brake systems

Brake particle sampling systems described in the literature can be classified into open systems, fully enclosed systems, and partially enclosed systems.

The PMP carried out an appraisal of brake dyno test rigs and their measurement systems, including studies by JARI, TU Ilmenau, Ford, Horiba/Audi, Brembo, and GM. In these studies, the brake disc and calliper (without wheel) are within an enclosure, with filtered air drawn or blown in, and exhaust (air and particles) drawn out for sampling. Although the designs differ, none are suitable for fitting to a vehicle.

Simple open systems, which place sample probe(s) near the brake-pad interface, were described by Mathissen et al (2011) [3], Kwak et al. (2013) [17] and Chasapidis et al. (2018) [8]. These studies are complemented by researchers at Ford (Farwick Zum Hagen, et al. (2019) [18]) who used Computational Fluid Dynamics (CFD) to analyse the airflow round the brakes during driving.

Data collected by researchers has indicated that particle emissions are significantly influenced by temperature, particularly of the brake pads. Thus, the choice of enclosed or open brake sampling system will not only affect the collection efficiency of brake particles produced but may also impact the rate of particle production through changing the brake system's temperatures.

As well as studies into measuring brake particles, there are already attempts to collect brake particles to prevent them being emitted. One system feeds air through slots cut into the brake pads and then into a filter. However, any system that involves modifying the brake pads is not be considered suitable as a sampling approach in this project, or for a certification procedure.

Filtration specialists Mann + Hummel have developed a brake particle filter that can be fitted to each brake of any disc-braked vehicle and can even be retrofitted. It consists of an enclosure with a slot to fit around the brake disc, of a similar size and outline to a brake calliper and fitted next to the calliper in the direction of the disc rotation. It is passive in operation; particles emitted from the brake pads enter the enclosure and are captured in a filter inside it. The filter is then replaced in routine servicing, although it is not clear what proportion of emitted particles may be captured as some may be emitted in other directions. The concept of the enclosure next to the calliper could be used as the basis for a partially open sampling system if connected to a sample line. However, the development of a sampling system for measurement should consider these filter systems because it is desirable that the effectiveness of such systems can themselves be measured.

2.2.2 Tyre systems

A fully or mostly enclosed system for the sampling of tyre particles is possible, but challenging, since a sampling system of this type needs to account for wheel movement, road imperfections, and any potential impact on the temperature of both tyre and brake. The necessary protrusion of this enclosure from the bodywork may also constitute a road hazard. Sampling inlets for tyres used in on-road measurements studies thus tend to fall into two broad designs:

1) one or more smaller diameter inlets mounted at various locations around the tyre and wheel housing,
2) a single large diameter sampling inlet mounted behind the wheel.

Key parameters include the number and diameter of the sampling inlets, and their cross section, their position relative to the tyre (wheel) and the road, and the volume of air sucked into the inlets. These inlets can be positioned directly adjacent to the tyre and open to the atmosphere, or anywhere around the rear of the tyre within a wheel enclosure - for example [19], near the top rear of the tyre.

As with brake particles, there are already ideas for capturing tyre particles at source. The Tyre Collective have demonstrated a device which is positioned around the tyre just behind and above the contact point with the road, and which uses an electrostatic charge to attract the tyre particles [20]. They claim that 60% of airborne particles were captured during rig tests though it is not clear how this was measured, and it has not yet been tested on a vehicle.

2.2.3 Background particle measurements

In addition to the measurement of particles generated by the braking system and tyres, the measurement of background particulates also should be considered. Some studies did not measure backgrounds, whilst others

used forward facing probes, or even ambient air sampling. A sampling probe facing forwards, under the vehicle (halfway across, and towards the rear) should allow for a background measurement that is better representative of re-suspended road dust, without being impacted directly by the wheels and tyres.

2.3 SAMPLE TRANSPORT

In our original proposal the focus was on sampling using the measurement instrumentation flows. The literature review has highlighted that a constant volume sampling (CVS) system and sub-sampling approach is favoured. Literature descriptions of sample transport from the sample inlets to the analysers were generally pragmatic. For example, where practical, sample inlets were fixed to the vehicle's body for both tyre and brake sampling systems. Some tyre studies used the wheel carrier, which moves with the steering wheel. A partially enclosed brake sampling system required a rotating joint to a stationary but flexible hose, to accommodate steering and suspension movement. Whereas another fully enclosed brake sampling system did not rotate, but too required flexibility in sample transport.

These practical constraints meant none of the systems described in the literature could achieve ideal sample transport conditions. The requirements of flexibility to accommodate wheel movements (steering and suspension), routeing samples out of wheel rims and arches and into vehicle bodywork to reach sampling instruments means some compromises are essential.

Notwithstanding, this project sought to adhere to the principles of good aerosol sampling practice. These include that isokinetic sampling should be used as far as possible, and sampling velocity should be high relative to the particle settling velocity in horizontal sections. Transport distances should be minimised (from sample to analyser), and where possible transport tubes should be:

- Straight (avoid bends wherever possible – eliminate inertial deposition).
- Of constant cross section.
- Vertical (to avoid gravitational settling).
- Metallic (such as stainless steel).
- Electrically earthed.
- Thermally insulated (where any part of the system is heated).

Achieving these demands is challenging enough in a laboratory, and measurements on a moving vehicle will involve practical constraints and requirements that involve a compromise from an ideal system. However, these compromises have been minimised in the design phase of this study.

2.4 SAMPLE ANALYSIS

Analysis instrumentation for the measurement of particle properties will need to consider equipment to quantify size distribution, particle number concentration, particulate mass emissions, and chemical analysis.

2.4.1 Particle size distribution

A review of particulate matter from NEE was performed by Piscitello, et al. (2021) [21]. In the review summaries of tyre wear and brake wear particle sizes are given. A large range of particle size distributions were observed from the reviewed studies; however, this may be expected as the distributions measured are limited by the detectable size range of the analysis instrumentation used, and also depend on the type of study.

For tyres, the reviewed studies showed that the mass-weighted distribution of particles was typically unimodal, peaking in the µm range (peaks from > 0.5 µm, up to 75 µm). The number-weighted size distribution was also mainly unimodal, peaking in the tens of nanometre range.

Brake wear studies also indicate a unimodal distribution in mass size distributions in most cases, peaking in the size range from 0.1 to 6 µm. For particle number the size distribution is more complex, and varies with brake system temperature, with at least one peak in the ultrafine fraction (diameter < 100 nm). Strong correlations between brake temperature and particle size distribution have been observed, with one study reporting a peak at 165 nm, and negligible ultrafine particles, for temperatures below 185°C, but a prevalence

of ultrafines (peak at 11 – 29 nm) for temperatures around 350°C. Peaks in number concentrations below 100 nm may be dominated by volatile particles, whereas coarse particles are primarily non-volatile.

Grigoratos & Martini (2015) [22], also reviewed studies on brake wear particle emissions and found that for particle number the distributions are usually bimodal and within the fine fraction.

2.4.2 Particle number concentration

An overview of particle number concentrations from brake wear (five studies) and tyre wear (three studies) under various conditions is given in Table 2-3 of the Literature Review report. The number concentrations for brakes range between 10^3 to 10^7 #cm^{-3}. The highest particle number emissions are typically observed during high-speed braking and cornering. However, it was often noted there can be a delay in the time between brakes being applied and the particles becoming airborne. Therefore, many studies calculate the particle number emissions (in PN emissions per km per brake) over a whole cycle.

The particle number emissions vary over different cycles and temperatures (Farwick zum Hagen, et al., 2019 [4]), At higher brake disc temperatures (above around 150°C) ultrafine particles begin to form, and are primarily comprised of volatile materials (see Section 2.4.4). Therefore, a number-based measurement system should consider measurements of both non-volatile and volatile particles.

There are few studies on particle number concentrations from tyres. Higher particle numbers were measured during braking and cornering when compared to driving at a constant speed, with mean particle numbers of 1.8x10^6 #cm^{-3} sampled 40 mm above the tyre road interface, during a cornering event.

2.4.3 Particle mass (PM) emission factors

An overview of PM emission factors from brake wear (seven studies) and tyre wear (three studies) is given in Table 2-3 and Table 2-4. Values listed can be for both PM_{10} and $PM_{2.5}$, and per brake, or per vehicle. Given the particle size distributions anticipated, and that this project will most probably be collecting samples one single brake assembly at a time, these are the metrics summarised here.

Table 2-3: Particle number concentrations from brake and tyre wear studies

Particle Source	Conditions	Sampling Method	PN concentration (#/cm^3)	Reference
Brake	Peak concentration during braking event at 80km/h	PN-PEMS without heating (> 23 nm)	2 x 10^5	Hesse & Augsburg, 2019 [23]
Brake	Peak concentration during braking event at 40km/h	PN-PEMS without heating (> 23 nm)	0.12 x 10^5	Hesse & Augsburg, 2019 [23]
Brake	Peak concentration during high velocity cornering	EEPS (5.6 nm and 562.3 nm)	3.5 x 10^6	Mathissen, et al., 2011 [3]
Brake	Peak concentration during full stop braking	EEPS (5.6 nm and 562.3 nm)	1 x 10^7	Mathissen, et al., 2011 [3]
Brake	Mean concentration over test runs	GRIMM (0.25 µm to 32 µm)	265 - 1252	Wahlström, et al., 2008 [5]
Tyre	Average at vehicle speeds of 50, 80, 110 and 140 km/h	FMPS (6-523 nm)	2.3 x 10^4 to 2.5 x 10^4	Kwak, et al., 2014 [17]
Tyre	Deceleration conditions	FMPS (6-523 nm)	7 x 10^5 to 1 x 10^6 (40mm above road/tyre)	Kwak, et al., 2014 [17]

Particle Source	Conditions	Sampling Method	PN concentration (#/cm^3)	Reference
Tyre	Cornering conditions	FMPS (6-523 nm)	$1.8x10^6 \pm 2.2x10^6$ (40mm above road/tyre) $3.8x10^4 \pm 1 x10^4$ (90mm above road/tyre)	Kwak, et al., 2014 [17]

Table 2-4: Particle number emissions from brake wear studies

Conditions	PN emission particles per km per brake	Reference
Over WLTP brake cycle	1.5 to 6 x 10^9	Mamakos, et al., 2019 [24]
20-min subsection of the 3h-LACT cycle < 153 °C	<1 x 10^{10}	Farwick zum Hagen, et al., 2019b [18]
20-min subsection of the 3h-LACT cycle > 153 °C	2 x 10^{12} to 1.3 x 10^{13}	Farwick zum Hagen, et al., 2019b [18]
Average over five tests on Ford F-150 vehicle (Non-Asbestos Organic, Low Metallic brakes)	4.5 x 10^{10}	Agudelo, et al., 2020 [25]
20-min subsection of the 3h-LACT cycle (LACT-20)	4 x 10^9 (solid particles) 7 x 10^{12} (total particles)	Mathissen, et al., 2019 [9]
3h-LACT cycle	3.5 x 10^9 (solid particles) 1 x 10^{10} (total particles)	Mathissen, et al., 2019 [9]
WLTP-Brake cycle (new brakes) first repetition	7.5 x 10^9 (thermally treated) 6.5 x 10^9 (untreated)	Mathissen, et al., 2019 [9]

PM_{10} brake system emission factors were found to be 5 ± 0.7 mg/km per brake over the WLTP-Brake cycle (all vehicles using low steel (LS) brake pads, four studies). As noted, there are fewer data regarding tyre emission factors. One study report gives a figure of 3.7 mg/km per vehicle for $PM_{2.5}$ for on road driving, whilst a laboratory study (using safety walk type 1 tape to simulate asphalt) quotes 0.03 – 0.05 mg/km. The authors of the laboratory study noted that the tyre tread wear rate underestimates the wear rate when compared to studies performed under real-world driving conditions. This may explain why lower $PM_{2.5}$ emissions ratios were observed in the laboratory study than the on-road driving study.

2.4.4 Chemical composition

Brake systems comprise two key components, with frictional contact between them generating particulate emissions through bulk physical abrasion, limited asperity contact and thermal mechanisms. These components are the brake discs, principally made from cast iron, and the brake pads. The literature review cited one analysis of a brake disc as containing 93.6% iron, 3.4% carbon, 3% all other elements.

In contrast the friction lining mixture on brake pads (the layer of the brake pad from which particles are generated) typically comprise five components: binder, reinforcement, filler, abrasive, and lubricants. Each

component can be comprised of a range of materials, such that brake-pads' composition is very varied between manufacturers. Moreover, several of these components (binders and reinforcements particularly) can have a high organic component content, which starts to decompose at high temperatures.

Figure 2-1: Chemical composition of key brake pad (adapted from Perricone et al. (2019) [10])

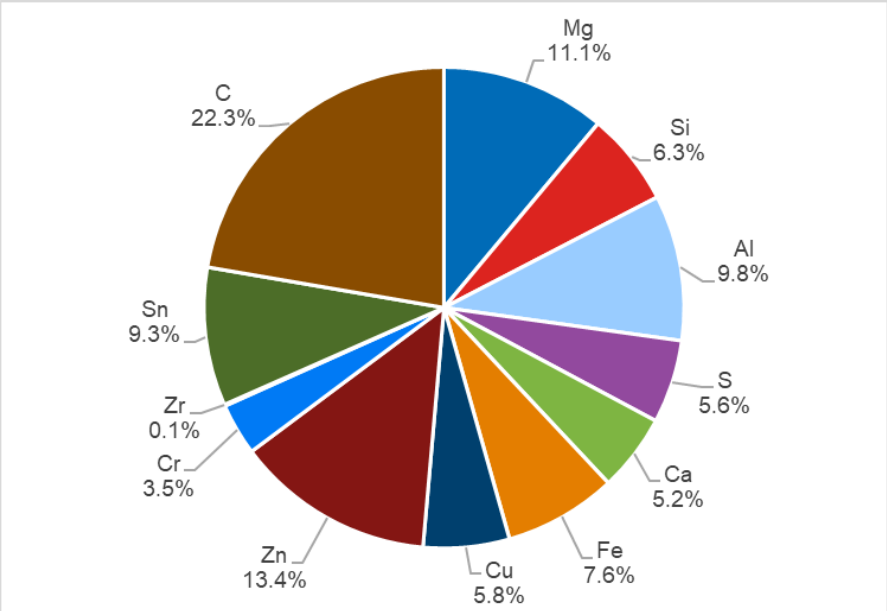

Figure 2-1 shows the chemical composition of a typical passenger car brake pad, as determined by x-ray fluorescence Perricone et al. (2019) [10]. This technique does not reveal the organic components in the brake pad, nor the oxygen present as oxides, only the principal heavier elements. Grigoratos & Martini (2015) [22] reviewed the metallic concentration ranges of brake dust emission analyses. This paper listed 20 metallic elements.

The tyre tread cap, the part of the tyre tread in contact with the road from which particle emissions are generated, comprises four principal components: elastomers, reinforcing fillers, plasticizers, and other chemicals. The elastomers and reinforcing fillers typically comprise 75 – 85% of this mixture. Elastomers are natural and synthetic rubbers (complex organic compounds) whilst the reinforcing fillers are generally carbon black and silica (often as nanoparticles).

Road surfaces comprise minerals and/or bitumen. Particles from the road surface mix with those from the tyre tread cap. In addition to road surface materials, re-entrained road dust will also contain legacy brake, tyre, and exhaust derived particulate matter.

Chemical analysis of the brake and tyre wear particles provides important information on the composition of airborne particles from NEE and their potential impact on human health. For this project performing detailed on-line composition analysis is not practical due to the limited power and space available in the vehicle. However, utilising an instrument that has the ability to collect particles, such as an Electrical Low-Pressure Impactor (ELPI), has allowed for off-line chemical composition analysis.

2.5 SUMMARY OF IMPLICATIONS FOR THIS STUDY

2.5.1 Brake Wear

A summary of particle size distributions (Piscitello et al., 2021 [21]) illustrates the difference in particle mass modal size distribution (typically 2 – 5 µm), and particle number modal size distribution (few 10s of nm). This is a consequence of the third power relationship between the two metrics, and, in part, the different ranges of the sampling instrumentation used during the study. In addition, differently sized particles are likely being generated by alternative mechanisms.

The two contributing components (the brake disc and brake pads) have very different compositions - The discs are made from predominantly iron. In contrast brake pads contain a number of organic polymers, that lead to large increases in particle number emissions with increasing brake (especially brake pad) temperature. Therefore, such particles emitted from the brake pads may be volatile, nucleation mode particles, and their number will be dependent on the brake pad's composition, temperature, and previous thermal cycles. This can make such particle number emissions quite irreproducible, even from the same brake pad-disc configuration as it ages. Solid nanoparticles may also be produced, but levels are likely to be orders of magnitude below the levels of volatile particles, and these will be difficult to detect without a dedicated non-volatile particle measurement system.

Whilst the particles emitted from the braking system are principally generated when brakes are applied, the aerodynamic flow round the brake callipers can mean a significant fraction of the solid particles become airborne after the braking event - during subsequent accelerations, or even steady speed driving.

Because different vehicle models have different geometric designs (not just the calliper but the whole wheel arch, ride height etc) and different aerodynamic flow patterns the extent of the "delay" in brake particles becoming airborne will vary. Therefore, brake emissions need to be integrated over the whole cycle (not just measured during braking). This aligns well with a mass or number per kilometre metric for brake wear emissions.

2.5.2 Tyre Wear

A summary of particle size distributions (Piscitello et al., 2021 [21]) again illustrates the difference in particle mass modal size distribution (typically 5 – 10 µm), and particle number modal size distribution (few 10s of nm).

The two contributing components are tyre wear (from the tread cap) and road wear. There is the additional complication of resuspension of pre-existing particles on the road being caught up in the air currents created by the passing car.

The tread cap is made predominantly of organic polymers (both natural and synthetic), and the majority of particles are created by mechanical abrasion, not volatilisation or decomposition of the organic materials.

However, increasingly nano particles (carbon or highly dispersed silica, HDS) are used to increase the longevity and strength of the organic polymeric elastomers. Their primary sizes are 5 – 100 nm (carbon) and 2 – 40 nm (HDS). But particles self-aggregate and agglomerate into larger particles during manufacture. Therefore, it is likely that part of the tyre emissions are these nano particles. If so, substantial levels of non-volatile nanoparticle emissions may be seen from tyres and, as with brake wear, a dedicated non-volatile particle measurement system would be necessary.

Road surfaces (the component in contact with the tyre intimately involved in generating the tyre and road surface wear particles) are generally concrete or asphalt based. Characterisation of road wear is complicated by pre-existing "dust" on the road which can become resuspended when a vehicle wheel passes over it. This legacy dust can be very difficult to discriminate from the real-time road wear emissions.

The review by Piscitello et al., gives the following PM_{10} emission factors for a range of vehicle types and surfaces: Tyre wear 1.9 – 9 mg km^{-1} $vehicle^{-1}$, road wear 3 – 40 mg km^{-1} $vehicle^{-1}$, and resuspension 0.3 – 733 mg km^{-1} $vehicle^{-1}$. These data illustrate the challenge of distinguishing between the three wheel-based emission sources.

3. CONCEPT DEVELOPMENT

3.1 HIGH LEVEL SPECIFICATION

Based on the literature review output and discussions with stakeholders a measurement solution for the prototype build and testing task was developed. A high-level specification for each component of the system is provided below.

Tyre sampling inlet: For the tyre inlet a large diameter nozzle, connected to a sampling duct (i.e., Feißel et al. (2020) [1]) to be located behind the tyre was found to be the most practical solution. The position of the

nozzle behind the tyre is important for maximum capture of a representative sample, therefore it is attached to the steering housing to allow the inlet to stay in line with wheel during cornering.

Brake sampling inlet: The brake sampling inlet consists of an enclosed system which can be continuously flushed with filtered air to allow for cooling of the brake pads and a high sample flow. To ensure the brake disc temperatures remain close to real-world driving, temperatures are monitored on both the enclosed brake and an unhoused brake, on the opposite wheel, for comparison.

Background: With an enclosed system on the brakes the influence from tyre wear, or road dust resuspension will be negligible, therefore a separate background measurement will not be necessary for the brake wear measurements. The tyres cannot be enclosed therefore a background measurement is required. For the background measurement a separate line and probe are used. Tests are performed with the inlet located in front of the tyre at different heights, and under the centreline of the vehicle. The aim is to be far away from any tyre-road interface effects, whilst still measuring re-suspended road dust.

Sampling Transport: For the sampling transport a constant volume system (CVS) seemed to be the best approach. Flexible ducting is used to sample from the brakes, tyres, and background inlets so the tubing can move with the vehicle. The flexible tubing is connected to a sampling tunnel from which the analysers sub sample from.

Sample analysers: To reduce the number of analysers required, we have investigated using common analysers to sample both brake and tyre wear. The peak particle size range from brakes and tyres ranges from the nm to µm range, therefore a combination of analysers is likely to be required.

Eight types of particle measurement equipment were investigated for this project. As volatiles are likely to dominate below 30nm, we will require a method of measuring both total and non-volatile fractions, from which the volatile fraction can be calculated. Chemical analysis can also be performed offline as the particles are collected. This may be achieved using two Electrical Low-Pressure Impactor (ELPI+) systems[1] in parallel, one with a heated inlet[2] to remove the volatile fraction. The ELPI+ system can measure particle concentration and size distributions over the size range 6 nm to 10 µm, in 14 size fractions. An eFilter analyser[3] was also used to obtain real-time particle mass concentrations. The eFilter can measure particulate mass up to 3 µm in real-time and also has a gravimetric filter holder to measure gravimetric particle mass. Further information on these analysers is provided in Table 3-1.

Table 3-1: Specifications of the ELPI+ (high resolution) and eFilter

Instrument	Size range	Size classes	Sampling rate	Sample temperature range	Sample flow rate
Dekati High resolution ELPI+	6 nm to 10 µm	14 (100/500 interpolated)	Up to 10 Hz	10-180 °C (High Temperature ELPI+)	10 lpm
Dekati eFilter	~5nm to 3µm	NA	1 Hz	NA	10–100 lpm (gravimetric filter) 0.5 lpm (real-time)

3.2 MODELLING OF SYSTEM PERFORMANCE

Feißel, et al. [1] used a CFD model to assess the flow conditions and particle sampling/transport efficiencies in their sampling system for brake and tyre wear. This type of complex analysis is beyond the scope of the current project; however, we can evaluate the sampling and transport efficiency of the candidate system, using particle penetration calculations. Particle penetration calculations are a useful tool to rapidly appraise the relative merits of a proposed sampling system.

[1] High Resolution ELPI®+ - Aerosol particle size spectrometer - Dekati Ltd
[2] High Temperature ELPI®+ - Real-time particle measurement - Dekati Ltd
[3] Dekati® eFilter™ - Dekati Ltd

3.2.1 Particle Sampling Efficiency

The sampling efficiency relates to the fraction of particles passing through the sampling inlet. As a first step we have assessed whether the particle transport calculations can be applied to the tyre sampling arrangement described in Feißel, et al.

No details are reported of the exact configuration or dimensions of the system used in the study, but some information can be gleaned from the diagrams and photographs provided:

- The sampling head is a 100 mm diameter funnel.
- The flow rate through the system is 1,330 l min^{-1}, resulting in a velocity of 2.8 m s^{-1} into the sampling funnel.
- The transport tubing must be narrower than the sampling funnel. A diameter of 80 mm is taken as an approximation.
- The system flow rate results in an approximate velocity of 4.4 m s^{-1} in the narrower tubing.
- A significant length of horizontal pipework exists in the system, potentially up to 2.5 m.
- Several bends are necessary to deliver the sample to the analyser.
- The exact location of the secondary sampling point (where the analyser samples from the “CVS”) is not specified.

Firstly, calculations were performed to estimate the velocity of materials leaving the tyre, under different vehicle speeds. The results from these calculations, shown in Table 3-2 demonstrate that to a first approximation, the vehicle speed is similar to the CFD entrained air velocity.

Table 3-2: Estimate of the CFD velocity of materials leaving the tyre, under different vehicle speeds.

Vehicle Speed		CFD Velocity Estimate at the Tyre
(kph)	(m s^{-1})	(m s^{-1})
30	8.33	10
60	16.67	15
90	25.00	20
120	33.33	30

Using the first condition (i.e., vehicle speed of 8.33 ms^{-1}) and duplicating other relevant parameters (inlet diameter, inlet flow, particle density) and assuming a non-isokinetic probe at non-ideal orientation (70°), calculations predict that 20 µm diameter particles would be sampled with 21.5 % efficiency. This is an encouraging initial result, but it should be noted that the calculation is very sensitive to orientation and that a one degree change in orientation results in a 5 % difference in the calculated efficiency.

The calculations were performed for other flow conditions, and particle diameters. The results of the efficiencies are provided in Table 3-3 and Figure 3-1.

Table 3-3: Sampling efficiency under different flow conditions and particle diameters.

Velocity (m s^{-1})	Sampling efficiency of specified particle diameter (%)			
	20 µm	10 µm	2.5 µm	1 µm
8.3	21.5	27.2	34.8	47.7
16.7	18.0	25.2	32.8	41.0
25.0	16.3	24.2	32.0	38.4
33.3	15.1	23.6	31.6	36.9

Figure 3-1: Sampling efficiency versus velocity for particle diameters of 20, 10, 2.5 and 1 µm.

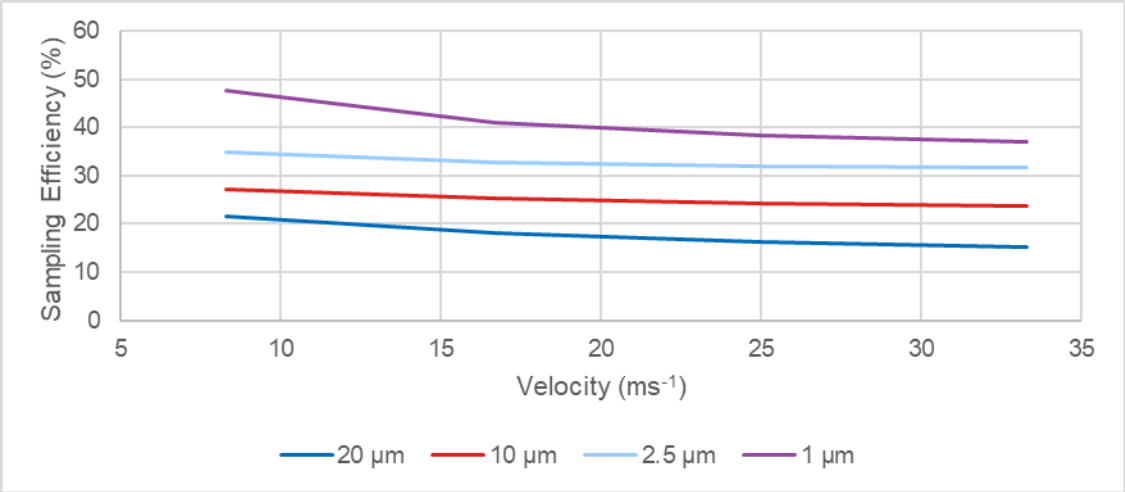

The trends evident in the results are consistent with typical particle aerodynamic behaviour:

- For a given diameter, sampling efficiency worsens with increasing flow velocity as the sampling becomes more anisokinetic.
- For a given flow velocity, sampling efficiency improves with decreasing diameter as the particles become more aerodynamically mobile.

These trends are also evident in the CFD modelled data in Feißel, et al. (2020), however, the magnitude of the sampling efficiency change, with respect to the critical diameters, is different. In particular, the CFD model predicts a significant reduction in efficiency at all velocities other than the slowest, whereas the simpler calculations predict a more gradual decline.

These different outcomes are most probably the result of the basis on which the sampling calculations are developed. The calculations assume that sampling is being undertaken from a well-developed flow, containing a homogenous particle concentration, within a well-defined duct. The features of this application that are a particular challenge are:

- The less well-defined sampling region behind a wheel – it is difficult to define appropriate boundary parameters within the calculations.
- The turbulent nature of the sampling location – this cannot be fully accounted for within the calculations.
- The degree to which the sample probe is in the particle stream of interest – the calculations do include an orientation parameter, but its usefulness is limited as it still assumes that the probe is fully within the particle stream.

Despite the challenges, the basic sampling efficiency calculations have demonstrated the importance of:

- Understanding the flow field from which sampling is taking place.
- Achieving near-isokinetic sampling where possible.
- The location of the sample probe.
- The orientation of the sampling probe.

While the significance of these should be apparent, it is easy to overlook their importance in a complex sampling situation. It is also valuable to have some degree of understanding of the sensitivity of the final sampling efficiency to each of these factors. Where compromises have to be made to accommodate the practical arrangements of performing this type of sampling, it is helpful to know their relative affect so those with fewer repercussions for the final sampling efficiency can be prioritised. Where possible we will also aim to apply a calibration approach to correct for any losses.

3.2.2 Particle Transport Efficiency

The transport of particles of a known diameter through such a system can be predicted by considering those factors that can cause particles to deposit within the system. In this case, the most relevant are:

- Gravitational settling (including turbulence where relevant).
- Inertial deposition in bends.
- Deposition in abrupt tube contractions.

Each mechanism can be approximated to a good degree of accuracy using fairly straightforward calculations derived from well understood interactions between the particles and the transport gas.

Other loss mechanisms have not been considered as their effect will be minimal or relatively easily negated:

- Diffusion – the magnitude of the effect is very small for the particle diameters and sampling conditions considered here (penetration better than 99.9%).
- Thermophoresis – it is not anticipated that there will be any significant temperature gradients with the sampling conditions to drive this mechanism.
- Electrostatics – there is evidence that the particle leaving the tyre are electrostatically charged (e.g., the Tyre Collective use the principle for particle capture), but the effects can be minimised in a sampling system by using well-earthed conductive components.

Firstly, the particle transport calculations were applied to the tyre sampling arrangement described in Feißel, et al. (2020).

Gravitational settling

Particles settle under the influence of gravity and may deposit within the tube before reaching the exit if their residence time in the tube is sufficiently long.

Under the flow conditions outlined above the effect of deposition was calculated for different particle aerodynamic diameters. The results of these calculations are given in Table 3-4.

Table 3-4: Calculation of the deposition per meter for different particle diameters sizes, using a flow of 1,330 $lmin^{-1}$.

Aerodynamic Diameter (µm)	Deposition Per Metre (%)
20	6.6
10	1.5
5.0	0.5
2.5	0.2
1.0	0.1
0.1	0

The magnitude of the loss is directly proportional to particle diameter due to larger particles having greater settling velocities.

The system being considered here is turbulent (flow Reynolds number ~23,000) and turbulence very slightly counteracts the gravitational settling, but the magnitude of the effect is very small. For example, in the first row in Table 3-4 above the result is 6.59% under turbulent conditions compared with 6.57% under laminar conditions.

Inertial deposition in bends

Particle inertia may mean that particles are unable to follow flow streamlines as flow direction changes around a bend, resulting in impaction on the internal surface of the sampling system. Calculations of deposition in a 90º and 45º bend, under laminar and turbulent flows, were performed, under same flow conditions outlined above. The results are shown in Table 3-5 and Table 3-6.

The effect is directly proportional to particle diameter, velocity and sharpness of bend. A shallower bend has a smaller effect on the deposition (all other parameters being constant). Turbulence has a much more significant role in this mechanism.

Table 3-5: Calculation of the deposition in a 90º bend under laminar and turbulent flow, for different particle diameters sizes.

Aerodynamic Diameter (µm)	Deposition in a 90° Bend (laminar) (%)	Deposition in a 90° Bend (turbulent) (%)
20	17	37
10	4	11
5.0	1	3
2.5	0.3	0.8
1.0	0.05	0.14
0.1	0.001	0.003

Table 3-6: Calculation of the deposition in a 45º bend under laminar and turbulent flow, for different particle diameters sizes.

Aerodynamic Diameter (µm)	Deposition in a 45° Bend (laminar) (%)	Deposition in a 45° Bend (turbulent) (%)
20	8	21
10	2	6
5.0	0.5	1.5
2.5	0.14	0.39
1.0	0.02	0.07
0.1	0	0

Deposition in abrupt tube contractions

If the particle laden flow encounters an “abrupt” contraction, then deposition is enhanced primarily due to the additional turbulence created by the flow velocity acceleration into the narrower tube. The magnitude of the effect is reduced by easing the abruptness of the contraction. Calculations were performed using the parameters already established in the previous calculations but includes a contraction to half the original tube diameter at two different contraction angles to illustrate the effect. The results are shown in Table 3-7.

Table 3-7: Calculation of the deposition in a 45º and 90º bend with a contraction to one half of the original tube size.

Aerodynamic Diameter (µm)	Deposition in a 45° contraction (%)	Deposition in a 90° contraction (%)
20	14	31
10	3	8
5.0	0.5	1.5
2.5	0.1	0.3
1.0	0.01	0.03
0.1	0	0

3.2.3 Application to sampling system

The authenticity of the calculated outcomes can be validated by comparison with the results of more detailed modelling as presented in Feißel, et al. (2020). In the sampling arrangement being considered here a combination of 2 m of horizontal tubing incorporating three 90° bends results in a similar efficiency profile to that reported from the modelling and this appears to be a realistic scenario.

The largest diameter particle (20 µm) is transported at close to 20% efficiency with an increase to greater than 85% efficiency for particle diameters of 5 µm and smaller. It has been necessary to estimate several of the crucial parameters, but these estimates have been based on reasonable assumptions and observations and have not been manipulated simply to produce the desired result.

One limitation that is acknowledged is that the calculations assume uniform conditions within the sampling system. They do not consider the influence of the complex flow field at the inlet of the sampling system and its subsequent effect on the initial velocity and direction of travel of the particles. Consequently, the calculations cannot replicate the transport efficiency profile of the modelling at a road speed of 120 km h^{-1}.

The particle penetration calculations presented here can be used to evaluate the relative merits of any proposed sampling system. For example, it has been postulated that it would be easier to route the sampling system through the vehicle if the pipe diameter was smaller. This would also have the advantage of requiring a smaller volumetric flow to maintain the same sampling velocity with the corresponding reduction in power required to drive the sampling pump during driving. These factors are summarised in Table 3-8 for 20 µm diameter particles.

There will be an increase in gravitational settling by a factor of ~1.8 due to the change in tube diameter despite the flow velocity and residence time in the sampling system remaining the same. However, the same velocity in a smaller diameter tube, while less turbulent, results in the losses due to inertial deposition in any 90° bend increasing by a factor of ~1.6 due to the smaller physical dimensions of the bend. In order to maintain the original losses in the bend, it would require the flow velocity to be half the original value. This may have additional favourable consequences for power consumption, but the slower velocity and longer residence time result in losses due to gravitational sedimentation increasing by a factor of ~3.2. However, there are three bends in the system under consideration so their relative contribution must also be accounted for.

Table 3-8: Calculation of the overall efficiency in a 2 m long tube with three 90° bends for different flow rates and tube diameters.

Flow Rate ($l\ min^{-1}$)	Tube Diameter (m)	Flow Velocity ($m\ s^{-1}$)	Efficiency 2m Horizontal Tube (%)	90° Bend Efficiency (%)			Overall Efficiency (%)
				1	2	3	
1330	0.08	4.4	87	63	63	63	22
330	0.04	4.4	76	39	39	39	5
165	0.04	2.2	58	63	63	63	15

4. LABORATORY EVALUATION

4.1 LABORATORY EVALUATION OF PROTOTYPE

Initially the laboratory evaluation focussed on the ELPI units to establish their measurement performance across a range of diameters, concentrations, and particle compositions. In addition, measurements were made to estimate their limit of detection. Thereafter, the ELPI units were employed in their role as particle detectors on the proposed measurement system to allow the determination of transmission efficiency as function of particle diameter and operating conditions.

4.1.1 ELPI to ELPI Comparison

Both units were challenged simultaneously with polydisperse soot particles to check their comparability. The high temperature unit (S/N 10082) was operated at room temperature. Both units report a similar modal diameter and width of distribution (Figure 4-1). Individual channel concentrations agreed to within 20% and this was sufficient to consider them as an equivalent pair in subsequent measurements.

Figure 4-1: Simultaneously measured particle size distributions

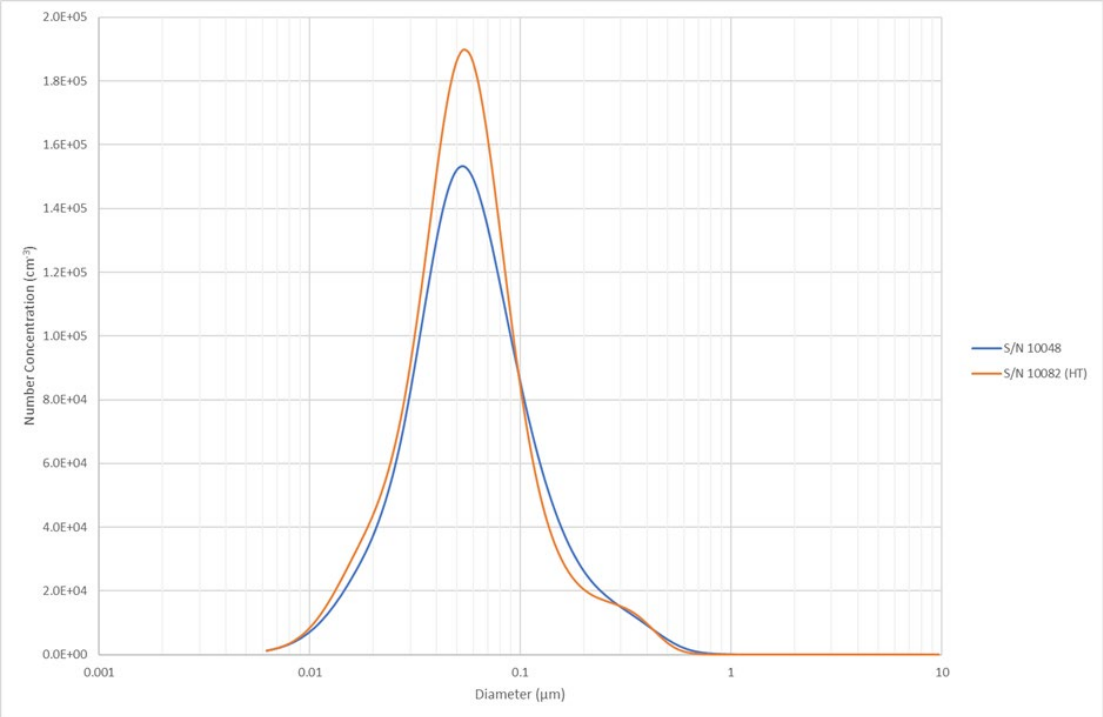

4.1.2 ELPI Detection Efficiency as a function of diameter, concentration and charge state

ELPI S/N:10048 was challenged with monodisperse 100, 50 and 30 nm soot particles produced by electrostatically classifying the output of a mini-CAST generator. The ELPI response was compared with a reference condensation particle counter. The ELPI detected particles with better than 95 % efficiency at all these diameters. Excellent linearity was observed over the measured concentration range in each case (Figure 4-2 to Figure 4-4). The comparison was undertaken both with and without an aerosol neutralizer after the electrostatic classifier which demonstrated that ELPI response was not sensitive to the charge state of the particles being measured. The charge state of the particles sampled in practise will not be known with any degree of certainty and there will be little opportunity to include a charge equilibrator in the final sampling system. This was an important observation giving confidence that the measured data will not be sensitive to this parameter.

Figure 4-2: Detection efficiency and linearity of 100 nm particles

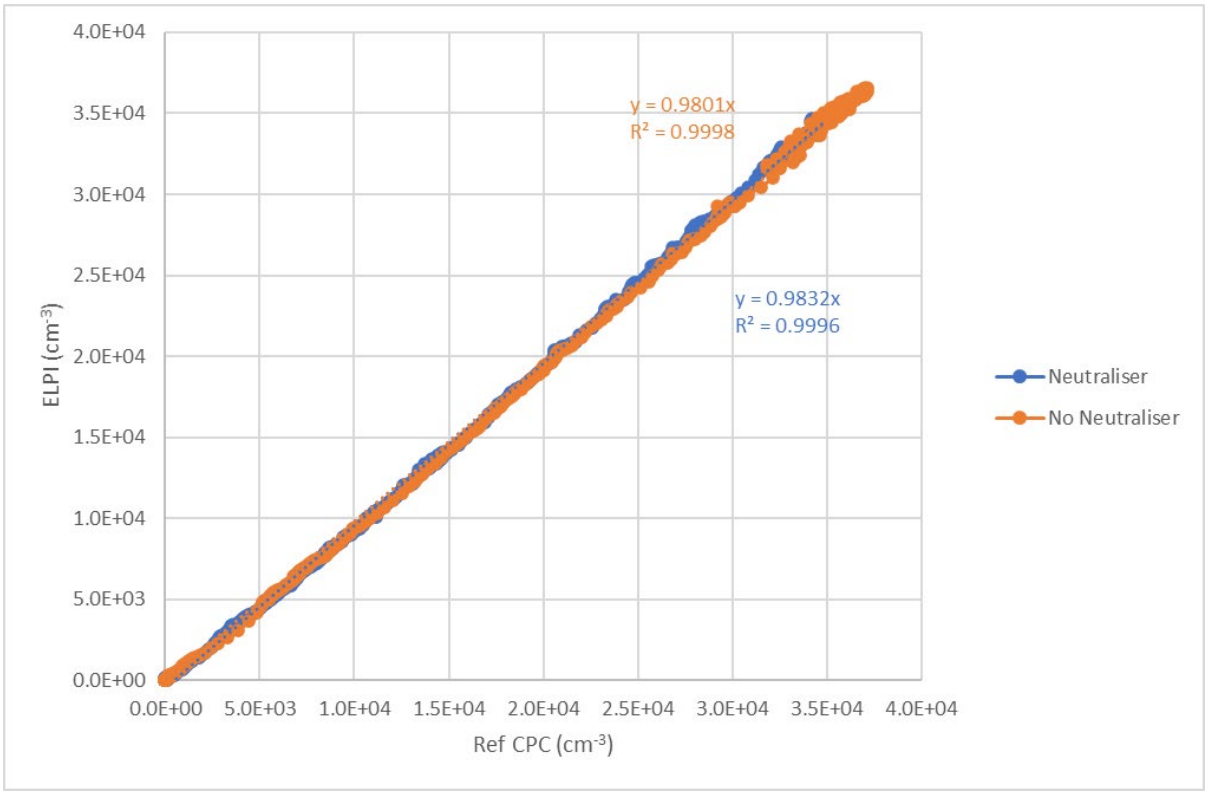

Figure 4-3: Detection efficiency and linearity of 50 nm particles

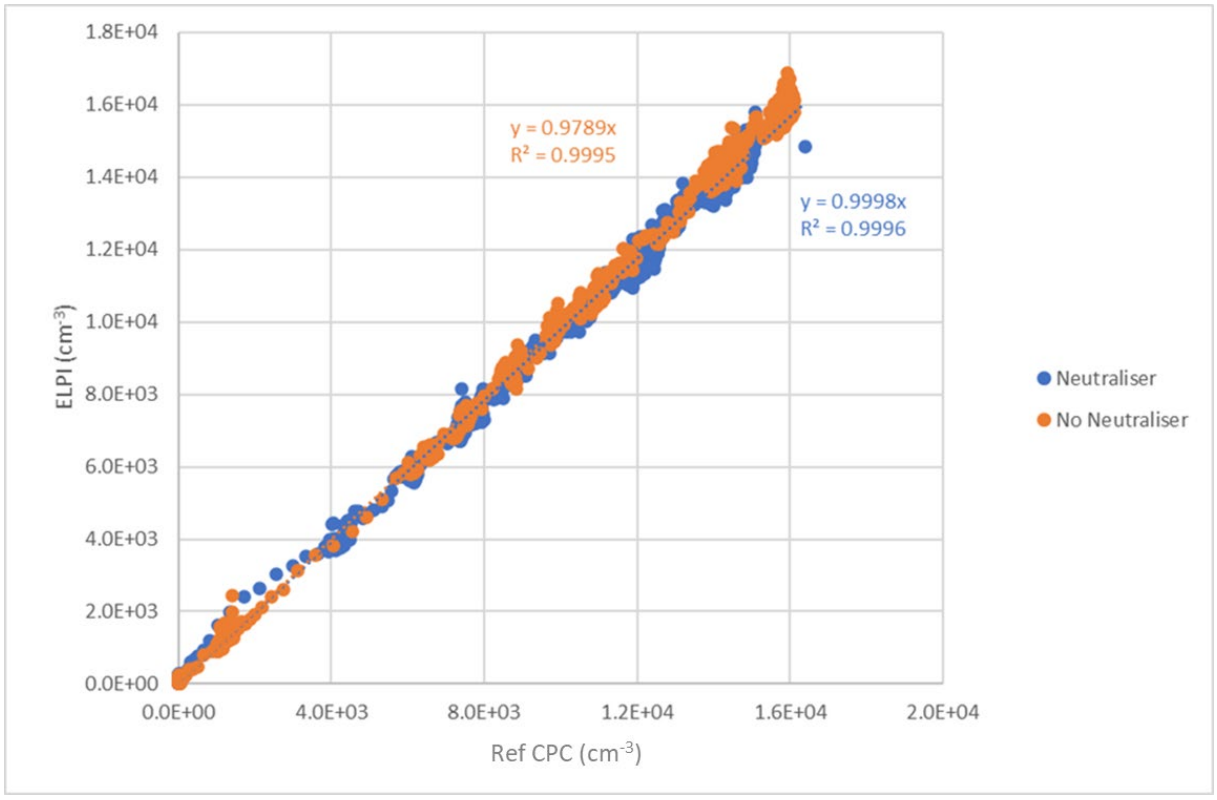

Figure 4-4: Detection efficiency and linearity of 30 nm particles

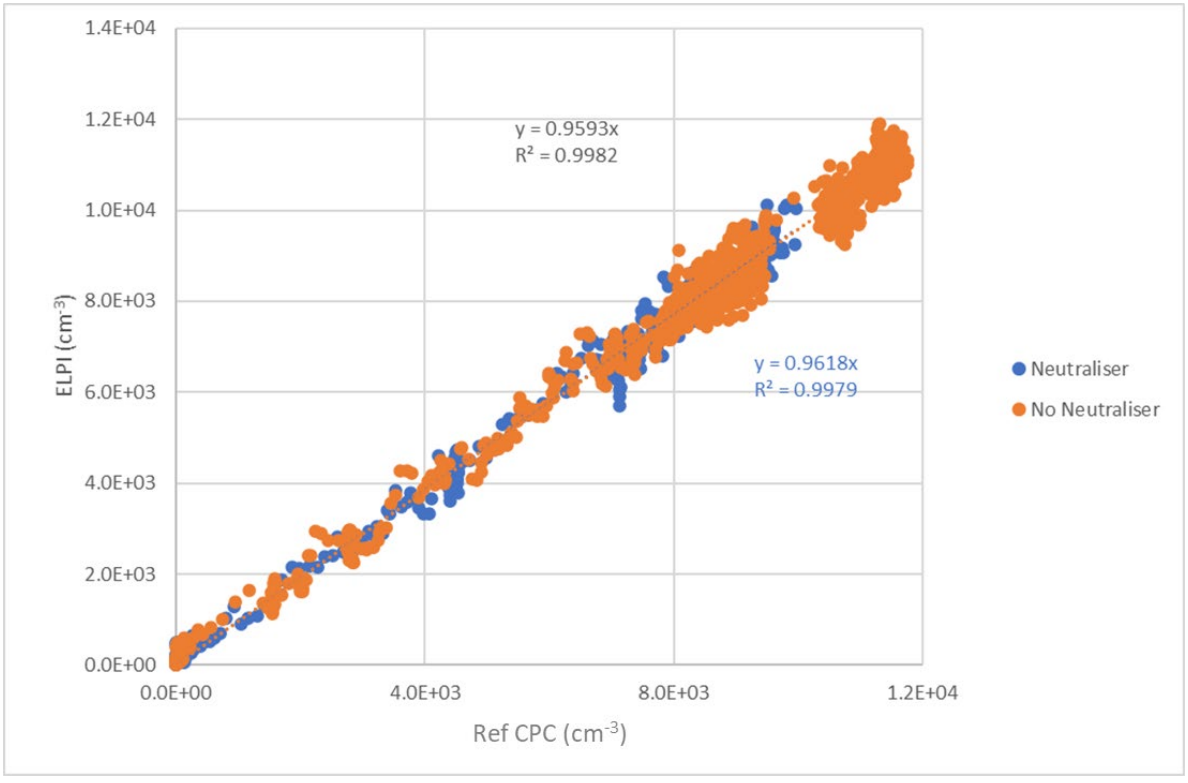

4.1.3 Limit of detection/baseline at zero particle concentration

The ELPIs have the facility to generate “zero air” with which to zero the stage electrometers before any measurements are made. Particle number concentrations were recorded with this facility turned on. An

additional measurement was made with the ELPIs operating normally but with a HEPA filter at the ELPI inlet to determine the typical "zero" concentration that the units can report. Both units were operated at room temperature and sampled from ambient air (Figure 4-5).

Figure 4-5: Ambient distribution at time of zero assessment

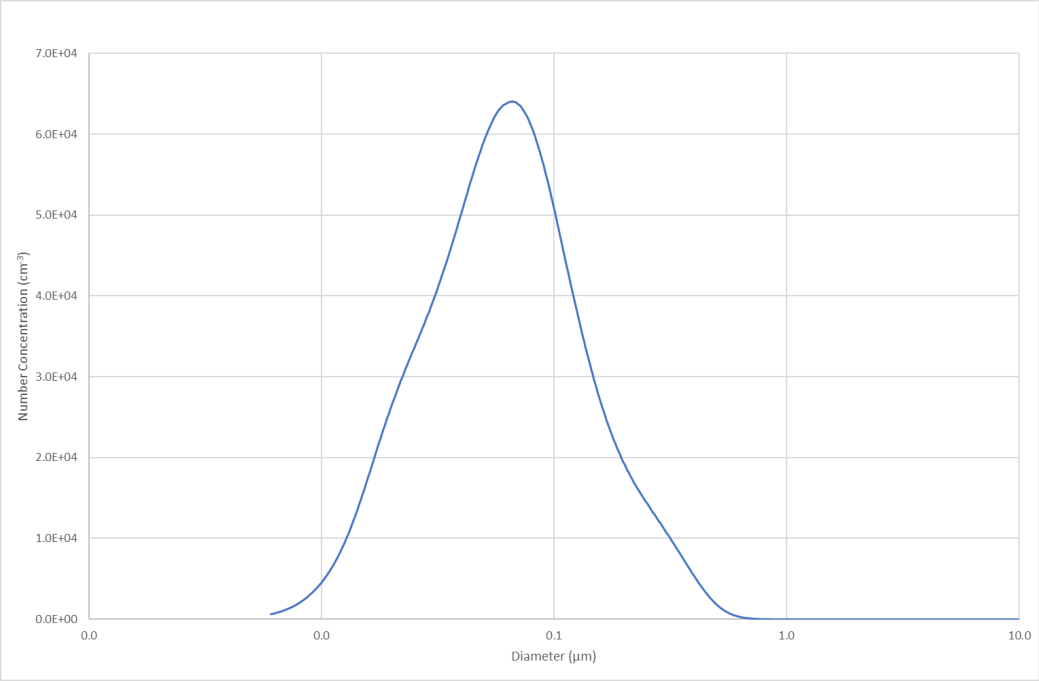

Table 4-1: "Zero" particle number concentrations

ELPI	Particle Number Concentration (cm^{-3})	
	"Zero Air"	HEPA Filter at Inlet
s/n: 10048	363	118
s/n: 10082	638	628

The "zero air" concentrations (Table 4-1) were comparable with those measured following the HEPA filtration of a significant challenge concentration (Figure 4-1). This provided confidence that the properly zeroed ELPIs are capable of measuring a zero-concentration equivalent to that generated by HEPA filtration.

4.1.4 Particle Composition

Tests were undertaken with two particle types that are considered to be good indicators of volatile particle behaviour. Tetracontane particles ($C_{40}H_{82}$) were generated by an evaporation/condensation process which produced a distribution at high concentration with a modal diameter of around 15 nm. Emery oil particles (Polyalphaolefin) were generated by pneumatic nebulisation which produced a distribution at more modest concentrations with a modal diameter of around 160 nm.

Both ELPI units were challenged with these volatile polydisperse particles. ELPI S/N 10048 was operated at room temperature and ELPI S/N 10082 was heated to 180°C with the sample line at a temperature of 200°C (Figure 4-6 and Figure 4-7).

Figure 4-6: Simultaneous “hot” and “cold” measurement of tetracontane particles.

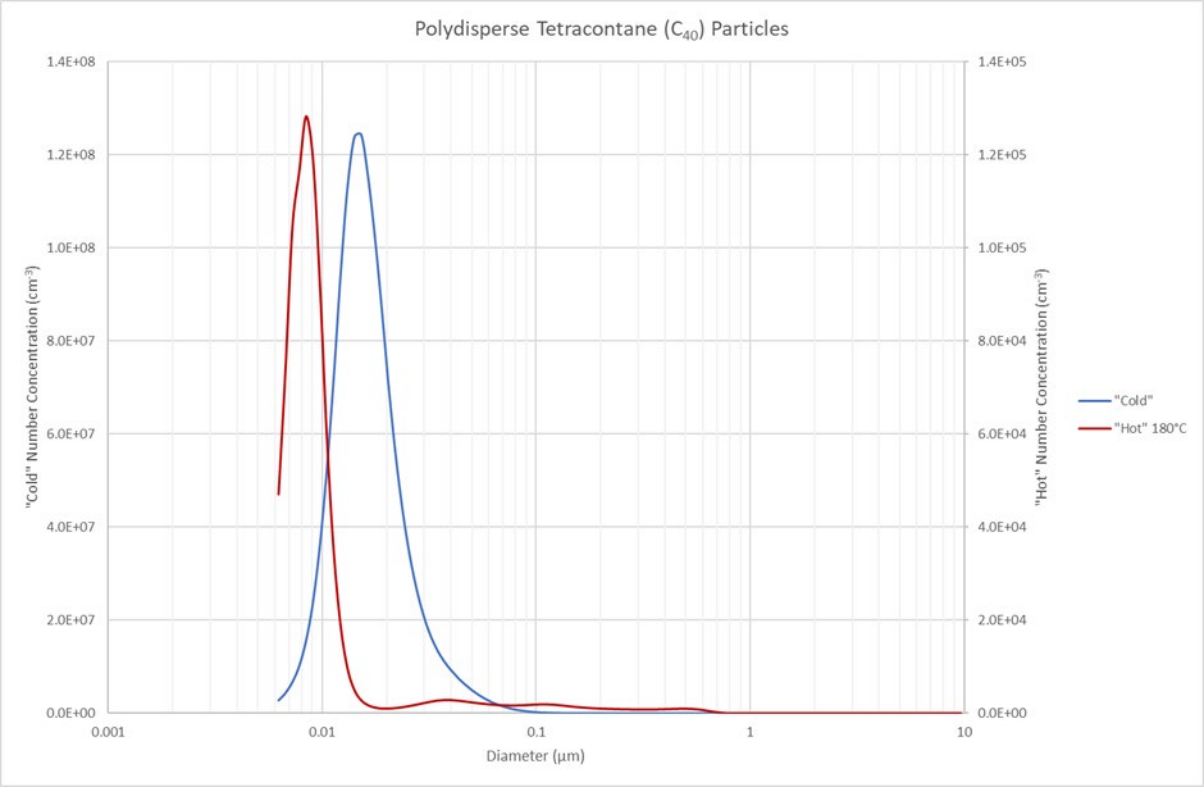

Figure 4-7: Simultaneous “hot” and “cold” measurement of emery oil particles.

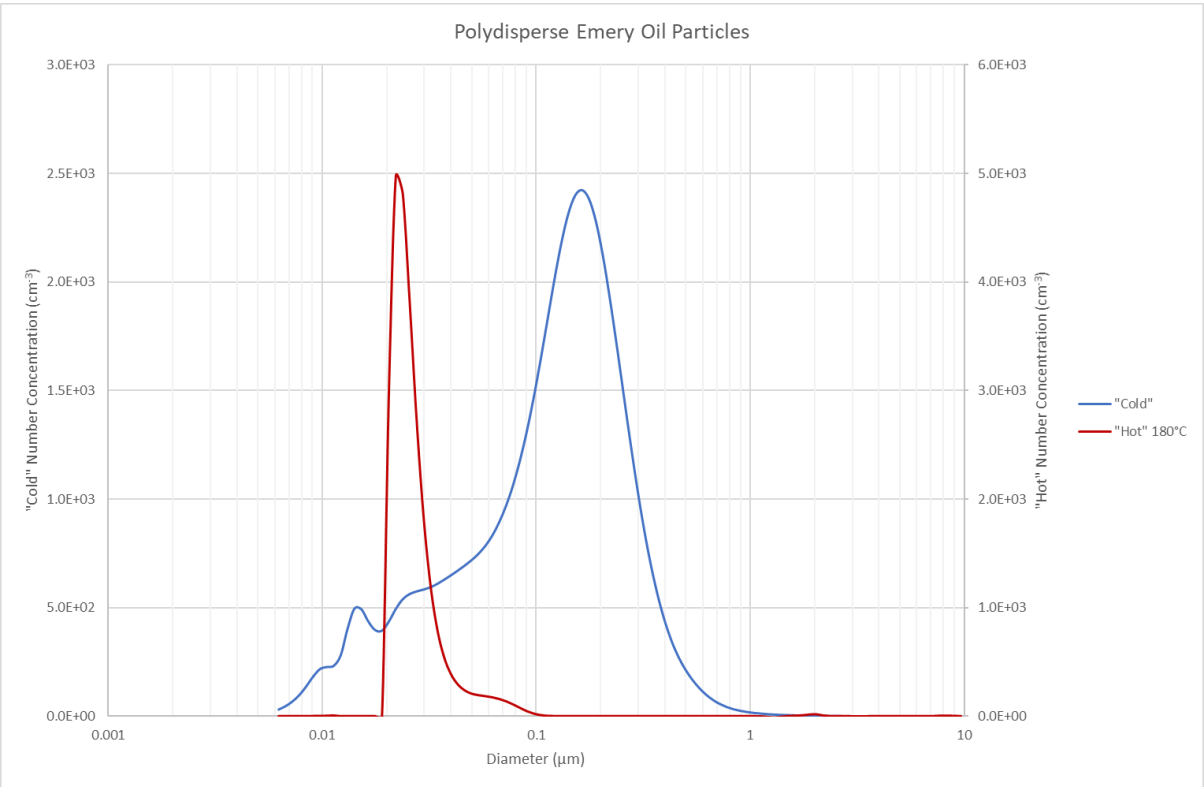

Table 4-2: Particle number concentrations measured under “hot” and “cold” conditions

ELPI	Number Concentration (cm^{-3})	
	Tetracontane	Emery Oil
s/n: 10048 “Cold”	4.25 x 10^7	1.85 x 10^3
s/n: 10082 “Hot” 180°C	3.05 x 10^4	1.31 x 10^3

Table 4-2 shows the particle number concentration measured by the ELPI+ under hot and cold conditions. For both particle types, the volatile particles that were detected in the “Hot” ELPI sample had been reduced to significantly smaller diameters. There was a substantial reduction (~x10^3) in concentration of the smaller primary tetracontane particles, but a smaller reduction (~x1.5) in the concentration of the larger primary emery oil particles. However, taking into account the diameter differences in the primary particle distributions, very substantial removal of volatile material occurred in both cases, demonstrating that simultaneous measurement under different temperature condition is a viable method to detect the presence of volatile particles.

4.1.5 Transport efficiency through prototype system

A surrogate of the proposed sampling tunnel was used to determine particle transmission efficiency as a function of particle diameter at the intended sampling conditions. The two fully characterized ELPI units were used simultaneously to measure the up and downstream particle size distributions, whilst challenging the system with a broad polydisperse distribution of mini-CAST generated soot particles and coarse test dust. The polydisperse distribution produced a modal diameter of around 100 nm and a coarse test dust with a modal diameter of around 2 µm.

Figure 4-8: Particle Transmission through the prototype sampling system.

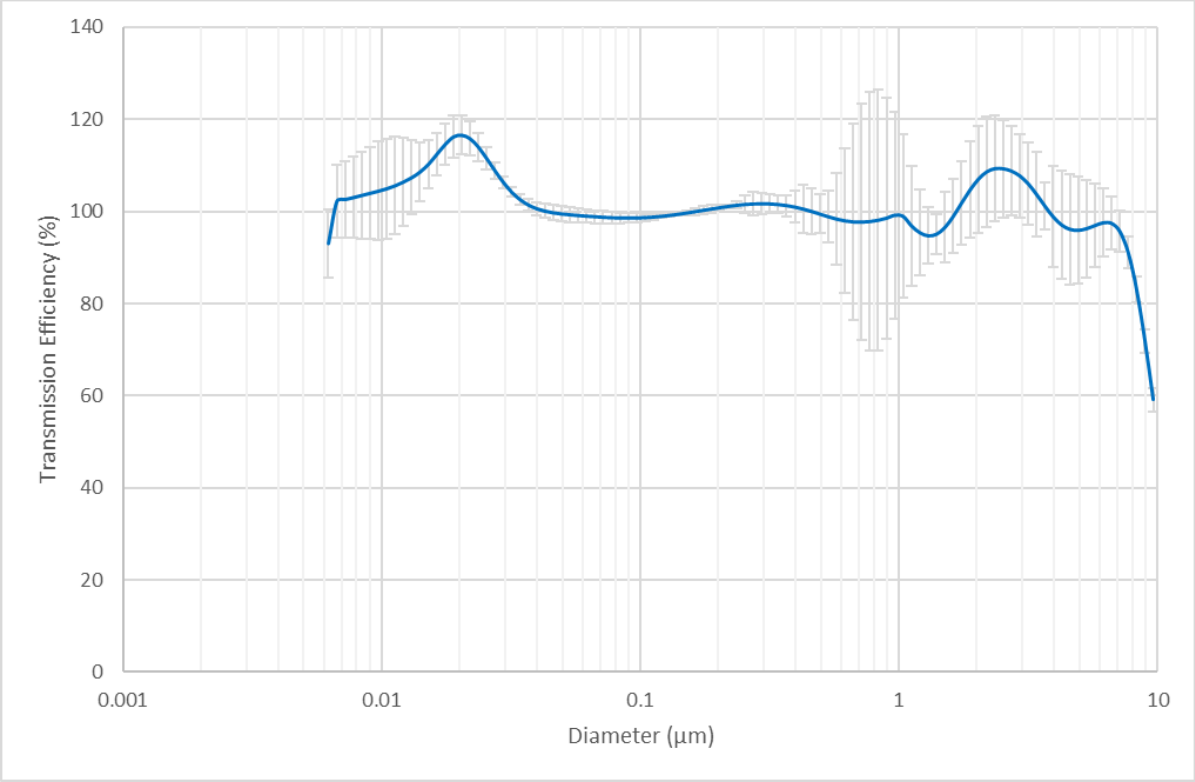

The overall performance was largely as expected from transport efficiency calculations (Figure 4-8). Particle efficiency was effectively 100% for the diameter range of interest. There was a decrease to around 60% at the largest particle diameters as would be anticipated from sedimentation in the horizontal tunnel. The under-sampling above ~5µm will impact the accuracy of PM_{10} determination but have minimal impact on particle number.

In some cases the calculated efficiency is above 100%. Measurement uncertainties were combined to give relatively large uncertainties in the final calculated efficiency. There was greater measurement uncertainty at those diameters where fewer particles were available to measure as would be expected. The error bars indicate where this is the reason for efficiencies above 100% (particularly at diameters greater than about 1 µm. At smaller diameters (< 40 nm) there also appears to be a degree of anisokinetic over sampling in the prototype system leading to larger calculated efficiencies.

4.2 FINAL LABORATORY EVALUATION

4.2.1 Transport efficiency through final transport system

The final sampling transport system consisted of the sampling tunnel studied at the prototype stage combined with a sample transfer line which connected the tunnel to the sampling location at the wheel. The transfer line was a 5 m length of 250 mm internal diameter conductive tubing. For the purpose of transport efficiency testing the line was arranged to include bends and vertical sections that were typical of the configuration used when routing it through the vehicle at final installation (Figure 4-9).

Figure 4-9: Schematic of sample tunnel and instrumentation

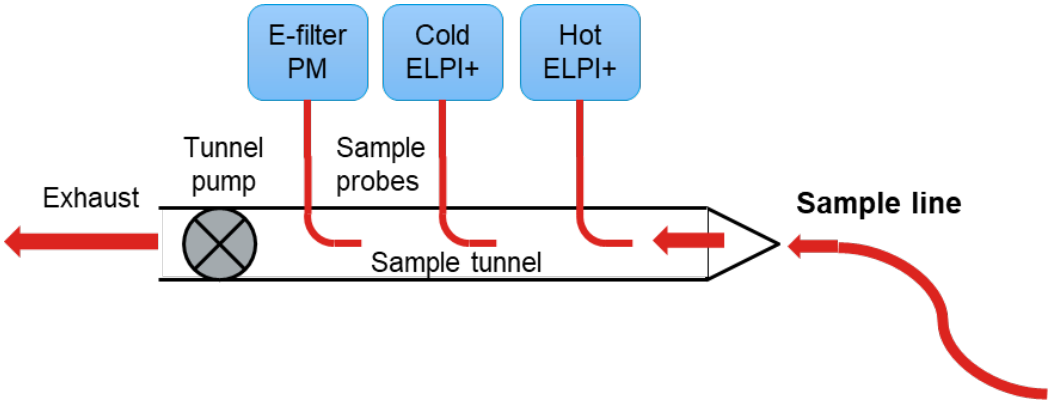

The system was designed to operate at a tunnel flow rate of 300 l min^{-1} to facilitate isokinetic sampling by the ELPIs. The flow was also towards the top end of what could be achieved with the pumps operating entirely on battery power. The portable power supplies had to run the sample tunnel pump, the supply pump for the brake enclosure (which also had to overcome the resistance of a high efficiency filter to generate the particle free air required) and the pumps for each individual measurement instrument.

The transmission efficiency testing performed on the prototype sampling tunnel (section 4.1.5) was repeated on the entire system. As before, the two fully characterized ELPI units were used simultaneously to measure the up and downstream particle size distributions, whilst challenging the system with a broad polydisperse distribution of mini-CAST generated soot particles and coarse test dust.

Figure 4-10: Particle Transmission through the final sampling system at 300 l min^{-1}.

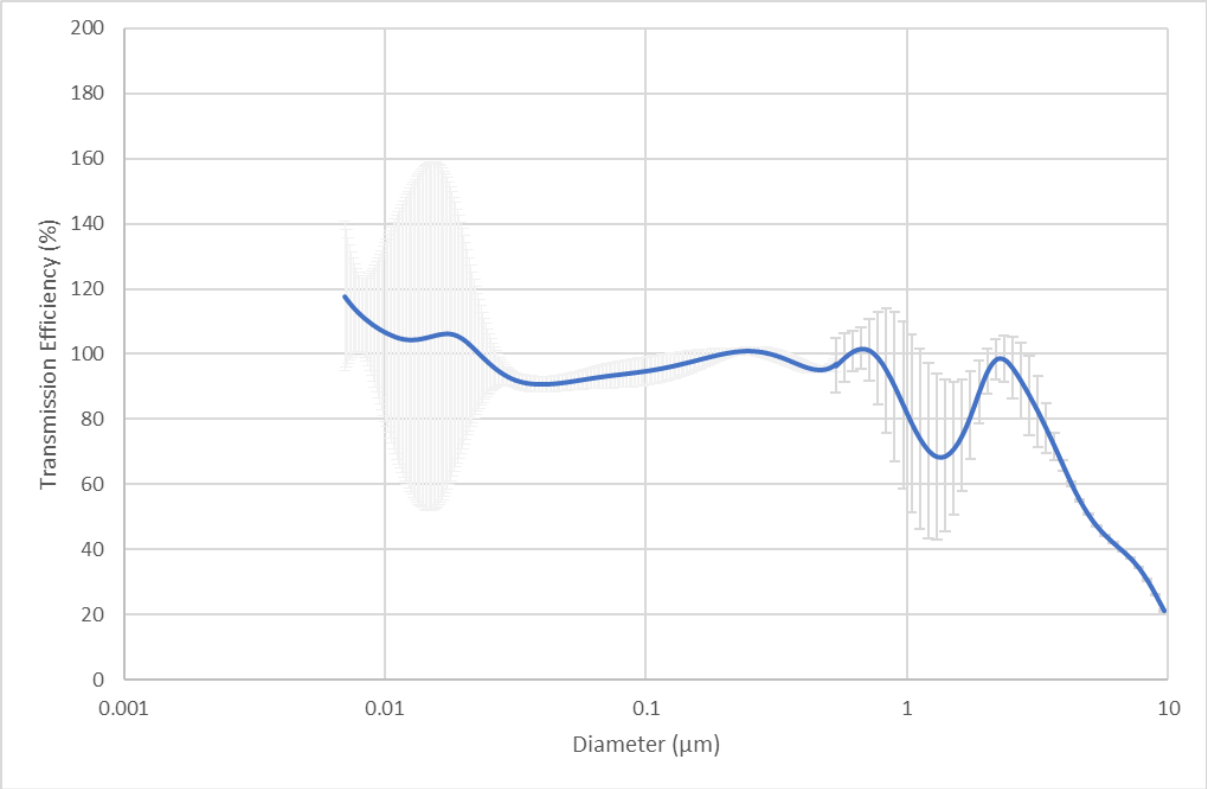

Particle efficiency remained high across the wide diameter range of interest (Figure 4-10) confirming the suitability of the system for the in-vehicle testing. There was greater measurement uncertainty at those diameters where fewer particles were available to measure as would be expected. There was a decrease in efficiency to around 20% at the largest particle diameters, accompanied by a general reduction in efficiency at diameters greater than 1 µm. This is to be anticipated from the addition of the sample transfer line with the associated opportunities for additional particle deposition.

Similar measurements were repeated at a tunnel flow rate of 200 l min^{-1} to confirm performance at a lower sampling flow rate (Figure 4-11). Overall transport efficiency was very similar to that measured at 300 l min^{-1} with only the very smallest hint of lower efficiencies at larger particle diameters. This provided confidence for using the system at the lower flow rate should such a compromise by desirable in practice.

An additional set of measurements were undertaken at a tunnel flow rate of 100 l min^{-1} (Figure 4-12). A significantly different transmission efficiency profile was obtained under this condition. None of the coarse aerosol was detected by the downstream ELPI. The data reported in Figure 4-12 shows the profile from the mini-CAST generated soot particles, with high measurement uncertainty at diameters greater than 1 µm due to the limited particle numbers available. The inclusion of the sample transfer tube was enough to prevent the coarser particles from reaching as far as the sample tunnel. The system remains suitable to measure particles smaller than 1 µm but anything larger is being effectively removed by the sampling system at this tunnel flow rate.

Figure 4-11: Particle Transmission through the final sampling system at 200 l min^{-1}.

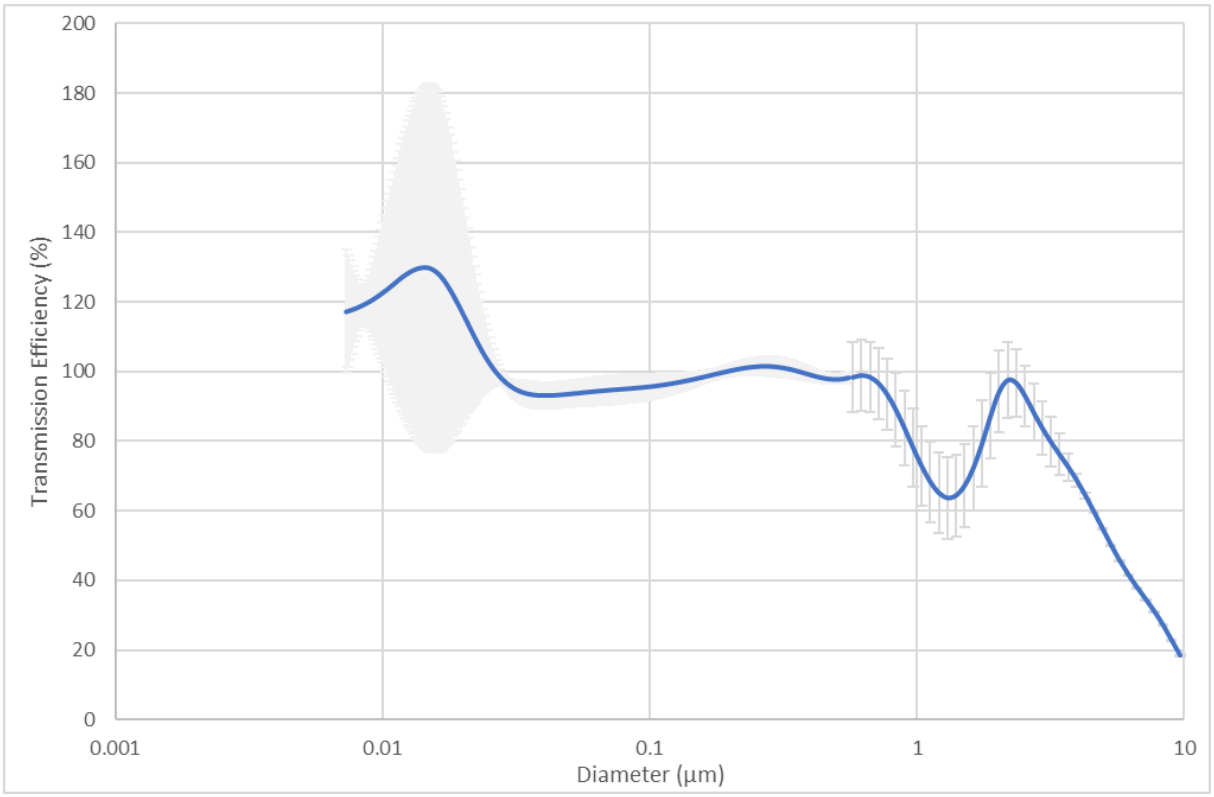

Figure 4-12: Particle Transmission through the final sampling system at 100 l min^{-1}.

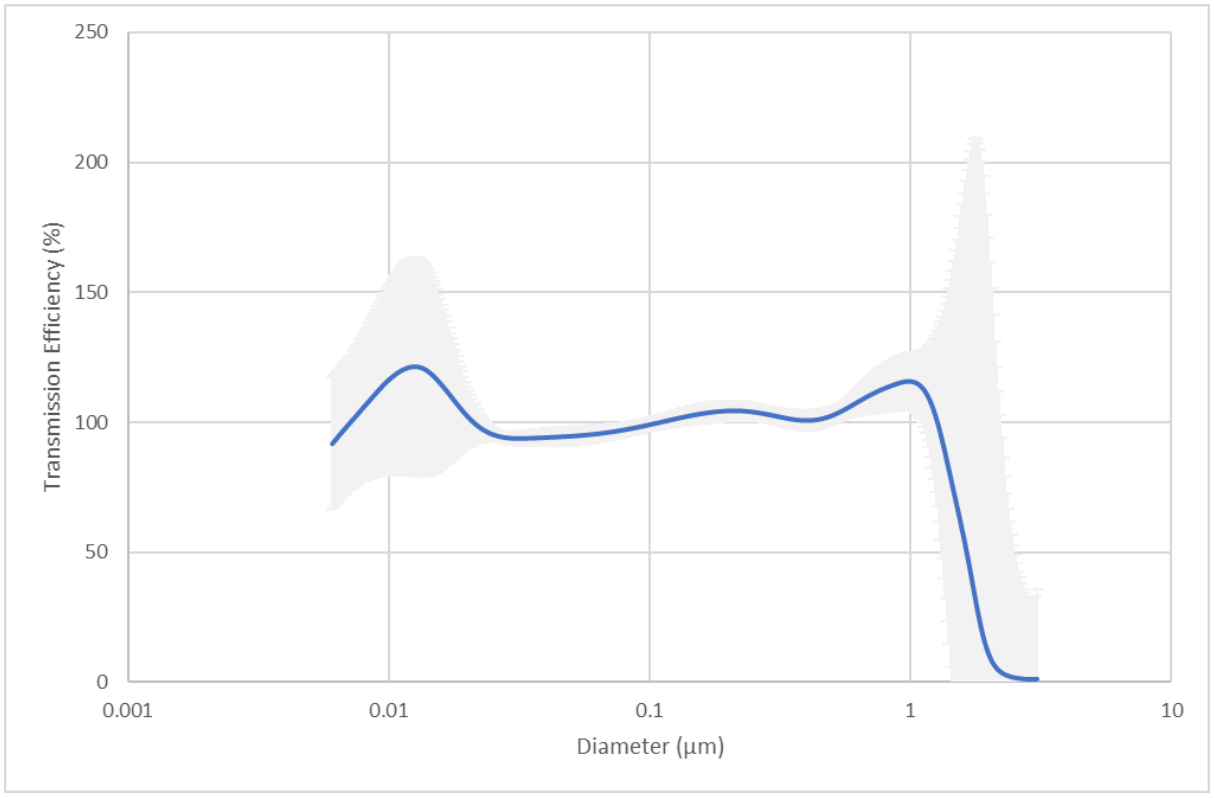

5. IN-VEHICLE TESTING AND VALIDATION PHASE

5.1 SYSTEM INSTALLATION AND OPERATION ON A LIGHT-DUTY VEHICLE

The prototype system evaluated in the laboratory was further configured to enable installation on a light duty vehicle and safety checks undertaken. The following sections provide details on the design of the individual components of the brake and tyre wear measurement system.

5.1.1.1 Test Vehicle#1: VW Caddy

The first test vehicle (Figure 5-1), used for testing front-wheel enclosures, was a diesel VW Caddy van, nominally “Caddy”. On receipt the vehicle was subjected to an MOT test and more rigorous Ricardo internal safety check. This included validating that the existing brake pads and discs were suitable for the test programme.

The vehicle was originally equipped with 16” wheels, but these were exchanged for 18” wheels (Figure 5-2) to provide greater space for the development of sampling for both brakes (accommodating enclosures) and tyres. It should be noted that the larger 18” wheels will allow better energy dissipation than 16” wheels and so particle emissions may have been higher if the original wheels had been employed.

Figure 5-1: VW Caddy van with original 16” wheels

Figure 5-2: VW Caddy fitted with 18” wheel

The 18” wheels were equipped with part worn – approximately 7000 mostly motorway miles - 225/40 R18 tyres (Table 5-1) taken from the vehicle of a Ricardo employee. These tyres can be considered fully run-in and representative.

Table 5-1: 225/40 R18 Tyre Specifications

Tyre Specification	Explanation
225	Width of the tyre measured in millimetres
40	Tyre profile; tyre height as percentage of tyre width
R	Radial tyre
18	Diameter of the wheel rim measured in inches

Specifications for the Caddy can be found in Table 5-2 below.

Table 5-2: Properties of the VW Caddy Test Vehicle

Transmission	Manual transmission, 5 forward gears, front wheel drive
Engine capacity (cc)	1598
Fuel type	Diesel
Gross Vehicle weight (kg)	2310
CO_2 emissions (g/km)	149
Peak power (kW)	55
Front Brakes	Vented disc
Date registered	28 Oct 2014

5.1.1.2 Test Vehicle 2: Audi A4

The second test vehicle was an Audi A4 estate. It was tested on the chassis dynamometer with an enclosure fitted to the rear right-hand wheel but with the majority of the sampling and measurement equipment and particle dilution tunnel (PDT) installed on a trolley as described in 5.1.7 (Figure 5-16).

Figure 5-3: Second test vehicle on dyno with external measurement system

Power was supplied from the mains, although battery packs were used to allow the instruments to be powered up and prepared before moving into the test chamber.

Table 5-3: Properties of the Audi A4 Test Vehicle

Transmission	Manual transmission, 6 forward gears, front wheel drive
Engine capacity (cc)	1798
Fuel type	Petrol
Gross Vehicle weight (kg)	2060
CO2 emissions (g/km)	141
Peak power (kW)	125
Rear Brakes	Solid disc
Date registered	08 Oct 2015

5.1.2 Brake sampling

The sampling approach selected adopts an enclosed brake, with sample air extracted for analysis replaced with filtered air entering the enclosure, the air flow through the enclosure also providing necessary cooling. This requires an enclosure around the brake being sampled with a sample line to the particulate measurement system, and a means of providing filtered air into the brake enclosure.

The brake enclosure is also an essential component for tyre testing since it isolates any brake emissions of that wheel from the tyre sampling system. Therefore, the brake enclosure must be present for tyre emissions sampling, with filtered airflow provided for cooling and exhausted away from the wheel, although measurement instruments for the brake emissions may not be present.

5.1.2.1 Brake enclosure design

There are challenges to the practical implementation of enclosing the brake, including:

- A non-rotating (static) element is required around the calliper, and to provide connections for the sample and inlet pipes.
- The wheel is rotating and therefore there must be a separation between rotating and non-rotating components.
- Clearances are tight between the calliper and the inside of the wheel rim and spokes (including balance weights), and between the brake components and vehicle suspension components.

- Rotating components must be balanced for safety.
- The safe operation of the brakes must not be inhibited including free movement of the calliper, integrity of the brake hose, and adequate cooling airflow.
- Sample and air pipes must be routed to avoid contact with vehicle body, suspension and powertrain components, and flex easily as the wheel moves relative to the vehicle body due to suspension travel and (if a front wheel) steering. The pipes must not inhibit such movement, nor be damaged by it.

The enclosure therefore needs both non-rotating (static) and rotating components, and consideration was given to providing a sealed interface between them. However, not only are there engineering difficulties in achieving this given the rotational speeds and necessary robustness, but the sliding contact surfaces of a rotating seal were also considered a risk of particles being emitted from friction and/or lubricant. A complete air-tight seal of the brake enclosure was found to be impractical in any case, since there must be some clearance to the brake line. Instead, clearances at the interface of rotating and static components would need to be as small as practical, and the sampling volume flow rate set to be lower than the inlet airflow. In this way leakage occurs out of the brake enclosure rather than into it, and its magnitude is understood.

Several approaches were identified for the design of the brake enclosure, which were refined into three basic options with differing interfaces of static and rotating components, as illustrated schematically in Figure 5-4. These design approaches are:

A. To seal the front face of the wheel using the wheel itself as the rotating outer enclosure, and construct a static inner enclosure with the interface between it and the wheel rim.
B. To construct a static enclosure around the brake, with the interface between the static enclosure and the rotating wheel hub.
C. To attach the outer part of the enclosure to the wheel, with which it rotates, and construct a static inner enclosure, with the interface between the static inner and rotating outer enclosure elements.

Figure 5-4: Brake design options

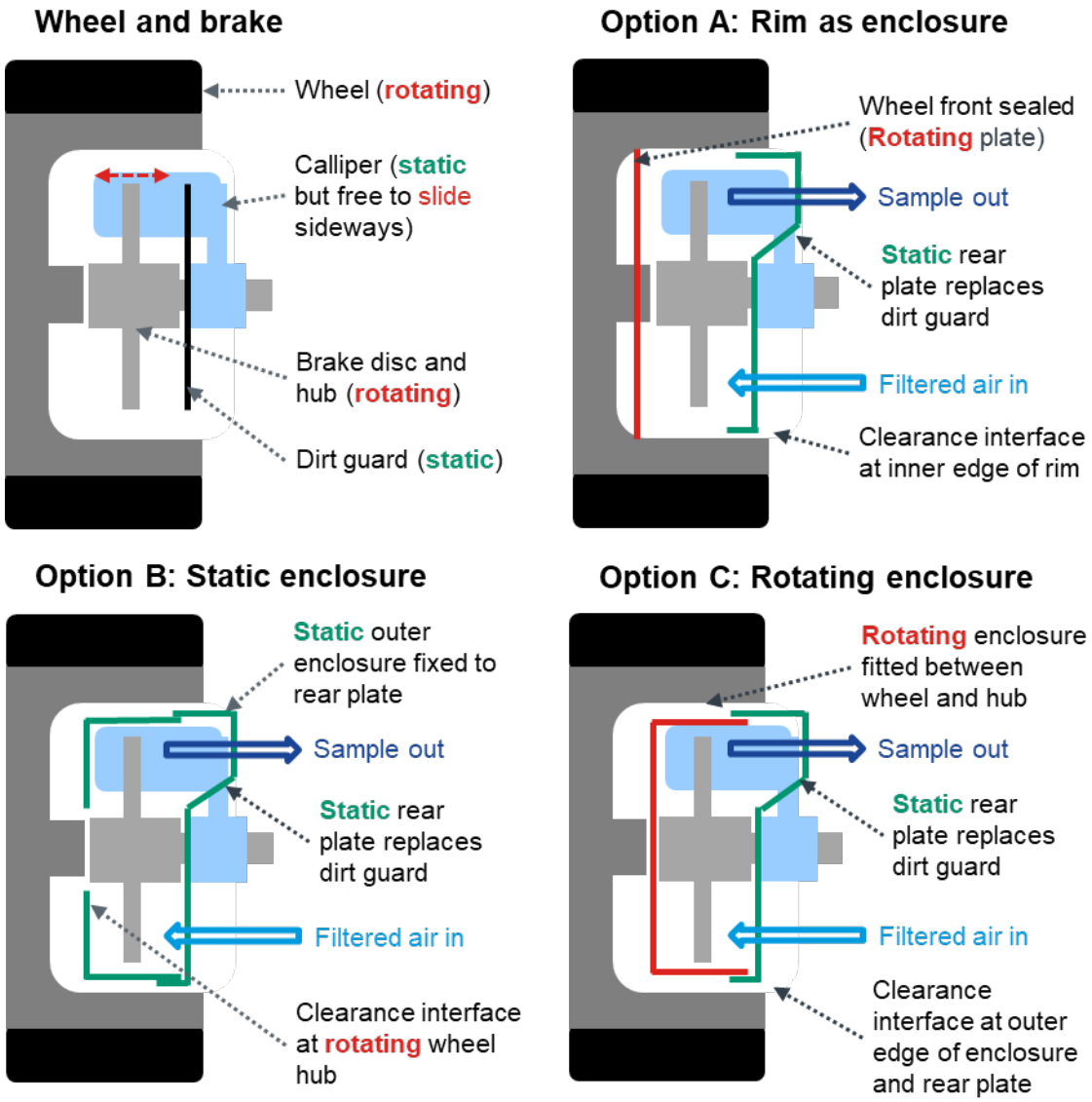

Each design option has its merits and demerits, especially when considering their ability to be applied to different vehicles. For example:

- Calliper to wheel rim clearance: Design option A requires the least clearance around the calliper[4] but designs B and C require adequate clearance between the calliper and the inside of the wheel rim and to the spokes for the internal enclosure.
- Ease of installation: Design options B and C have the potential to utilise more standardised prefabricated components for the enclosure and potentially the rear plate, whereas design A could be more intrusive to the vehicle since a wheel must be modified, and requires that the rear plate design is adapted to the wheel fitted.
- Volume: Design options B and C allow a slightly smaller volume to be enclosed which may reduce the volume flow of air needed.
- Cooling: The separate enclosure with thin metal walls using in options B and C provides a large surface area to help radiate heat, with a little air space between the enclosure and the wheel, whereas in option A the thick wheel rim surrounded by the tyre and its hot air may limit the cooling ability.

[4] The inner of the wheel rim usually tapers such that there is more clearance at its inner edge than at its centre or near the spokes, and the calliper often protrudes further out than the face of the wheel hub with the wheel spokes shaped around it.

- Leakage: Design option B has the clearance interface between rotating and static parts at the wheel hub, providing the shortest length of clearance, whereas options A and C have the clearance at the outer edge leading to a longer clearance interface and potentially greater air leakage and inlet airflow requirement. Also, the larger particulates may concentrate towards the outer edge due to centrifugal force.

Design option A was selected for the initial installation since with the least requirement for clearance it was considered applicable to the widest number of vehicles. However, to allow the other enclosure options to be evaluated, the test vehicle was fitted with larger wheels (and lower profile tyres) to increase clearance between the calliper and the wheel rim (See section 5.1.1.1).

5.1.2.2 Brake enclosure fabrication: design A

The front face of the wheel is closed using an aluminium disc cut and shaped to fit snugly into the wheel, around the hub fixing, and sealed to the wheel hub and rim, as seen in Figure 5-5, the wheel then being rebalanced by a tyre fitter.

Figure 5-5: Brake enclosure design option A: Wheel face sealed with an aluminium disc

The static inner enclosure is fabricated to fit in place of the brake disc guard, which would normally fit close to the inner side of the disc and uses the same mountings. It consists of a circular plate which just clears the inside of the wheel rim, with a cut-out to clear the calliper which is covered by a shaped pocket bolted to the plate, and a gap for the brake line to pass through safely. A deep lip protrudes from just inside the outer edge of the plate into and just clearing the wheel so that the clearance gap between the rotating wheel and the static enclosure is a narrow passage approximately 2 mm wide and 15 mm deep, improving the sealing effect, as well as providing rigidity to the plate.

Two ports are provided in the static part of the enclosure: one connects to the inlet air hose, and as space allowed an elbow inside the enclosure directs the air onto the edge of the disc; the other connects to the outlet sample hose. The ports were positioned with the inlet “upstream” of the calliper and the sample “downstream” for forward rotation of the wheel, and so that the flexible pipes connected to them cleared suspension and engine components. The two flexible pipes were routed in a large-radius curve forming a “?” shape to where they entered the vehicle, and supported by brackets under the vehicle, so that they could freely flex in the vertical plane as the suspension moved and twist and slide in the horizontal plane as the wheel steered.

The inner part of the enclosure, as fabricated and fitted to the test vehicle, is shown in Figure 5-6, with the wheel removed. Visible in the pictures is the rubbing thermocouple in contact with the brake disc, a thermocouple was also fitted into one of the brake pads but only the cable is visible. The cables exit the enclosure with the brake hose.

Figure 5-6: Brake enclosure design option A: Static inner brake enclosure.

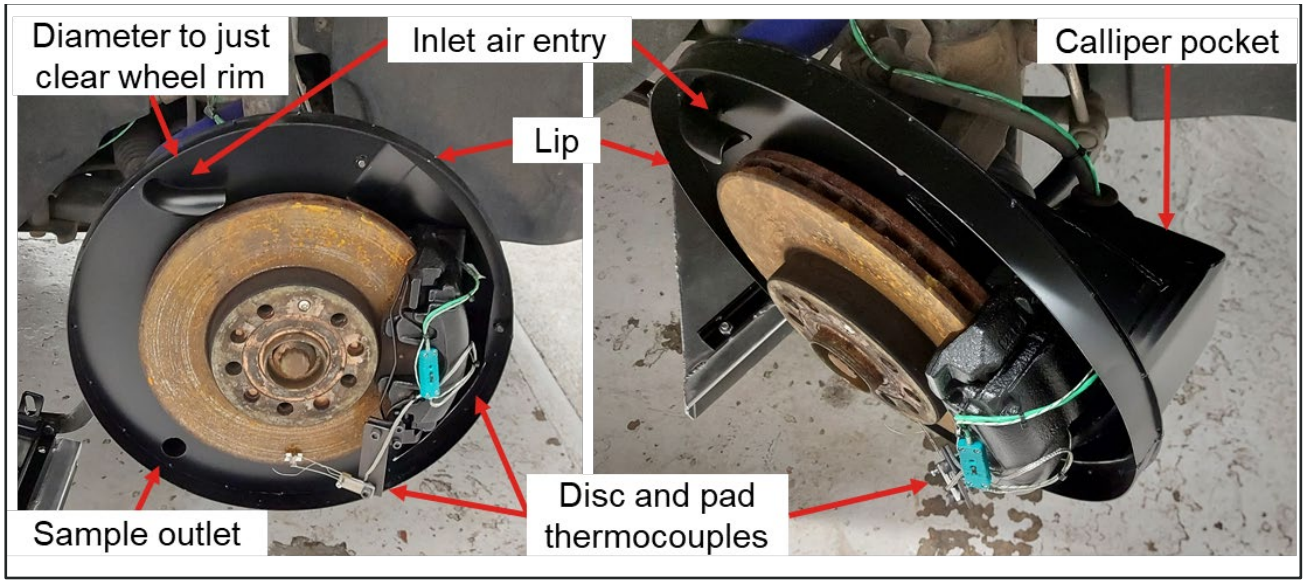

Brake enclosure design option A was also used for the second test vehicle, and Audi A4. In this case the rear brake was chosen, which reduced the complexity of the rear plate of the enclosure slightly and meant the air and sample hoses had only to accommodate suspension movement, not steering. The wheels were not changed as they were already large enough, and their offset combined with a smaller rear brake calliper allowed a flat disc to be used to seal the front of the wheel. This vehicle was only used for dyno tests and so the measurement equipment was mounted on a trolley separate to the vehicle rather than on-board, hence the sample and air hoses were routed to the rear of the vehicle rather than into the body of the vehicle.

Figure 5-7: Rear brake enclosed using design option A for the second test vehicle

5.1.2.3 Brake enclosure fabrication: design B

A single-piece outer enclosure assembly was designed to fit within the wheel and clear the brake calliper and spun from aluminium to produce a thin-walled concentric “bowl” shape, as shown in Figure 5-8.

Figure 5-8: Single piece spun aluminium enclosure for designs B and C

For design option B the centre of the spun enclosure was cut out to clear the wheel hub with a small gap, while the depth was set to clear the inside face of the wheel when touching the rear plate, as shown in Figure 5-9. The rear plate of the enclosure was the same as used in design option A, with the same pocket to clear the calliper and the air entry and sample outlet pipes in the same location. With the design of this enclosure the diameter of the rear plate could be smaller to match that of the spun outer enclosure, but for convenience it was not trimmed. The spun enclosure was fixed to the rear plate and provided clearance to the wheel hub, and the unmodified wheel attached over the enclosure as normal.

Figure 5-9: Brake enclosure design option B (static)

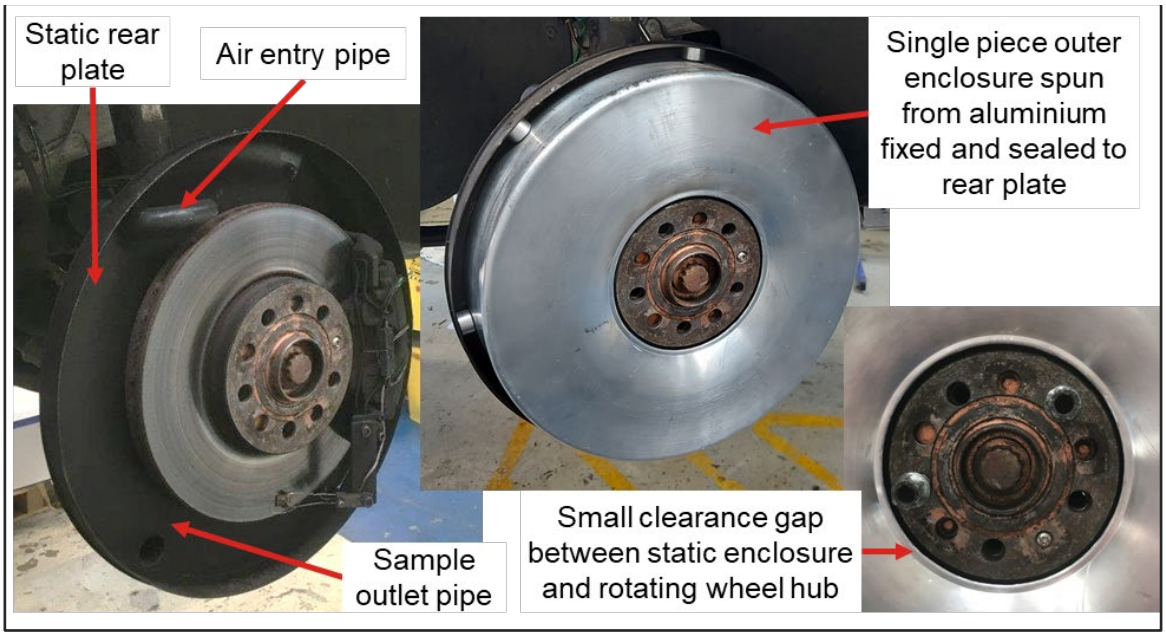

5.1.2.4 Brake enclosure fabrication: design C

The same single-piece outer enclosure design as used in option B (Figure 5-8) was used to form the rotating part of the enclosure. Rather than being cut to clear the wheel hub, it is fitted to the front of the hub with holes

machined for the wheel studs to pass through as seen in Figure 5-10. In this way it is clamped between the wheel and the hub and rotates with them, since the spun aluminium enclosure is very thin (approx. 2 mm) there was no need for longer studs and the impact on the wheel offset was negligible. The depth of the enclosure was trimmed to just clear the static rear plate, which was the same as that used in design options A and B.

Figure 5-10: Brake enclosure design option C (rotating)

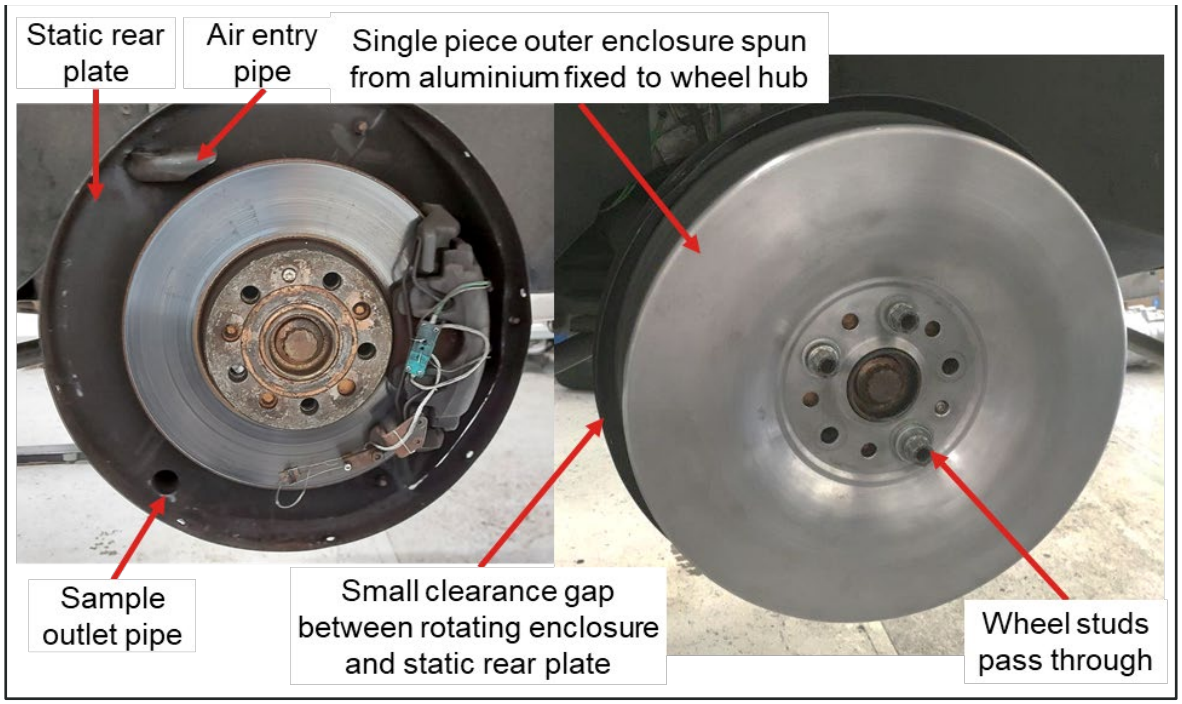

5.1.2.5 Air handling

The brake enclosure needed to be supplied with filtered air to replace that being sampled from the enclosure, providing excess air to allow for leakage since, as noted in Section 5.1.2.1, it would not be practical to fully seal the enclosure, and to provide adequate cooling to the brake. An air flow meter was necessary to account for the leakage from the enclosure. The filtered and metered air would need to be fed into the brake enclosure via a flexible pipe of 25 mm diameter and around 3 m in length. The need to provide the filtered air on-board the vehicle to allow on-road testing created challenges:

- The space and weight limitations inside a moderate size light-duty vehicle.
- The power demand given the significant power requirement of the necessary sampling equipment and pumps.

For these reasons, a lightweight and low power air handling system was created using two axial air fans feeding into two high-efficiency particulate absorbing (HEPA) filter boxes, the output from both being ducted into the flexible pipe via the air flow meter. In use this system proved capable of delivering around 180-190 litres/minute of air into the brake enclosure. This was restricted by the ability of the axial fans to overcome the restriction of the pipe, and future testing should consider improving the airflow while reducing the bulk of the system, without significantly increasing weight or power consumption.

The HEPA filter boxes are relatively bulky but fitted on one side of the test vehicle with the inlet to the fans at the rear, one of the rear doors of the van being fixed partly open during testing to allow fresh air to enter. However, the second test vehicle was only tested on the dyno, so the air system was mounted on castors to be fitted externally to the vehicle for the tests. Figure 5-11 shows the air system outside of a vehicle, the footprint including the fans, filters, and flow meter being around 1.8m long and 0.6m wide.

Figure 5-11: Filtered air system for brake enclosure

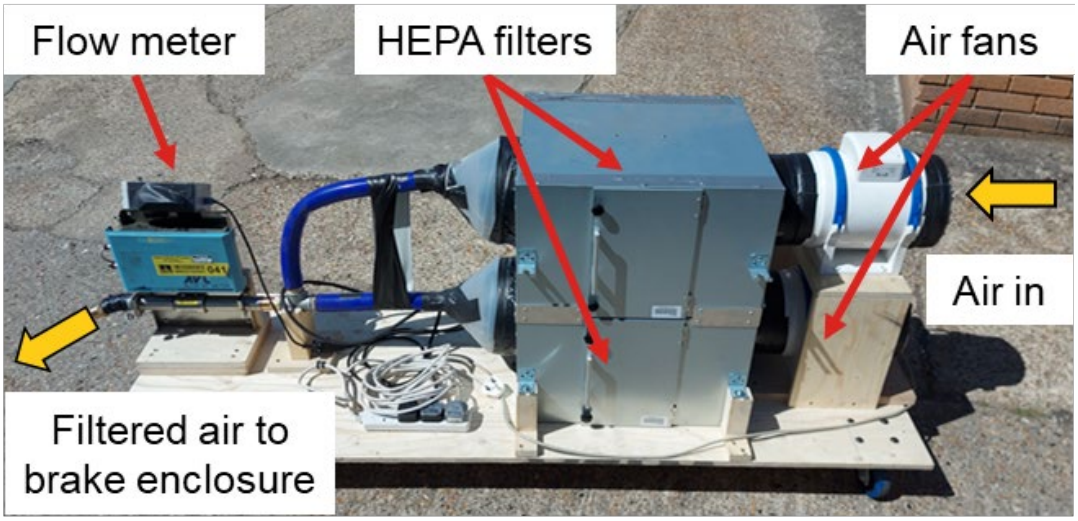

5.1.3 Tyre sampling

The tyre sampling approach selected uses an open duct (scoop) to draw sample from behind the tyre-road contact patch into the measurement system. The area of the opening is limited to ensure a reasonable flow velocity at the entry within the flow capability of the measurement system, particularly the pump drawing sample through the tunnel, and the constraints of equipment size and power demand on-board the vehicle. The tyre sample duct and its mounting arrangement is shown in Figure 5-12.

Figure 5-12: Tyre particulate sample duct

The tyre sample duct was fabricated from aluminium sheet for light weight and corrosion resistance. At the front the inlet was sized at 350 mm wide to be slightly wider than the tyre, and 7 mm high to keep sufficient

entry velocity at around 300 litres/minute of sample flow. The duct increased in depth to 15 mm behind the opening and tapered in width along its outer edge to blend into the 25 mm sample hose at the rear. Tapering the outside edge also limited the protrusion of the duct and sample hose on full right-hand steering lock.

The duct was mounted to a bracket which in turn was fixed to the rear of the wheel hub carrier, so that the duct position is fixed relative to the wheel and swings with the wheel as it steers. A complication was found due to the axis of the wheel steering rotation not being vertical but inclined rearwards (the castor angle) and the duct being mounted to the right of this axis, meaning that as the wheel steered left the duct swung right and upwards, and as it steered right it swung left and down. On sharp right-hand bends there was a risk of the end of the duct hitting the road, and this constraint set the minimum height at which the duct could be mounted. The maximum height was also limited by the floor of the vehicle when the suspension compressed, and because the duct was mounted angled with the opening downwards to minimise the entry of water and stones.

Within these constraints and the objective to sample as close as possible to the tyre-road contact patch the duct was fixed approximately 55 mm from the road surface and 5 mm behind the tyre. The duct was positioned so that the sampling direction was aligned with the contact patch, this resulted in an approach angle of ~ 20° to the horizontal. Even so, care had to be taken when driving on the road, particularly uneven surfaces on sharp right-hand bends, and speed bumps had to be avoided, or approached at minimum speed. As a precaution against injury or damage to others in the event of bracket failure, the duct was fitted with a safety wire attached to the wheel hub. The sample hose was routed from the rear of the duct into the vehicle to the sampling system via large radius S-curves, and through brackets, allowing movement with the suspension and steering movement, and via a hole cut into the floor.

As already noted, the brake enclosure with its air entry and sample exit also forms an essential element of the tyre sampling system. Containing the brake particulate emissions and piping them away from the wheel ensures the tyre measurement duct does not sample brake emissions from that wheel.

5.1.4 Ambient sampling

Sample probes for background ambient particulates were fitted to the front of the vehicle at three locations as shown in Figure 5-13:

- In the centre of the vehicle, just below the bumper/air-dam – **Centre**.
- In line with the right-hand tyre, just below the bumper/air-dam – **Right Upper**.
- In line with the right-hand tyre, a similar height as the tyre sample duct above the road surface (approx. 50 mm from ground level) – **Right Lower**.

Figure 5-13: Tyre background sampling positions

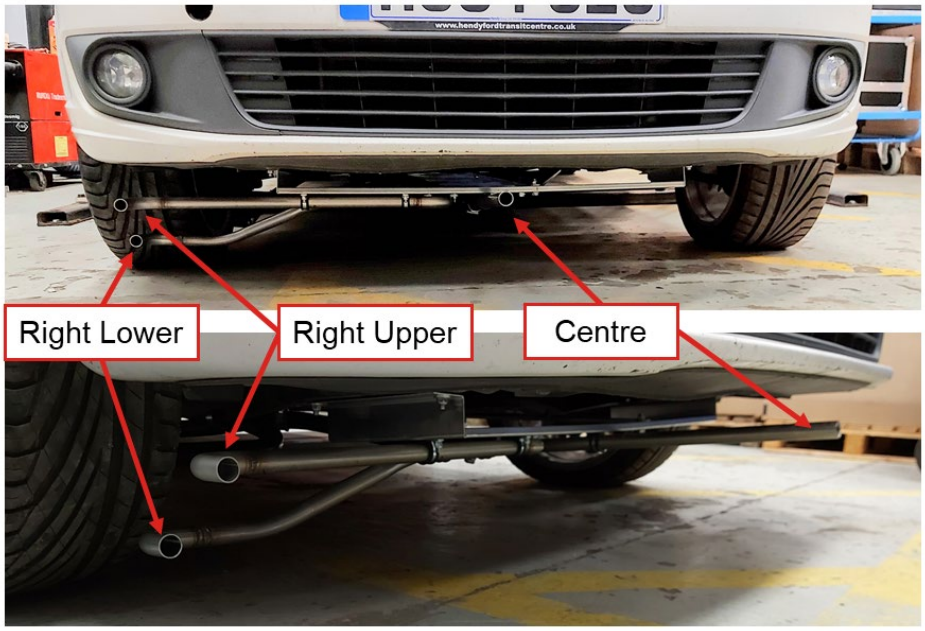

The sample probes each consisted of a 25 mm diameter stainless steel pipe mounted horizontally and in line with the vehicle, open to the front, and set 20mm behind the front of the vehicle for safety. A 25 mm inner diameter flexible sample pipe was connected to the rear of sample probe in use, and at the other end connected to the sample tunnel in the vehicle.

In practice it was found that the right lower sample probe was prone to grounding such as where left-hand bends combined with uneven road surfaces, a change in gradient, or a braking event, as well as fouling on speed bumps. This sample probe was removed after initial tests.

5.1.5 Instrumentation and measurement systems

In order to conduct on-road tests, the test vehicle needed to carry the sampling system and instruments for particulate measurements, plus the necessary additional instrumentation. A general layout of the sampling system and instrumentation is shown schematically in Figure 5-14. Logging is provided by a Dewesoft DEWE-43A which can acquire analogue, digital, and Controller Area Network (CAN) sources at high speeds, although just 10Hz was used in these tests.

Figure 5-14: Schematic of final sampling system and instrumentation

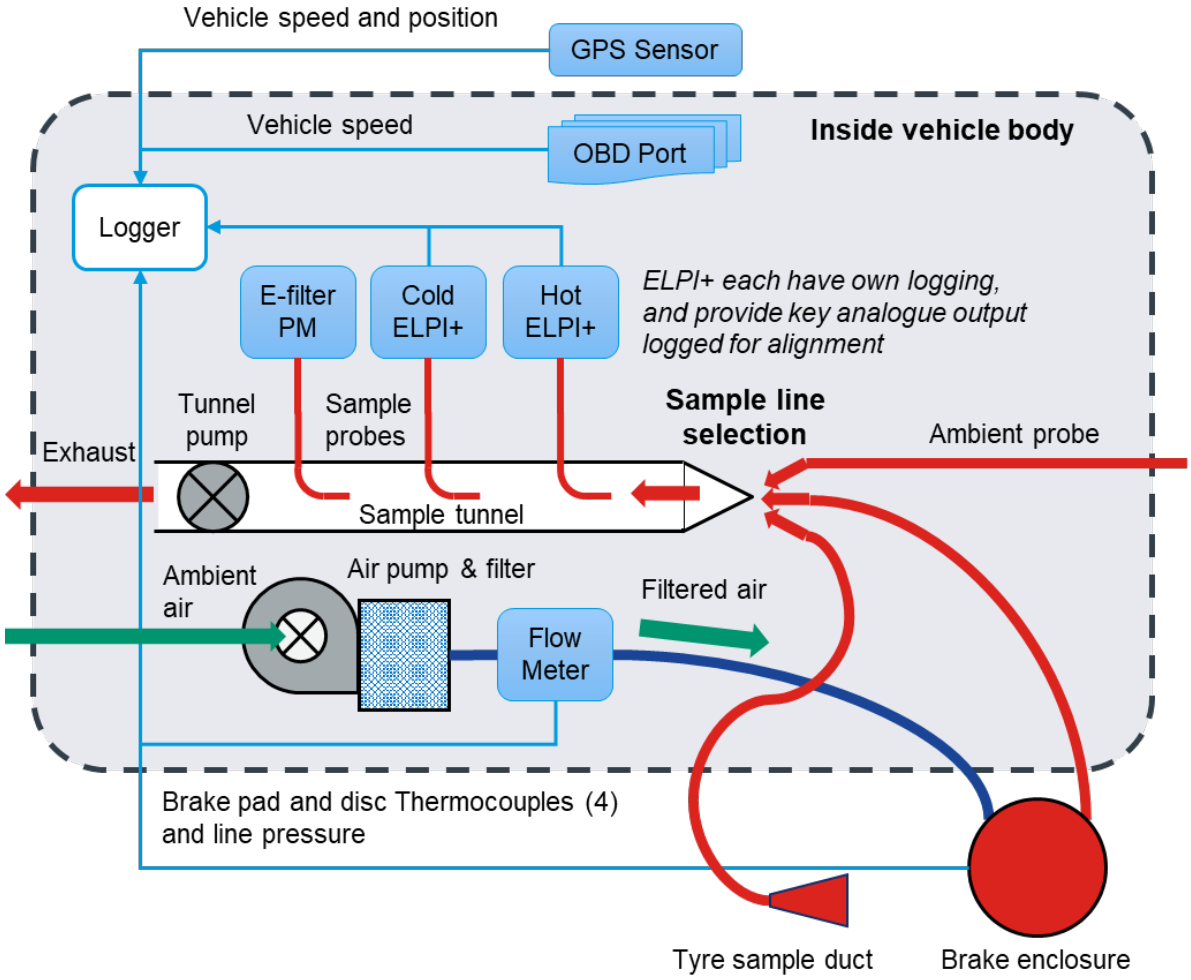

5.1.5.1 Particulate measurement instrumentation

A pair of Dekati ELPI+ analysers were used for real-time evaluation of particle number and size distribution (Table 3-1). One was run at ambient temperature (“cold ELPI”) to measure “total” solid plus volatile particles, the other (“hot ELPI”) was internally heated to 180°C, and sampled via a heated line to evaporate volatile particles and hence provided a measurement of non-volatile particles. The two ELPI+ were installed into the vehicle along with their sample vacuum pumps and controlling laptop computers. These have their own high-resolution logging which provided the full breakdown of particle size distribution but were also configured to provide an analogue output of total particles to be recorded by the Dewesoft logger for data alignment purposes.

The on-board Dekati eFilter (Table 3-1) measured particulate mass in real time, but also allowed a glass-fibre filter to be used to capture a total mass weight. The e-Filter recorded data to a memory card and had a glass-fibre filter inserted for each test.

During chassis dynamometer testing an external Horiba MEXA-2100SPCS Solid Particle Counting System (SPCS) was also used, this recorded data separately. This system employs the principles of the measurement systems designed for regulatory tailpipe emissions when sampling from a dilution tunnel, but is designed for raw exhaust sampling. In overview, heated dilution at 150°C and an evaporation tube at 350°C are employed to eliminate volatile particles and create a non-volatile particle metric that is enumerated by an integrated condensation particle counter[5]. Further detail is given in Section 5.2.4, lab-based equipment.

The three on-board particulate measurements all sample from the sample tunnel, which can be connected to any of the three sample lines to the brake enclosure, the tyre sample duct, or the ambient probe. Not shown in the figure, a fourth sample probe allowed the SPCS to be connected to the sample tunnel, though situated externally, during dyno tests.

5.1.5.2 Other instrumentation

The air flow into the brake enclosure was measured using an orifice type meter with range calibrated up to 548 litres/min. This provided an analogue output recorded by the Dewesoft logger.

The brake being measured, and the brake of the opposite wheel, were both instrumented for pad and disc temperature with specialist thermocouples being inserted into the brake pads, and set to slide across the surface of the brake disc. This allowed the temperatures of the brakes and discs to be compared between the enclosed brake and the unaffected opposite brake. A pressure sensor was fitted into the brake line (at the flexible brake hose to the wheel) to measure the brake fluid pressure, and so the braking force applied. The pressure sensor and thermocouples were recorded by the Dewesoft logger.

The Dewesoft logger also recorded vehicle speed and position on the road[6] using the satellite Global Positioning System (GPS) with a sensor antenna which was attached to the roof of the vehicle. The Dewesoft CAN interface was used to record vehicle On-Board Diagnostics (OBD) data via the OBD port, which included vehicle speed (available on both road or dyno) and ambient air temperature and pressure.

Finally, during road tests, a dash-camera was used to record video through the windscreen of the vehicle to gather qualitive information about the driving conditions, environment, and nearby vehicles, that might provide cause for any unusual measurements.

5.1.5.3 Ancillary equipment

In total, four air sampling pumps were fitted in the vehicle; the tunnel sample pump, vacuum sample pumps for each of the two ELPI+ instruments, and a pump to draw sample through the e-filter. These pump outlet vents were piped out through the rear door of the test vehicle. In addition, two air fans and HEPA air filters were used to provide air into the brake enclosure as described in Section 5.1.2.5, these must be running even when sampling from the ambient or tyre to provide cooling to the enclosed brake.

While the filtered air fans had been selected for their low power demand, the four sample and vacuum pumps drew between 400 W and 800 W each, with the heating system for the hot ELPI+ requiring a similar power. With the filtered air fans, logging instruments, and laptop computers, the total power requirement was found to be around 3.5 kW continuously, up to 4 kW while the hot ELPI+ was heating to a stable temperature, and with a higher peak on start-up of the pumps. The alternator of a typical car or van might provide 1 kW to 1.4 kW, depending on vehicle specification, although of course much of that power is required for vehicle systems (a cigarette lighter auxiliary output might be 120-240 W), so it was clear that an alternative source of power was required.

To meet the power demand and energy requirement EcoFlow Delta Max[7] lithium-ion battery packs were employed, which have an on-board inverter to directly power mains powered equipment through standard 3-pin sockets. Three packs of 2 kWh capacity and 2.4 kW peak load each were used, and the electrical load spread across them allowing for start-up peak demand. The batteries allowed about an hour of autonomy

[5] MEXA-2000SPCS series - HORIBA

[6] Since GPS data was invalid during dyno tests

[7] Specifications at https://uk.ecoflow.com/products/delta-max-portable-power-station

(between 95% and 20% charge) for road or track testing and took 1.5 to 2 hours to charge, while being relatively compact, and at 22 kg each, relatively low weight.

5.1.6 System Installation on the VW Caddy

The first test vehicle was a VW Caddy van, which although being of similar size and weight (and brake and tyre components) to a typical mid-size car, offered valuable extra space for the installation of the equipment. The use of a van had the additional advantages of a load bay separated from the driver's cabin by a bulkhead since the pumps proved to be noisy in use, and three large doors to access the equipment.

As outlined already, the key components were:

- The sample tunnel, which with hose entry and exit required at least 1.5 m of length, and needed space for the sample lines, and the e-Filter, which fitted directly to it.
- The two ELPI+ instruments. Although the ELPI+ instruments were relatively compact and rugged themselves, the heated stack for the hot ELPI increased the footprint and stood around 0.6m tall.
- Each ELPI+ needed a large, powerful, and heavy vacuum pump.
- The sample tunnel also needed a large pump, and a smaller pump was required for the e-Filter.
- The air handling for the brake enclosure (see 5.1.2.5) required two fans, two bulky filter boxes, a flow meter, and connection hoses.
- Two laptops were required for the two ELPI+ instruments.
- The datalogger input/output (I/O) hardware and its laptop.
- Three Li-Ion battery packs.

The installation considered the need for access to the instruments and battery packs while keeping the heavier components low in the vehicle and distributed across it, and for safety reasons ensuring all items were securely fixed to avoid movement or damage during driving, or in the event of an accident. Thus, the heavy pumps and batteries were fixed directly to the wooden floor of the van, as was the air handling system. A raised plywood bench was installed on which was mounted the tunnel and particulate measurement instruments, and a second plywood shelf provided a secure location for the ELPI+ laptops. The data logger was installed in the passenger footwell (to allow access to the vehicle OBD connection). The resulting installation is shown in Figure 5-15 through the three doorways of the van.

Figure 5-15: Measurement equipment installation in VW Caddy

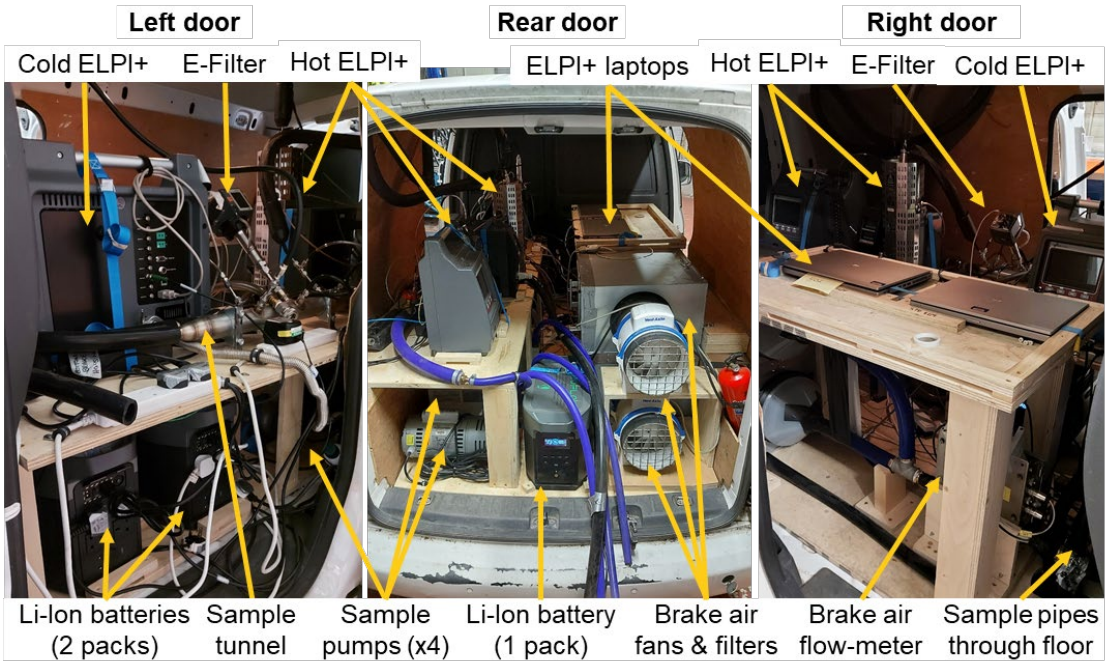

The sample hoses from the brake enclosure, tyre sample duct, and ambient probes, plus the filtered air to the brake enclosure were routed through a hole cut into the floor just behind the bulkhead. This allowed short and

safe routing of the hoses. One of the rear doors of the van was arranged to be securely latched in a partially open position of 100 mm. This allowed fresh cooler air into the air handling system fans just inside the door, as well as heat rejection from the equipment within the van, and venting of the tunnel and the sample pumps – which had their outlets piped through the door towards the road.

The vehicle was weighed using vehicle corner-weight scales both with and without equipment installed, the difference showed the total weight of the installed equipment to be approximately 270 kg, including the air system and batteries but excluding the wooden support framework, brake enclosure, and sample hoses.

5.1.7 System Installation for the Audi A4

The second test vehicle was an Audi A4 Avant, an estate car which offered reasonable space inside. It was clear that installing the necessary equipment inside the vehicle would be challenging and, for wider applicability in any further work, some of the components (such as the air handling system and sample pumps) would need future reduction in size. Since the testing was restricted to chassis dyno tests it was decided to mount the equipment onto trolleys which could be quickly connected to the vehicle once in the dyno. The trolleys allowed easier access to the equipment, and in general this approach would allow one set of instruments to be used on different vehicles without re-installation.

The sample tunnel, along with the particulate measurement instruments and their pumps, was mounted onto a 3-tier trolley, along with a battery pack allowing the instruments to be powered up and stabilised before the trolley was wheeled into the test chamber. The air handling system was mounted on a board fitted with castors which was easily moved into place alongside the vehicle. These are shown in Figure 5-16. The datalogger was installed in the vehicle with connections to the brake thermocouples and the vehicle OBD connector. The connection of the sample and air hoses to the trolleys, and the instrumentation between the trolleys and the logger, took just a few minutes.

Figure 5-16: Trolley-mounted sampling and measurement equipment for dyno testing only

5.1.8 Operational procedures

Given the range of measurement instruments and their operational requirements, a procedure to initiate and operate the instruments was established and documented ensuring their correct and repeatable operation. Broadly, this involved:

- Preparing and weighing filters in advance.

- Power up of all instruments, warm-up and stabilisation of the heated ELPI+.
- Zeroing of the ELPI+ sensors.
- Power up of the sample pumps and brake air supply.
- Checking the correct sample hoses are connected (for brake, tyre, or ambient) and flow rates and sample pressures are within expected range.
- Ensuring all instruments are reading correctly – including thermocouples, the GPS sensor and the OBD connection to the vehicle.
- Inserting a filter into the e-filter ready for the test.
- Configuring log-files ready to commence logging.

The procedure also covered the post-test activities including filter removal, collecting the data files, and battery charging where appropriate. The same procedure applied to both dyno tests and road or track tests with minor differences:

- The use of battery power or mains power.
- The GPS was not used when in the dyno – even if a signal was obtained there would be no movement. The OBD vehicle speed was used.
- The SPCS was only available for dyno tests.

5.1.8.1 Dyno tests

The Vehicle Emissions Research Centre (VERC) at the Ricardo Shoreham Technical Centre was used for vehicle dyno testing. The tests carried out on the vehicle dyno followed many of the conventional procedures, although procedures relevant only to achieving repeatable engine emissions were not necessary. For example, no pre-conditioning cycle was run prior to the tests, and procedures around charging of the vehicle battery were not relevant. However, the vehicle was prepared and checked in the usual way, fixed in place on dyno using the front and rear towing eyes, and the exhaust connected to the dyno extract. Exhaust tailpipe emissions were monitored to understand test repeatability only.

The instruments on-board the vehicle could be initiated while the vehicle waited in the soak area prior to the test to make efficient use of the time on the dyno, the on-board batteries keeping them powered up while the vehicle was moved. Once in place on the dyno as seen in Figure 5-17 the instruments could switch to mains power to remove the limitation of battery capacity. A connection was made to the SPCS, which is resident in the facility. The test cycle was followed by the driver as for a conventional emissions test, although gear selection was not specified since it had no bearing on brake or tyres.

Figure 5-17: The VW Caddy test vehicle on the Ricardo VERC dyno

5.1.8.2 Road and track tests

The test vehicle was garaged between tests allowing the battery packs to be charged, and instrument preparation to take place protected from the weather. The instruments were prepared while the batteries were connected to mains power, and when the test was ready to commence, they were unplugged. Vehicle and track tests were limited to around an hour by the capacity of the batteries. Since the equipment had to be distributed between the battery packs to keep the peak load (on power-on) within their limits the continuous load was not evenly balanced, and the test duration was limited by the battery with the highest continuous load. Where appropriate instruments could be started or stopped away from base – such as at the test track or end of the route – and the sample lines switched and/or filters changed between test runs, to maximise testing time.

On-road testing used local routes which could provide urban, rural, or high-speed road conditions, the routes are detailed in the next section. Track testing used a short private test track owned by Ricardo and adjacent to the Ricardo site. This track is intended for measuring “drive-by” noise and so is often referred to as the drive-by site. It provides a safe environment away from the public and other traffic to carry out low to medium speed manoeuvres, such as the braking tests described below.

5.2 TESTING AND MEASUREMENT SCOPE

5.2.1 Test plan and drive cycles

In order to explore the generation and magnitude of particle size distribution, number and mass of brake and tyre wear emissions, the testing element of the programme involved 4 parts:

- Background measurements: a brief measurement campaign was undertaken to explore background emissions sampled from the three potential locations. Background measurements were primarily aimed at tyre emissions because the design and function of the brake enclosure should inhibit the ingress of external aerosols. Occasional measurements of background from the brake enclosure, with the vehicle static, were taken to validate this assumption.
- Chassis dynamometer measurements: repeated measurements were made of a single ~42 minutes duration chassis dynamometer drive cycle. This cycle was constructed to contain aggressive braking events in order to increase the probability that sufficient particle emissions would be generated for measurement. The same cycle was used for both brake and tyre wear measurements.
- Urban road driving measurements: a ~20 km section of the urban part of a valid real driving emissions (RDE) route was driven. Test duration was approximately 45 – 50 minutes. This includes speed limits between 20mph and 40mph and both level and hilly topography. The same route was used for both brake and tyre wear measurements.
- Test track measurements: repeated braking events from moderate speeds (≤ 80kph) were conducted on the Ricardo “drive-by” test track. Both normal braking and emergency braking styles were considered. These data were used to study the repeatability of emissions between nominally identical braking events, the impact of increasing brake disc and pad temperatures on particle emissions and to enable the consideration of other factors such as the relationship between initial braking velocity and particle emissions.

5.2.1.1 Background Measurements

Tyre background measurements were made on three roads in the vicinity of Ricardo (Figure 5-18) using three different background sample probes, located to the front right or the front centre of the vehicle. Frontal locations were employed to avoid collecting materials thrown up from the road surface by the tyres, but these could not avoid sampling airborne background materials. Measurements of background were sampled and analysed exactly as if they were sample acquisitions, using both hot and cold ELPIs plus the eFilter, with vehicle data recorded using the Dewesoft logger.

Background measurements were collected from:

1. “A27”: loops on the main A27 from the Ricardo test track site via the cloverleaf, then heading west to the Lancing Manor roundabout and back. Three repeat measurements were made, one with each of the three sampling probes (centre, right upper, right lower).
2. “A283”: loops on the rural A283 from the Ricardo heading north from the test track, clover leaf towards Bramber Castle and back. Three repeat measurements were made, one with each of the three sampling probes (centre, right upper, right lower).

Additional measurements were made on a further road:

3. “A270”: a short eastbound urban trip towards Brighton. Measurements were made with one sampling probe (centre).

In addition, a static measurement, with the upper right sampling probe, was made at the A27 roadside.

Testing is summarised in Table 5-4.

Table 5-4: Summarised Background Testing

Ref YYYMMDD_HHMM	Sampling probe	Theme	Test details
20220330_1040	Ambient - Centre	Highway	A27: STC-Lancing-Cloverleaf, 3 laps, light traffic
20220330_1430	Ambient - Right Upper	Highway	A27: STC-Lancing-Cloverleaf, 3 laps, light traffic
20220330_1520	Ambient - Right Lower	Highway	A27: STC-Lancing-Cloverleaf, 2.5 laps, heavy traffic
20220330_1700	Ambient - Centre	Rural road	A283: STC-Steyning, 2 laps took 30 mins, traffic near STC
20220401_0940	Ambient - Right Lower	Rural road	A283: STC-Steyning, 2 laps, quiet traffic
20220401_1020	Ambient - Right Upper	Rural road	A283: STC-Steyning, 2 laps, quiet traffic
20220401_1330	Ambient - Right Upper	Urban	A270: STC-Shoreham to Southwick eastwards, little traffic. GPS failed. Sleet near end
20220401_1600	Ambient - Right Upper	Static background - traffic	A27: Lancing roundabout westbound layby (by crossing). Easterly wind

Figure 5-18: Roads around Ricardo Shoreham used for background sampling (map created in Leaflet (https://leafletjs.com/),map source © OpenStreetMap contributors https://www.openstreetmap.org/copyright).

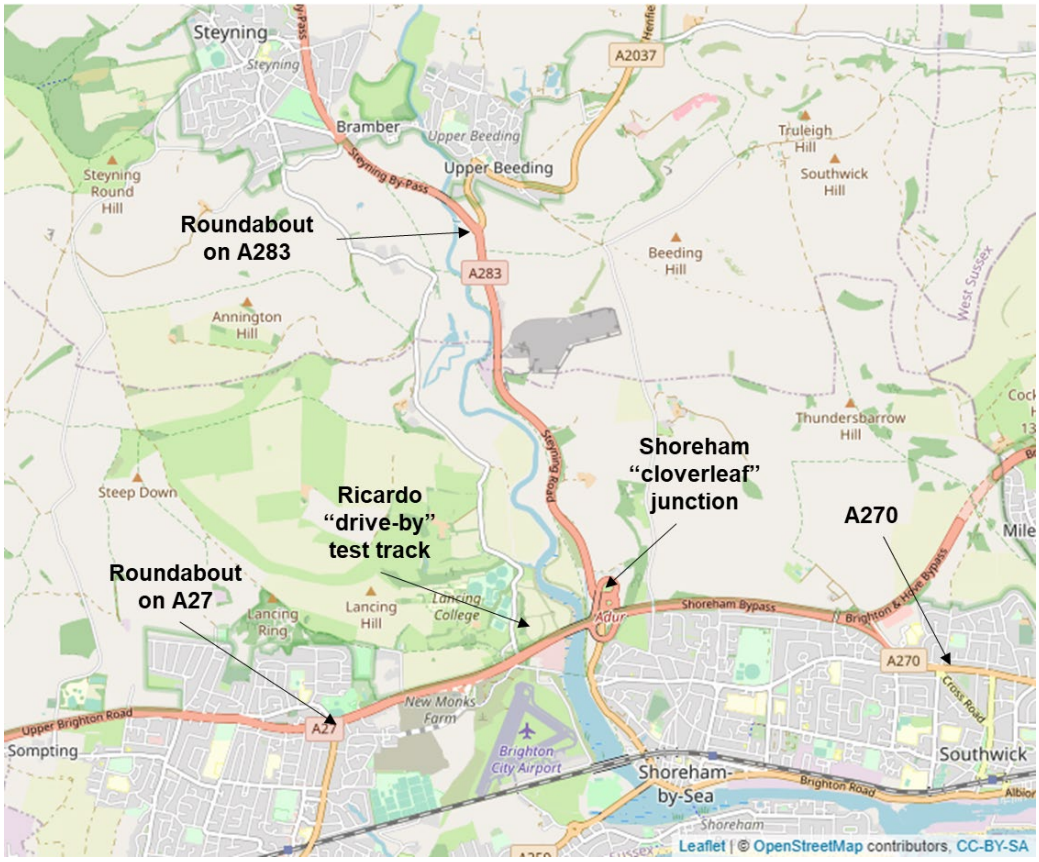

5.2.1.2 Chassis Dynamometer Measurements

Chassis dynamometer testing was undertaken using the Ricardo-designed ~42 minutes duration particle generation "PG-42" cycle. This cycle was created from sections of the WLTP brake dynamometer cycle (Figure 5-19), specifically Trip 10 (Figure 5-20) and from the Los Angeles City Traffic Test Cycle (LACT, Figure 5-21). In both cases the sections of the drive cycles that have previously demonstrated highest brake wear emissions were selected.

Figure 5-19: WLTP Brake Dynamometer Cycle

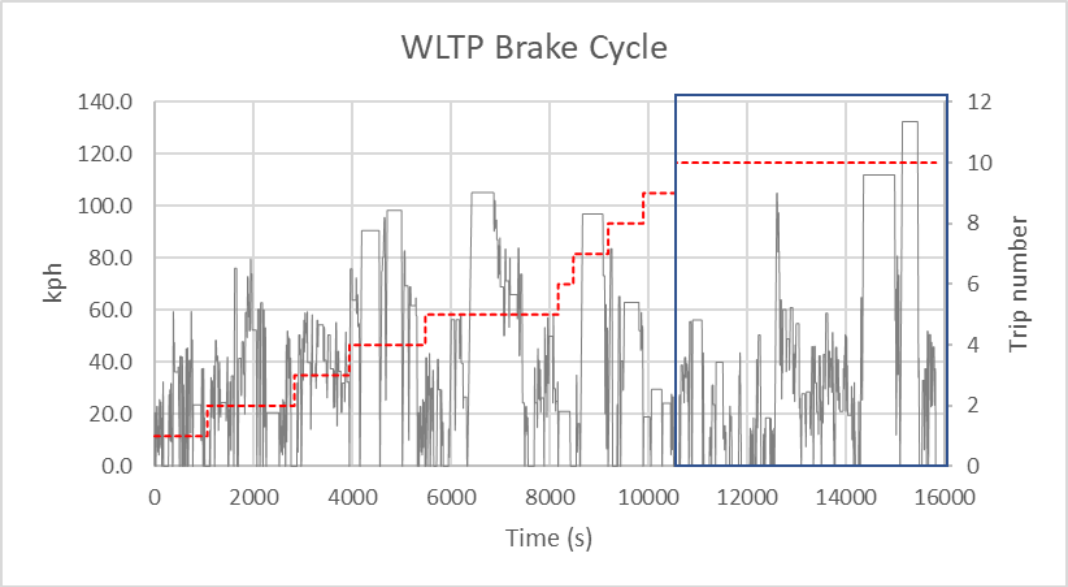

Figure 5-20: WLTP Brake Dynamometer Cycle, Trip 10

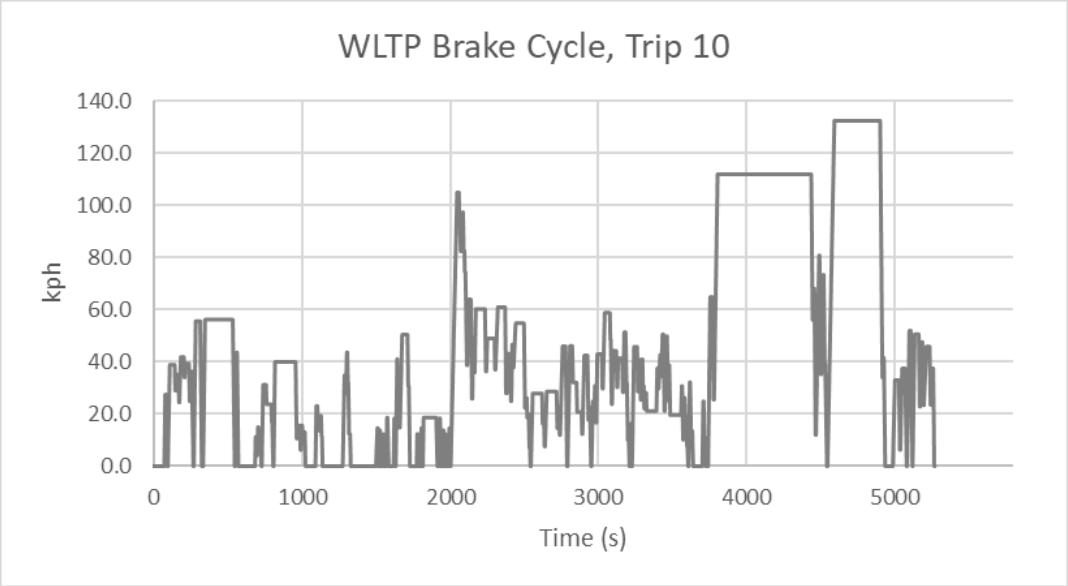

The PG-42 cycle was constructed using an approximately 1330s section of the LACT, followed by the ~1200s section of WLTP Trip 10 that contains two high speed accelerations and braking events (Figure 5-22) plus cruises for the consideration of steady state emissions. Steady state emissions may indicate cooling effects for brakes and cooling (post braking events) and heat-up (tyres warming on dyno roller effects) for tyres. The final PG-42 Cycle is shown in (Figure 5-23).

Figure 5-21: LACT Cycle (1335s orange section used in PG-42 cycle)

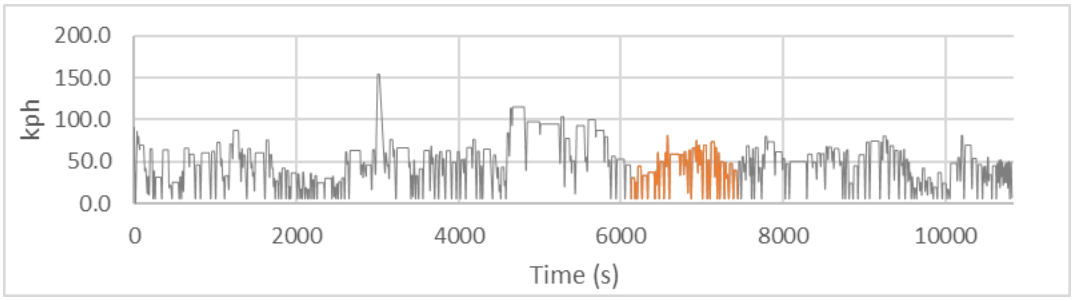

Figure 5-22: 20 minutes section of WLTP Trip 10

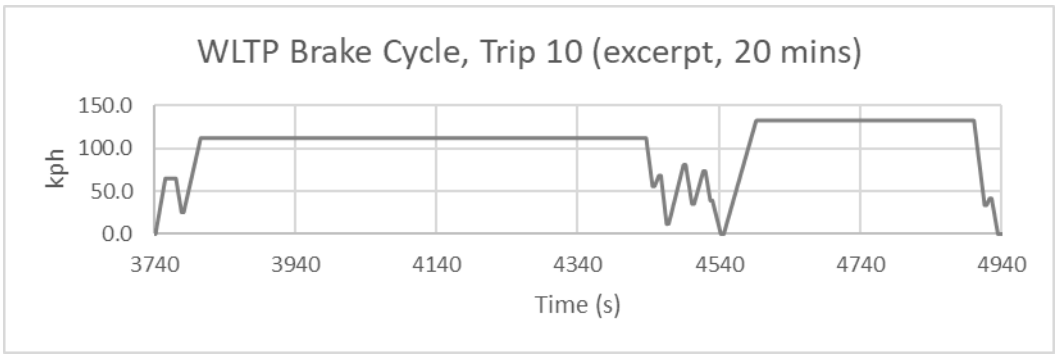

Figure 5-23: PG-42 Cycle used for brake and tyre chassis dynamometer testing

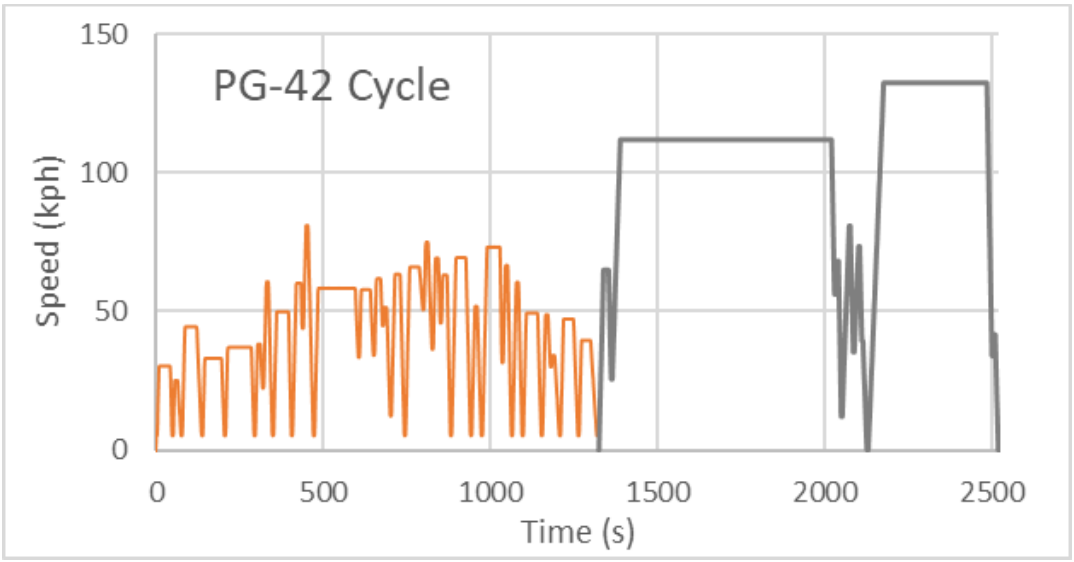

5.2.1.3 Chassis Dynamometer Measurements: Brakes

Nine repeat PG-42 cycles were tested, and brake emissions were sampled using hot and cold ELPI systems plus the e-filter. The eFilter gathered continuous data and was also equipped with a 47mm glass-fibre filter for cumulative particulate mass determination. Tests are summarised in Table 5-5.

Table 5-5: Summarised Chassis Dynamometer Brake Testing

							Extra		Tailpipe
Date/time	Theme	Location	Details	ELPI (hot)	e-filter	ELPI (cold)	ELPI (cold)	SPCS	CO_2
20220405_1305	Brakes	VERC	PG-42	Y	Y	Y	-	Y	Y
20220405_1425	Brakes	VERC	PG-42	Y	Y	Y	-	Y	Y
20220405_1530	Brakes	VERC	PG-42	Y	Y	Y	-	Y	Y
20220406_1330	Brakes	VERC	PG-42	Y	Y	Y	-	Y	Y
20220406_1505	Brakes	VERC	PG-42	Y	Y	Y	-	Y	Y
20220407_0946	Brakes	VERC	PG-42	Y	Y	Y	Y (mass distribution)	Y	Y
20220407_1100	Brakes	VERC	PG-42	Y	Y	Y		Y	Y
20220407_1210	Brakes	VERC	PG-42	Y	Y	Y		Y	Y
20220408_1040	Brakes	VERC	PG-42	Y	Y	Y	-	Y	Y

5.2.1.4 Chassis Dynamometer Measurements: Tyres

Nine nominally identical PG-42 tests were also executed for tyre emissions sampling. In addition, one further PG-42 test (***20220413_1415***) was undertaken with partially deflated tyres (see Section 5.2.5). A summary of PG-42 tests for tyre emissions measurements is given in Table 5-6.

Table 5-6: Summarised Chassis Dynamometer Tyres Testing

							Extra		Tailpipe
Date/time	Theme	Location	Details	ELPI (hot)	e-filter	ELPI (cold)	ELPI (cold)	SPCS	CO_2
20220408_1135	Tyres	VERC	PG-42	Y	Y	Y	-	Y	Y
20220411_0945	Tyres	VERC	PG-42	Y	Y	Y	-	Y	Y
20220411_1100	Tyres	VERC	PG-42	Y	Y	Y	-	Y	Y
20220411_1145	Tyres	VERC	PG-42	Y	Y	Y	-	Y	Y
20220412_1145	Tyres	VERC	PG-42	Y	Y	Y	Y (mass distribution)	Y	Y
20220412_1245	Tyres	VERC	PG-42	Y		Y	-	Y	Y
20220412_1405	Tyres	VERC	PG-42	Y		Y	-	Y	Y
20220413_1200	Tyres	VERC	PG-42	Y	Y	Y	-	Y	Y
20220413_1315	Tyres	VERC	PG-42	Y	Y	Y	-	Y	Y
20220413_1415	***Tyres***	***VERC***	***PG-42***	***Y***	***Y***	***Y***	***-***	***Y***	***Y***

5.2.2 Urban drive cycle

An example speed-time trace of the urban drive cycle is shown in Figure 5-24. The distance of the cycle is essentially fixed between repeat tests, but clearly the speeds and time taken can vary due to road conditions, other road users and many other factors.

Figure 5-24: Example urban drive cycle

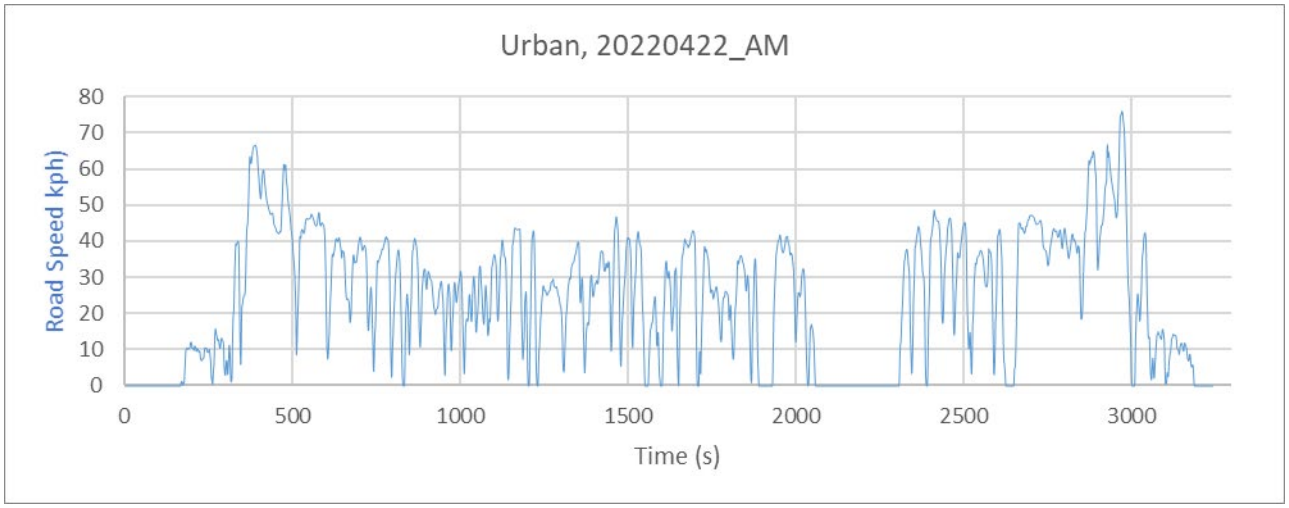

5.2.3 Track-based testing

Repeated braking events were executed on the short private test track situated close to the Ricardo site (Figure 5-18) at Shoreham-by-Sea. A driver with a moderate natural style was used. The test vehicle was driven back and forth (north to south) along the ~450 m track (Figure 5-25) accelerating to target speed and then either braking normally (moderate braking sessions) or in the manner of an emergency stop (extreme braking sessions). Repeat braking events from discrete speeds up to and including 50 mph (80kph) were studied. Speeds greater than 50 mph in the VW Caddy were not achievable in the 450m of available distance.

Figure 5-25: "Drive-by test track (map created in Leaflet (https://leafletjs.com/),map source © OpenStreetMap contributors https://www.openstreetmap.org/copyright).

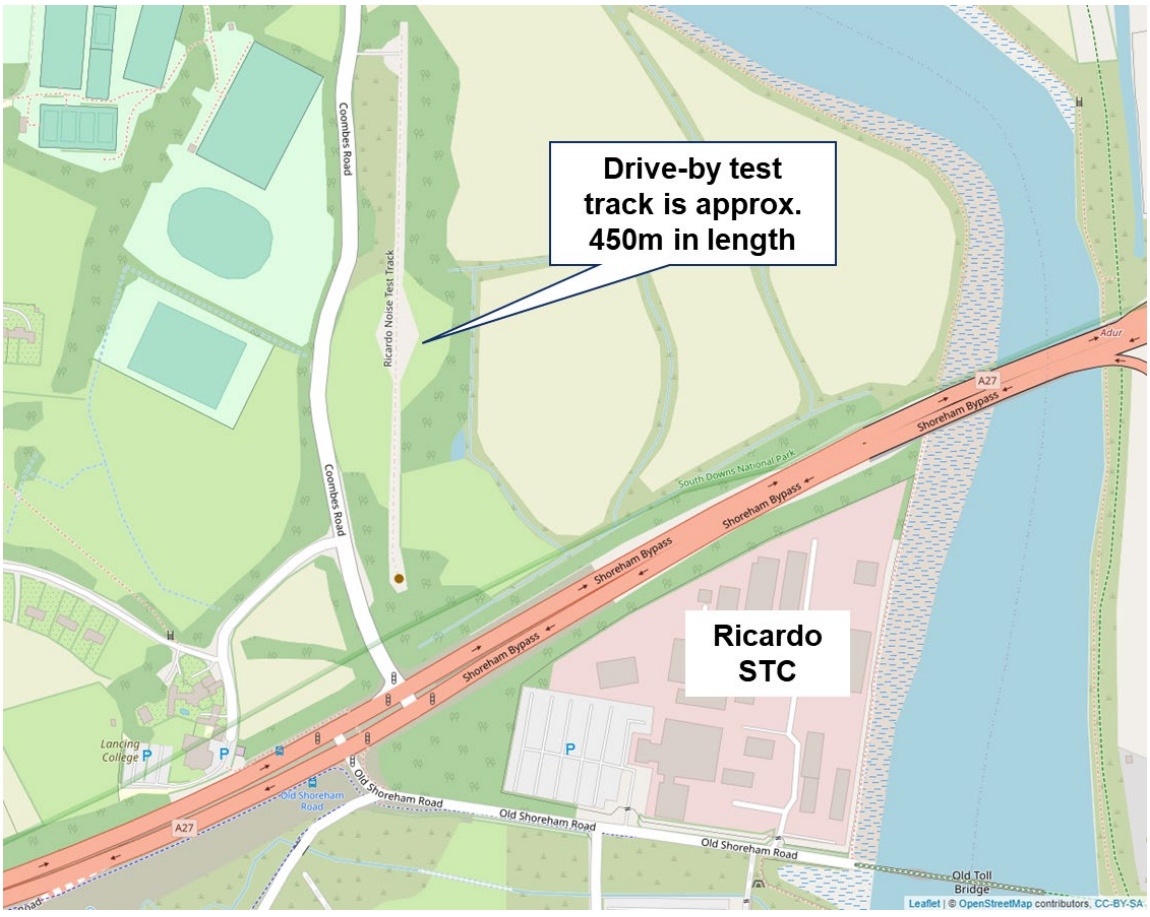

5.2.4 Lab-based equipment

Chassis dynamometer testing was undertaken in the Vehicle Emissions Research Centre (VERC) at the Shoreham Technical Centre (STC) of Ricardo. Detailed specifications of the VERC twin-axle chassis dynamometer facility used are given in Table 5-7.

Table 5-7: Specifications of the VERC Test Facility

	STC VERC
Dynamometer	4WD
Max speed	250 km/h
Max Power	170 kW
Vehicle wheelbase length	1800 to 4400 mm for 4WD
Vehicle height	3000 mm
Vehicle track width	800 to 2300 mm
Max vehicle weight	4500 kg total
	2500 kg maximum axle weight
Temperature control	-30 to +55 ºC
Humidity control	5.5 - 12.2 g H2O/kg dry air
Vehicle cooling fan	Adjustable cooling fan 1400 x 550-900 mm / 165 km/h
Automation	Horiba Ricardo STARS VETS
Emissions measurement	MEXA ONE
CVS tunnels	3
Soak capacity	Ambient soak chamber ~ 16 vehicles
	Climatically controlled transit /soak area
	2 x dedicated climatic chambers

In addition to the particle size distribution, number and mass emissions measured by the equipment used while installed on the test vehicle, a Horiba MEXA ONE[8] analyser with non-dispersive infra-red analyser was employed to measure continuous, 1Hz, raw CO_2 emissions from the tailpipe. CO_2 determination enables the evaluation of test-to-test variation in exhaust emissions as a baseline to compare with simultaneously sampled brake and tyre emissions.

Non-volatile particle number concentration was measured directly from the sampling tunnel on-board the test vehicle, in parallel with the ELPIs and eFilter, using the Solid Particle Counting System (SPCS). The SPCS uses an initial mass-flow controlled diluter, then primary hot dilution (150°C) to commence evaporation of volatile and semi-volatile species while reducing partial pressures, a heated evaporation tube (350°C) to eliminate volatiles from the sample aerosol, then secondary cold dilution to further reduce partial pressures of gas-phase species to avoid recondensation of volatiles. Non-volatile particles (defined as non-volatile by the measurement process) are then passed to a condensation nucleus counter where they are enumerated. The lower size range of particles that the SPCS measures is tuned to a roughly 50% counting efficiency at 23nm, with a nominal upper limit of ~2µm, though in practice few particles larger than ~500nm are likely to reach the particle counter.

Both hot ELPI (180°C) and SPCS (350°C) use high temperatures to stabilise the sample aerosol by elimination of volatiles. However, the substantial difference in temperatures of the two devices, and the potential for recondensation of semi-volatiles following heating in the hot ELPI (which does not have secondary dilution), may mean that SPCS and ELPI do not necessary correlate particularly well.

[8] MEXA-ONE - HORIBA

5.2.5 Vehicle chassis dynamometer test parameters

The Caddy and Audi were tested with demanding chassis dynamometer load terms and high inertia to maximise the stresses on both tyres and brakes during the PG-42 cycle. These measures were implemented with the intention of generating elevated levels of particle mass and number emissions. This extreme approach was undertaken to increase the chances of:

- Discriminating emissions from test facility backgrounds.
- Establishing representative particle size distributions, including in the >1µm region.
- Determining repeatability from multiple nominally identical tests.

Both front and rear tyre pressures were set to 2.9 bar, excepting the final test for tyre emissions where the tyres were deflated by ~30%, to 2 bar. This change was undertaken to increase the surface contact between the tyre and dyno roller to explore whether this had any impact on measured emissions levels.

Highway and dynamometer load terms, test inertia and details of relevant test parameters are given in Table 5-8 and Table 5-9 respectively.

Table 5-8: VW Caddy Chassis Dynamometer Test Parameters

Property	Value
Test Inertia (kg)	2405
Dyno Configuration	Four Wheel
Highway A (N)	71.748
Highway B (N/km/h)	0.8485
Highway C (N/km/h2)	0.0381
Dyno A (N)	35.874
Dyno B (N/km/h)	0.1697
Dyno C (N/km/h2)	0.0381

Table 5-9: Audi A4 Chassis Dynamometer Test Parameters

Property	Value
Test Inertia (kg)	1825
Dyno Configuration	Four Wheel
Highway A (N)	255.5
Highway B (N/km/h)	0
Highway C (N/km/h2)	0.04941
Dyno A (N)	127.8
Dyno B (N/km/h)	0
Dyno C (N/km/h2)	0.04941

5.2.6 Calculation of non-exhaust emissions and estimation of total emissions

5.2.6.1 Calculation of brake emissions

The sampling approach employed enables brake emissions to be simply calculated. The total flow from the brake enclosure is flushed into the particle dilution tunnel (PDT) from which particle measurement instruments are sampled. Since the brake enclosure is not completely sealed, the flow in the PDT is set to be a little lower than the flow of filtered dilution air into the brake enclosure. In this way it can be assumed that while air and brake particulates may escape from the enclosure, external air and background particles should not be drawn in, and since the dilution air to the enclosure is HEPA filtered it can then be assumed that all particles measured derive from the braking system. This is confirmed by carrying out a “background” sample of the brake enclosure system while the vehicle is stationary (i.e., no braking events), just drawing the filtered dilution air through the brake enclosure and into the PDT.

For the purposes of calculating the total emissions, the filtered dilution air flow into the enclosure is measured and logged as this is assumed to be carrying particulates whether drawn into the PDT or escaping from the brake enclosure.

Therefore, the emissions for eFilter, ELPIs (and SPCS) can be calculated as follows:

- The instantaneous particle or mass concentration (µg/m^3 or #/cm^3) is multiplied by the dilution air flow into the brake enclosure (units are adjusted for standard volume and time) to produce emissions per second.
- The emissions per second are summed over the test duration to produce emissions per test.
- The per test emissions are divided by the cycle distance (or time if required).

The calculation for eFilter, ELPIs (and SPCS) test total emission is therefore:

[total PDT volume (litres) * 1000 * particles/cm^3 or mass/cm^3] / cycle distance (km) or time (s).

Similarly, the total test mass emission from the PM filter mass can be calculated as follows:

[total PDT volume (litres) /filter flow (litres) * filter mass (mg)] / cycle distance (km) or time (s).

The flow to the filter is set by the eFilter sample pump which remains constant during the test.

This measurement provides the total emissions from the brake measured since the measured airflow is the total airflow passing over the brake, and the enclosure ensures the particulate measurements represent the emissions from that brake alone.

Background particle mass and number levels were determined in the same manner as samples, by running the measurement systems with the vehicle static (either while the wheels are stationary and the vehicle was situated on the chassis dynamometer, or while the vehicle was stationary in the soak area of the test facility). Since there was positive pressure within the brake enclosure, and so zero or minimal ingress of particles, the actual location at which background was sampled was not considered to be critical.

5.2.6.2 Calculation of tyre emissions

A very similar approach is used to calculate tyre wear emissions as is used to calculate brake emissions, except that a fixed nominal total flow of 350 litres/minute is used for the PDT volume. This flow is set by the total of the PDT pump and the sample pumps for the two ELPI+ and the eFilter, once set these do not vary throughout the test.

The tyre is not enclosed by the sample system and so the sample measured will not constitute the total emissions from the tyre, indeed the small opening of the sample duct relative to the tyre means it will only capture a small fraction of the emissions. However, without a means of measuring the total emissions of the tyre over the test, qualifying the proportion of emissions collected by the sample duct (that is, the sample efficiency) is not possible. This is discussed further with consideration of upper and lower bounds for the sample efficiency in section 5.6.2.

In a dyno test the tyre runs on a smooth steel cylindrical surface, which is unlikely to either retain or emit particles. However, on the road or track the road surface will both retain particles from the tyre on or within it, and emit particles from the road material or deposited from other vehicles, dust, pollution, etc. The ability to retain or emit particles will depend on the road surface material, and other factors such as age and weather.

In addition, since the tyre sample duct is drawing in air from near the tyre without any isolation, the sample will include ambient airborne particles such as from the engines, brakes, or tyres of other vehicles (or even of the test vehicle), other pollution, dust from the road or carried by the wind, etc. These may be reduced on a test track and much reduced in a dyno but can never be eliminated with the open sample duct approach. The use of the brake enclosure removes particles from the brake of the measured wheel from the tyre sample system, while background measurements allow the other external ambient particles to be quantified, as in 5.3.1.

5.3 TEST RESULTS 1: VW CADDY INITIAL ENCLOSURE

5.3.1 Background measurements

Since the method used in this study to determine brake wear emissions involves enclosing the brake pad and disc system, with filtered air constantly flushing out the enclosure, background levels were anticipated to be low. Typical maximum background levels in the brake enclosure were assessed by considering static measurements (with the vehicle stationary), but primarily through considering the baseline levels within the enclosure between braking events from the real-time signals of ELPIs and eFilter, for example in Section 5.3.3.3.1. The main focus of background investigations was then comparison between ambient measurements from the test vehicle, and real-world tyre scoop measurements.

The Caddy was equipped with three sampling probes for ambient measurements (Figure 5-13) and testing was performed on, or by, three different roads (A27, A283, A270) with the three different probes (centre, C; right upper, RU and right lower RL) as described in Table 5-4. Emissions results in unit/s are shown in Table 5-10 and Figure 5-26 for the hot and cold ELPI integrals, the eFilter mass and the mass determined by the PM filter (also from the eFilter).

Emission per second units were chosen as this:

(1) Enables a straightforward comparison between background and test results without further calculation.

(2) Permits a background equivalent total mass or number to be calculated for an on-road drive cycle of any duration, and then with cycle distance from that test, a #/km background can be simply calculated.

Table 5-10: Unit/s background emissions for ELPIs, eFilter and PM

Date/time/road/probe	cold ELPI (#/s)	hot ELPI (#/s)	eFilter (µg/s)	PM (µg/s)
20220330_1040_A27_C	2.88E+08	5.43E+07	4.15	0.343
20220330_1430_A27_RU	2.12E+08	7.23E+07	4.35	0.494
20220330_1520_A27_RL	1.34E+08	5.48E+07	4.01	0.802
20220330_1700_A283_C	1.95E+08	7.93E+07	4.75	0.537
20220401_0940_A283_RL	1.23E+08	3.26E+07	1.12	0.460
20220401_1020_A283_RU	1.66E+08	2.52E+07	0.97	0.395
20220401_1330_A270_RU	1.78E+08	6.19E+07	1.53	0.371
20220401_1600_A27_RU	2.06E+08	4.58E+07	1.95	No sample
Average	1.88E+08	5.33E+07	2.85	0.486
STDEV	5.16E+07	1.85E+07	1.60	0.156
CoV %	27.50	34.65	56.17	32.05

Figure 5-26: Unit/s background emissions for ELPIs, eFilter and PM

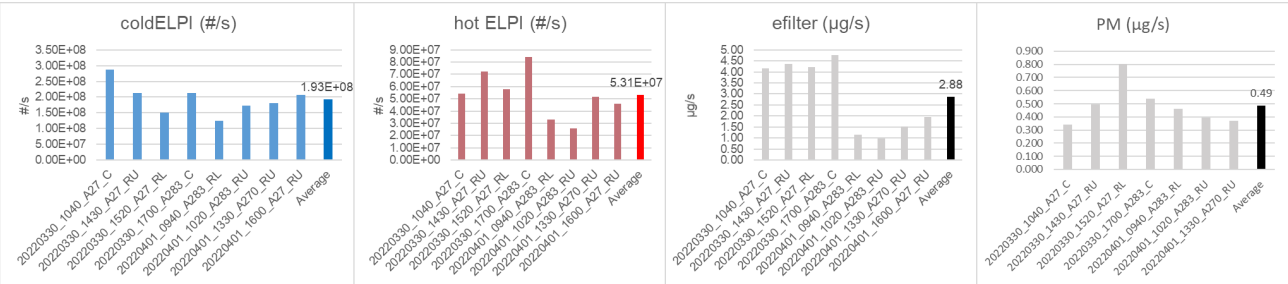

Background PN emissions from the cold ELPI are a factor of 2-3x higher than the hot ELPI, consistent with the hot ELPI eliminating some volatile particles. Variability of the cold ELPI between ambient runs is lower than that of the hot ELPI, suggesting that the composition of the background, and balance between solids and

volatiles, or the volatility of the ambient aerosol, is changing from test to test. Emissions from the eFilter range from a factor of 3 to a factor of 10 higher than from the PM filter. It is not clear why, but this could be due to numerous highly volatile particles (for example from gasoline exhausts) being identified by the eFilter, which then attributes them an instantaneous mass value. These particles would also collect on the PM filter but might evaporate with air flow through the filter as sampling progresses and would not be detected gravimetrically. This would result in lower masses from the PM filter. Mass conversion from current to mass is size distribution dependent. The difference between eFilter and PM may also suggest a variable particle size distribution, alongside the nucleation mode.

There is no clear evidence that the sampling probe used has any impact on particle emissions rates measured. From Figure 5-26, it appears that for the cold ELPI the central probe might show highest PN emissions, and the right lower probe might show lowest emissions, but this is not apparent with hot ELPI, eFilter or PM results.

For comparative purposes the average values from the background measurements shown in Table 5-11 will be used to compare with measured emissions from road and test track tyre emissions sampling. For comparative purposes, Table 5-11 also contains the result of a ~25 minutes duration background sample through the tyre scoop in the VERC. This shows substantially lower PM and PN background levels than on the road. It should be noted that that the VERC background may also vary depending on the prior vehicle tested, although the air exchange in the cell during testing is quite rapid.

Table 5-11: Average unit/s values from the background measurements: ELPIs, eFilter and PM

	cold ELPI (#/s)	hot ELPI (#/s)	eFilter (µg/s)	PM (µg/s)
Average background (roadside)	1.88E+08	5.33E+07	2.85	0.486
VERC background (vehicle static)	1.25E+07	6.00E+06	0.78	0.06[9]

To put these values into context, the roadside hot ELPI background would equate to ~1.5x10^{10} #/km over a WLTC cycle, with the eFilter background representing ~0.22 mg/km. Both these levels are consistent with the tailpipe particulate emissions of a very clean gasoline PFI vehicle.

5.3.2 Test repeatability: cycle replication, distance and CO_2 emissions

5.3.2.1 Cycle replication

The PG-42 cycle is derived from cycles intended for a brake dynamometer and contains some aggressive accelerations and braking events. The relatively low-powered Caddy struggled to achieve some of the accelerations in the drive cycle, which is unsurprising given the elevated test inertia and dynamometer loading applied. Nevertheless, as Figure 5-27a shows, the drive cycle was followed closely and repeatably throughout the PG-42 cycles driven for both brake and tyre evaluations. The 5 different drivers of the Caddy were unable to match the defined accelerations in three locations (Figure 5-27 b, c and d) but these accelerations were addressed at full load each time and consequently the comparative speed vs. time profiles repeat well. It is interesting to note that the blue line visible in Figure 5-27 b, c and d, with slower acceleration rates, corresponds to the tyre test with the lower inflation pressure, potentially indicating higher friction limiting the vehicle's acceleration rate.

[9] VERC PM filter background was found to be equivalent to ~0.06µg/s from one test

Figure 5-27: PG-42 drive cycle replication

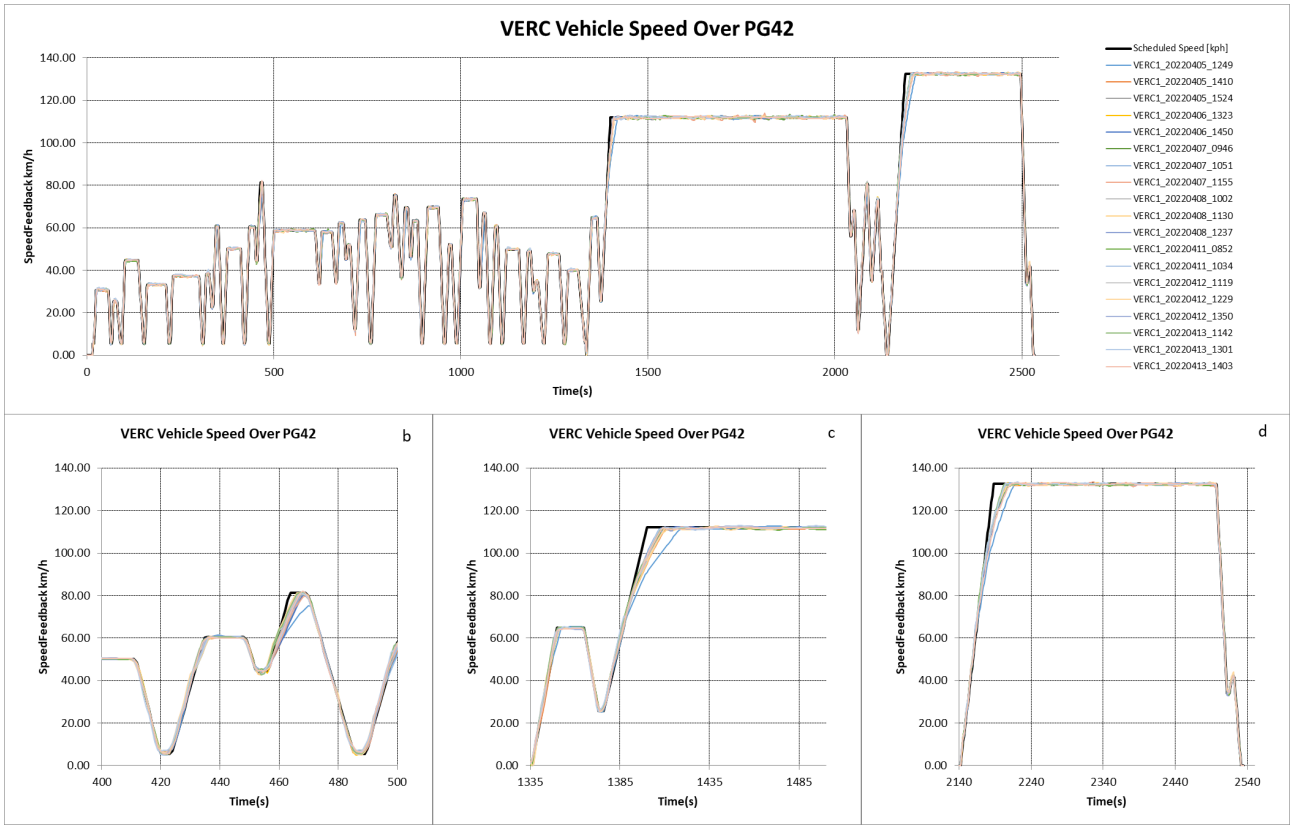

Test to test consistency of the drivers during the PG-42 cycles can be assessed through the repeatability of overall drive cycle distance (for following the cycle accurately and for CO_2 (for the driving style). As Figure 5-28 shows, CoV for cycle distance was 0.22% and for CO_2 emissions it was 1.57%. Error bars show 1-sigma in these, and all results, charts throughout this report. These levels of repeatability provide confidence that brake and tyre emissions from multiple PG-42 tests are legitimate comparisons of similar tests.

Figure 5-28: Repeatability of PG-42 cycle distance and CO_2 emissions

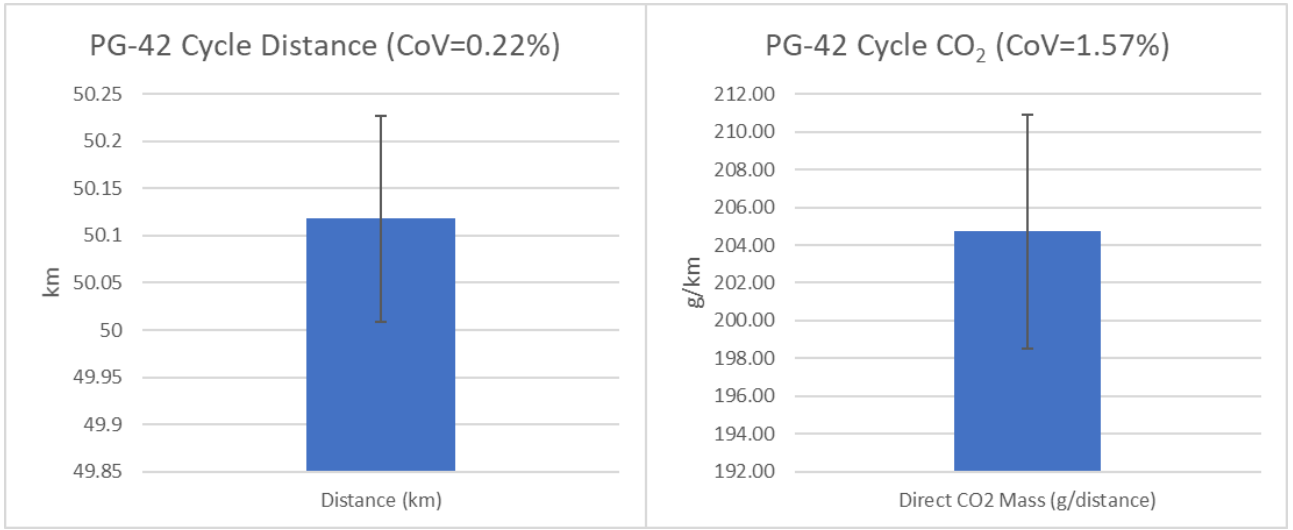

5.3.3 Brake emissions: repeatability and measurements

5.3.3.1 PG-42 Cycles

Average, standard deviation and CoV brake emissions from the 9 chassis dynamometer-tested PG-42 cycles are shown in Table 5-12.

Table 5-12: Average, standard deviation and CoV brake emissions from the PG-42 cycle

	PM (uncorr), mg/km	eFilter, mg/km	Cold ELPI (/1e9), #/km	Hot (180°C) ELPI (/1e9), #/km	Hot (350°C) SPCS (/1e9), #/km
Brake-PG-42 mean	1.602	0.482	2.47	4.81	4.91
Brake-PG-42 STDEV	0.116	0.110	3.05	1.95	0.20
Brake-PG-42 CoV	7.2%	22.8%	123.4%	40.4%	4.0%

These data show the best repeatability for SPCS at 4%. Since the evaporation tube of the SPCS removes the majority of volatile and semi-volatile particles this indicates that volatile materials are likely to be the greatest source of variation in brake wear particle emissions. Filter-based PM emissions, both with and without an ambient background subtracted, are also highly repeatable, with CoV in the range 7 – 8%. eFilter PM results are less repeatable (CoV ~23%). This may indicate that instruments, such as the eFilter and ELPIs, that are "detecting" particles, especially when volatile particles are included, are more variable. This could be due to evaporation and condensation of particles in the instruments and in the brake enclosure. This appears to be borne out by the cold ELPI, which shows the highest CoV (~123%) and improved CoV of the hot ELPI (~40%).

The glass-fibre PM filters used have a high affinity for volatile materials and will collect these largely independent of particle size. This may at least partially explain why filter-based PM is more repeatable than ELPI. This also partially explains why PM filter mass is higher than eFilter mass. Both e-filter and gravimetric PM will be impacted by reduced sampling efficiencies for larger particles, with the impact on the filter measurement potentially lower due to high sample flow rates. The mismatch between eFilter and filter-based PM is discussed in more detail in Section 5.3.3.1.3. PM filters collected from PG-42 tests on the chassis dynamometer are clearly black in colour (Figure 5-31), with this seemingly most likely deriving from elemental carbon or from black-coloured metal oxides (such as iron).

Real-time brake wear events are clearly observable in PG-42 cycles, with emissions spikes coincident with decelerations and braking events for both eFilter (Figure 5-29, left) and SPCS (Figure 5-29, right). These figures also show stable and consistent baseline (maximum background) emissions in the test facility (for example during long cruises, when brake wear would not be expected). SPCS baseline levels were of the order of 3.5×10^7 #/s (~1.76×10^9 #/km), with eFilter baseline around 1.25 µg/s (0.063 mg/km).

Figure 5-29: Real time brake PN (SPCS) and PM (eFilter) emissions during PG-42 Cycle

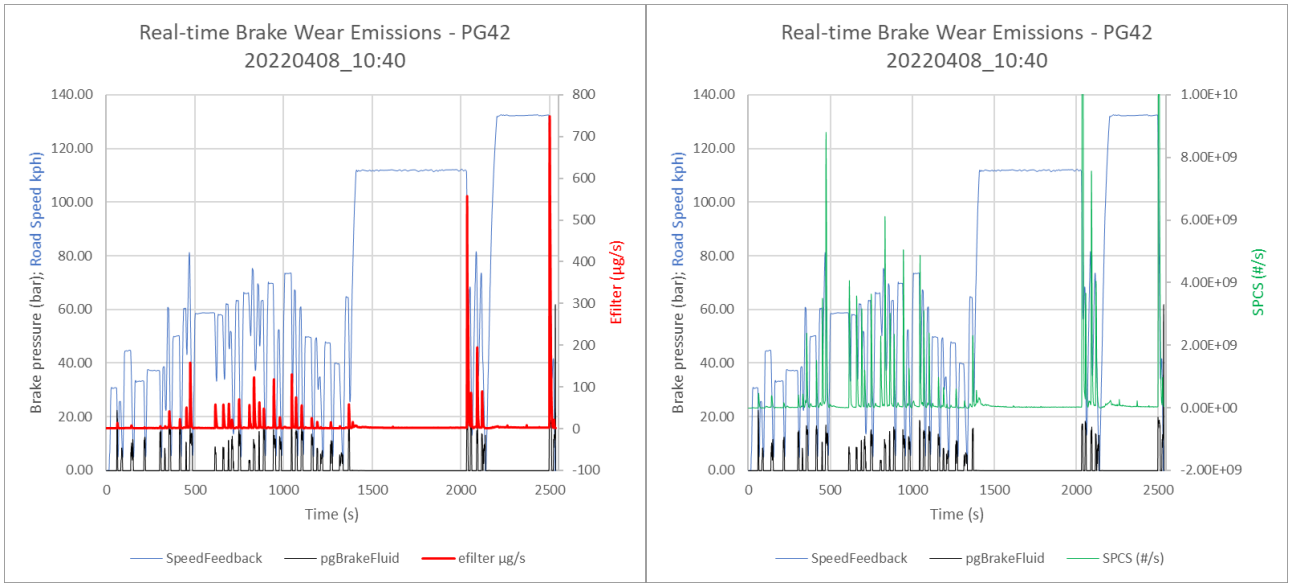

PN emissions from the cold ELPI indicate coincidence with some braking events, but the discrimination from the baseline/background level is poorer than from the SPCS, with levels at ~7x10^7 #/s. Conversely, the hot ELPI has a lower baseline (~4x10^7 #/s) and braking peaks are discriminated in a similar manner to the SPCS.

Figure 5-30: Real time brake PN (cold and hot ELPI) emissions during PG-42 Cycle

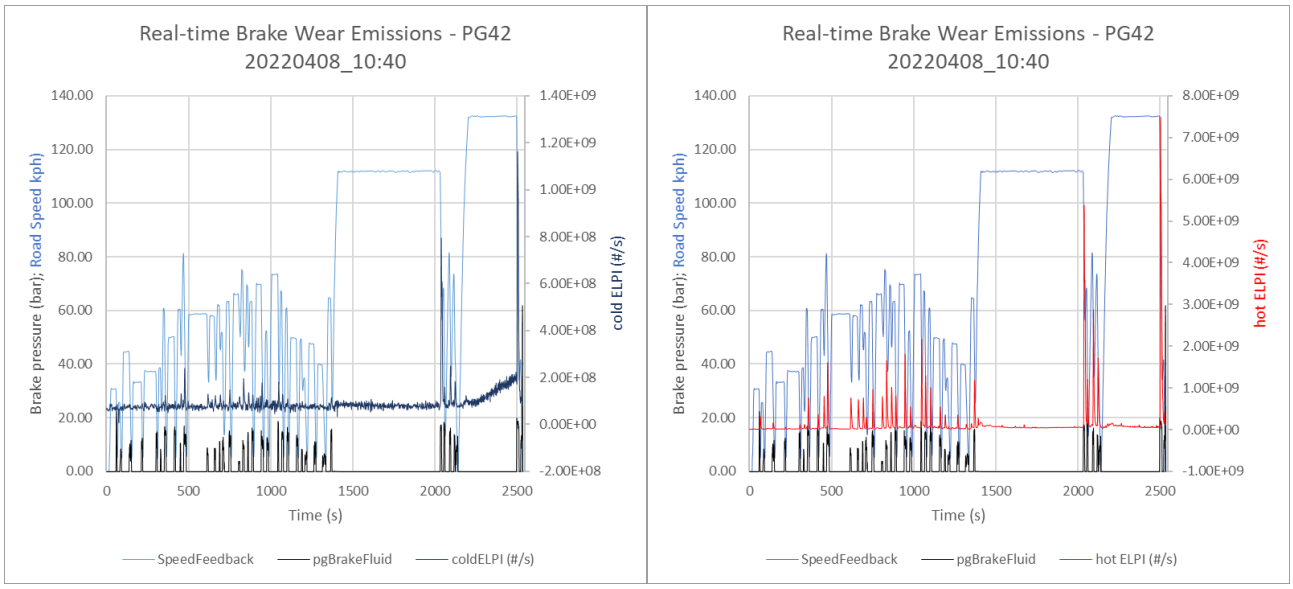

Figure 5-31: Three repeat PM filters from PG-42 brake testing

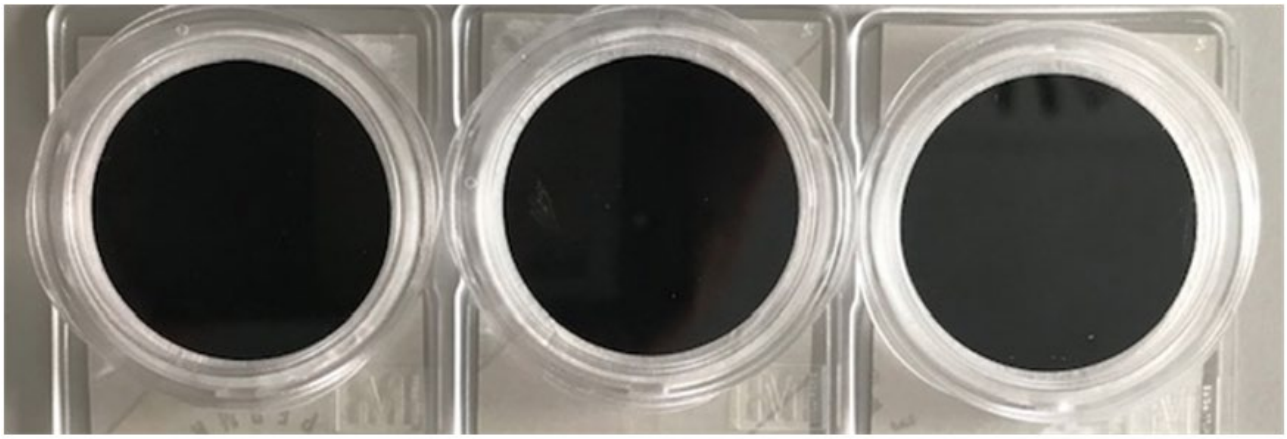

To investigate the chemical nature of the collected material, a thermogravimetric analysis (TGA) of a PG-42 filter was performed. In this analysis a sample filter section containing a known mass of particulate material is placed on a microbalance contained within an oven. The atmosphere within the oven can be switched between flows of bottled nitrogen or synthetic air, as required. The oven is initially ramped to 550°C with a nitrogen atmosphere, and components volatile below 550°C evaporate and register as a weight loss. Air is then introduced to the oven, with the temperature held at 550°C, and any remaining materials are oxidised. In diesel particulate samples the dominant material is usually carbon. The carbon oxidises to carbon dioxide and is lost, producing another weight loss. It is also possible that low volatility organic materials are present, and these too will oxidise to CO_2 and contribute a weight loss. A weight gain with air introduction suggests the presence of elemental materials (for example metals) that are not volatile at 550°C. The sum of the weight losses can be compared with the mass on the filter. The difference between the total mass loss and the mass on the filter section is the “remainder fraction” – so this quantifies the material on the filter that is neither volatile nor oxidisable (though could include some oxygen from any weight gain observed with the switch to air).

The thermogravimetric analysis (Figure 5-32) showed that ~95% of the PM material collected is almost completely non-volatile and this is most likely derived from metals and metal oxide emissions from the brake pad and disc, plus possibly ceramic contributions. Small masses of elemental carbon/graphite (~2%), volatile materials (from brake pad binders etc, ~1.7%) and water (~1%) were also detected.

Figure 5-32: Results of thermogravimetric analysis of PG-42 brake filter

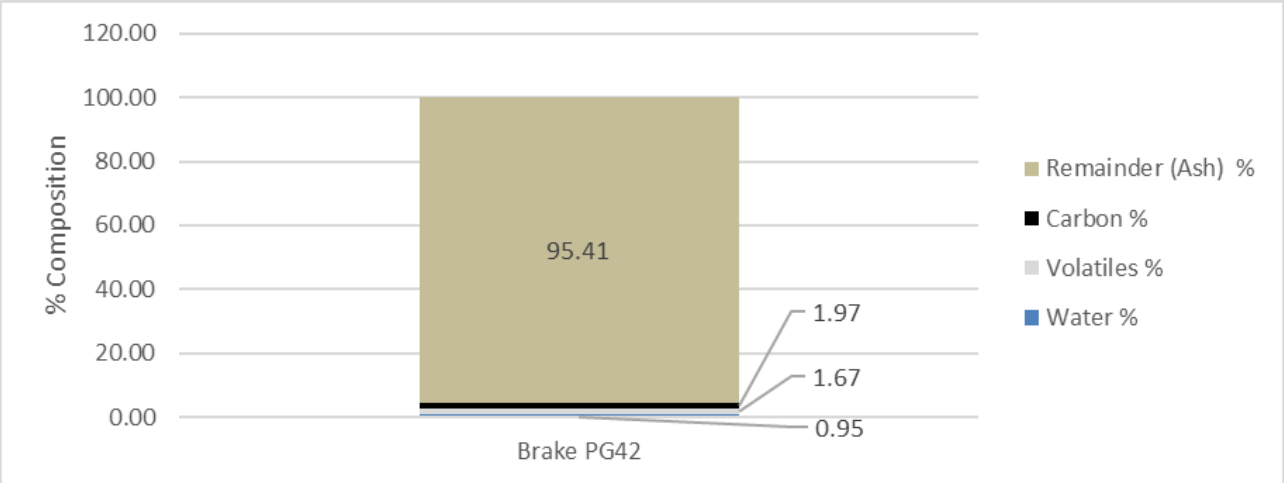

The residual material on the filter post thermogravimetric analysis is reddish-brown (Figure 5-33) indicating that the majority of the non-volatile mass may be iron (III) oxide.

Figure 5-33: Residual material on brake PG-42 PM filter section post TGA analysis

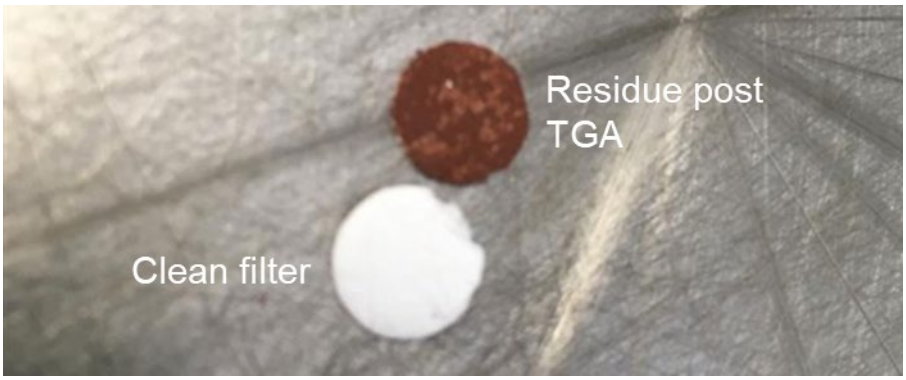

Emissions levels from the individual tests with both ELPI and SPCS are shown in Figure 5-34 left, with eFilter data shown in Figure 5-34 right.

5.3.3.1.1 PG-42 Particle Emissions Repeatability

Individual PG-42 repeat tests' brake PN and PM results are shown in Figure 5-34. These figures show that the cold ELPI has poorest PN repeatability, due to occasional high results. Hot ELPI data are more consistent, but there is a trend of increasing PN during the first 5 tests and then, potentially, the emissions stabilise. This may be related to brake pad/disc stabilisation for the higher demand braking of the PG-42 compared to the Caddy's prior driving. PN emissions from the SPCS were most repeatable, excepting the last test where the instrument malfunctioned. This result should be considered an outlier and that result excluded.

The hot ELPI reports lower emissions than the SPCS. This is counterintuitive as the SPCS has a more effective approach to eliminating volatile particles than the hot ELPI. Certainly, the Particle Concentration Reduction Factor (PCRF) correction for small particle losses would increase SPCS results relative to the hot ELPI, but perhaps the most likely factor is that the aerosol size distribution, for any single test, that reaches the counter of the SPCS is different to that seen by the hot ELPI and different again to that seen by the cold ELPI sampled simultaneously. This is explored in the discussion of Figure 5-35.

The eFilter gives similarly consistent results to the hot ELPI and also appears to evolve over the first 5 tests (but in the opposite direction, with mass reducing). This may also indicate a shift in the size distribution between repeat tests. If this effect is related to the size distribution this must be through a change in the ratio of volatiles in the particle phase that the eFilter can detect, and the volatiles in the gas phase that the eFilter does not detect.

Figure 5-34: Individual PG-42 repeat tests' brake PN and PM Results

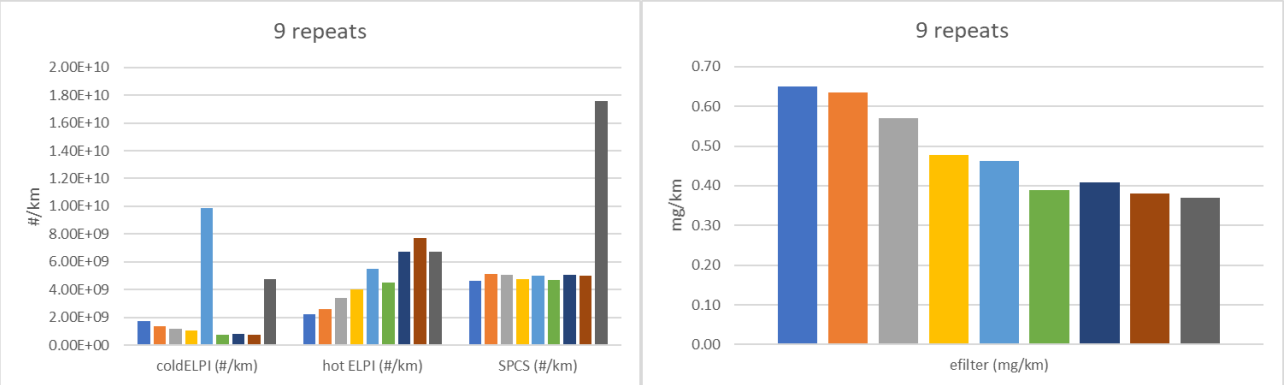

5.3.3.1.2 Particle Size Distributions

Figure 5-35 shows some example brake wear particle size distributions from three consecutive PG-42 tests conducted on a single day on log (Figure 5-35a) and linear (Figure 5-35b) ordinates. In Figure 5-35, the order of the three tests can be identified by line thickness, with the earliest test the thickest line with the dates identified in different colours.

There are several clear observations that can be made from Figure 5-35a and b:

- There are substantially fewer particles present in the size range between 1µm and 10µm with the hot ELPI. These particles must be removed by the heater (180°C) and thus are volatiles / semi-volatiles.
- In some regions of the particle size distribution (e.g., between 10 (0.01µm) and 100nm (0.1µm) and between 0.1µm and 0.3µm) the peaks observed from the hot ELPI are higher than the peaks observed from the cold ELPI in the same size range. This indicates that new particles form, or particle growth is occurring, during the hot ELPI sampling and measurement process and the heating aspect does not eliminate all volatiles. These volatiles are likely removed from the larger end of the size spectrum (the top stages of the ELPI stack) and recondense on lower stages, and some particle simply shrink during transition through the hot ELPI. This means that the hot ELPI size distribution is not representative of the real-time emissions from the brakes.
- Emissions from the cold ELPI are occasionally very high but using hot ELPI means that PN emissions may be higher than cold ELPI PN emissions.

Figure 5-35: Example repeat PG-42 brake particle size distributions

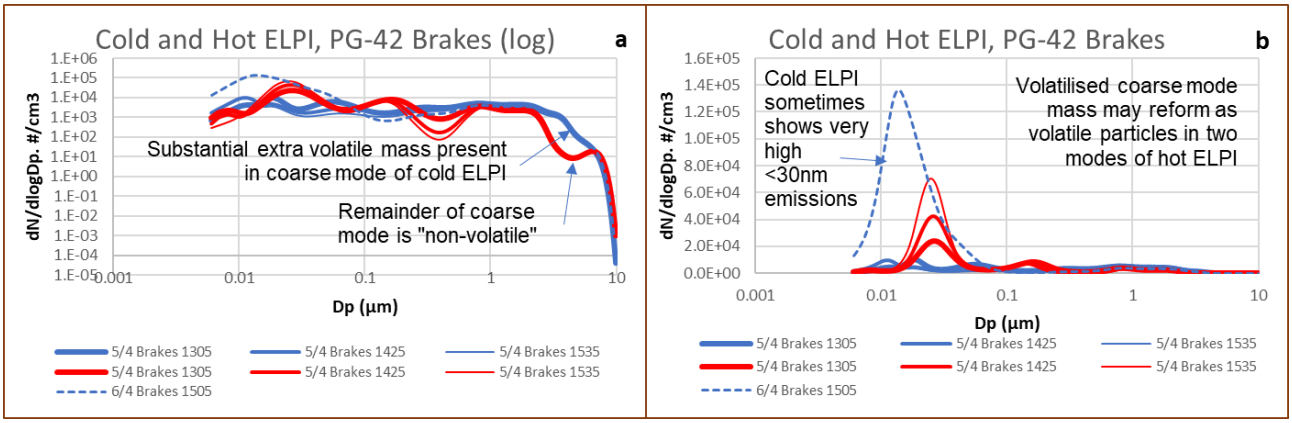

The detail of PG-42 brake particle size distributions from hot and cold ELPI are shown in Figure 5-36 and Figure 5-38 respectively.

Hot ELPI size distributions show trimodal character with size distribution shapes generally repeatable on a day-to-day and test-to-test basis. The first mode (lowest diameter, <0.03µm) increases in peak height as PG-

42 tests progress through the day (Figure 5-36b), while the magnitude of the second mode (0.1µm - 0.3µm) decreases and the final mode (> 0.5µm) is relatively consistent (Figure 5-36c).

Figure 5-37 illustrates for 3 consecutive PG-42 tests on 5th May, that initial and continuing brake pad temperatures are higher with subsequent tests. Temperatures differentials across these 3 tests are consistent, indicating that the major cause of higher pad temperatures is the higher initial temperature from heat stored during the prior test. This suggests that as temperatures of the disc and pad rise, the quantity of volatile material liberated from the 2nd modes increases, and this leads to the formation of more particles in the first mode. The third mode has limited volatility at the hot ELPI temperature.

It seems clear that the size distributions determined by the hot ELPI are neither fully non-volatile, nor representative of the size distributions produced by the braking event. However, the >0.5µm section of the size distribution may be non-volatile and therefore representative. This mode may originate from direct bulk wear of the pad and/or disc, or alternatively derive from 'dust' lost from the coarse surface of the pad.

Cold ELPI size distributions also seem to suggest three modes, but the first two are far more variable than seen with the hot ELPI (Figure 5-38a, b). It should be noted that the three distributions shown in red appear slightly different to the others, and these were sampled when the cold ELPI was using impaction plates to measure mass weighted particle size distributions. It is possible that this has some influence on the particle size distribution.

Cold ELPI particle size distributions may be highly variable due to inconsistent particle formation during sampling, through high sensitivity to temperature and from variable local volatile, semi-volatile and non-volatile particle concentrations within the brake enclosure during sampling. The >0.5µm section of the size distribution may be largely non-volatile as it appears similar to same region of the size distribution from the hot ELPI.

The cold ELPI size distributions are representative of the emissions from the braking system, but with the potential exception of the 0.5µm region are likely to be too unrepeatable to use for a regulatory procedure.

Figure 5-36: Magnified particle size distributions from hot ELPI brake measurements

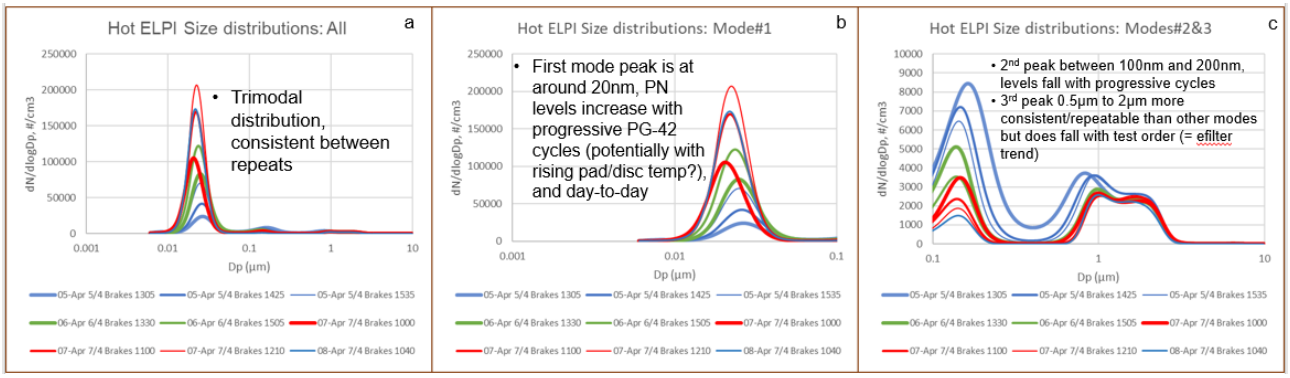

Figure 5-37: Repeat PG-42 brake pad temperatures, Enclosure A

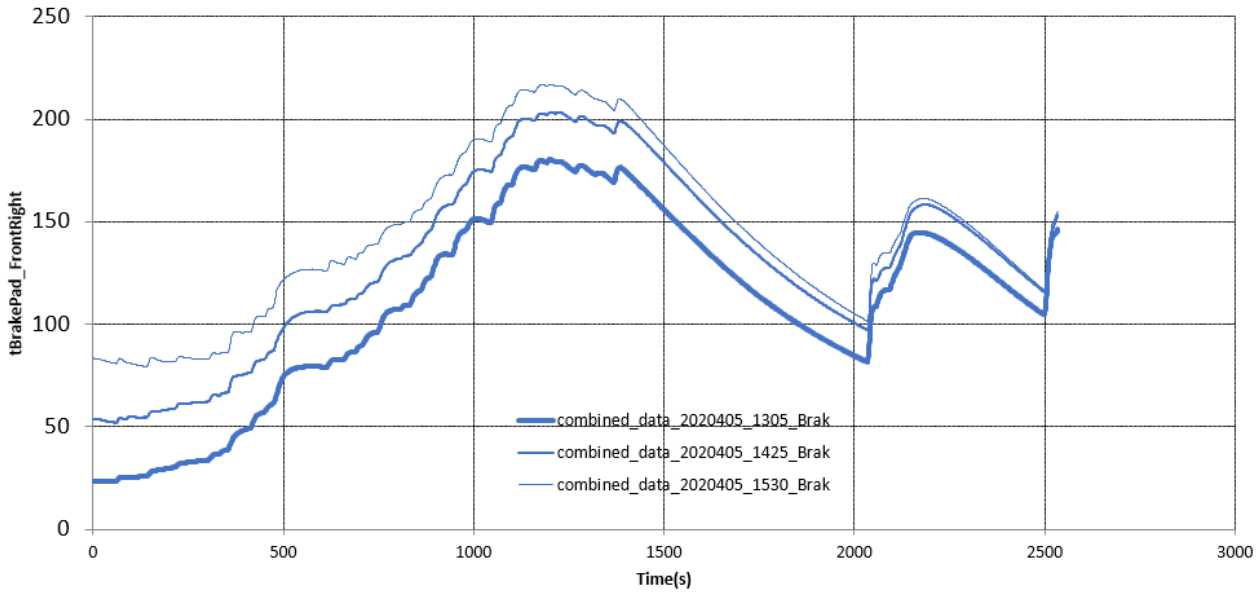

Figure 5-38: Magnified particle size distributions from cold ELPI brake measurements, PG-42

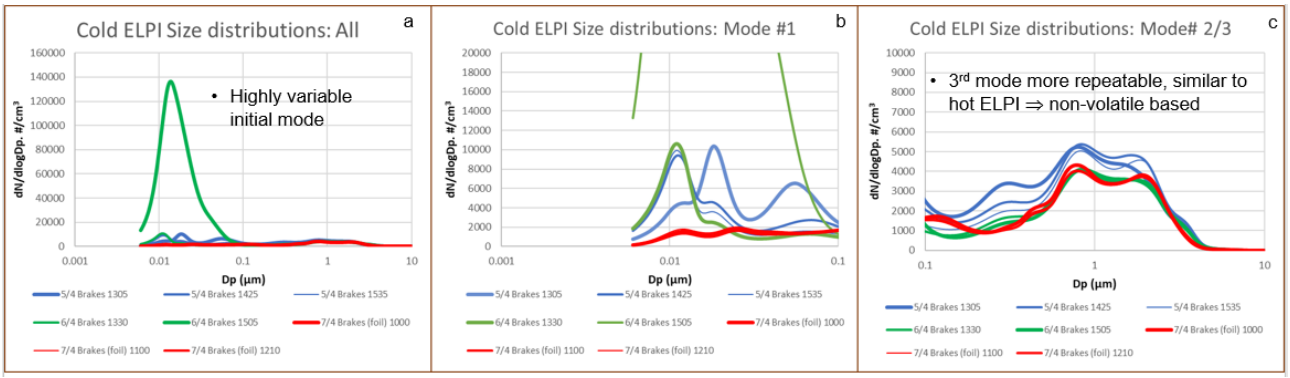

For regulatory purposes high repeatability is required in order to discriminate different products. From the PG-42 evaluations in this study it would seem wise to focus on non-volatile particles (PG-42 repeatability via SPCS was ~4%) potentially measured using a PMP -type device with catalytic stripper or evaporation tube, with a mass measurement alongside to capture volatile emissions effects. However, a future modification could look at measuring total particles (like the cold ELPI) but first stabilising the volatiles via, for example, a high dilution ratio step.

5.3.3.1.3 Comparative magnitudes of PM and PN Emissions

Figure 5-39 shows that filter-based PM indicates approximately 1.5 mg/km PM emissions from the PG-42 cycle. Error bars show 1-sigma. Filter PM level is roughly 3 to 4 times the level determined by the eFilter. This disparity likely derives from a combination of the following factors:

- The filter method collects gas-phase volatiles as well as volatile and solid particles, the real-time eFilter method detects only particles, and so the filter-based method would be expected to report higher mass. The eFilter data can be considered to reflect the lung deposited surface area (LDSA) of the particles, so might be a better indication of health effects related to particles (rather than to particle mass + chemistry) than the filter result.
- The eFilter calculates mass depending on charges transferred to particles, a charging efficiency model, an assumed particle size distribution, and assumed density of the particles. It is likely that materials released from brakes may produce a different particle size distribution, tending towards

larger particles, be of different chemical composition and likely higher density than the eFilter defaults. These would all tend towards underestimating the actual mass.

- It should be possible to optimise the eFilter algorithm to provide a mass metric suitable for brake wear measurement.

Figure 5-39: Mean PM and PN emissions from PG-42 braking tests

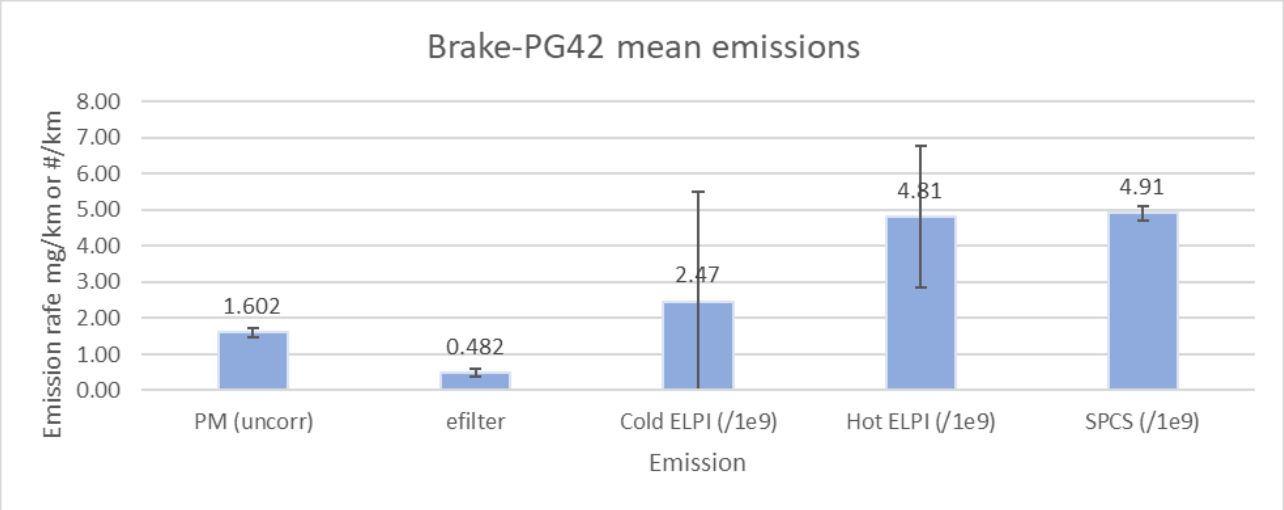

PN emissions from the SPCS and Hot ELPI were in the region of 5 x 10^9#/km, with cold ELPI about 50% lower (although the high variability of cold ELPI measurements means all three instruments' emissions were statistically similar).

If a PN metric is to be used for brake wear emissions, a non-volatile measurement should be considered to maximise repeatability. This might use an evaporation tube or catalytic stripper.

5.3.3.2 Urban Drive Cycles

Real-time particle number (cold and hot ELPI, middle and right respectively) and particle mass (eFilter, left figure) data compared with road speed and braking pressure are shown in Figure 5-40 for an urban road drive. These figures indicate that the eFilter and hot ELPI show emissions events that are coincident with decelerations and reported braking pressure events. At least some emissions events due to braking are also reported by the cold ELPI, but these are accompanied by many more spikes in the data, and it seems challenging to resolve distinct emissions that are due to braking from this instrument. Interestingly, baseline emissions levels on the road appear lower than observed on the chassis dyno during the PG-42 cycle for the eFilter (0.3µg/s v 1.26 µg/s).

Figure 5-40: Real time braking events on an urban road can be discriminated by eFilter and hot ELPI

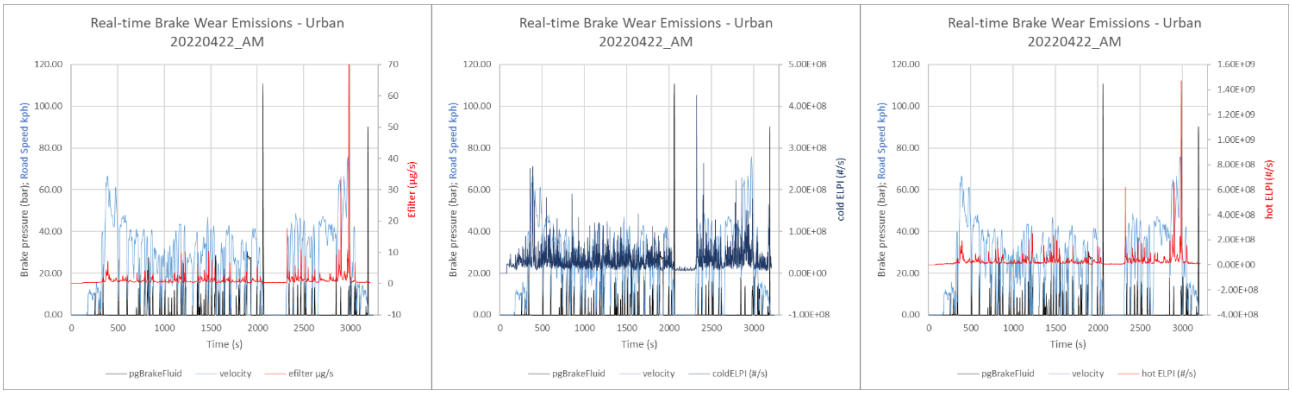

5.3.3.2.1 Urban Cycle Brake Particle Emissions Repeatability

Repeatability of the ELPI and eFilter instrumentation from 3 repeated on-road urban drives is given in Table 5-13. The SPCS data are not available as this is only a lab-based instrument. As with the chassis dyno measurements, the cold ELPI (CoV ~ 58%) is less repeatable than the hot ELPI (~27%). The eFilter is most repeatable at 5%, compared to 29% for the filter PM, but it should be noted that these data are averages of only 3 (cold ELPI, filter PM) or 4 (other) tests. Note that one of the 3 tests was of double length to accumulate PM for mass weighted particle size distribution determination.

As with the PG-42 cycle samples, urban PM filters are clearly black in colour (Figure 5-41), indicating the presence of elemental carbon or other black components.

Figure 5-41: Three repeat PM filters from urban cycle brake testing

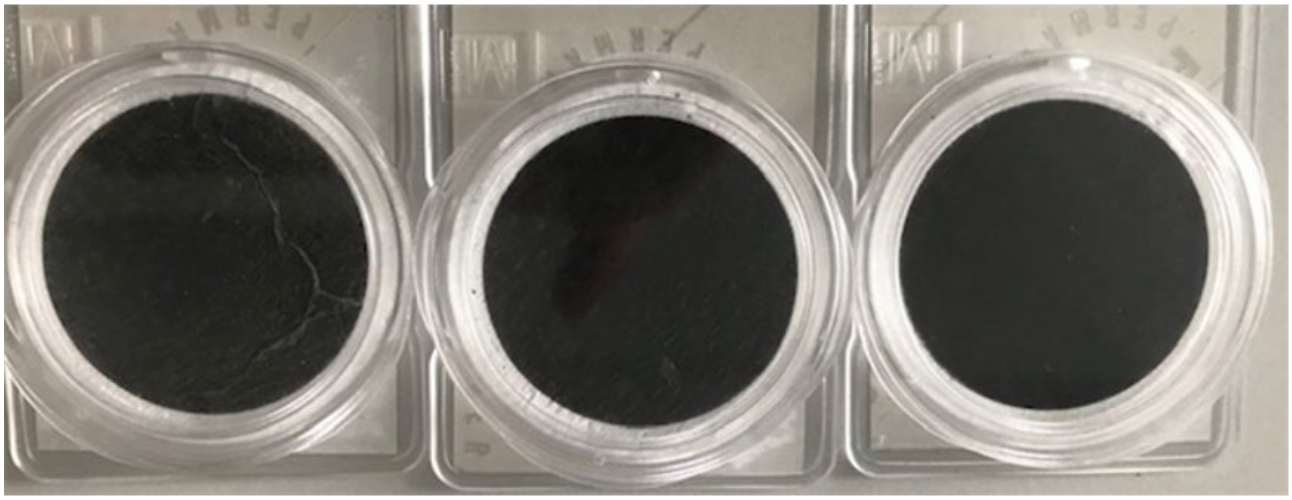

Figure 5-42: Results of thermogravimetric analyses of PG-42 and urban brake filters

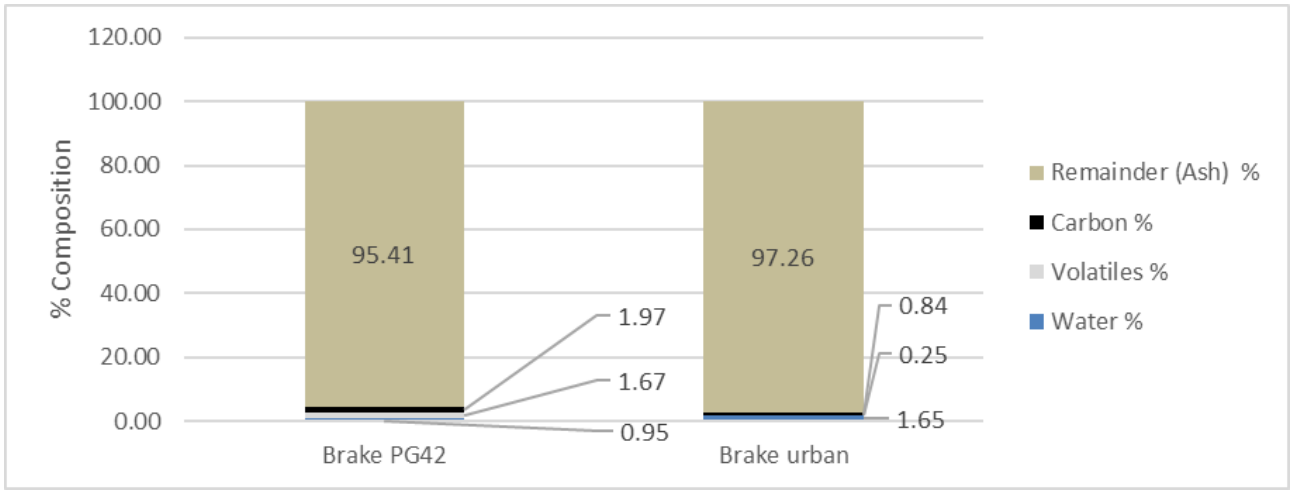

Thermogravimetric analysis of an urban filter (Figure 5-42) shows a breakdown consistent with that from the on-dyno PG-42 cycle, with the remainder fraction entirely dominant. This suggests that there is limited, if any, ingress of ambient volatile materials into the brake enclosure during sampling.

Table 5-13: Average, standard deviation and CoV brake emissions from the on-road urban drive cycle

	PM (uncorr), mg/km	eFilter, mg/km	Cold ELPI (/1e9), #/km	Hot (180°C) ELPI (/1e9), #/km	Hot (350°C) SPCS (/1e9), #/km
Brake-PG-42 mean	0.916	0.192	4.18	5.38	Not on-board
Brake-PG-42 STDEV	0.200	0.010	2.42	1.44	Not on-board
Brake-PG-42 CoV	22%	5%	58%	27%	Not on-board

Repeat urban cycles data are shown for ELPIs, eFilter and filter PM in Figure 5-43.

Figure 5-43: Individual urban cycles repeat tests' brake PN and PM Results

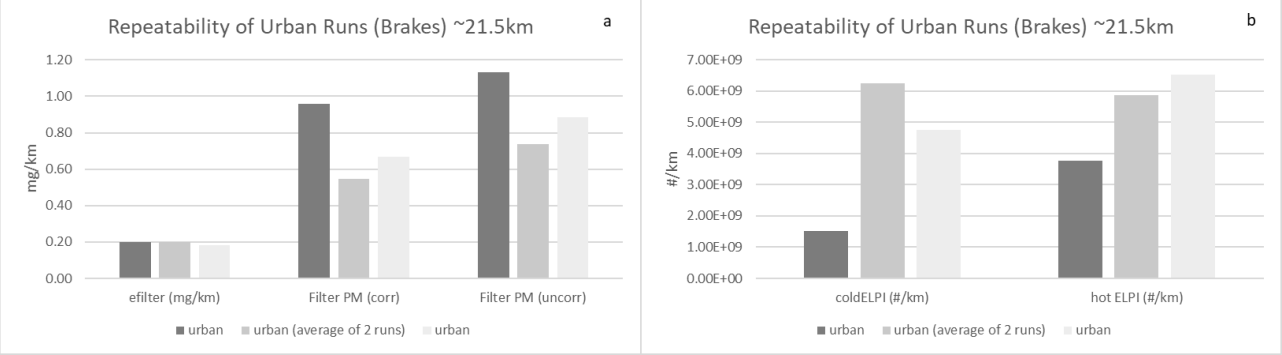

Mean urban cycle brake emissions from ELPI, eFilter and PM filter measurements are compared in Figure 5-44. Urban eFilter mass is ~4.5x lower than the filter-based PM measurement, and eFilter and PM emissions are ≥43% lower than from the PG-42 cycle.

Urban PN emissions from cold ELPI were on average slightly lower than from the hot ELPI, and slightly higher than from the PG-42 cycle, but not statistically different at 1-sigma.

Lower mass from the urban cycle, combined with similar PN levels suggests either generally lower density particles with the same particle size distribution or a shift in the particle size distribution to smaller particle sizes than from the PG-42 cycle.

Figure 5-44: Mean PM and PN Emissions from PG-42 and urban cycle braking tests

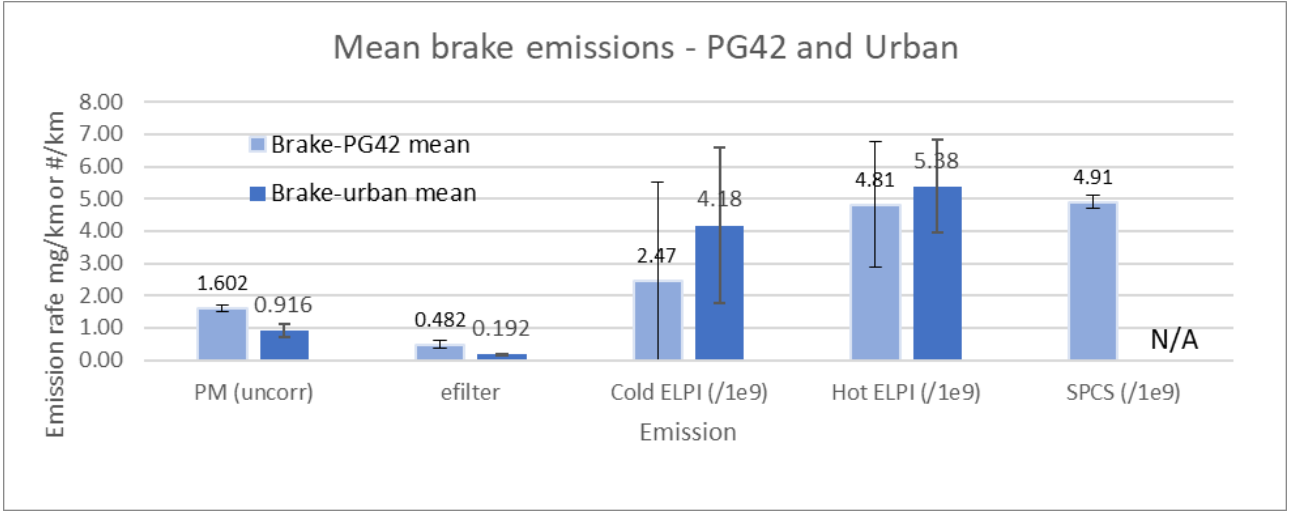

5.3.3.2.2 Number Weighted Particle Size Distributions

Brake particle size distributions from the cold and hot ELPI are shown in Figure 5-45a-c and Figure 5-45d-e respectively. A comparison of Figure 5-45a and d, shows that while there are 5 clearly resolved modes in the hot ELPI data, the cold ELPI data is much less well resolved into individual peaks. In both cold and hot ELPI data (Figure 5-45b and e) total particle number is dominated by the 0.01 to 0.1µm range, with similar concentrations, though the mode of the hot ELPI size distribution tends towards a larger diameter (25nm) than the cold ELPI. The cold ELPI clearly shows greater particle numbers and variability than the hot ELPI above 0.5µm, Figure 5-45c and f. This suggests that for urban cycle brake emissions there are significant levels of volatile particles, and/or volatile material in the size distribution above 0.5µm than are removed in the hot ELPI.

Figure 5-45: Particle size distributions from cold and hot ELPI brake measurements, urban cycle

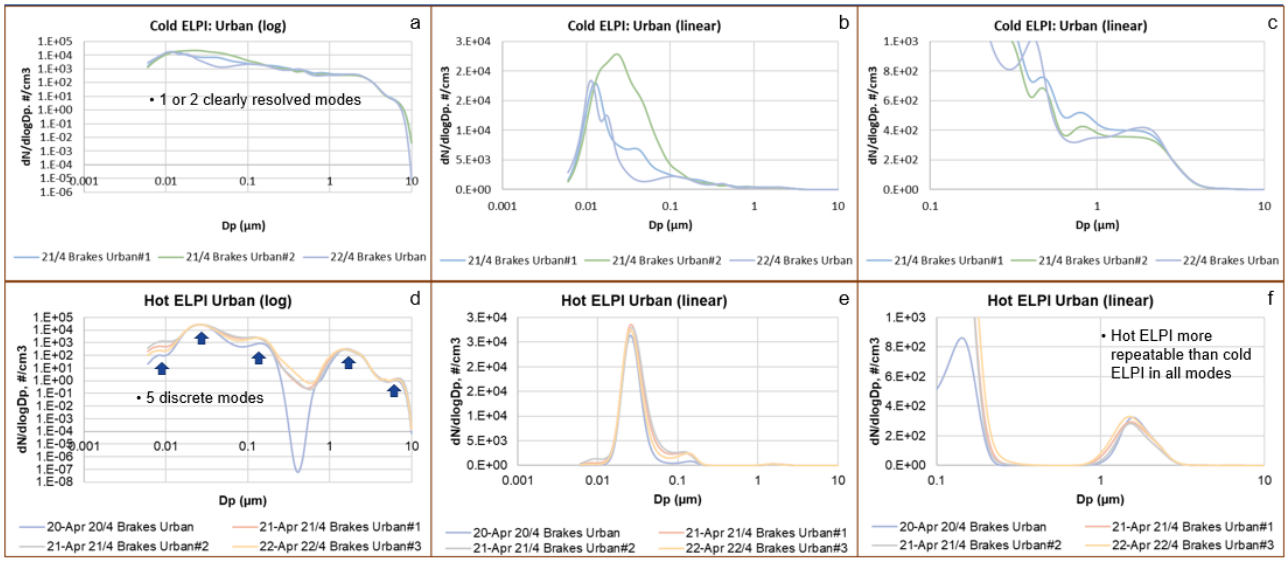

Hot ELPI size distribution data is more repeatable than cold ELPI data and there is a clearly discriminated non- or low volatility mode present above 0.5µm. However, particle number emissions in this size range are very low, and since this size range is likely to have a substantial contribution to measured mass, a mass metric may be a better way of monitoring and limiting these emissions.

5.3.3.2.3 Mass Weighted Particle Size Distributions - Brakes

One-off measurements were conducted using the cold ELPI to obtain mass weighted particle size distributions. Samples were accumulated during triplicate on-dyno PG-42 and duplicate on-road urban drive cycles and show in which size ranges the particulate mass is primarily concentrated. Figure 5-46 shows mass weighted particle size distributions on linear (left) and log (right) ordinates for PG-42 and urban cycles.

Figure 5-46: Mass Weighted Particle Size Distributions, Cold ELPI, PG-42 & Urban Cycles, Brake Emissions

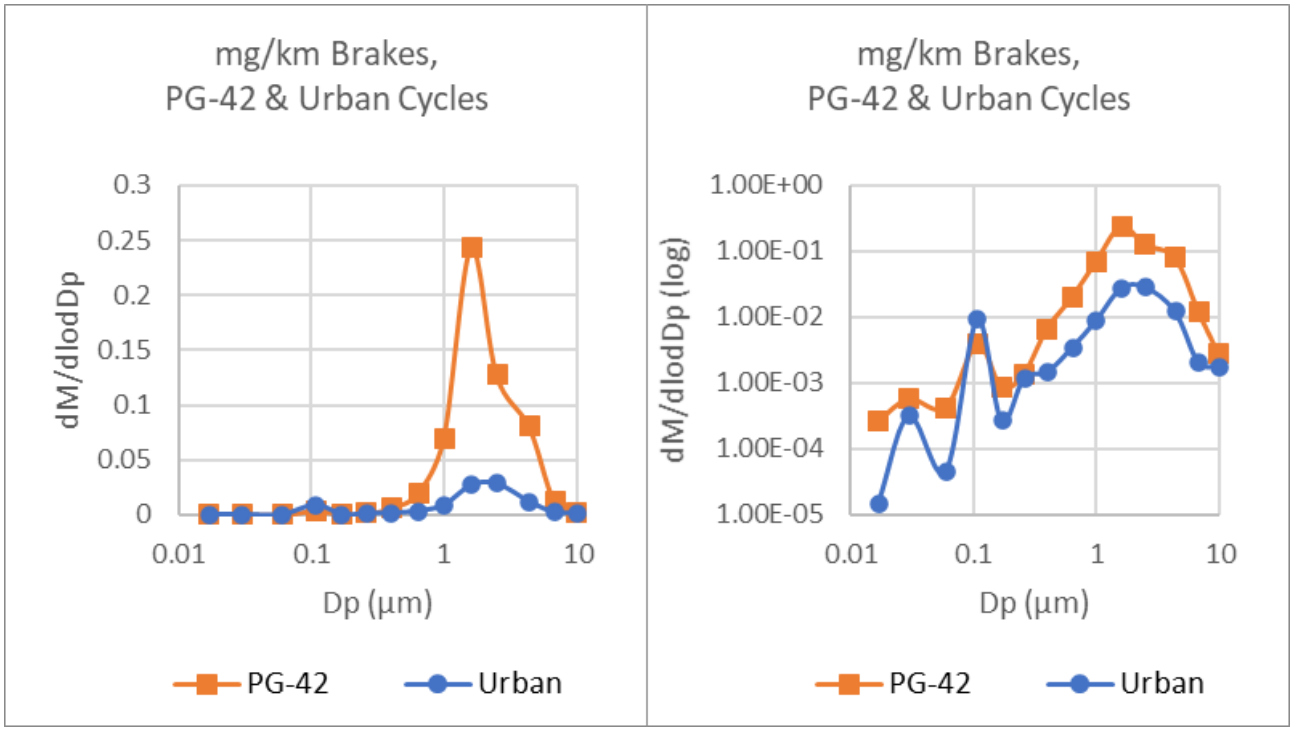

Particle size distributions from the PG-42 and urban drives are generally similar, showing two modes: a minor mode at ~100nm (0.1µm) and a dominant mode at ~1.6µm. The >1µm mode is likely to be mechanically generated wear materials primarily released from the brake pad. A coarse mode above 3µm is not observed, possibly due to poor transmission of larger particles to the analysers. The emissions from the PG-42 cycle, which contains more aggressive braking events, are substantially higher than from the urban drives. The similarity between the size distributions indicates that the use of the brake enclosure is protecting both lab and on-road brake wear samples from ingress of ambient materials.

5.3.3.3 Test Track Experiment#1: Moderate Braking

A dedicated measurement session was conducted on the Ricardo test track with the aim of performing repeatable, comparable braking events from different speeds.

- A series of moderate (WLTC-like) repeated braking events were performed on the test track, from ~50mph (80kph), 40mph (64kph), 30mph (48kph), 20mph (32kph) and 10mph (16kph). Particle emissions were measured with the hot and cold ELPI plus eFilter following a static background acquisition from the brake enclosure.
- Brake pressure plus pad and disc temps (both front left and right brakes) were recorded using the Dewesoft logger, along with other metrics, including vehicle speed.
- PN and PM emissions data corresponding to individual braking events were isolated and then compared between different braking events from the same starting speeds. Data from different speeds were also compared.
- The entire ~1340s measurement session was also treated as a single “drive cycle” to establish cumulative emissions/km. An overall particle size distribution was also determined for comparison with PG-42 and urban results.

The measurement session included six replicate braking events from each of 50mph, 40mph and 30mph, with more numerous events at 20mph and 10mph. Figure 5-47 shows these events along with the braking pressure.

Figure 5-47: Speed v time and braking pressure (bar) for the moderate braking experiment on the test track

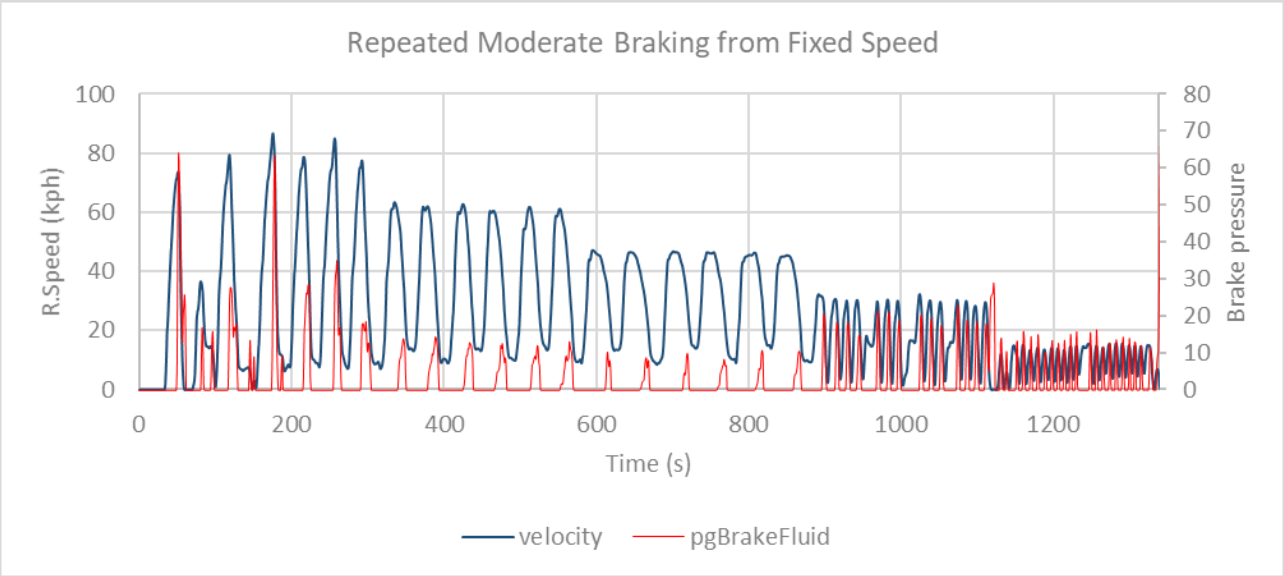

Particle emissions, and related parameters such as braking pressure and brake and disc temperatures, were isolated for each braking event. Using the 50mph events as an example (Figure 5-48, left), time-aligned data were inspected for each velocity peak and the integrated particle number or mass data extracted on a per second basis. The box bounded by dashed lines in Figure 5-48 right shows how the deceleration event is isolated from the speed peak (light blue line), how a coincident spike of particle emissions is seen from the hot ELPI (grey line) and how brake pad temperatures in the enclosure on the right hand wheel (orange line) and left hand side (dark-blue line) increase as the brakes are applied.

Figure 5-48: Braking events from 50mph and isolation of particle emissions data

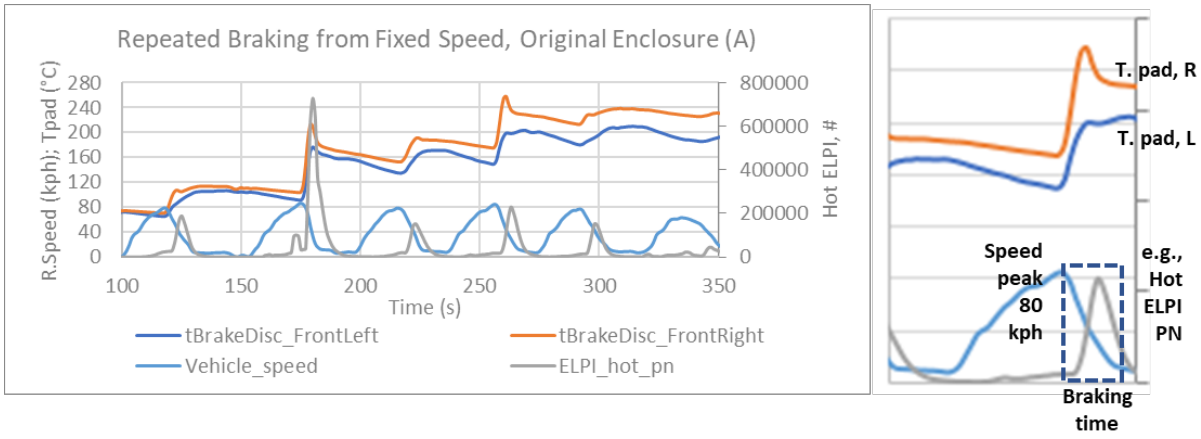

5.3.3.3.1 Brake enclosure backgrounds

Particle number and mass backgrounds from the ELPI and eFilter instruments are shown in Figure 5-49. These data were sampled for ~22 minutes shortly prior to the start of the sequence of braking events with the vehicle static and the engine off.

These data show that the cold ELPI background levels (average 1.4 x 10^7 #/s) were ~50x higher than the hot ELPI levels (average ~2.3x10^5 #/s) which is consistent with volatile particles dominating the cold ELPI particle size distributions, and the hot ELPI eliminating these. Average particle concentration from the hot ELPI for the sampling period was ~85 particles/cm^3. Background for the eFilter was ~4.4 µg/m^3 (0.82 µg/s).

Figure 5-49: Brake Enclosure ELPI and eFilter backgrounds

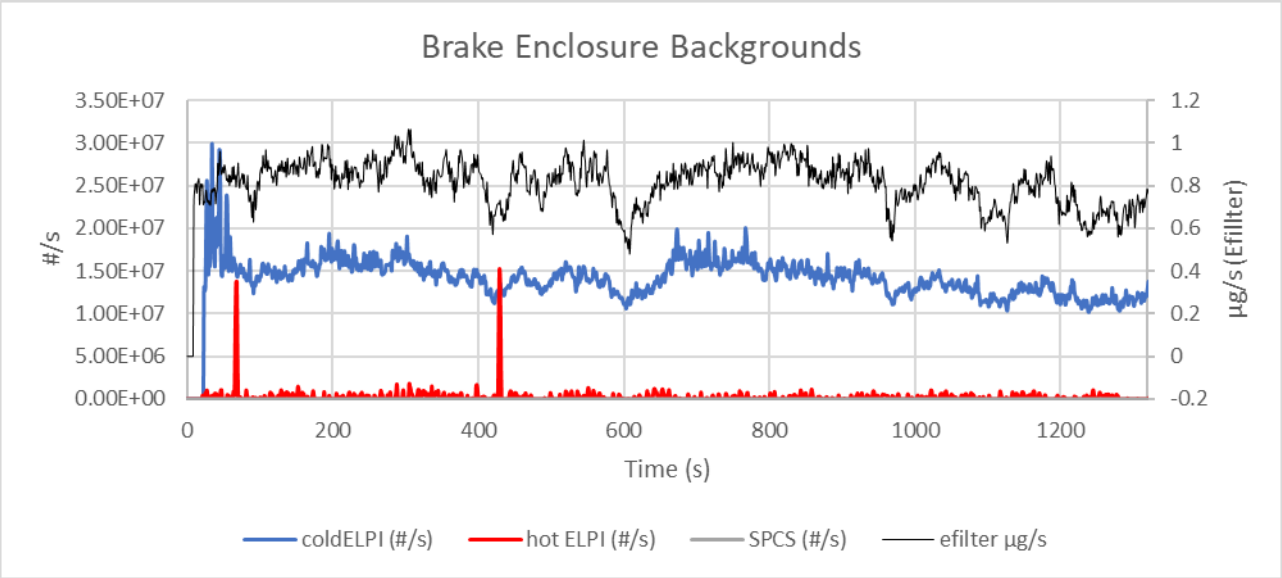

The PN background levels were consistent with baseline levels (between accelerations) seen during the moderate braking experiment (Figure 5-50) but PM background was more than three times the eFilter baseline levels (0.82µg/s v ~0.25µg/s). Consequently, it seems possible that brake enclosure backgrounds, for eFilter at least, taken with the vehicle static are not representative of backgrounds experienced during active testing.

Figure 5-50: Baseline emissions levels cold ELPI, hot ELPI and eFilter

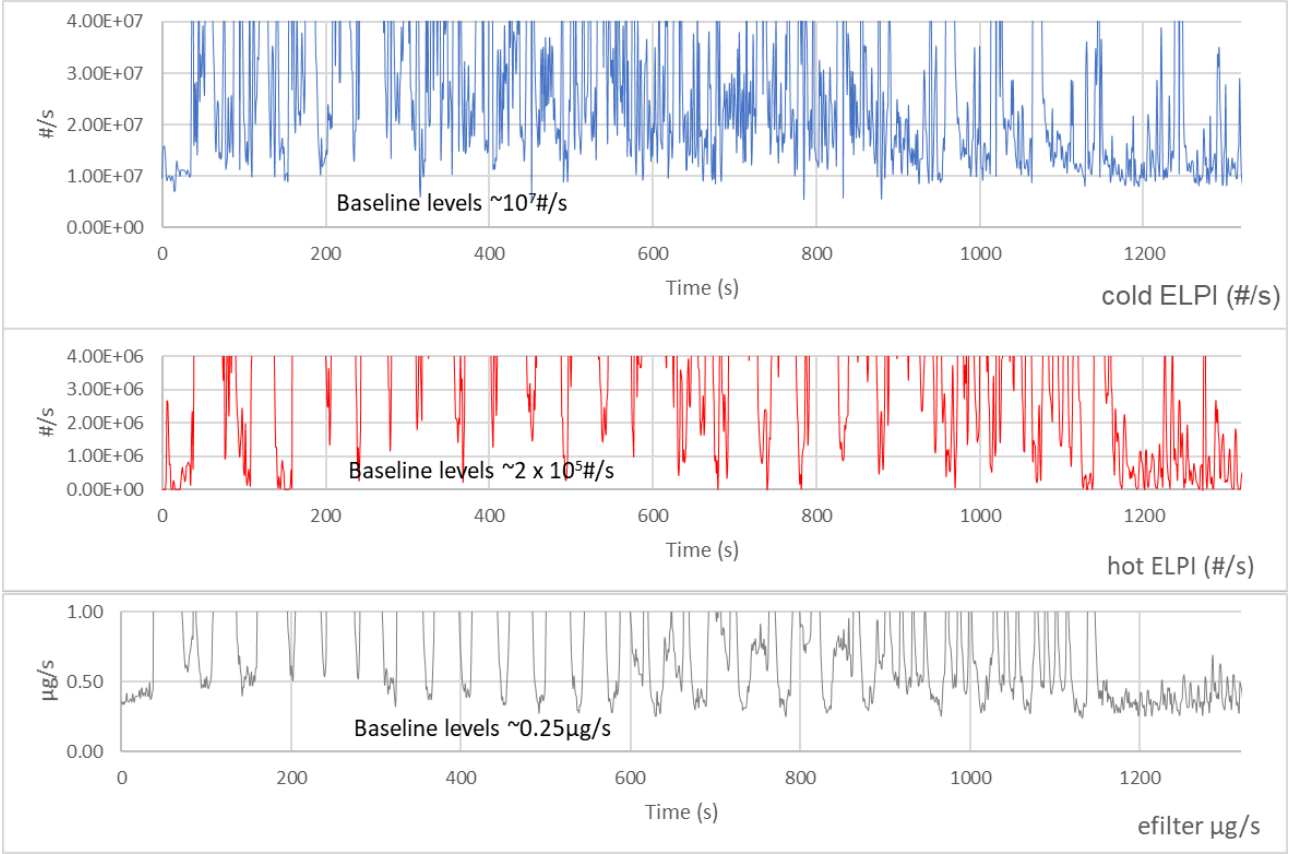

PN backgrounds from the cold ELPI are quite similar to measured particle emissions at 10 and 20mph and approach 50% of emissions levels at 30mph and 40mph. Hot ELPI backgrounds are always < 30% of measured PN (Figure 5-51) even at 10mph, but at this speed the contribution is still considered substantial.

Consequently, in the following figures exploring brake emissions, ELPI backgrounds of 1.4 x 10^7 #/s (cold ELPI) 2.3x10^5 #/s (hot ELPI) have been subtracted.

Figure 5-51: Average particle/s emissions compared with backgrounds

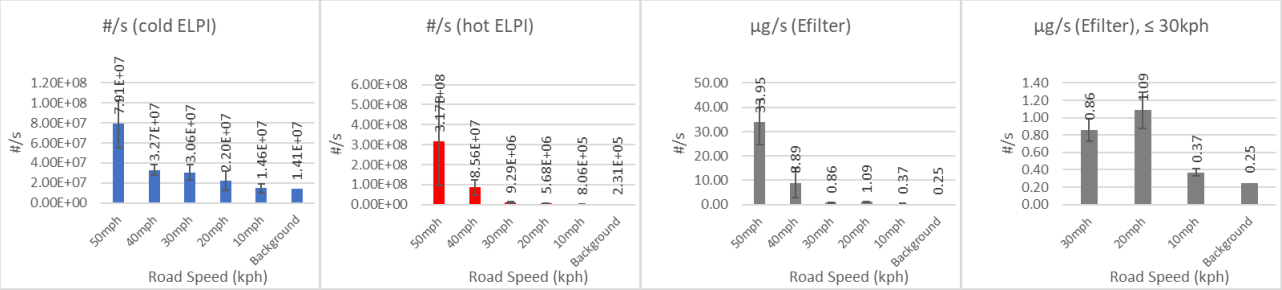

The assumed eFilter background (0.25 µg/s) is lower than emissions observed at all speeds from 10mph to 50mph but is ~70% of the emissions level at 10mph. Therefore, a background subtraction has also been performed. It should be noted that the emissions at 10 mph were 0.49µg/s from an average of 17 separate measurements with CoV of 24% and ranging from 0.031µg/s to 0.102µg/s. It seems unlikely that this level of consistency would be possible if the background was legitimately contributing > 0.8µg/s.

5.3.3.3.2 Brake Particle Emissions' Relationships

Figure 5-52 illustrates that all number and mass metrics appear to show an approximately quadratic relationship between peak speed (at which braking commences) and particle number and mass emissions. This is consistent with emissions being proportional to the kinetic energy transferred to the braking system (a function of velocity squared).

Figure 5-52: Relationship between particle/s emissions and peak speed of braking event

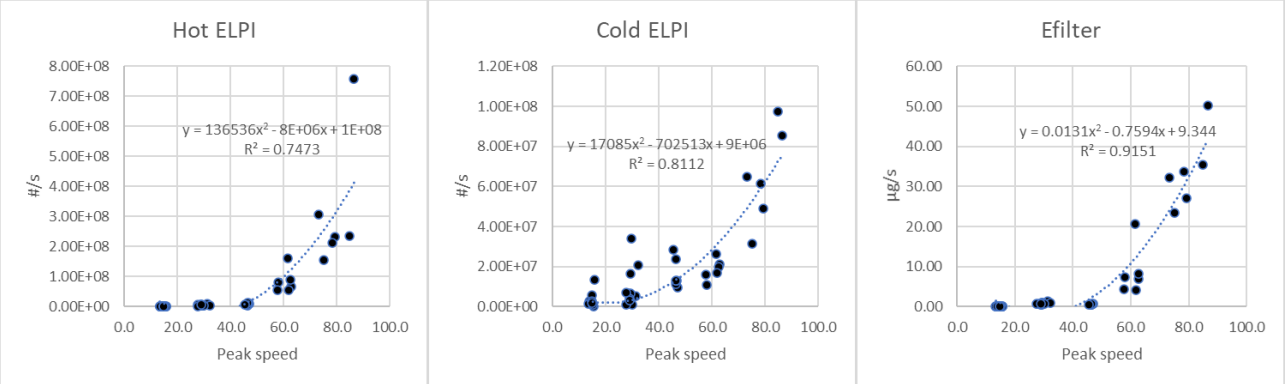

Interestingly, the particle emissions rate in both #/s and µg/s appears to decrease with average brake pad temperature (Figure 5-53) when all vehicle speeds are considered. The same effect is also observed when comparing average disc temperature with particle emissions (not shown). It should be noted that this could be a function of the higher speed braking events being tested first in the sequence.

When PN emissions at individual speeds are considered (Figure 5-54), there is no strong evidence of any temperature-related evolution in emissions in either cold or hot ELPI data. Interestingly, at the higher road speeds (50mph and 40mph) emissions from the hot ELPI are higher than from the cold ELPI, while at lower speeds the cold ELPI concentrations are higher. In both the 50mph data, Figure 5-55 left, and the 20mph data (righthand figure) the hot ELPI shows lower emissions in the >0.5µm region. It is likely that volatile material in this size range is being evaporated and recondensing in the small sizes. At a 50mph braking event more material is liberated, and more nucleation mode particles are created, and PN levels exceed cold ELPI integrals. Less material is liberated at lower speeds and nucleation mode formation is insufficient to surpass cold ELPI emissions levels.

Similarly, there is no obviously consistent effect on temperature on eFilter emissions at different average brake pad temperatures (Figure 5-56). Effects with brake disc temperatures were similar to those observed for brake pads.

Figure 5-53: Relationship between average brake pad temperature and particle emissions rate (#/s)

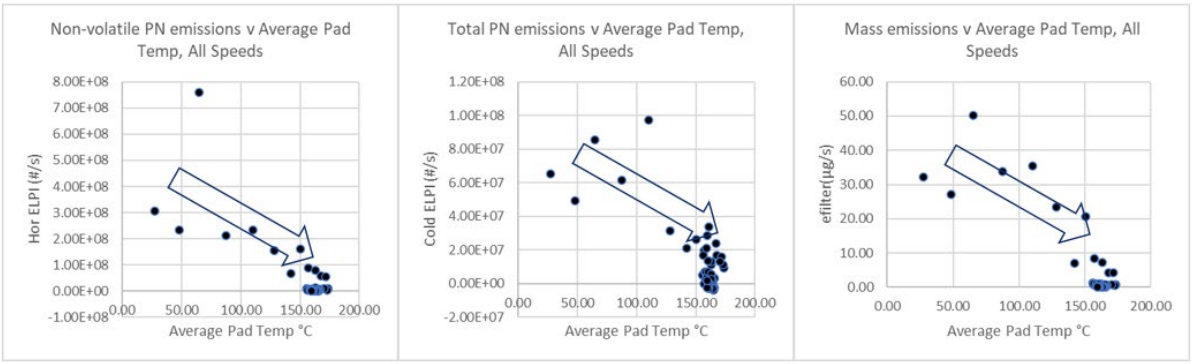

Figure 5-54: No consistent relationship between average brake pad temperature and PN emissions rate (#/s)

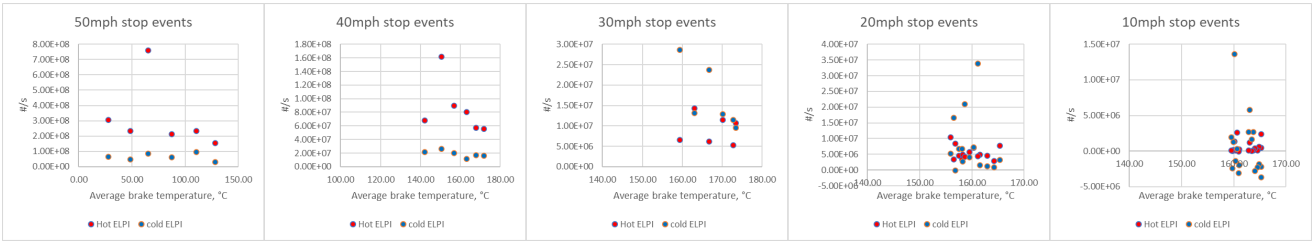

Figure 5-55: Particle size distributions from hot and cold ELPI at 50mph and 20mph

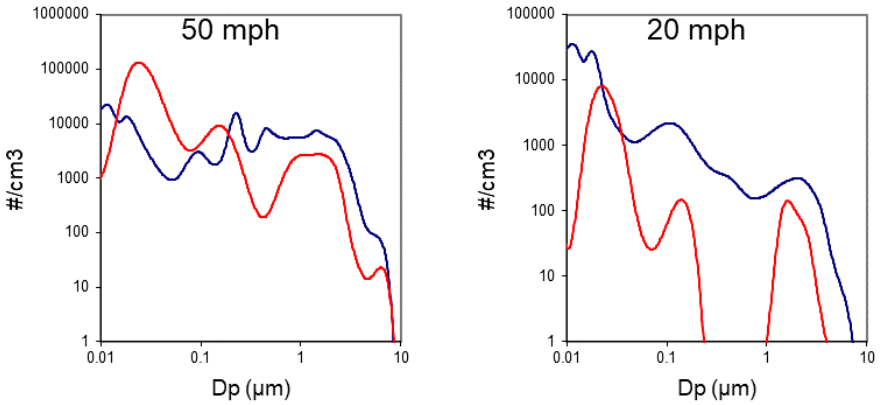

Figure 5-56: No consistent relationship between average brake pad temperature and PM emissions rate (µg/s)

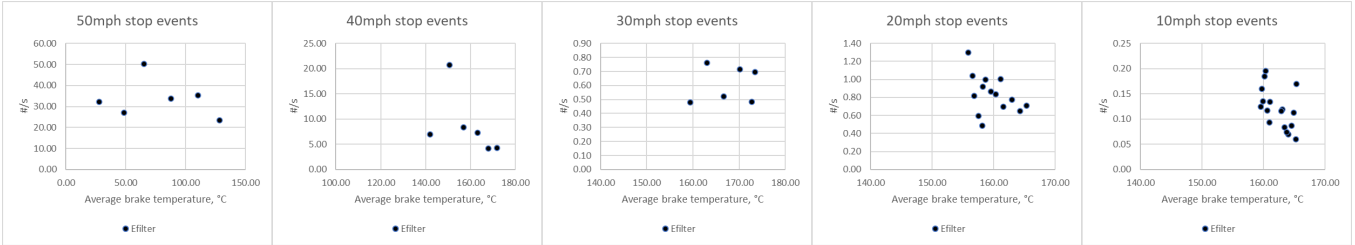

As would be expected, there is a clear relationship of increasing particle number (and mass) emissions with the product of peak braking speed and brake pressure in bar (Figure 5-57). The higher rotational speed of the wheel at higher road speeds and greater braking force will supply more energy to the braking system.

Figure 5-57: Particle emissions rate correlates with max speed * brake Pmax

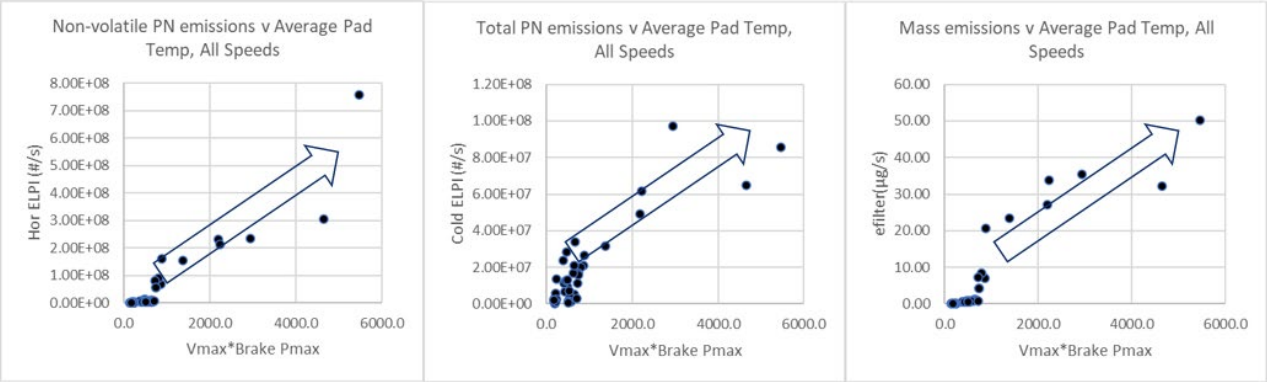

5.3.3.4 Test Track Experiment#2: Extreme Braking

The original objective of the second track experiment was to generate particle emissions at a higher level than observed in the moderate track braking experiment. This was to be achieved by using repeated, more aggressive, “emergency stop-like” braking events at different speeds. Two measurement sets were made, one from ~900s to 1500s and the other from ~1900 to 3050s. Both sets were also viewed holistically to create “drive cycles” for determining particle size distributions and overall particle number concentrations.

For this measurement set, only the ELPI systems were used due to a temporary issue with the eFilter. As Figure 5-58 shows for the first measurement set, brake pressure can be used to discriminate aggressive braking events (high spike above 20 bar) from braking events when the vehicle is turning or getting into position.

Figure 5-58: Speed v time and braking pressure (bar) for the moderate braking experiment on the test track

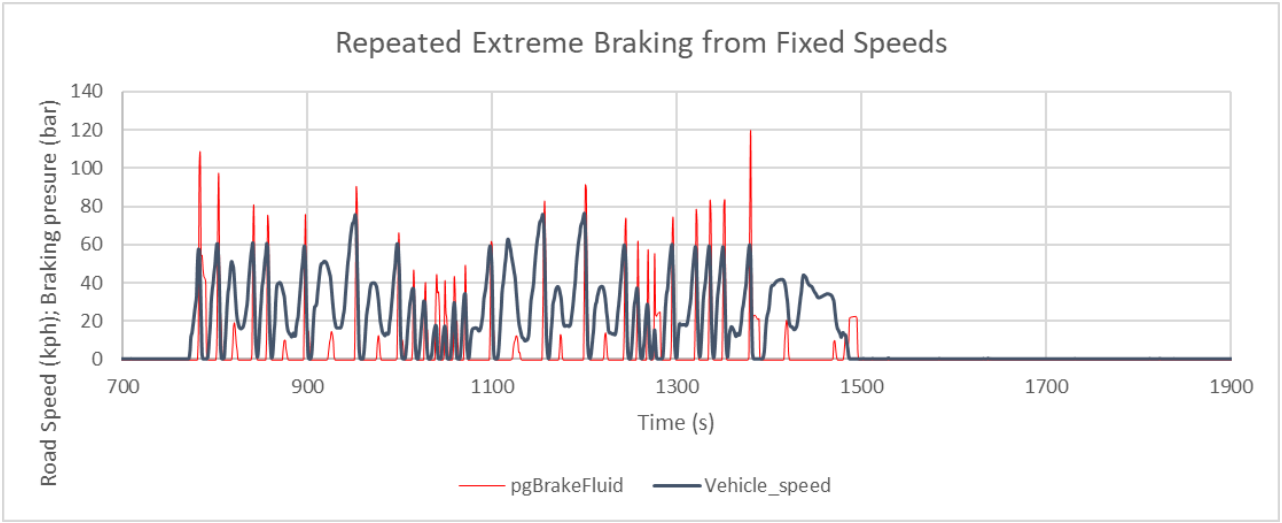

The more aggressive braking events have a marked impact on the temperatures of brake discs and pads on both left-hand and righthand (enclosure) wheels, while the lower (<20bar) braking events do not, as Figure 5-59 shows. It appears that, with the current pad/disc combination on the Caddy, when the brake disc temperature reaches almost 400°C (~1350s) and the brake pad temperature reaches ~300°C the individual braking events are no longer easily discriminated in the particle number emissions. This may indicate that the brake pad reaches a temperature at which some constant thermal release (outgassing) of materials occurs independent of braking. This is borne out by the continuing, but decreasing, emissions of both cold ELPI and hot ELPI PN after the cessation of driving shown in Figure 5-59 from ~1500s. The cold and hot ELPI emissions

converge at ~1750s indicating that outgassing of volatiles from the pad has ceased. These effects make it difficult to extract much individual braking peak data from the exercise.

Figure 5-59: First set of extreme braking measurements

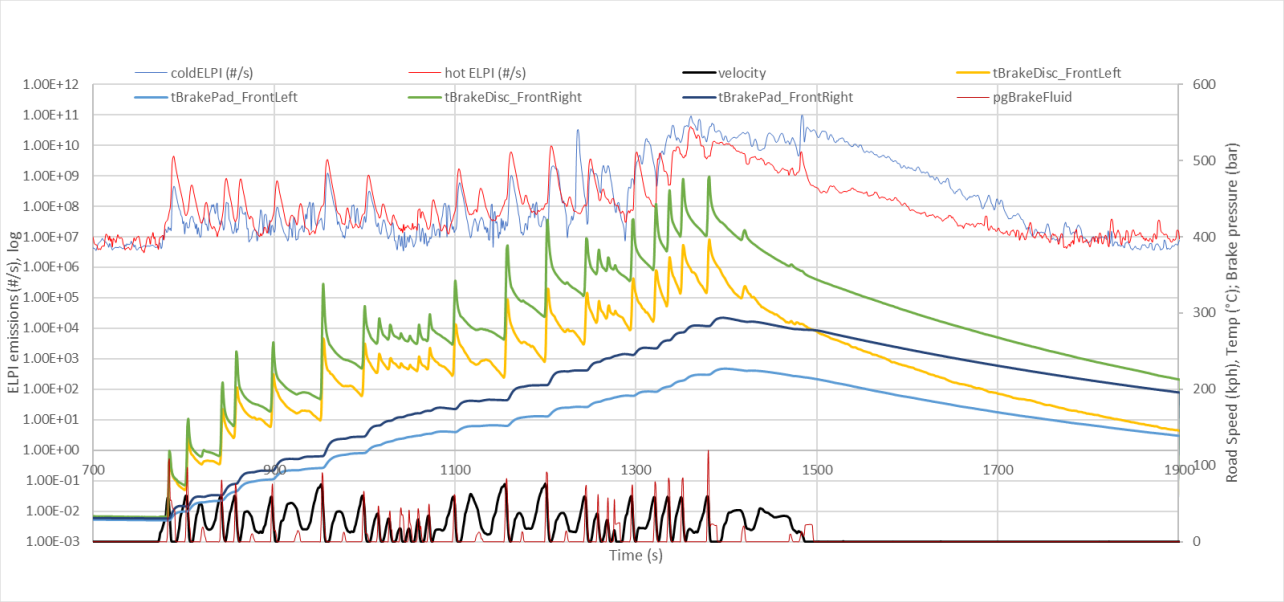

However, the early part of these data does allow us to compare two similar braking events taken at different times and with very different brake pad/disc/ enclosure temperatures. Figure 5-60 shows that braking event 1 from 50kph occurs at ~785s, with disc temperature at ~120°C and pad temperature at ~30°C. Braking event 2, occurs at ~1100s with disc temperature at ~350°C and pad temperature at ~175°C. Despite these large differences in pad and disc temperatures the cold and hot ELPI PN emissions from the two events are broadly similar, and at third braking event at intermediate time (~1000s) and temperatures also has similar PN emissions.

Given that PN levels appears to be almost independent of pad and disc temperatures up to a pad temperature of ~300°C, this may indicate that an enclosure with pad and disc temperatures 50°C – 70°C higher than the opposite wheel may still produce representative brake particle emissions measurements.

Figure 5-60: Two braking events with different pad and disc temperatures giving similar PN emissions

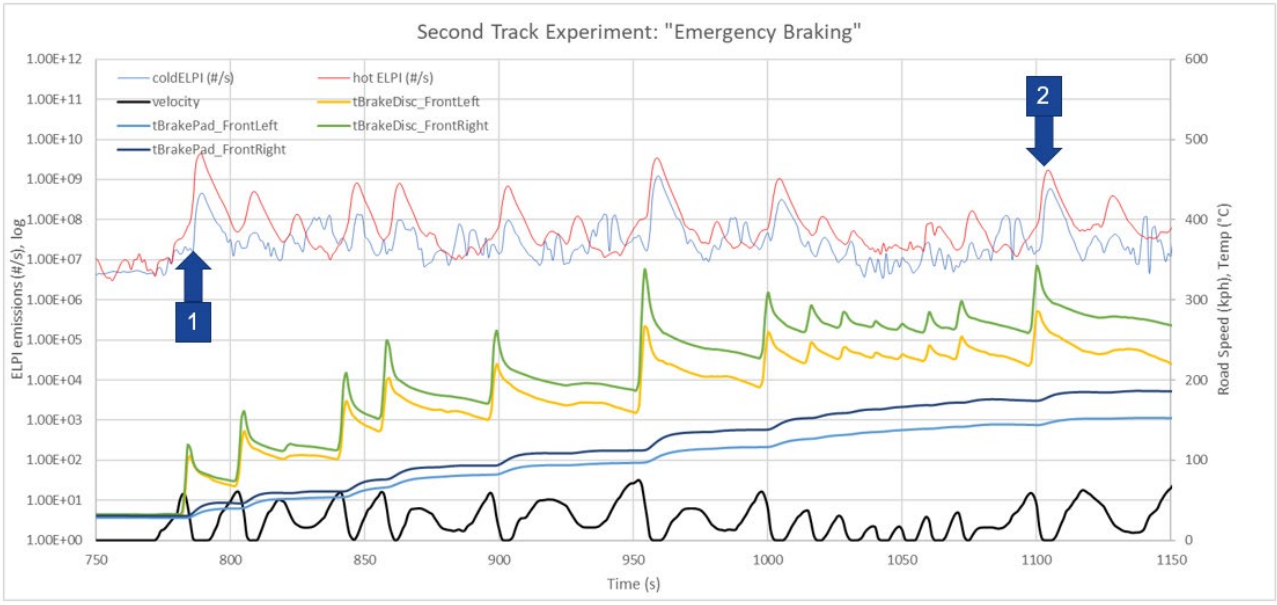

The eFilter, cold ELPI and hot ELPI were all used to measure particle emissions during the second data set. As Figure 5-61 shows, pad and disc temperatures continue to rise, PN and PM emissions (dotted line, eFilter) do not return to baseline between braking occurrences, and it is not possible to discriminate emissions from individual braking events. These data were only used for the cumulative emissions and particle size distributions comparisons.

Figure 5-61: Second set of extreme braking measurements

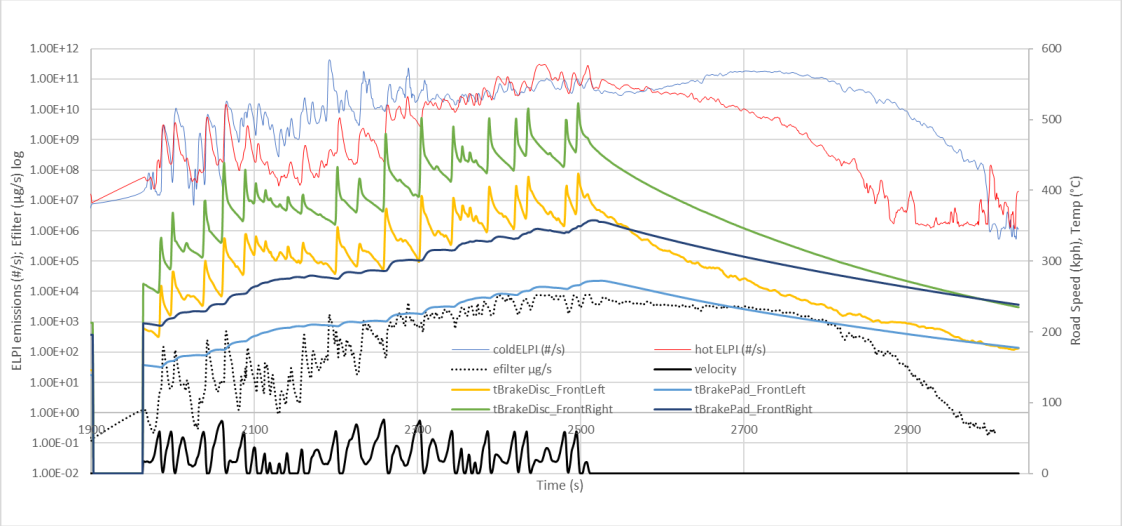

5.3.4 Brake Particle Emissions and Size Distributions Compared Between Drive Cycles

Comparative particle number (Figure 5-62, left) and eFilter particle mass (Figure 5-62, right) emissions are shown below. For both cold and hot ELPI, particle number emissions from urban, PG-42 and moderate track braking experiments are broadly similar, but emissions from the extreme braking events are 1-3 orders of magnitude higher. eFilter mass emissions increase by a factor of >300 with the braking events in extreme set 2 compared to the moderate track experiment.

Very high particle mass and number emissions can be generated by repeated aggressive braking events over a short duration. Cumulative energy fed to the pads and discs appears to result in quasi-continuous release of particulate materials which would likely fail any regulatory limit. This braking behaviour is almost certainly unrealistic for normal road use, but some more aggressive braking and more frequent braking behaviour might be seen with certain drivers under certain conditions. It would be useful to define some boundaries for what represents aggressive driving (analogous to driving above the RDE v*apos95 limits for tailpipe emissions) and what would be classified as abusive driving (i.e., that which might be performed only to intentionally generate unrealistically high levels of particle emissions).

Figure 5-62: Averaged cumulative #/km emissions all cycles

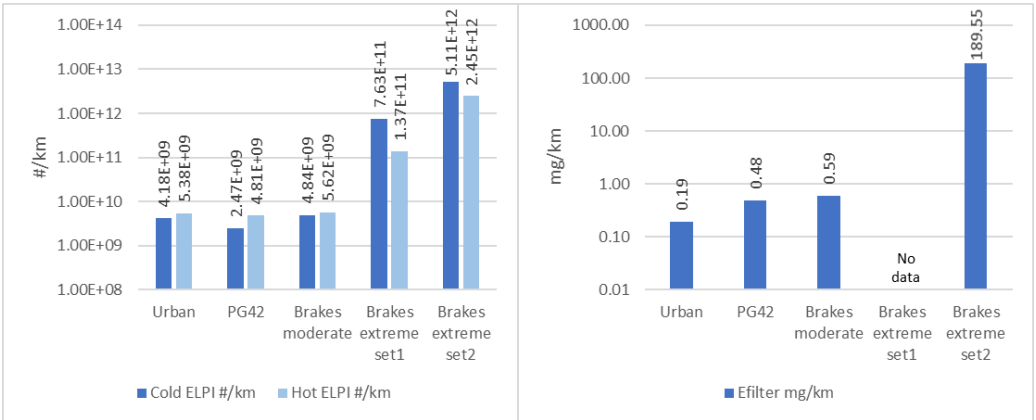

Average particle size distributions during urban cycles, PG-42 cycles, the moderate track experiment and both extreme track sets are shown in Figure 5-63 for hot ELPI data and Figure 5-64 for cold ELPI data. From left to right each figure shows: all size distributions on a log y-axis, all size distributions on a linear y-axis and all size distributions on a down-scaled linear y-axis with the x-axis scaled to show a narrower size range (> 0.1µm).

Figure 5-63: Hot ELPI size distributions, all cycle types, average data

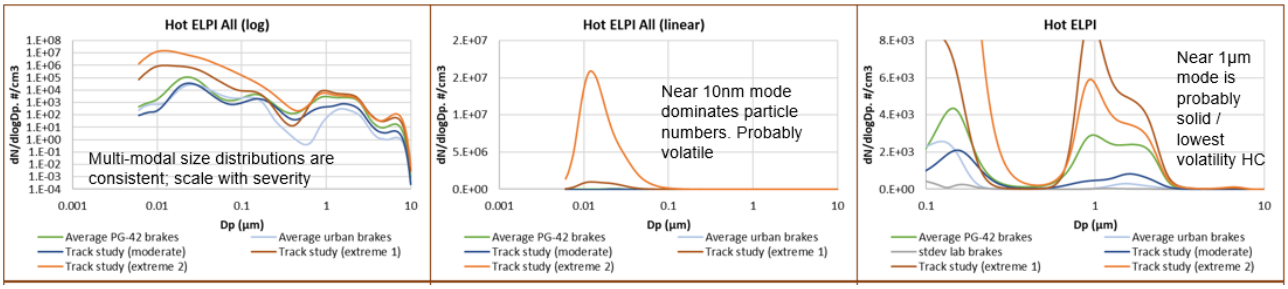

Hot ELPI particle size distributions are consistent between all the driving cycles, with just the magnitude varying. The heating approach of the instrument appears to stabilise the aerosol. The urban, PG-42 and moderate track size distributions appear to show broadly similar particle concentrations below 0.2µm, with emissions from the extreme sets 2-3 orders of magnitude higher. In the size range above 0.5µm it's clear that there is a bimodal distribution of predominantly non-volatile particles.

Cold ELPI particle size distributions are less well defined but are discriminated in magnitude similarly to the hot ELPI size distributions. One major difference seen with the cold ELPI is the greater abundance in volatile material seen in the particles present between ~10nm and 100nm. While particle concentrations are broadly the same, mean particle size in the cold ELPI is much larger. The similarity of size distributions in the >0.5µm region is also diminished relative to the hot ELPI data, indicating that volatiles are present in this size range.

Figure 5-64: Cold ELPI size distributions, all cycle types, average data

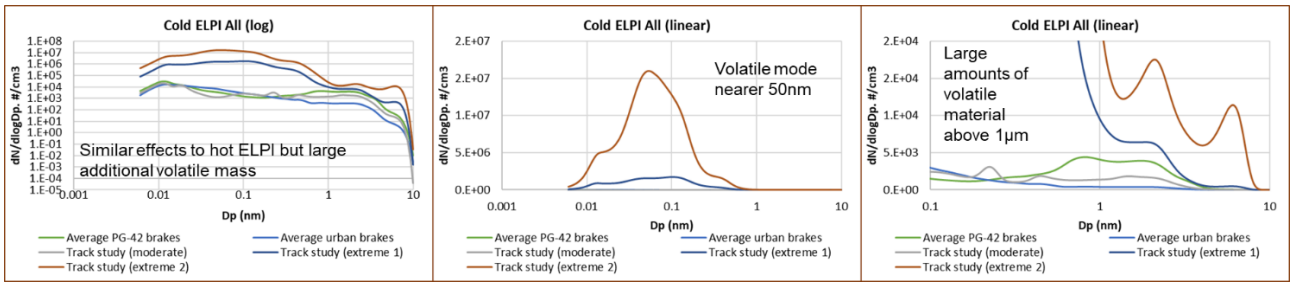

- Heat treatment of brake particle emissions during hot ELPI measurement can create similar / standardised particle size distributions even across wide concentration ranges. For a consistent and repeatable non-size specific particle number measurement, it would appear wise to aggressively thermally condition / remove the volatiles, such as in the PMP approach. A second measurement is then required to ensure that volatile particles/materials are also considered. This could be a mass measurement that captures both solid and particle phase volatile materials, such as an eFilter.

5.3.5 Tyre emissions: repeatability and measurements

5.3.5.1 PG-42 Cycles Tyre Emissions

Average, standard deviation and CoV tyre particle mass and number emissions from the 9 chassis dynamometer-tested PG-42 cycles are shown in Table 5-14. The PM (corr) data has the A27 background subtracted (corrected for cycle time). It should be noted that unlike the measurements from the brake enclosure, into which all the particles are emitted during and following a braking event, these measurements reflect what is sampled through the scoop inlet that is facing a small area of the total circumference of the tyre, and this is unlikely to be representative of the entire emissions of the tyre from the braking event as discussed in 5.2.6.2. The likely relationship between the measured sample and the total tyre emissions is considered in 5.6.2.

Table 5-14: Average, standard deviation and CoV tyre emissions from the PG-42 cycle

	PM (corr)[10], mg/km	PM (uncorr), mg/km	eFilter, mg/km	Cold ELPI (/1e9), #/km	Hot (180°C) ELPI (/1e9), #/km	Hot (350°C) SPCS (/1e9), #/km
Tyre-PG-42 mean	0.034	0.067	0.056	3.33	0.55	1.12
Tyre-PG-42 STDEV	0.012	0.012	0.010	3.67	0.35	0.30
Tyre-PG-42 CoV	36.3%	18.5%	18.2%	110.2%	62.8%	27.0%

Figure 5-65 shows that real-time emissions spikes of particle mass (eFilter) and particle number (SPCS) both correspond to braking events in the speed time trace, and to brake pressure rises. This is clear evidence that tyre-derived non-volatile particle emissions are measurable on the chassis dynamometer above any facility background. It is also apparent that any background is relatively stable during the cycle as seen during the cruise events (for example, from ~1400s to ~2000s). PN background is of the order $1.2x10^7$ #/s and eFilter background 1 µg/s.

Figure 5-65 Real-time tyre particle mass (eFilter) and number (SPCS) emissions from PG42 cycle

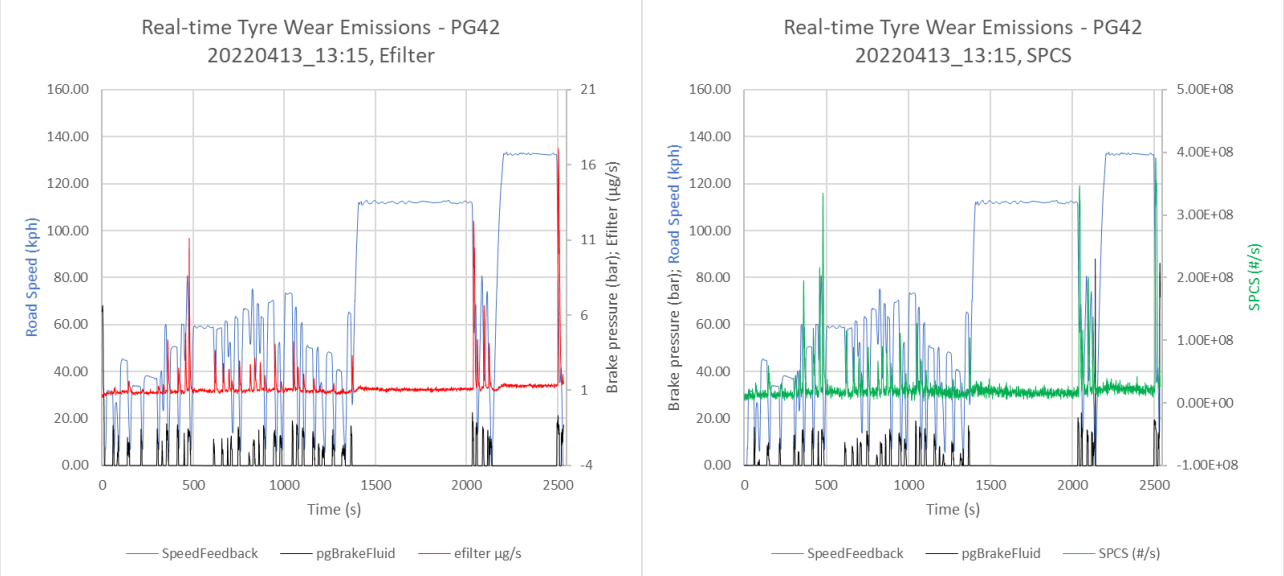

While emissions of non-volatile particle number and mass from tyres during the PG-42 cycle seem to be clearly related to braking events, particles of different volatilities may affect both cold ELPI and hot ELPI emissions. Figure 5-66 (left) shows that for the cold ELPI there are many spikes of particle emissions during the PG-42 cycle, both during braking events but also during accelerations and cruises. Many of the spikes seen during cruises are similar in magnitude to those seen during braking events. Background levels are of the order $2x10^7$ #/s. This is an order of magnitude lower than the $1.88x10^8$ #/s average tyre backgrounds measured on-road (Table 5-10). The hot ELPI emissions profile appears more similar to that of the SPCS, and many of the braking events are observed, particularly those at highest braking pressures. However, there are also some additional spikes of particles that appear during cruises Figure 5-66 (right).

[10] Ambient PM background from the VERC at ~0.06µg/s

Figure 5-66: Real-time tyre particle number (cold and hot ELPI) emissions from PG42 cycle

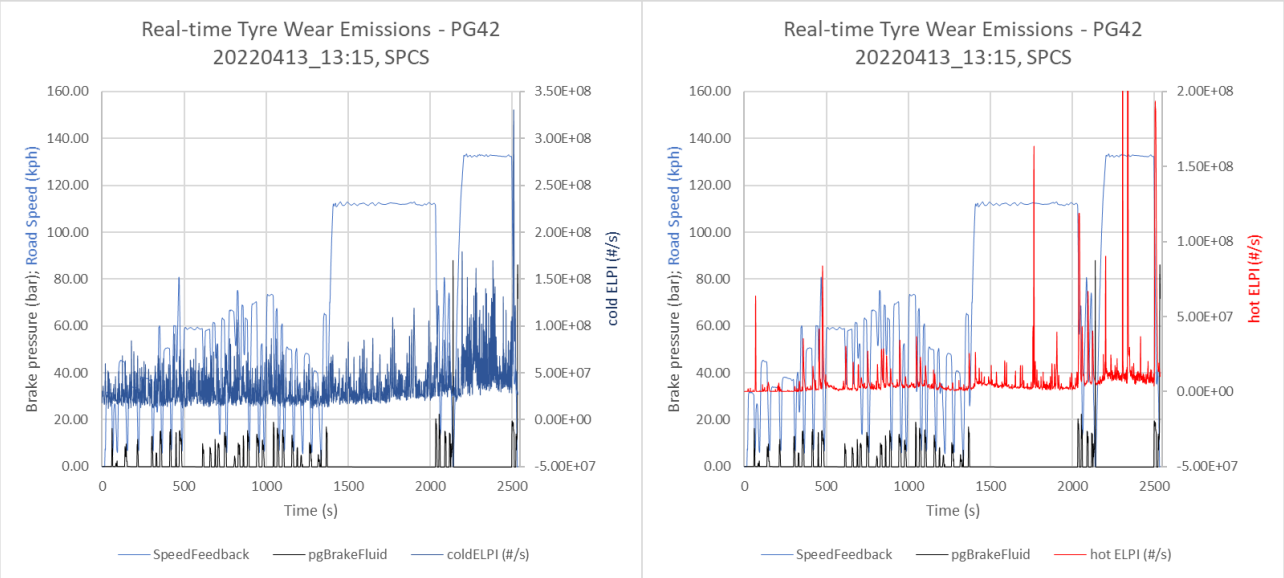

During PG-42 tyre testing, the highest repeatability levels were observed from the mass measurements, PM (uncorrected) and eFilter, (~20% CoV) with the SPCS most repeatable of the number metrics and the hot ELPI more repeatable than the cold ELPI (~63% and ~110% respectively).

Collected filter masses, and per km emissions, were much lower than observed from brake testing. This is apparent in Figure 5-67 which shows the light-grey particulate material that was collected, this compares starkly with the deep black brake emissions filters shown in Figure 5-31. The grey colour may indicate finely divided tyre materials, but also some low volatility materials, for example partially pyrolyzed HC.

PM emissions measured by the GF/A filter method and eFilter were much closer than observed with the brake emissions. This may indicate that the average density of the materials sampled (e.g., rubber) is closer to that of soot than the material collected during the brake tests. There may also be substantially more volatile contribution to the PM with tyre emissions than with brake emissions, which would bring the average density down.

Figure 5-67: Three repeat PM filters from PG-42 tyre testing

A thermogravimetric analysis of the tyre-derived PM material collected during a PG-42 cycle (Figure 5-68) showed that non-volatile components were dominant: 63% remainder materials (non-volatile at 550°C and non-oxidisable in air at 550°C), so potentially steel and inorganic materials plus ~2% carbon. The remaining 35% of the PM mass comprised water and general volatiles. These volatiles could be decomposed rubber, oils, resins, plasticizers etc.

Figure 5-68: Results of thermogravimetric analysis of PG-42 tyre filter

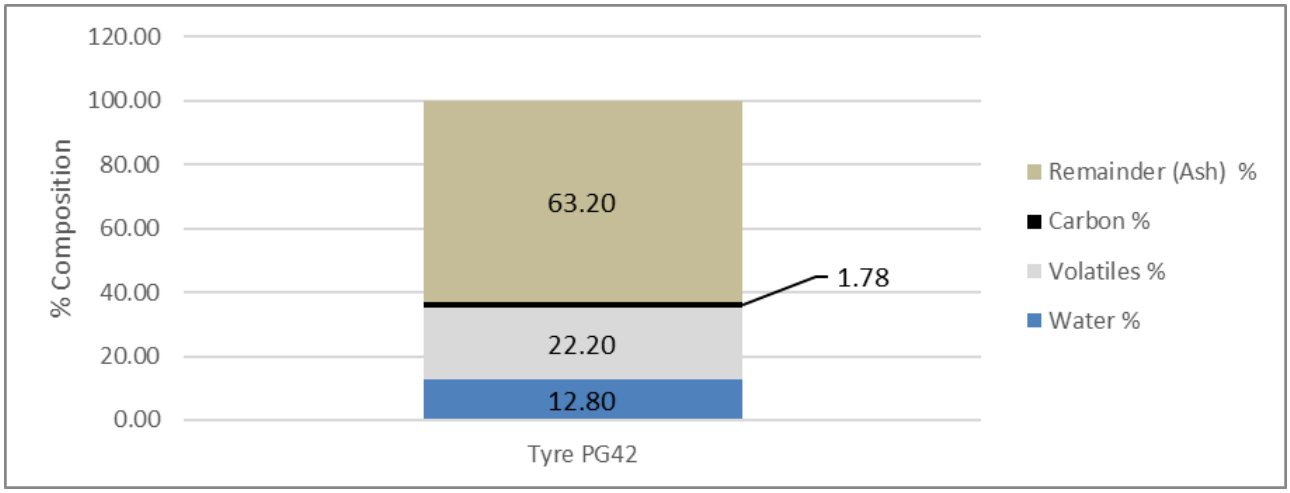

The residual material on the filter post thermogravimetric analysis is a whiteish-pink (Figure 5-69) indicating that the non-volatile mass may contain iron (III) oxide and some white inorganic materials. It does not appear that any substantial quantity of rubber survives the thermogravimetric analysis, so this must contribute to the fraction of tyre-derived PM identified as volatiles. It is possible that there is some contribution of brake wear to the measured PM from tyres in these experiments. However, the probability of this is diminished since the brake system is completely enclosed on the wheel that is being sampled for tyre wear.

Figure 5-69: Residual material on tyre PG-42 PM filter section post TGA analysis

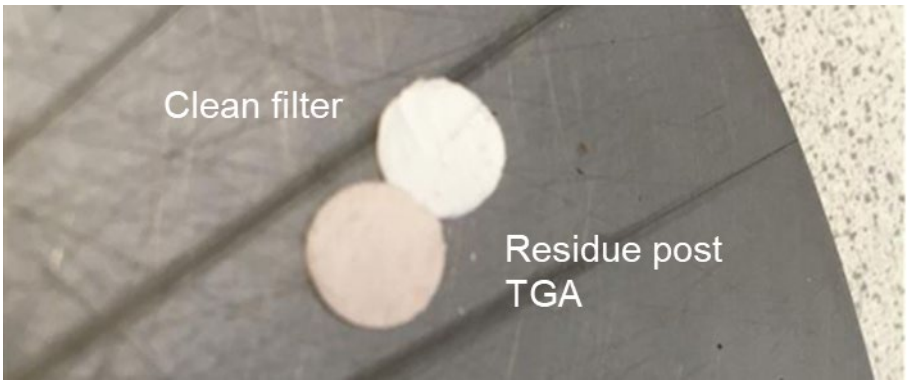

5.3.5.1.1 PG-42 Tyre Particle Emissions Repeatability

Emissions levels from the nine individual PG-42 tyre emissions tests with both ELPI and SPCS are shown in Figure 5-70 left, with eFilter data shown in Figure 5-70 right. These results reflect the trends shown for PG-42 brake emissions measurements (Section 5.3.3.1.1) which revealed sporadic high PN emissions from the cold ELPI leading to high variability, more consistent results from the hot ELPI and most consistent PN from the SPCS. The eFilter also produced consistent results. The 4th test in sequence showed results that were amongst the lowest or were the lowest recorded by the various instruments from the sequence of 9 tests. There were no indications this was not a legitimate test result.

Figure 5-70: Individual PG-42 repeat tests' tyre PN and PM results

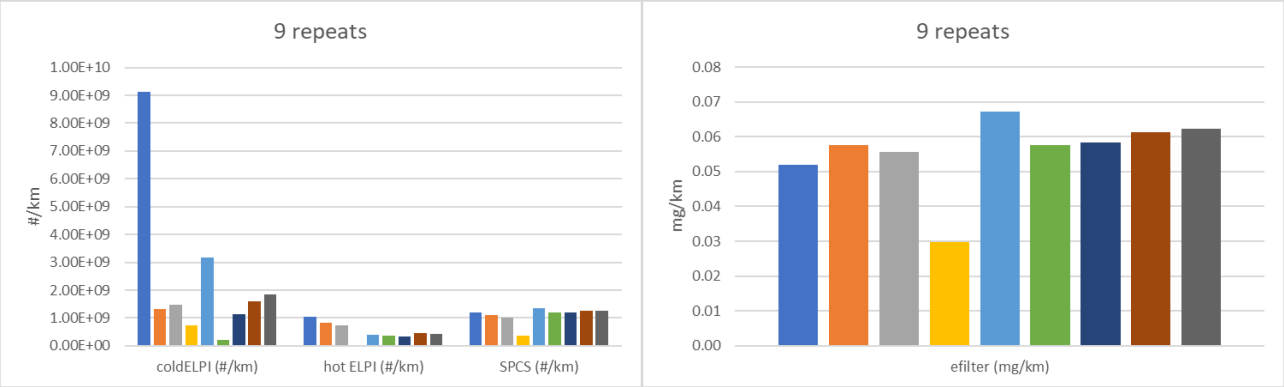

Using the same colour scheme as Figure 5-70, Figure 5-71 (upper) shows brake pressure repeatability for 3 PG-42 tests (2nd, 3rd and 4th in Figure 5-70) conducted on the same day, with the lower figure showing tyre particle number emissions from the SPCS. There is no evidence of consistently lower brake pressures, but non-volatile PN emissions are lower throughout the cycle.

Figure 5-71: One PG-42 Cycle shows lower tyre PN emissions despite similar braking pressures

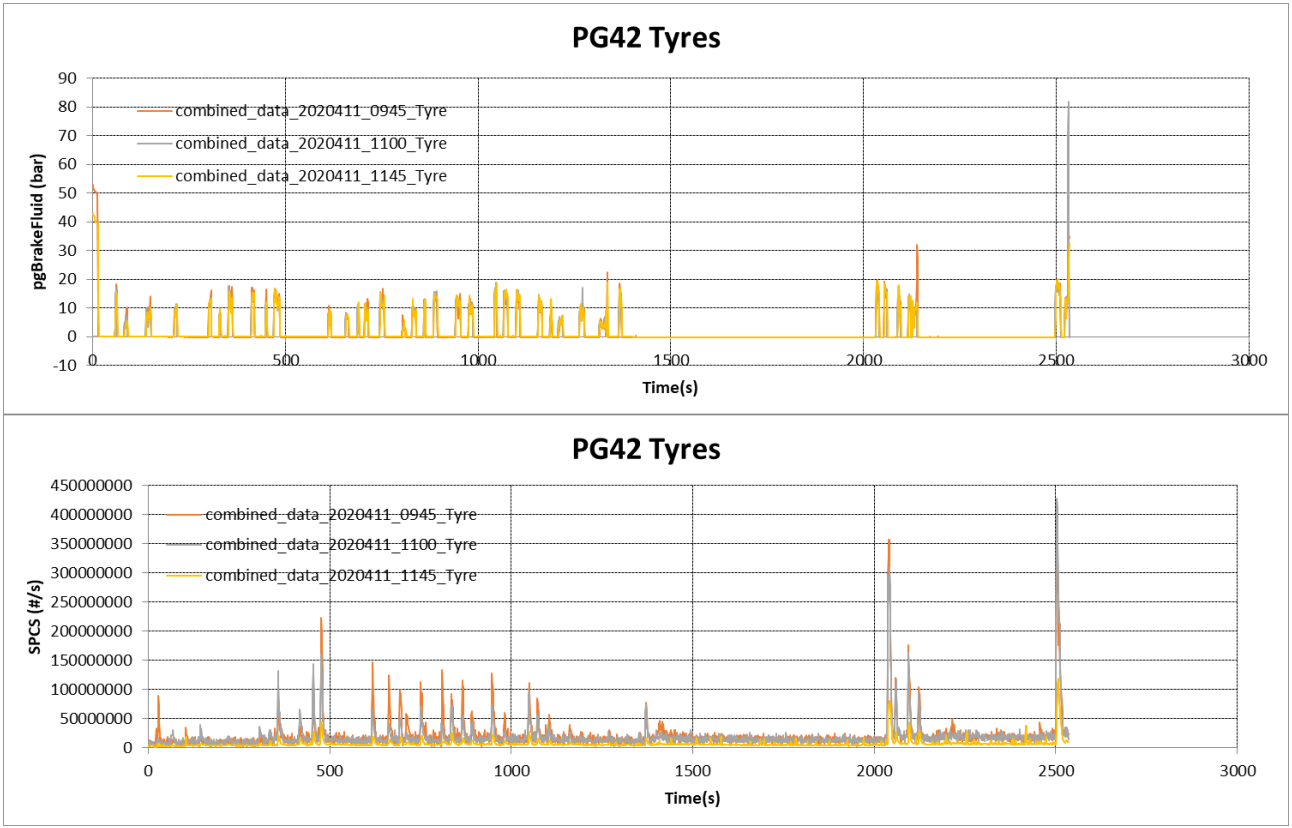

5.3.5.1.2 PG-42 Tyre Particle Size Distributions

Particle size distributions from two PG-42 tests conducted on the same day, and with both hot (shown in red) and cold ELPIs (blue), are shown on a log scale in Figure 5-72 left and on a linear scale in Figure 5-72 right. Test order is shown with greater line thickness denoting an earlier test.

Figure 5-72: Example repeat PG-42 tyre particle size distributions

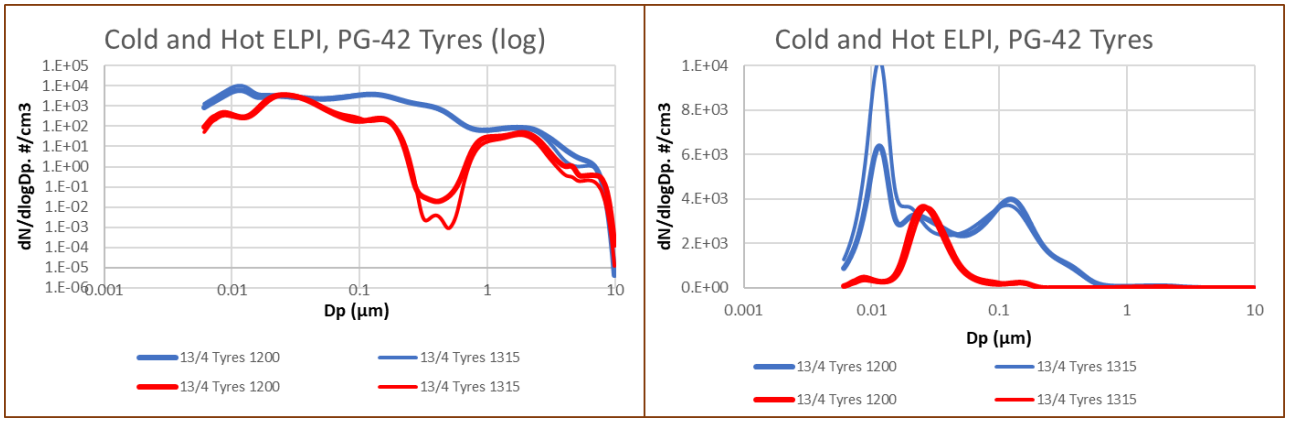

In general, hot ELPI size distributions are lower in magnitude than cold ELPI across the size range, excepting between approximately 25nm (0.025µm) and 35nm. This indicates that a substantial amount of material is being removed by the 180°C heating mechanism of the hot ELPI, and so this material must be of reasonably high volatility (perhaps similar to the light fractions of diesel or heaviest components of gasoline). Some of this material recondenses in the 25nm – 35nm region, but this would represent very little of the evaporated mass. The third of the three tests shows the highest levels of <100nm particles, which must be volatile. These are very effectively removed by the hot ELPI.

As was seen with the brake measurements, the heating aspect of the hot ELPI stabilises the particle size distribution, but this results in some restructuring of the volatile materials. To avoid this restructuring and to ensure a standardised non-volatile particle metric, a more aggressive volatile removal approach would be required.

The hot ELPI shows 3 groups of modes at around 10nm, between 10nm and 100nm and above ~0.4µm (Figure 5-73). Data are relatively consistent between repeats, but there is mass redistribution from the mode around 30nm to the mode at around 10nm, indicating that excepting perhaps the >0.4µm region, where PN levels are very low, the hot ELPI size distributions undergo significant changes during sampling.

Figure 5-73: Magnified particle size distributions from hot ELPI PG42 tyre measurements

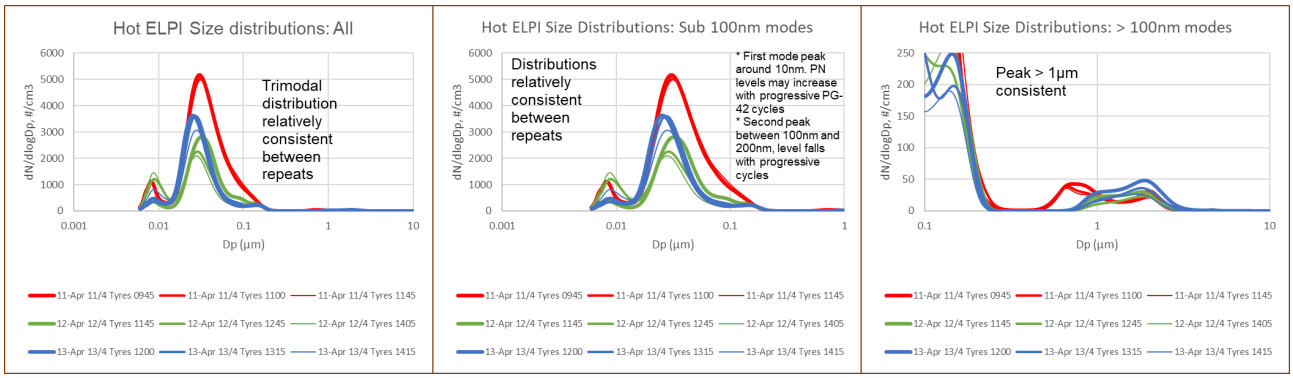

The cold ELPI size distributions are much more variable than the hot ELPI data, except in the region above 1µm where PN levels are very low. While it might be possible to discriminate between background and wear in this region, it is unlikely that a regulation could be established addressing only the few particles present above 0.5 or 1µm due to the complexities of sampling and measurement in this distinct size range.

Figure 5-74: Magnified particle size distributions from cold ELPI PG42 tyre measurements

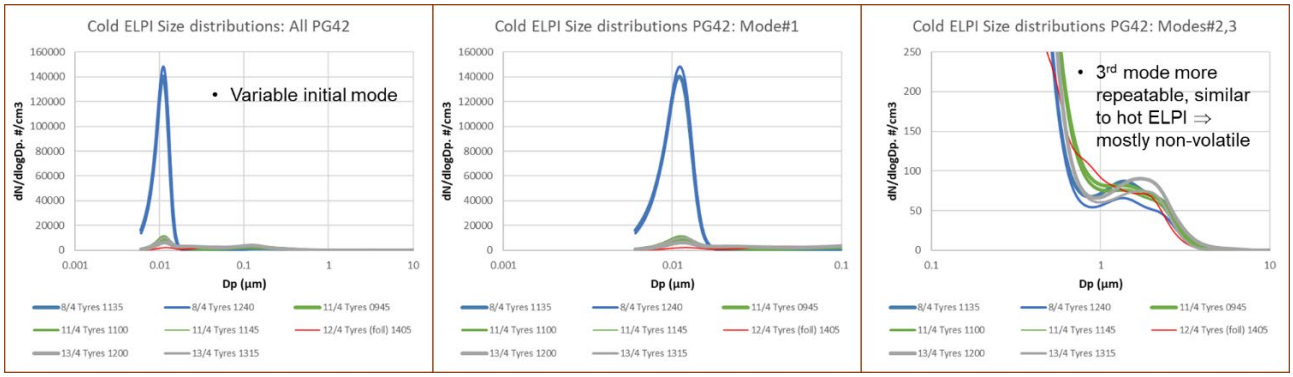

5.3.5.1.3 Comparative magnitudes of PG42 tyre PM and PN emissions, and background

Figure 5-75 shows average unit/km emissions of mass and number metrics from PG-42 tests. Results illustrated are corrected for (PM filter), or show, a facility background taken on a different day.

Mass emissions from the PM filter and eFilter are well below 0.1 mg/km, with corrected eFilter and PM filter results broadly similar at ~0.03 mg/km. Both PM and eFilter measurements are above background levels. Similarly, mean PN emissions from cold ELPI, hot ELPI and SPCS are all above background levels. It should be noted that the SPCS was not available for the background measurements, but it is assumed that background levels would be similar to, or lower than, the hot ELPI.

Mean PN emissions from the cold ELPI were substantially higher (~3x10^9 #/km) than the hot ELPI and SPCS emissions, though the scatter of data was very large, and the differences were not significant. Best repeatability was observed with the SPCS at emissions of ~1x10^9 #/km and comparing non-volatile particle emissions would appear to be the most reliable method for discriminating between emissions of different tyre types.

- Background correction may not be appropriate or relevant in the test facility and this needs further study. For example, the materials sampled in the facility with all wheels stationary, may not be the same materials as collected on the filter or by real-time instruments during a test. During test execution a proportional fan is running, and test cell air exchange is rapid, but this is not the case when the vehicle is stationary. Outgassing from the tyre opposite the scoop might displace ambient aerosol, so that background is not sampled during those braking events. If this was the case, subtracting a background for the whole test duration would be excessive.
- If background should be subtracted, then facility design could be optimised to minimise ambient contributions during the test.

Figure 5-75: Mean PM & PN tyre emissions from (blue) and background (grey) from PG-42 braking tests

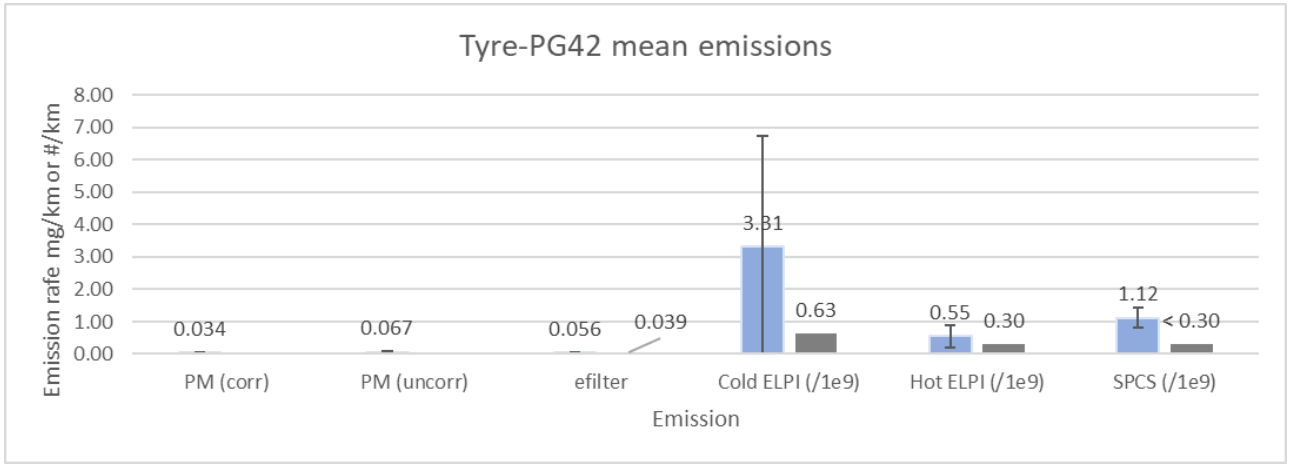

5.3.5.2 Urban Road Tyre Emissions

Tyre measurements were made from 4 repeat urban drive cycles with the cold and hot ELPI, and the eFilter. From selected tests PM filters were collected. Additionally, two tests on the same day were combined to sample and determine a mass weighted particle size distribution using the cold ELPI.

The coincidence of brake pressure increases (and decelerations) and particle emissions spikes for the on-road urban drive cycles is shown in Figure 5-76. These figures show that while some urban braking events register an emissions response, not all do, and other peaks can also be found during the drive cycle that are not related to instantaneous braking events. In general, the eFilter and hot ELPI better reflect the braking events than the cold ELPI. Qualitatively, the relationship between braking and emissions spikes with the real-time PM and PN systems was substantially poorer than observed for tyre measurements with the PG-42 cycle, and also poorer than observed for the urban cycle brake measurements.

Figure 5-76: Real-time tyre particle number (cold and hot ELPI) emissions from urban cycles

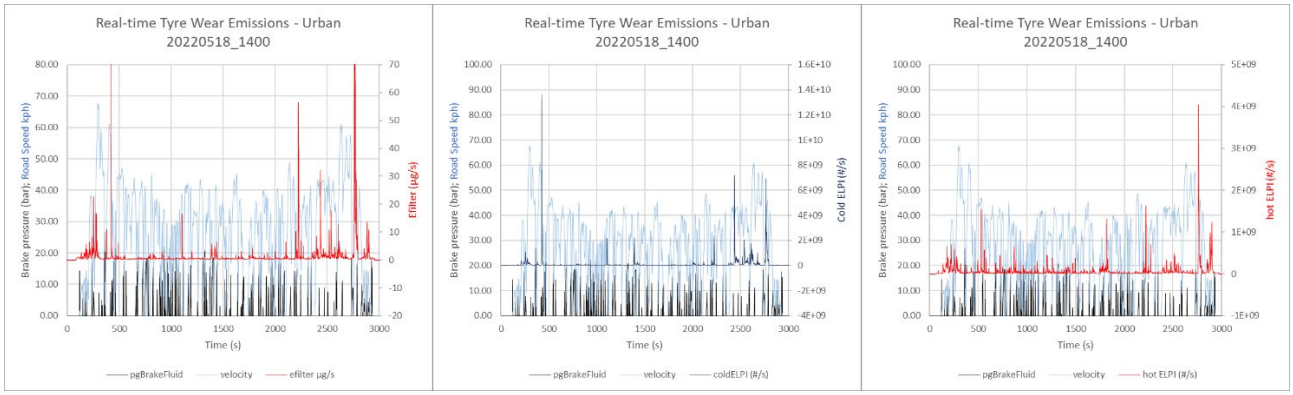

5.3.5.2.1 Urban Cycle Tyre Particle Emissions Repeatability

Average, standard deviation and CoV tyre particle mass and number emissions from the on-road urban cycles are shown in Table 5-15 and Figure 5-79. The PM (corr) data is background subtracted according to the value shown in Table 5-11.

The repeatability seems generally good, from <15% CoV for mass approaches to a maximum of ~40% from the cold ELPI. However, eFilter and cold ELPI masses were lower than typical backgrounds. It is likely that there were both volatile and non-volatile components in the background leading to this effect, as discussed below. Hot ELPI emissions were lower than the background, but it is probable that volatile components present in the background are still contributing to reported ELPI emissions levels: for example, these may restructure from large particles to the 10nm to 100nm mode within the hot ELPI.

Table 5-15: Average, standard deviation and CoV tyre emissions from the Urban cycle

	PM (corr)	PM (uncorr)	eFilter	Cold ELPI (/1e9)	Hot ELPI (/1e9)
Brake-urban mean	0.753	1.608	0.247	13.53	18.50
Brake-urban STDEV	0.120	0.176	0.032	5.61	6.22
Brake-urban CoV	16%	11%	13%	41%	34%
Background mean	-	-	0.431	28.33	7.79

Figure 5-77 shows two PM filters, each collected from a pair of urban on-road drive cycles. The grey colour of the filters is not dissimilar to that seen from the chassis dyno brake testing filters (Figure 5-67), but this does not guarantee that colouration derives solely from tyre wear. The grey colour could come from background diesel soot, brake wear, or asphalt dust as well as from tyre wear. The speckled nature of the filters suggests

that some additional large particles of dust or grit are being sampled. This speckling was not observed on the chassis dyno and so the large particles are unlikely to be from real-time tyre wear, and may be road dust of various compositions.

Figure 5-77: Two repeat PM filters from Urban Cycle tyre testing – each collected from two urban cycles

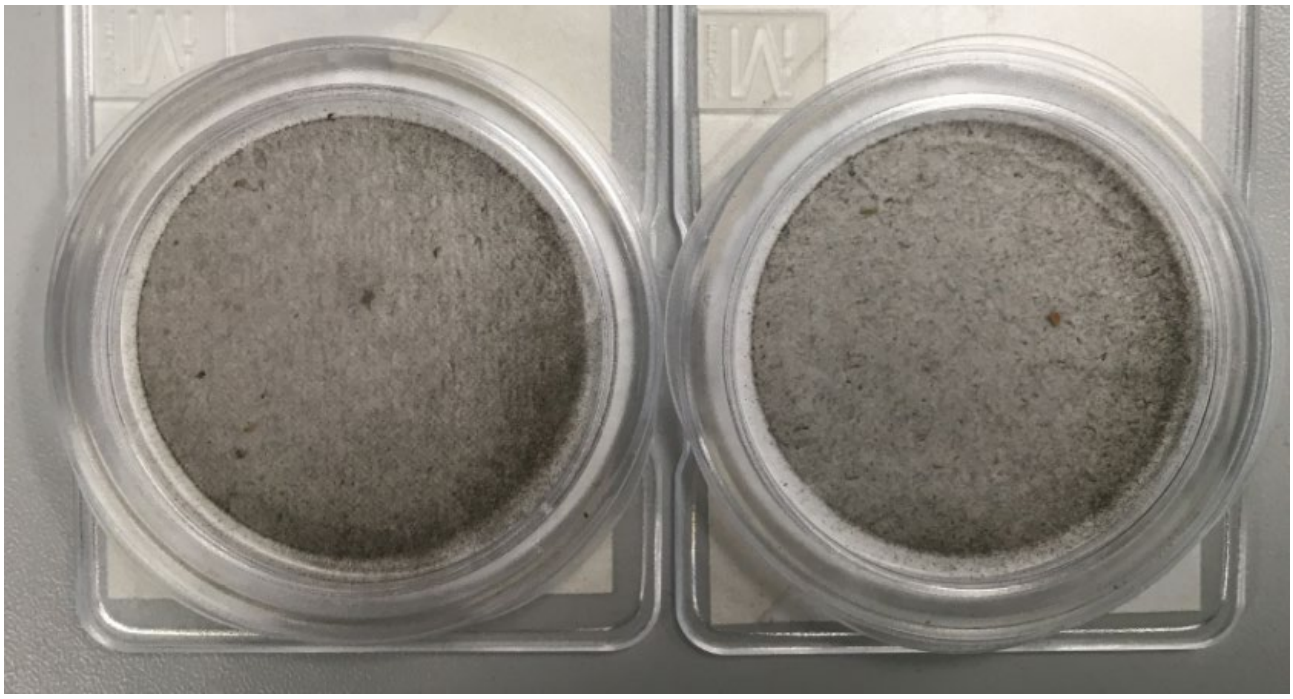

A thermogravimetric analysis of an urban tyre test filter revealed a substantially higher remainder (non-volatile, non-carbon) fraction of the PM than observed from the chassis dynamometer PG-42 test (Figure 5-78). This suggests that some non-volatile materials that are not derived from the tyre are being sampled

Figure 5-78: Results of thermogravimetric analyses of PG-42 and urban tyre filters

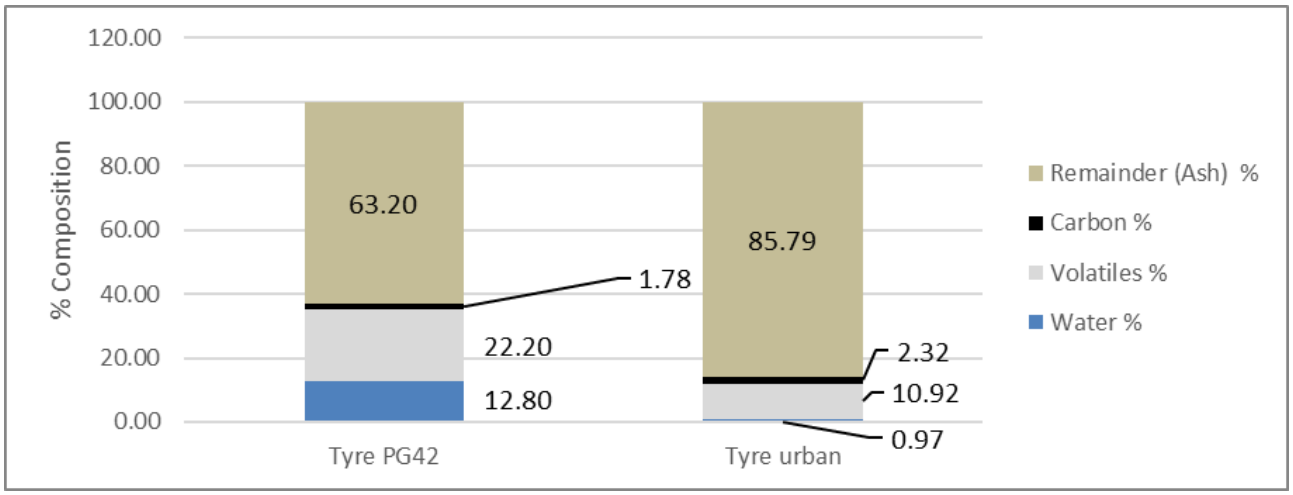

As Figure 5-80 shows, PM emissions were higher from the filter-based method than from the eFilter, at 0.75 mg/km (corrected) or 1.6mg/km (uncorrected). This contrasts from the PG-42 on-dyno test results (Figure 5-75) where emissions levels were more similar between filter and eFilter, but also much lower (typically < 0.06 mg/km). This suggests that the on-road urban tyre tests either produced a great deal more tyre wear, or the samples contain materials not released by the tyres. Since the braking events in the PG-42 cycle were selected to maximise emissions, and the urban drives take place in normal traffic, it is most likely that non-tyre emissions are the source of the additional mass.

PN measurements showed slightly higher emissions from the hot ELPI than the cold ELPI, though these were statistically similar at between 1 and 2 x10^{10}#/km. For the cold ELPI, PN emissions were ~4x higher than from the PG42 cycle and for the hot ELPI ~35x higher. Size distribution measurements with the ELPIs (Figure 5-79) show that the urban drives have higher levels of particles present in both the 10-100nm size range and above 2-3µm.

Figure 5-79: Urban and PG-42 tyre emissions, cold and hot ELPI

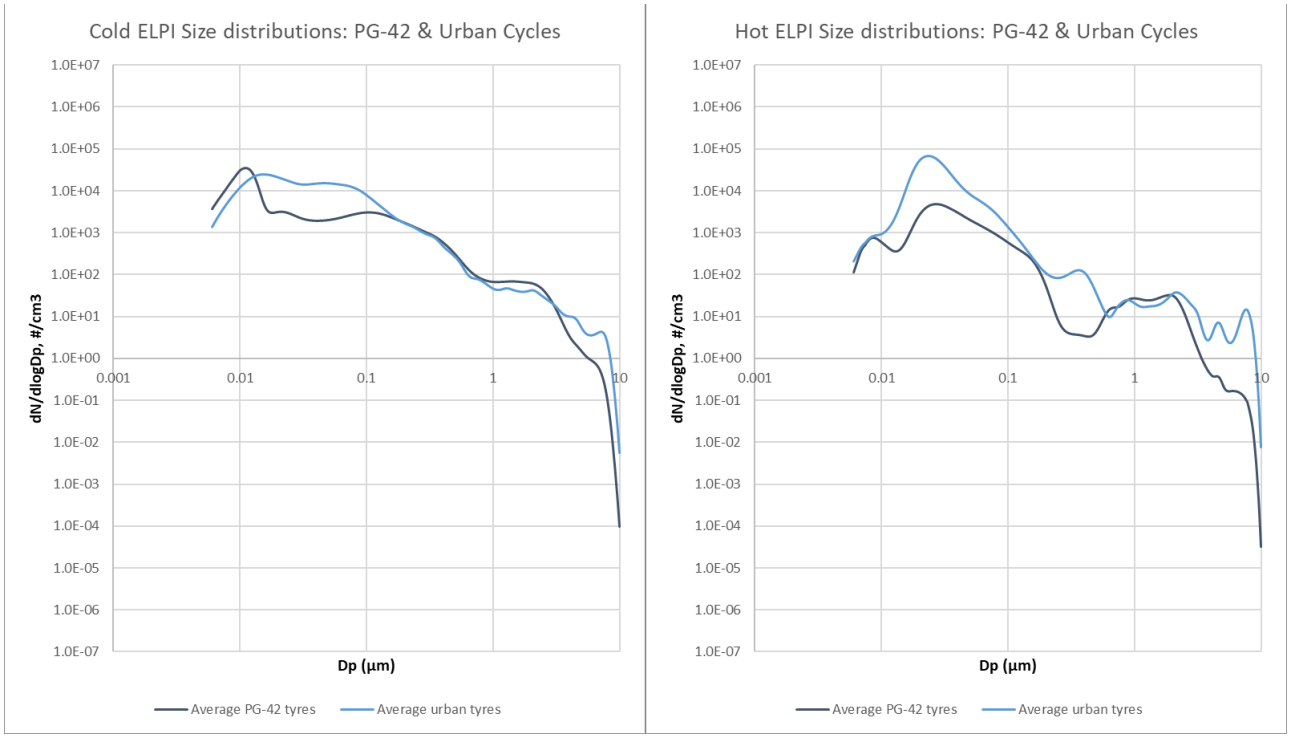

Figure 5-80: Mean PM and PN emissions from Urban Cycle braking tests, with typical backgrounds

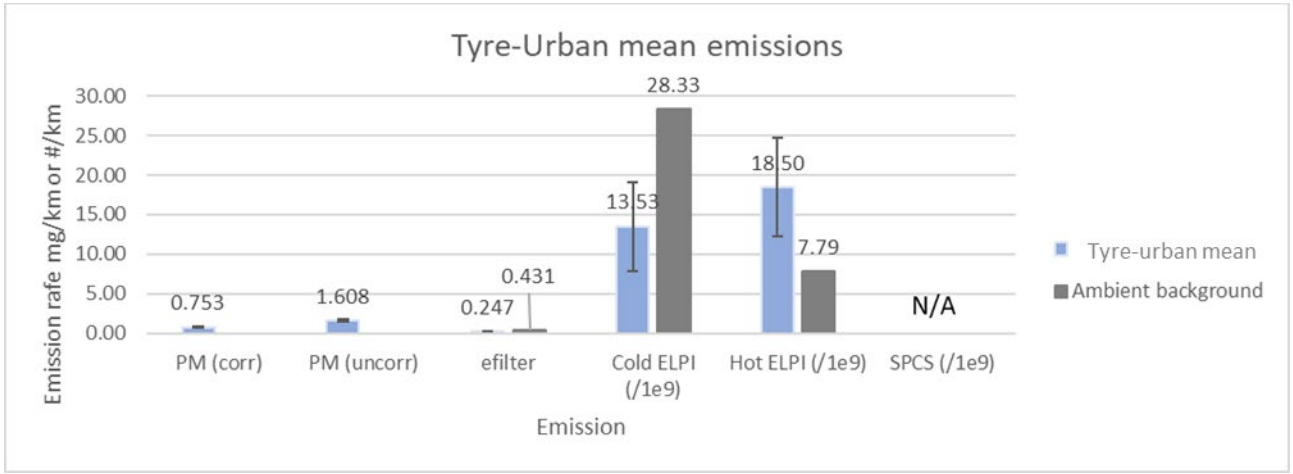

Visually the repeatability of urban tests appears good (Figure 5-81), particularly for mass metrics, but this may be more likely an indication of a repeatable background than of repeatable tyre emissions.

- In overview, real-time PN and PM (ELPI and eFilter) measurements suggest that some real-time tyre wear can be detected during urban testing, but not all braking events are apparent. The discrimination is improved when non-volatile particles are considered, but spikes of particles are observed between braking events. In comparison with PG-42 cycle results, very high PM emissions levels are observed, which suggests that materials that are not derived from the tyres of the test vehicle are being collected. Visual inspection of PM filters indicates that grey material is being collected on the filters along with

large particles, visible to the naked eye, that speckle the surface. The grey material may indicate the presence of some tyre wear material, but might also indicate that diesel soot, brake wear, road surface materials and other dark materials may be collected. From these analyses it does not seem practical to measure tyre wear from urban tests on-road.

Figure 5-81: Individual urban cycles repeat tests' brake PN and PM results

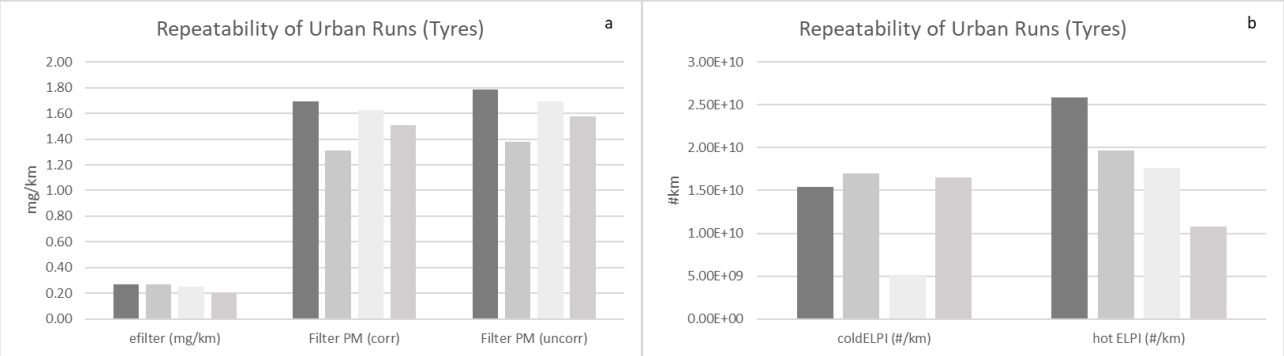

5.3.5.3 *Mass Weighted Particle Size Distributions – Tyres*

Mass weighted particle size distributions were obtained using the cold ELPI during repeated PG-42 and urban drive cycles. Data are shown on linear and log ordinates in Figure 5-82.

Figure 5-82: Mass Weighted Particle Size Distributions, Cold ELPI, PG-42 & Urban Cycles, Tyre Emissions

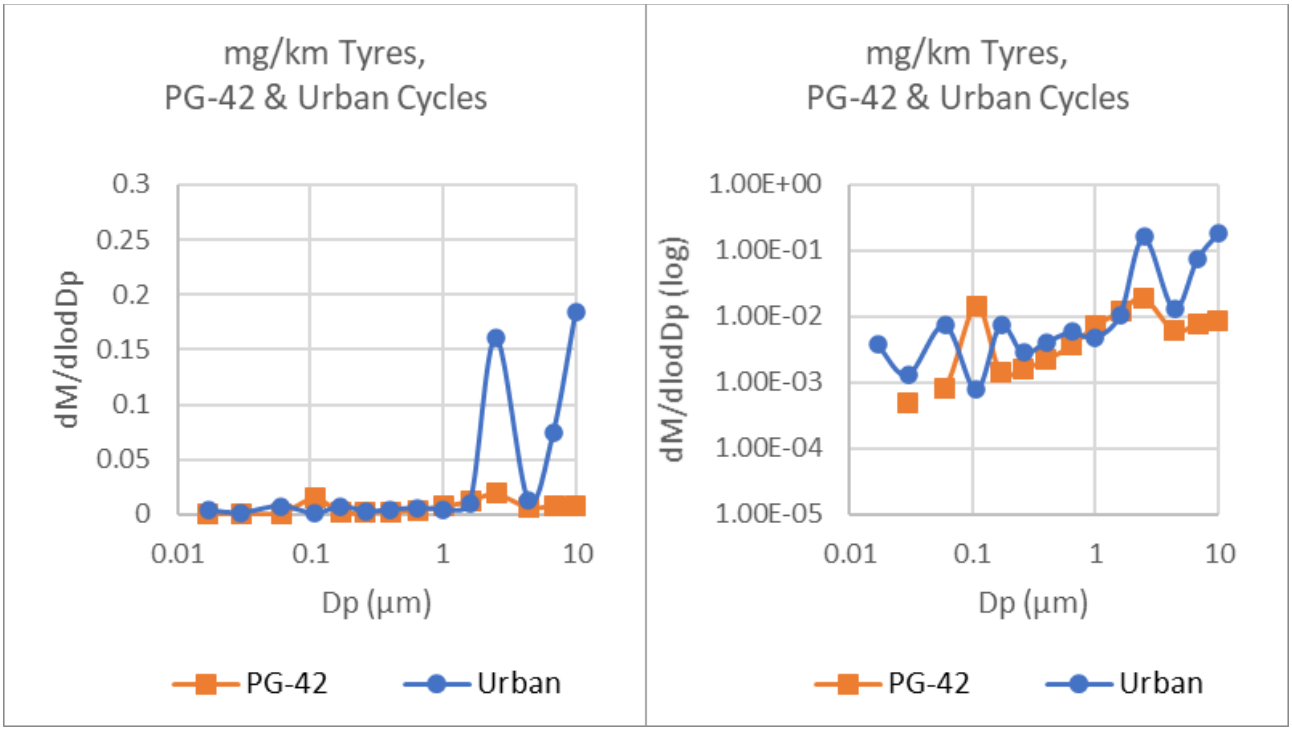

The size distribution data from the PG-42 cycle measured in the laboratory (orange lines and squares), with low particulate mass and particle number backgrounds, shows two modes of similar magnitude at ~100nm and 2.5µm, plus an indication of increasing PM above 4µm. The urban drive is entirely dominated by coarse materials present above 1µm. Since braking events in the urban drive are less vigorous than in the PG-42, it is highly unlikely that this >1µm particle mass comes from braking events and it is much more likely that this is background from the air or from road wear. This is consistent with the appearance of the PM filters from urban tests (Figure 5-77) which indicated both a dirty grey (mixed chemical) appearance of the filters and the presence of discrete particles. This dominance of background in on-road measurements means that it will be

extremely difficult to isolate tyre wear effects in the real world, but this does appear to be possible on the chassis dynamometer.

5.3.5.4 Test track studies

Two sessions were conducted on the Ricardo test track to explore whether using more predictable moderate braking and more aggressive braking approaches might enable real-world assessment of tyre wear. Track-based testing is also conducted in isolation from potential contributions from other vehicles that might be simultaneously present on the road.

5.3.5.4.1 Moderate braking Tyres Emissions

The first session measured tyre emissions during repeated moderate braking from a maximum speed of ~50mph/80kph, with emissions measured with both ELPI systems and the eFilter. Speed vs. time and braking pressure vs. time charts are shown in Figure 5-83. Peak braking pressures are around 50 bar. The session comprised three groups of acceleration and braking events, with each nominally a repeat.

Figure 5-83: Road speed and braking pressure from the track-based moderate tyre emissions tests

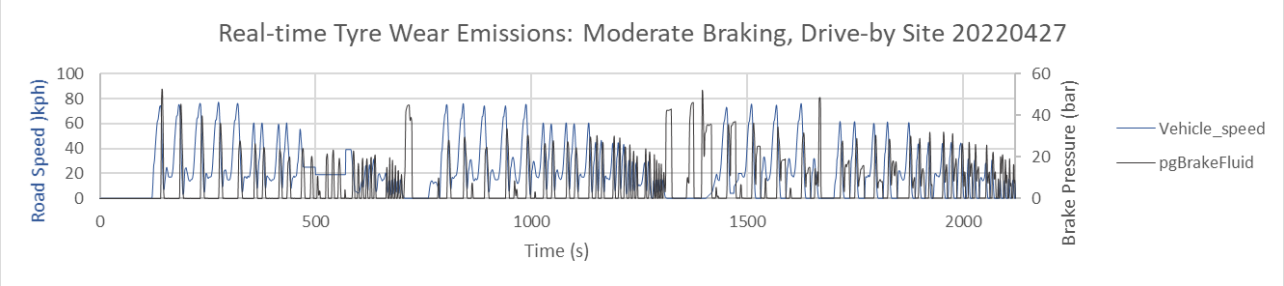

Both cold ELPI (Figure 5-84) and hot ELPI (Figure 5-85) showed emissions peaks coincident with some brake events. However, as shown in the areas enclosed with dashed lines in Figure 5-86, where hot and cold ELPI real-time emissions are compared, the cold ELPI can indicate emissions peaks not associated with braking events, while still indicating many of the same peaks as the hot ELPI. It is of course possible that these additional spikes are related to the release of volatile particles from the tyres, but if that is the case they do not seem to be predictable.

In fact, it appears that the production of particle emissions from tyres may not occur with every braking event, as seen with brake system emissions, and may not be repeatable between events. Figure 5-87 shows eFilter and road speed traces. The first ~400s of the cycle contains 5 repeat braking events starting from ~80kph (~50mph). The eFilter reports particle emissions spikes from braking events 1, 3 and 5 with the emissions magnitudes 3 > 5 > 1, but with no obvious particle production from braking events 2 and 4 in-between. The hot ELPI (Figure 5-85) also shows this effect, but the cold ELPI does not to the same extent. The hot ELPI also appear to show substantially higher peak PN emissions than the cold ELPI ($8x10^{10}$ vs. $2x10^{9}$ #s). This may be due to a difference of the distribution of volatiles as measured by the two systems. This is investigated in Section 5.3.5.4.3. Emissions of particles from hot ELPI and eFilter do not appear to be impacted by any substantial background contribution, so these effects seem to be real.

Due to the unpredictability of the appearance of emissions from nominally identical braking events and the differences in their magnitudes, emissions from individual braking events were not compared specifically.

Potentially there may be some accumulation of heat energy in the tyres from repeated braking that leads to periodic releases of particles. This may be an artefact of the pattern (proximity of one braking event to the next) of braking in the track-based tests conducted. However, if this is a real phenomenon, then a test aimed at measuring tyre wear would need to account for this possibility.

Figure 5-84: Track-based moderate braking tyre emissions tests – cold ELPI data

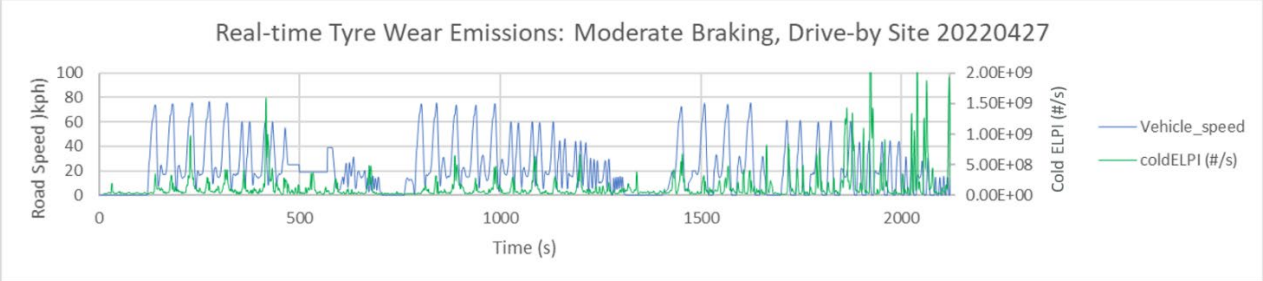

Figure 5-85: Track-based moderate braking tyre emissions tests – hot ELPI data

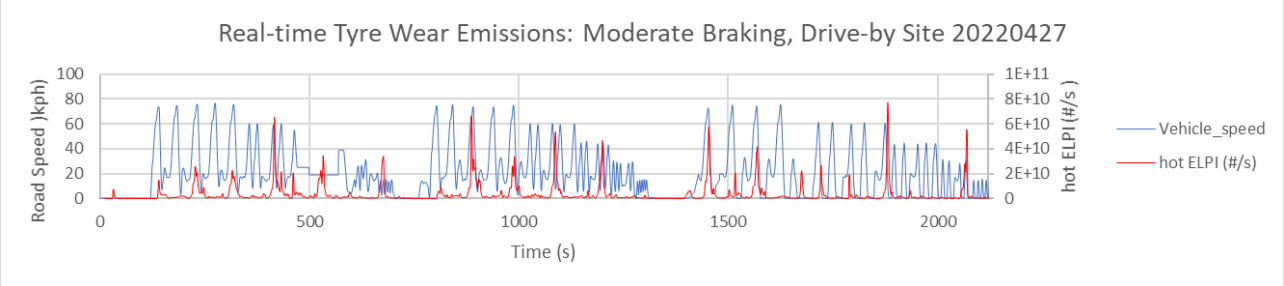

Figure 5-86: Track-based moderate braking tyre emissions tests – cold ELPI data shows non-braking peaks

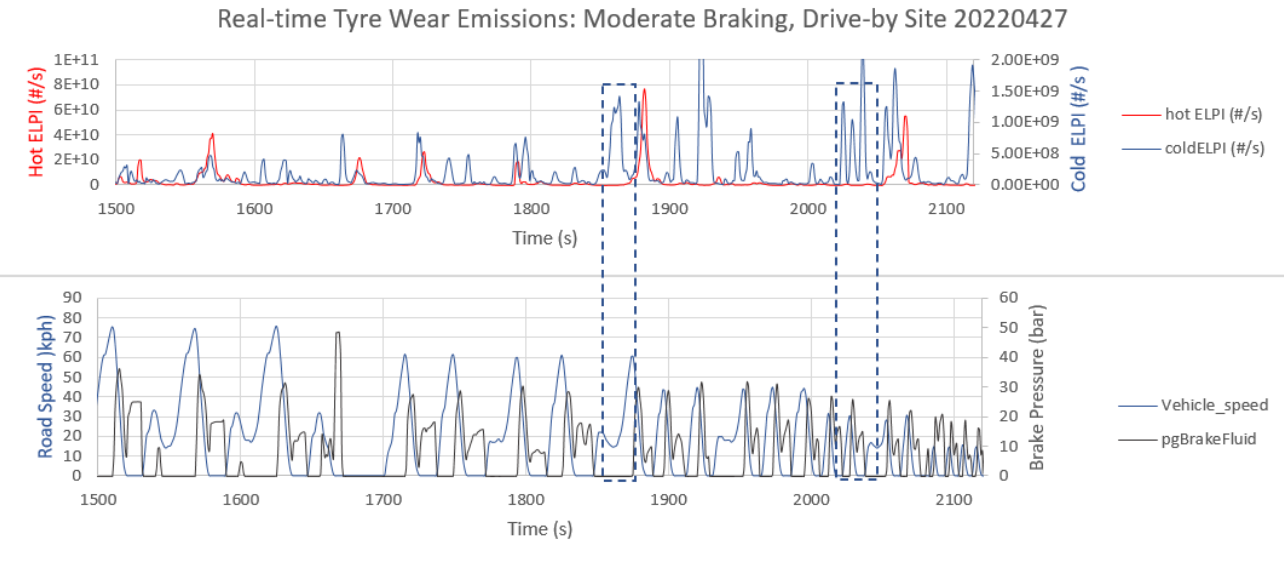

Figure 5-87: Track-based moderate braking tyre emissions tests – eFilter data

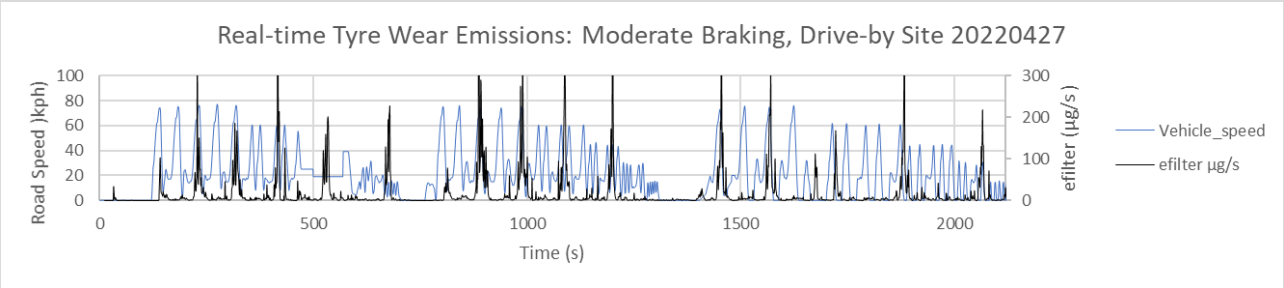

Contrary to the urban tests, where it was difficult to resolve emissions produced by braking events in the real time particle number and mass data, these track-based measurements show clear particle emissions peaks. This suggests that it could be possible to have a standard track-based drive cycle where tyres could be compared on a whole cycle basis. For example, an average emission from a cycle comprising e.g., 20 braking events at different speeds. This would need to be run several times and averaged to consider inconsistent particle production (that could be related to potential energy storage effects on emissions).

5.3.5.4.2 Aggressive Braking Tyres Emissions

A follow-up session was conducted on the same test track, this time with more aggressive braking. These events were similar to “emergency stops”. The aims of the study were to:

- Confirm the sporadic nature of tyre emissions
- Generate per second and per km emissions for comparison with the moderate track testing
- Generate particle size distributions for comparison with the moderate track testing

Road speed and braking pressure data for the aggressive braking session are shown in Figure 5-88. Peak braking pressures approach 90 bar, compared to 50 bar for the moderate braking experiment. Braking events were conducted in three groups with the second group (~920s to 1700s) a repeat of the first group (~120s to 900s), and the third group a set of repeated braking events from ~50mph.

Figure 5-88: Road speed and braking pressure from the track-based aggressive tyre emissions tests

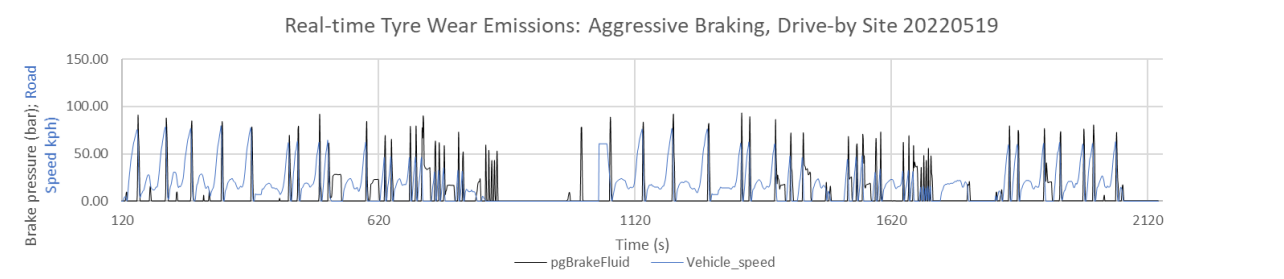

There is little similarity between the eFilter (Figure 5-89), cold ELPI (Figure 5-90) and hot ELPI (Figure 5-91) particle production events in the first and second groups, and similarly little consistency between the repeat 50mph events in the third group. In all cases the magnitudes of peak heights are inconsistent between repeat events and between repeat groups, and in some cases, particularly at lower initial braking speeds (for example, immediately after 620s with all three instruments), there are no obvious emissions with braking events.

Figure 5-89: Track-based aggressive braking tyre emissions tests – eFilter data

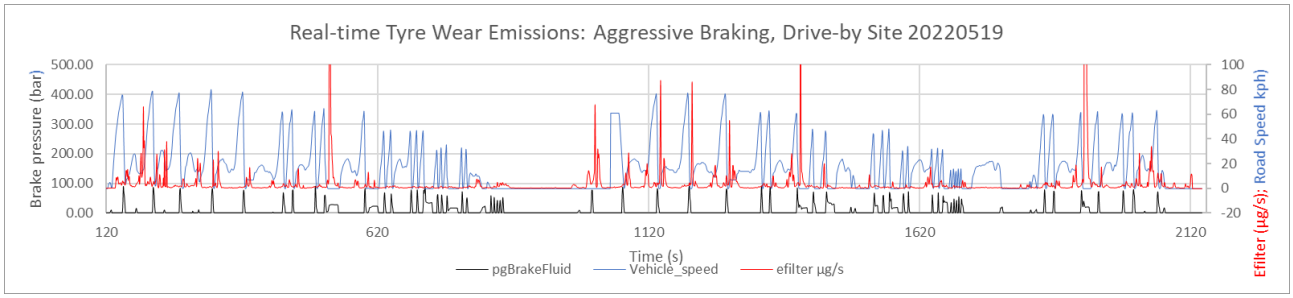

Figure 5-90: Track-based aggressive braking tyre emissions tests – cold ELPI data

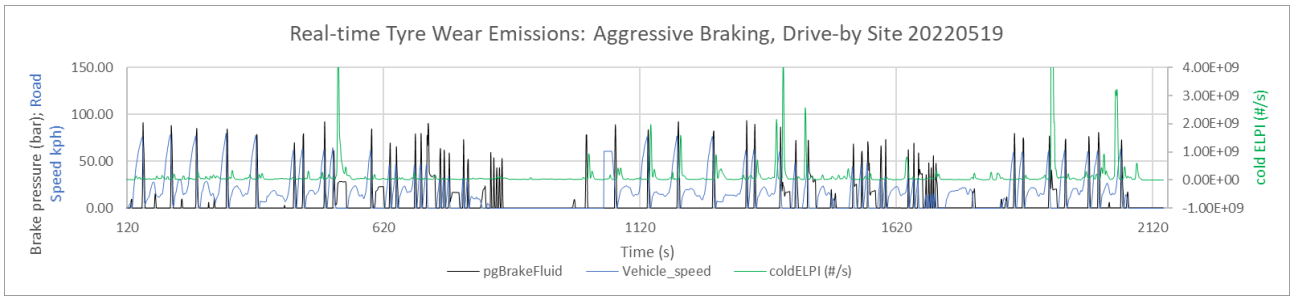

Figure 5-91: Track-based aggressive braking tyre emissions tests – hot ELPI data

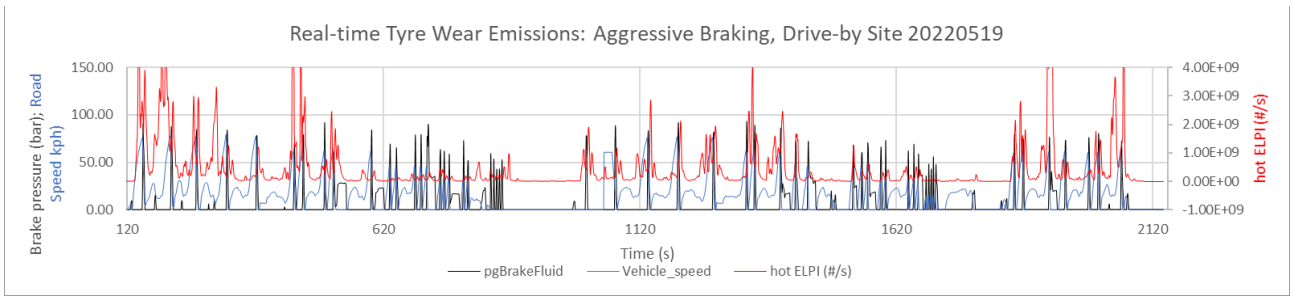

Results indicate that the inconsistency in the generation of particle emissions peaks seen from the moderate track exercise was repeated with more aggressive braking. In the following section, emissions levels and particle size distributions between moderate and aggressive braking will be compared.

5.3.5.4.3 Moderate and aggressive braking, tyre particle number emissions compared

Comparing integrated hot and cold particle number emissions from cold and hot ELPI from the moderate and aggressive braking sessions (Figure 5-92) reveals generally higher PN is measured by the cold ELPI during the aggressive braking experiments, but higher PN from the hot ELPI during the moderate experiments. In addition, the moderate experiments' hot ELPI emissions are an order of magnitude higher than from the aggressive tests.

Figure 5-92: ELPI integrated particle numbers from moderate and aggressive tyre emissions tests

Particle size distributions from the cold and hot ELPI indicate that during the moderate testing (Figure 5-93, left) there was a much larger coarse mode of particles (>0.5µm) present than during the aggressive braking testing (Figure 5-93, right). It appears that volatiles redistributed from the larger particle sizes (>100nm) to smaller particle sizes (10nm to 100nm) with both moderate and aggressive driving, is potentially due to the displacement of more materials from the larger coarse mode. This was greatest during the moderate testing, leading to overall much higher PN emissions from the hot ELPI.

It is most likely that the increased coarse mode materials identified by the ELPIs during the moderate testing are from an ambient background source. These coarse mode materials contain volatiles that interact with the hot ELPI to generate high levels of 10 – 100nm particles. Since testing cannot control the background contributions during tyre sampling, there will always be a risk, with real-world brake emissions sampling, of this effect occurring with a heated system, such as the hot ELPI, that does not remove all (or nearly all) of the volatiles.

Figure 5-93: ELPI particle size distributions from moderate and aggressive tyre emissions tests

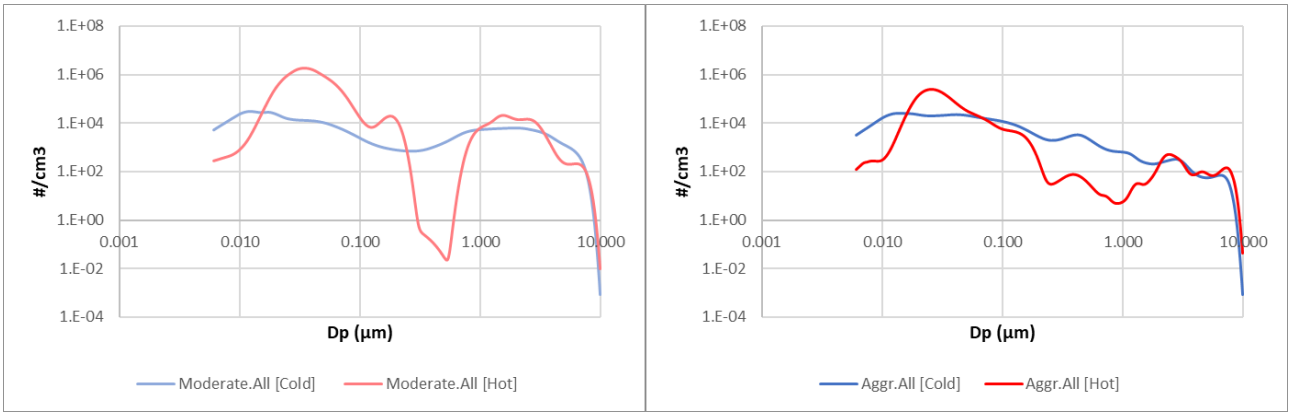

It appears that despite the benefits of better repeatability from the hot ELPI when compared to the cold system, the redistribution of volatiles in the hot ELPI can lead to substantial increases in PN emissions. These volatiles can derive from both the tyre (as observed in the test facility) and from the ambient (as observed on the test track). The cold ELPI most realistically illustrates the particle size distribution from braking events and is useful to understand the particle sizes released. The hot ELPI data is less valuable as the size distributions shown are not representative of the point of emissions. For potential particle number control from tyres a non-volatile approach (using catalytic stripper or evaporation would likely provide high repeatability.

5.3.5.5 Tyre pressure effects on particle emissions during an on-dyno PG-42 cycle

Reducing the tyre pressure likely increases the surface area contact between the tyre and dynamometer roller leading to higher friction. When lower pressure, 2.0 bar, tyre emissions were compared with the average particle size distribution determined from the set of PG-42 tests at 2.9 bar, a marked effect of increasing

production of particles of <0.1µm diameter, as measured by the cold ELPI (Figure 5-94 a (log scale), c (linear scale)) was observed. Conversely, the impact on the hot ELPI measurements (Figure 5-94 b, d) was minimal. This strongly suggests that the lower tyre pressure, increased contact surface area and elevated friction releases an increased level of volatile particles but has minimal impact on non-volatile particles. It should be noted that cold ELPI data has shown substantial variation in particle number emissions, but this variation has been related to a mode very close to 10nm, whereas the mode that appears with the low-pressure tyres is closer to 30nm.

This is supported by comparing integrated particle number emissions from the two ELPIs and the SPCS. Of these three instruments (Figure 5-95), only the cold ELPI shows a substantial change in particle number emissions - a near 10-fold increase in volatile particle emissions.

The eFilter also reported increased mass emission with lower pressure tyres (Figure 5-96) relative to the higher-pressure tyres' PG-42 results.

Figure 5-94: Cold and hot ELPI size distributions over PG-42 cycle tests at low and high tyre pressures

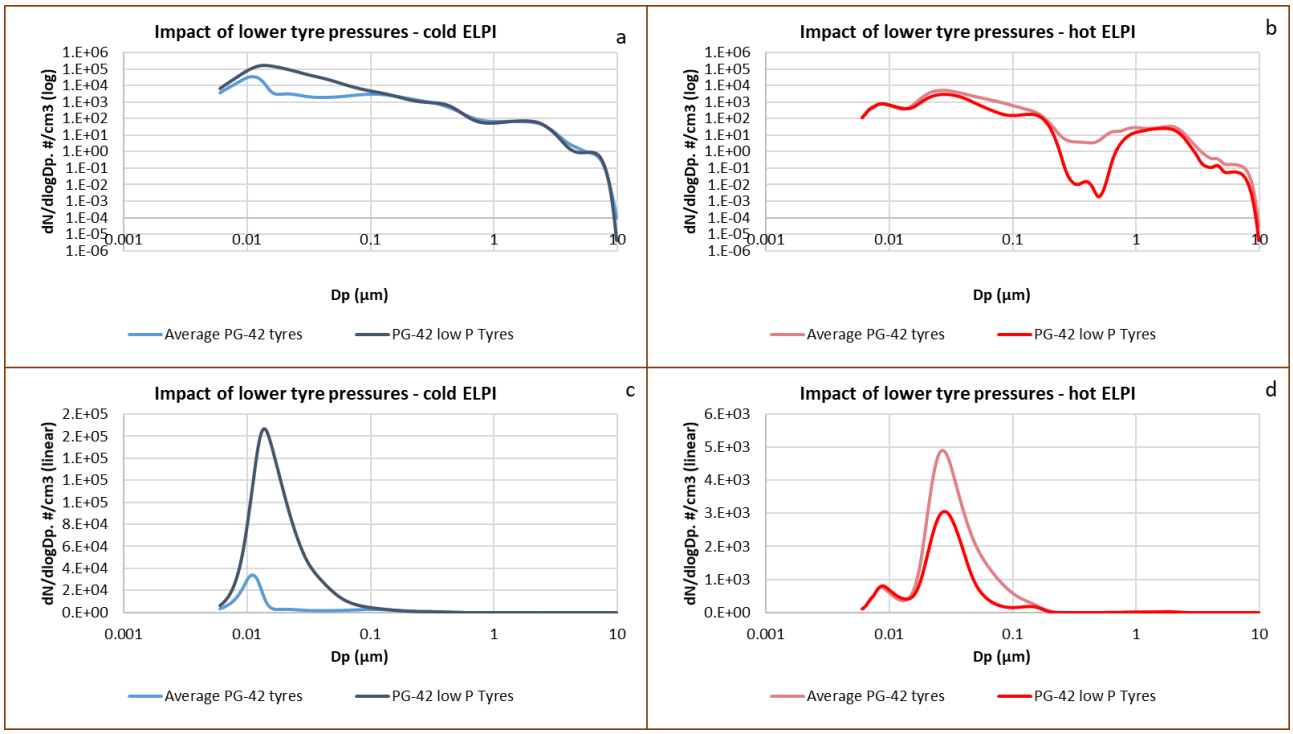

Figure 5-95: Integrated PN from ELPIs and SPCS over PG42 cycle tests at low and high tyre pressures

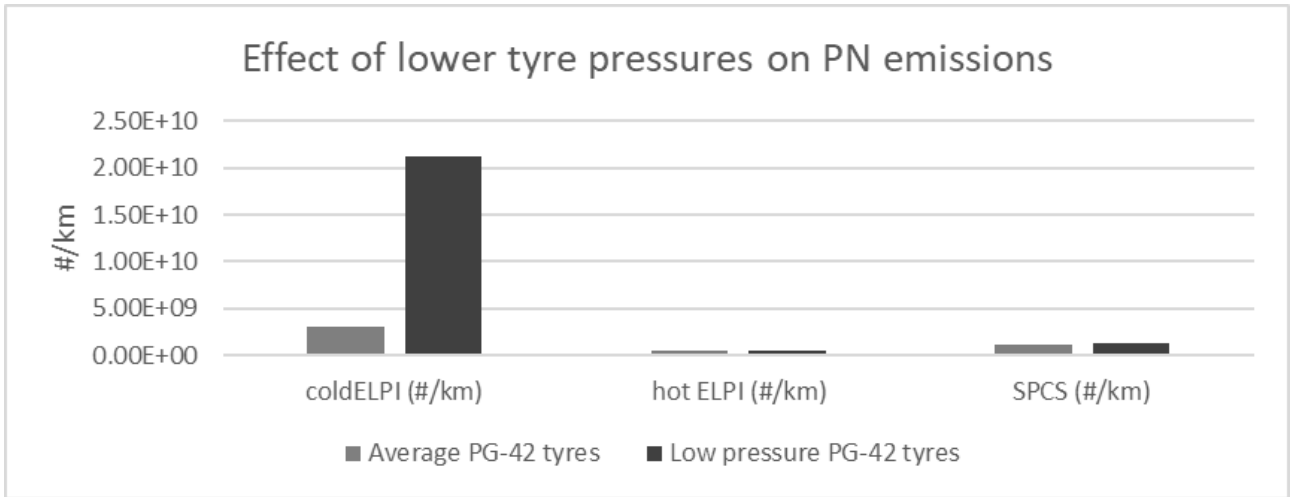

Figure 5-96: eFilter PM over PG42 cycle tests at low and high tyre pressures

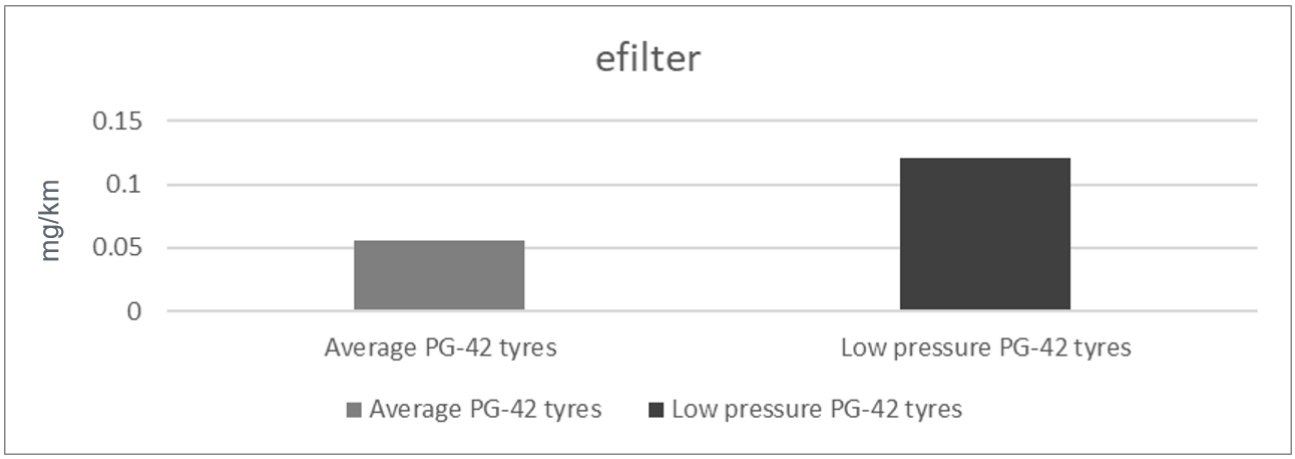

5.3.5.6 Comparative Tyre Emissions and Particle Size Distributions

Tyre emissions from the PG-42, on-road urban plus on-track moderate and extreme driving are compared in this section.

Mass emissions data are predominantly available from the real-time eFilter system. Figure 5-97 shows how measured mass increases substantially when moving from the chassis dynamometer facility (PG-42 tests) to any road or track-based testing. The PG-42 cycle is more demanding in terms of braking aggressiveness than the urban cycle driven in the vicinity of Ricardo at Shoreham, so intuitively higher tyre wear emissions would be anticipated from the PG-42. Moderate and extreme track-based braking, with greater braking frequency and potential to add heat energy to the tyres, does lead to higher tyre mass emissions than urban driving, but moderate braking emissions were generally higher than extreme braking emissions. This suggests that another factor not related to braking frequency or severity is responsible for the majority of the mass emissions during the track-based tests, and probably also during the urban tests.

Figure 5-97: Tyre mass emissions from various driving

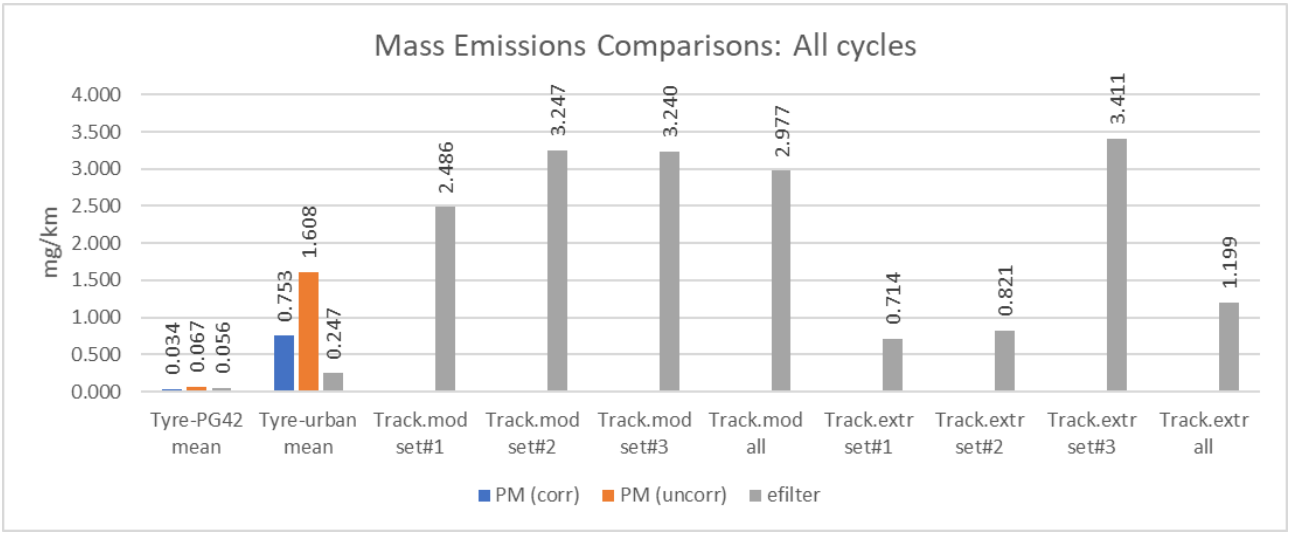

Particle number emissions from cold (blue) and hot (red) ELPI systems are shown given in Figure 5-98. As with the mass data a substantial increase in emissions is seen with urban PN emissions compared to PG-42 emissions, despite the reduction in braking severity. PG-42 tests show > 5x higher levels of PN from the cold ELPI than from the hot system. With the cold ELPI, PN emissions increase from PG-42 to urban to moderate track to extreme track driving, which may indicate increased volatile PN emissions with increased driving severity and frequency in the real-world. Lower emissions from PG-42 in the lab than from urban driving on the road likely indicates a background contribution to urban emissions, that is not present in the chassis

dynamometer facility (or that real world tyre wear from tarmac is much greater than from the roller in the test facility, but this seems less likely).

Tyres-derived hot ELPI PN emissions from urban, moderate track and extreme track driving are in all cases substantially higher than from the cold ELPI. This suggests a restructuring of the particle size distribution, where larger particles are evaporated and then at least some of the evaporated material recondenses into more numerous smaller particles, despite an overall mass loss.

The moderate track testing indicated an anomalous observation where extremely high hot ELPI PN levels 20 – 30x those of the cold ELPI were observed. These increases were consistent with the generally higher moderate track exercise PM emissions recorded with the eFilter described above and suggest that there were large volatile particles present during the moderate track testing that weren't present during the extreme testing. It is unlikely that these were generated by the testing itself and these are most likely a contribution from the ambient background. The presence of these particles can be studied in the particle size distributions (Figure 5-99). The lower levels of hot ELPI PN than cold ELPI from the PG-42 cycle suggests a reduction in evaporable particles from this test cycle in the chassis dynamometer facility, indicating a consequent reduction in volatile particles formed through evaporation and recondensation.

Figure 5-98: Tyres Integrated PN emissions from various driving

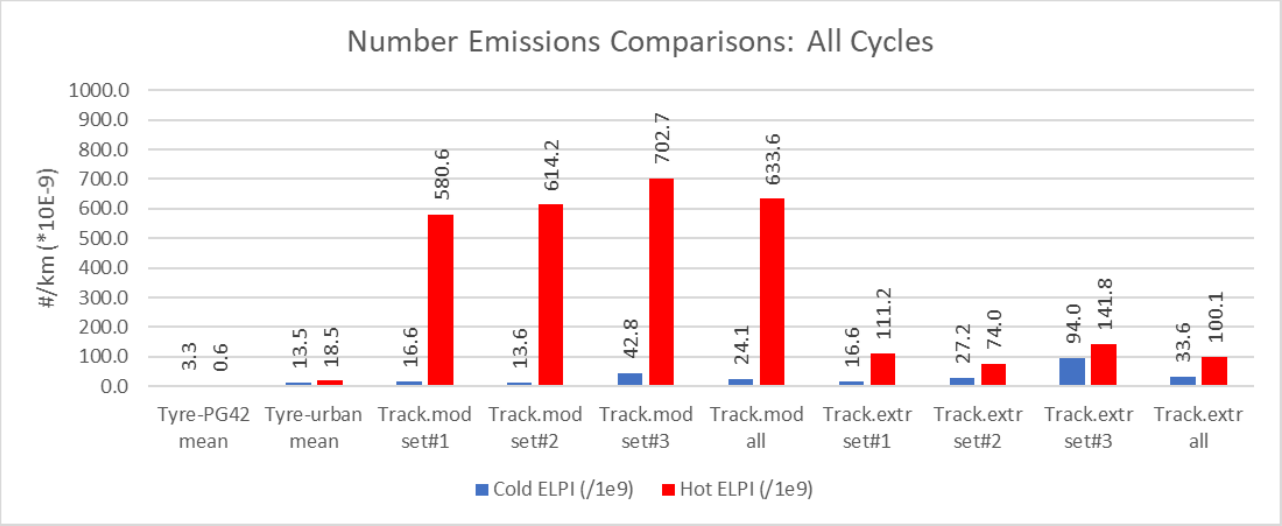

Both cold and hot ELPI particle size distributions show much higher coarse mode particle emissions in the region 1µm to 10µm from the moderate track testing than from the extreme track testing (Figure 5-99). These appear to be converted to significant levels of < 0.1µm particles in the hot ELPI, resulting in the high PN levels observed in Figure 5-98. There is no obvious mechanism for the moderate track braking to produce more tyre wear or outgassing of volatile emissions than extreme track braking, so it is most likely that these coarse particles are a background contribution not related to the braking events.

Lowest coarse mode particle emissions are observed from the PG-42 cycle, with urban cycle emissions also lower than emissions from the track-based exercises. The PG-42 PN emissions were ~10x lower from the cold ELPI, and closer to 100x lower from the hot ELPI, when compared to the urban cycle emissions. It seems likely that there are ambient contributions to the coarse mode that both substantially influence particle mass, and which contain substantial volatile levels which confound PN emissions measured by the hot ELPI through evaporation and recondensation. These background coarse mode contributions are almost absent from testing in the chassis dyno facility making it much easier to detect discrete tyre emissions.

Figure 5-99: Tyres particle size distributions, cold and hot ELPI

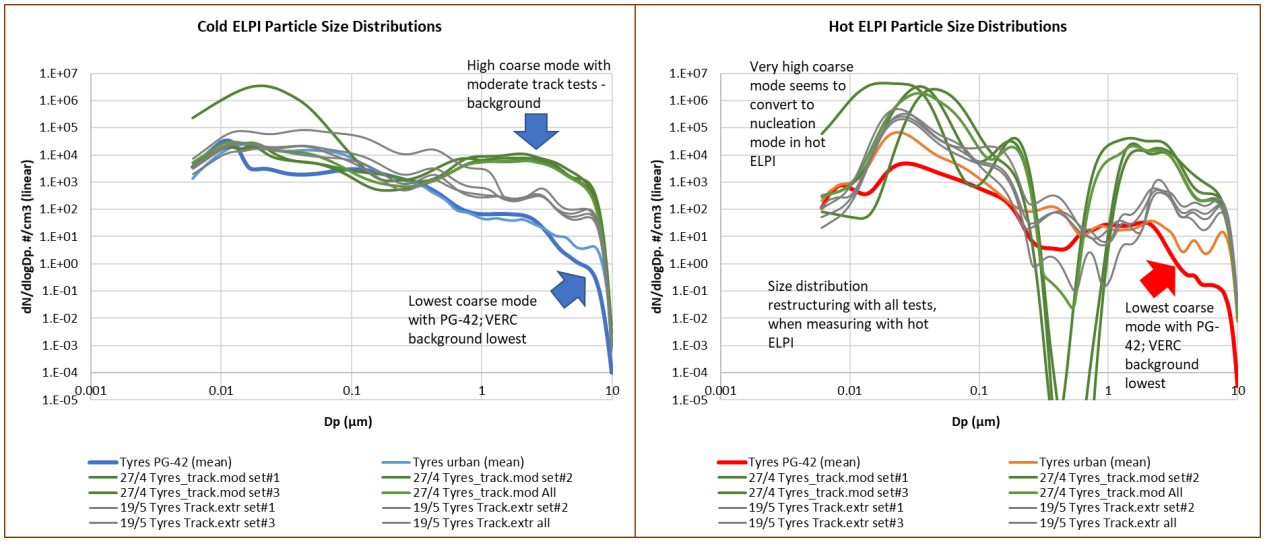

5.4 TEST RESULTS 2: VW CADDY FURTHER ENCLOSURES

Three enclosure design options were developed as described in Section 5.1.2 and illustrated schematically in Figure 5-4. These were:

A. In the **original** design the **whole wheel** is used as a **rotating** enclosure, with the front face of the wheel sealed with a plate attached to and rotating with the wheel. A static (non-rotating) rear plate covers the back face of the wheel, fitted around the calliper, with a clearance gap at the inner edge of the wheel rim. This design was used for the majority of testing, and also used for the second test vehicle

B. A **separate static** (non-rotating) enclosure is fitted around the brake and within the wheel. This is formed of a single-piece outer "bowl" which is fixed to the rear plate and has a clearance gap around the rotating wheel hub at its centre.

C. A **separate rotating** enclosure is fitted around the brake and within the wheel. This has the same design and dimensions as the static enclosure, except that it is instead fitted between the wheel and hub and rotates with them, having a clearance gap to the static rear plate.

All three designs shared the same rear plate with the filtered air inlet and sample outlet pipes in the same location. Their different designs mean that the enclosures could differ in several respects:

- The volume enclosed: that of the separate enclosure designs (B, C) being less than that of the original whole-wheel design (A). A lower enclosed volume leads to the air exchange period being shorter for a given flow, but also provides less space for the air to move around the brake and mix.
- Heat dissipation: The separate enclosures (B, C) have thin metal walls surrounded by air between them and the wheel, which may help dissipate heat. The test vehicle had larger wheels fitted which increased the air gap between the enclosures and the wheel. The original enclosure (A) used the wheel rim itself, which being surrounded by the tyre and the hot air within it, will not be able to dissipate heat around its circumference. The thin metal plate across the wheel face will be able to dissipate heat to air beyond the wheel, but the spokes will ensure it is turbulent and that may hinder heat transfer
- The rotation effect: the static enclosure (B) does not rotate, although the disc within it, and the wheel outside it are both rotating. The combination of the enclosure and calliper being static with little clearance between (the enclosure being designed to fit between the calliper and the original smaller wheel) them may limit air movement within the enclosure and around the disc and calliper, which could result in both reduced cooling and particulate movement, with some air trapped, while some dilution air passes through with little mixing. Both the rotating enclosure designs (A, C) should encourage more movement of the air around the disc and calliper, with the rotation of the wheel ensuring dilution air is moved around the brake, which could impact both cooling and particle mixing, although this effect would only be meaningful at higher rotational speeds (vehicle speeds).

- The clearance gaps: the original whole-wheel enclosure (A) had a gap to the static rear plate around the inner circumference of the rim. While the gap is narrow it is long and being at the outer edge of the wheel the particulate emissions may be concentrated in this region due to centrifugal force. However, the force will be unlikely to influence particles within the size-range (PM10) studied in this project. The separate rotating enclosure (C) similarly has a clearance gap at its outer edge, but the static enclosure (B) has the clearance gap around the wheel hub, so it is much shorter and at the inner of the enclosure. For mass flows, any leakage is accounted for by using the measured airflow *into* the enclosures.

Tests were carried out using designs B and C applied to the VW Caddy, and the results compared to design A to identify if differences were present that could be attributed to the enclosure design.

5.4.1 Static Enclosure

The original rotating enclosure (Option A, Figure 5-4) was removed from VW Caddy and replaced with a static enclosure (Option B, Figure 5-4). Both designs use the same fixed (non-rotating) rear plate behind the wheel and the brake calliper, with the air inlet and sample pipes in the same location. The original enclosure approach (A) was to seal the outer face of the wheel to use the wheel as a rotating outer enclosure, with the interface between the static inner and rotating outer enclosure elements being at the inner edge of the wheel rim. The static enclosure (B) instead has a non-rotating enclosure around the brake, attached to the fixed rear plate, and within the rotating wheel, the interface between static and rotating parts being around the wheel hub just inside the wheel.

The vehicle was then subjected to the following tests, a subset of those conducted on the original rotating enclosure:

- 9 x PG-42 tests on the chassis dynamometer.
- 2 x Urban route tests on the roads.
- A moderate braking exercise on the test track.

During these experiments a fault was detected with the hot ELPI and so data are only presented from the SPCS (PG-42 tests only), cold ELPI and eFilter.

5.4.1.1 PM and PN Emissions from PG-42 and Urban Cycles

From PG-42 tests, PN emissions measured by the SPCS were ~35% lower from the static enclosure than from the original rotating enclosure, this being a significant difference (at 1-sigma) due to the high repeatability of the SPCS in the rotating enclosure tests. Emissions from the cold ELPI were directionally lower from the static enclosure, but statistically similar. Distance-based emissions from both systems and enclosures were < 5 x 10^9 #/km.

Mass emissions from the eFilter and measured on GF/A filters were also directionally slightly lower from the static enclosure than from the original rotating enclosure, but differences were not statistically significant (at one standard deviation). Filter mass emissions were in the range 1.2 to 1.6 mg/km and eFilter emissions 0.4 – 0.5 mg/km.

Figure 5-100: Comparison between PN and PM emissions from PG-42 cycles with original rotating and static enclosures

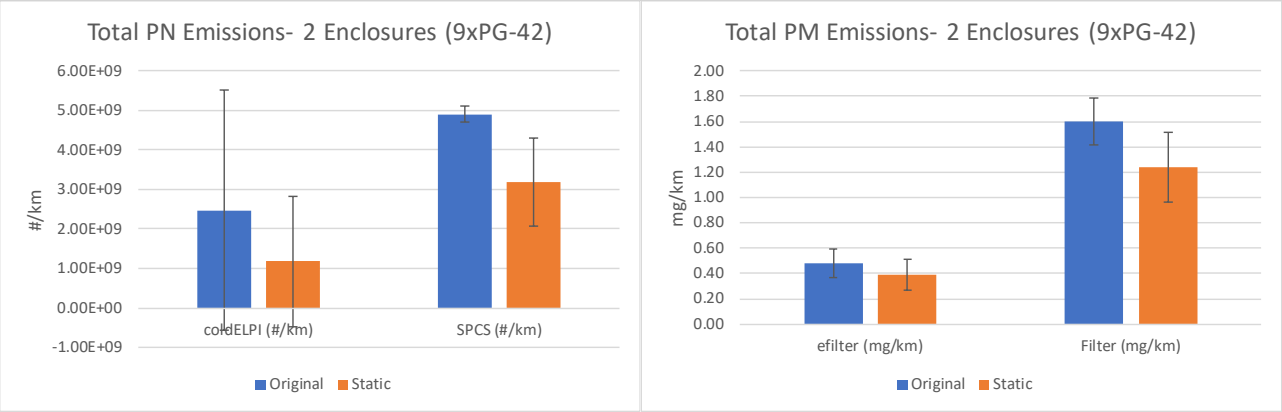

Similar trends were observed from urban testing, though it should be noted that results are from fewer tests than the PG-42 cycles. Cold ELPI PN emissions were directionally higher from the rotating enclosure than from the static enclosure, but with overlapping 1-sigma error bars. Mean emissions were < 5 x 10^9 #/km.

Urban PM emissions were lower than from the PG-42, and broadly similar from two enclosures. Filter-based PM emissions were ≤ 1mg/km and eFilter masses < 0.25 mg/km.

Figure 5-101: Comparison between PN and PM emissions from urban cycles with original rotating and static enclosures

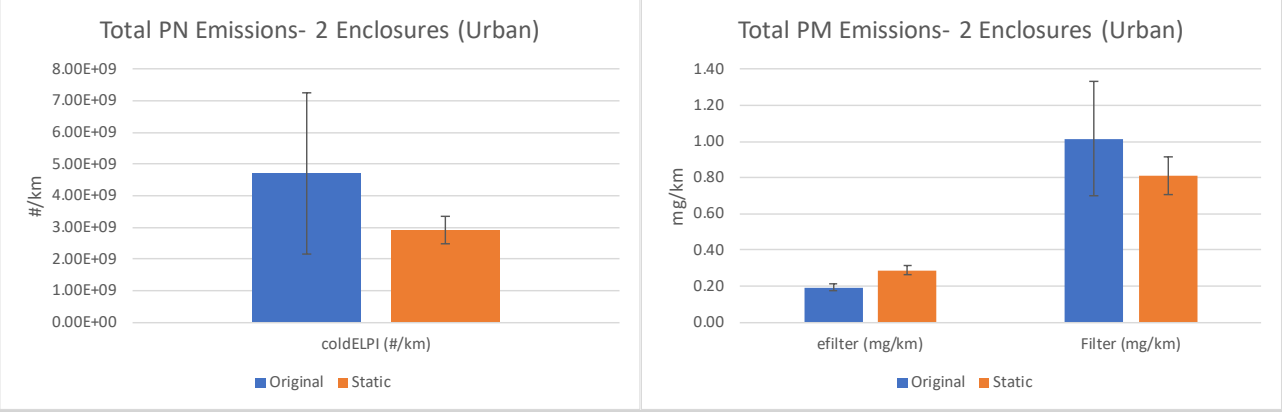

5.4.1.2 Particle emissions from moderate track exercises

The static enclosure moderate track tests were conducted with a different driver than with the original rotating enclosure tests, and these tests may also have been on a slightly wetter surface. This may lead to some differences in results. As described for the original enclosure (Section 5.3.3.3), the exercise comprises repeated (at least 5) consecutive moderate braking events at approximately 50mph/80kph, 40mph/64kph, 30mph/48kph, 20mph/32kph and 10mph/16kph. The sequence commenced at 50mph descending stepwise to 10mph.

Particle emissions were observed to be coincident with braking events at all speeds with cold ELPI (Figure 5-102) and eFilter (Figure 5-103), but reproducibility of peak magnitudes was not consistent.

Figure 5-102: Static enclosure real-time cold ELPI PN production, moderate track exercise

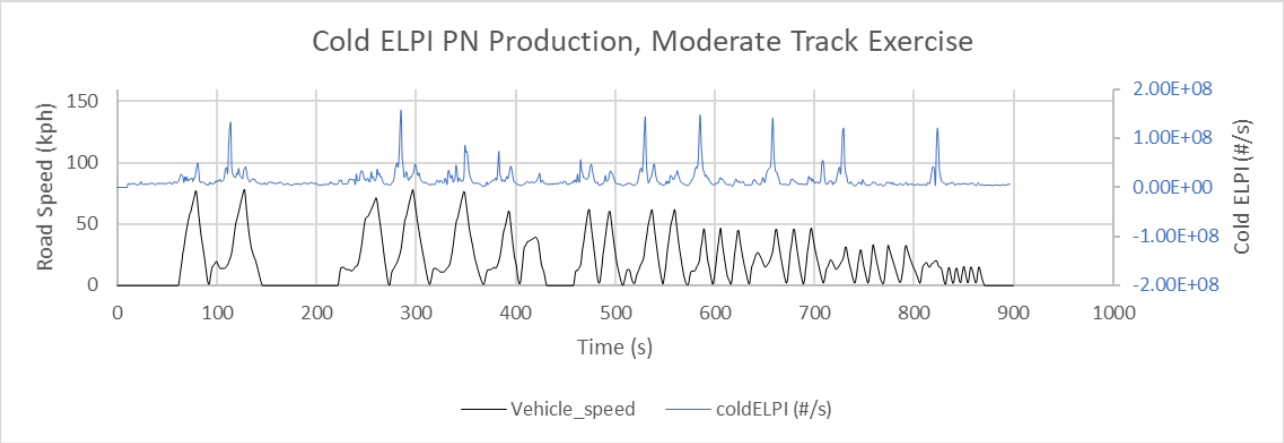

Figure 5-103: Static enclosure real-time eFilter PM production, moderate track exercise

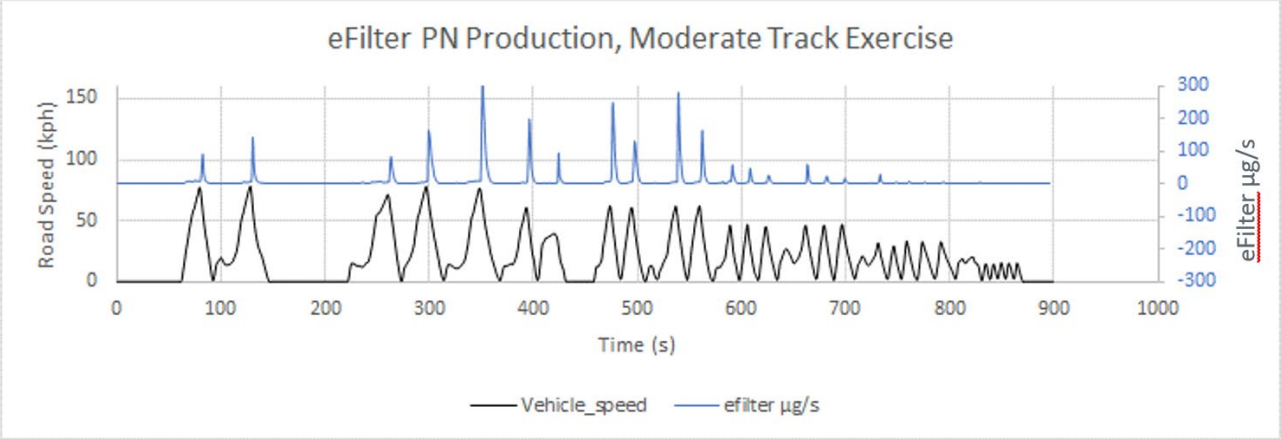

A comparison of track PM and PN results obtained from braking speeds from 80kph (50mph) down to 16kph (10mph) is shown in Figure 5-104 for the two enclosures. Cold ELPI PN emissions are shown in the left-hand figure, with eFilter results on the right.

Figure 5-104: Moderate track exercise PN (left) and PM (right) emissions from static and original enclosures

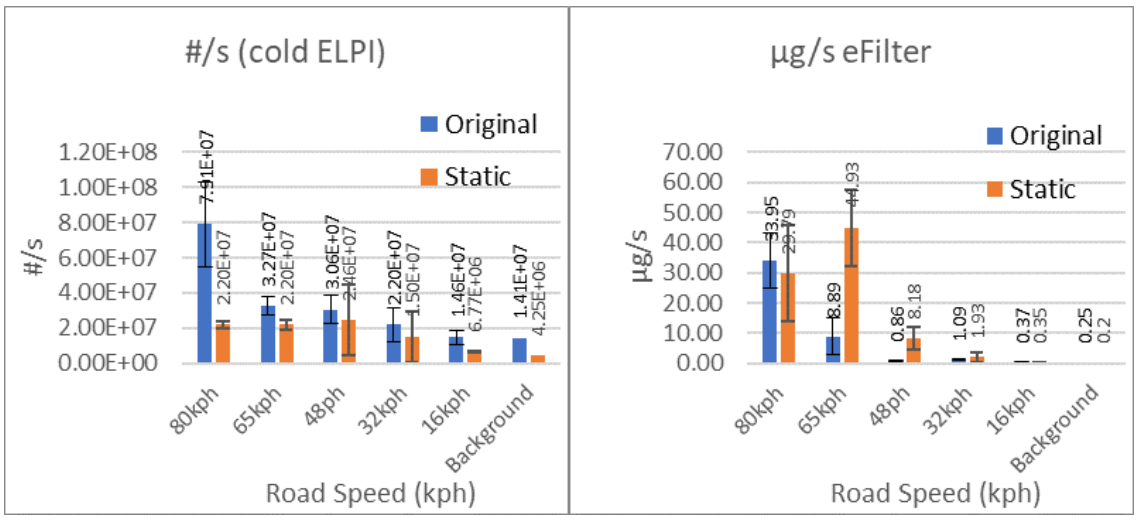

Broadly similar cold ELPI PN emissions are observed across the speed range, with perhaps slightly lower emissions from the static enclosure. This is consistent with observations from the PG-42 and urban cycle data. The exception is at 80kph, where there were markedly higher emissions from the original enclosure. It may be that this was due to a higher average braking pressure events during the exercise (Figure 5-105).

Figure 5-105: Average braking pressure by speed, two enclosures

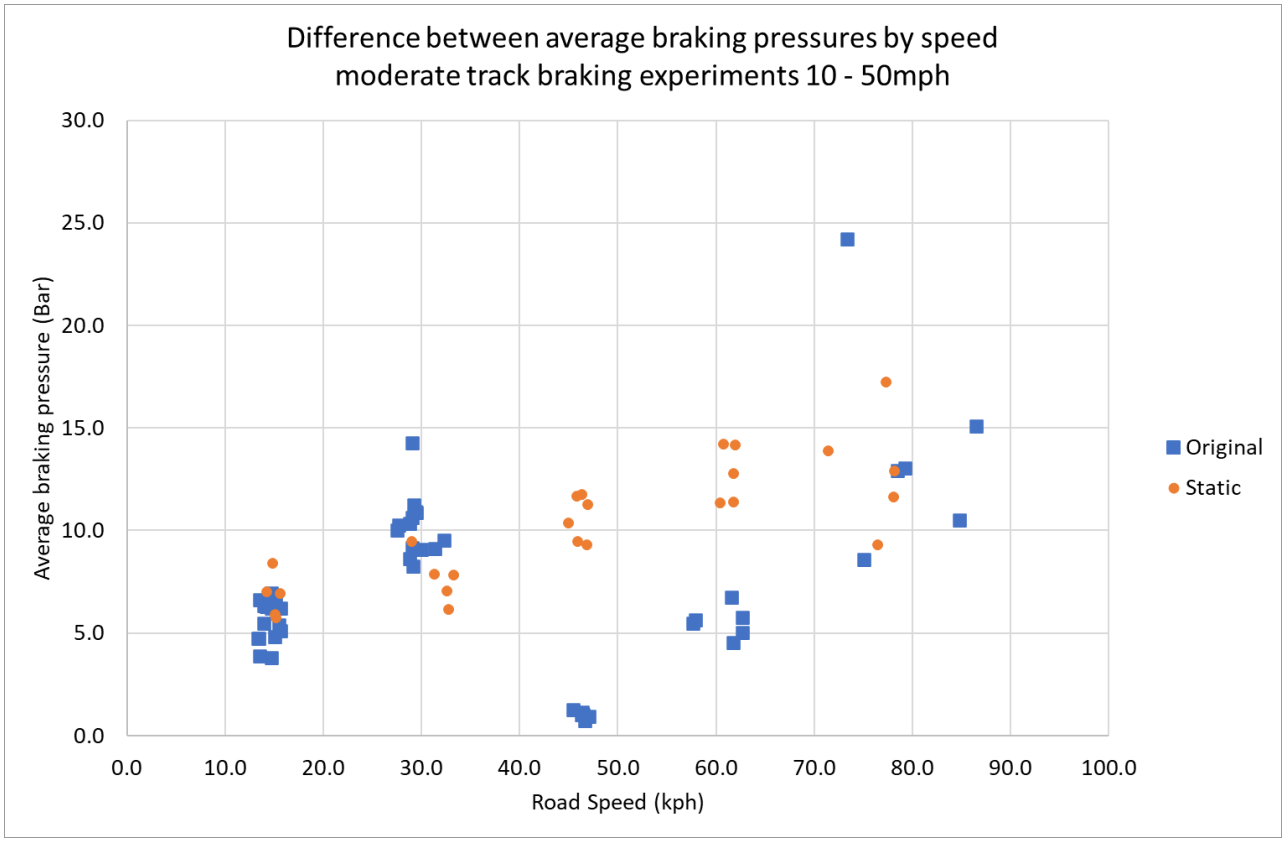

PM emissions from the eFilter (Figure 5-104, right) were similar between enclosures at ~80kph and at ≤ 32kph, but emissions were higher from the static enclosure at ~65kph and ~48kph. At these speeds there were clearly higher average braking pressures during the exercise with the static enclosure than during the exercise with the rotating enclosure.

The static and rotating enclosures also resulted in different brake disc temperatures between the enclosed (right-hand front, sampled) wheel and unenclosed left-hand front wheel. A comparison of these temperatures from the moderate track exercises, covering braking events from ~16kph up to ~80kph, is shown in Figure 5-106.

Figure 5-106: Differences between enclosed and unenclosed disc temperatures, 2 enclosures

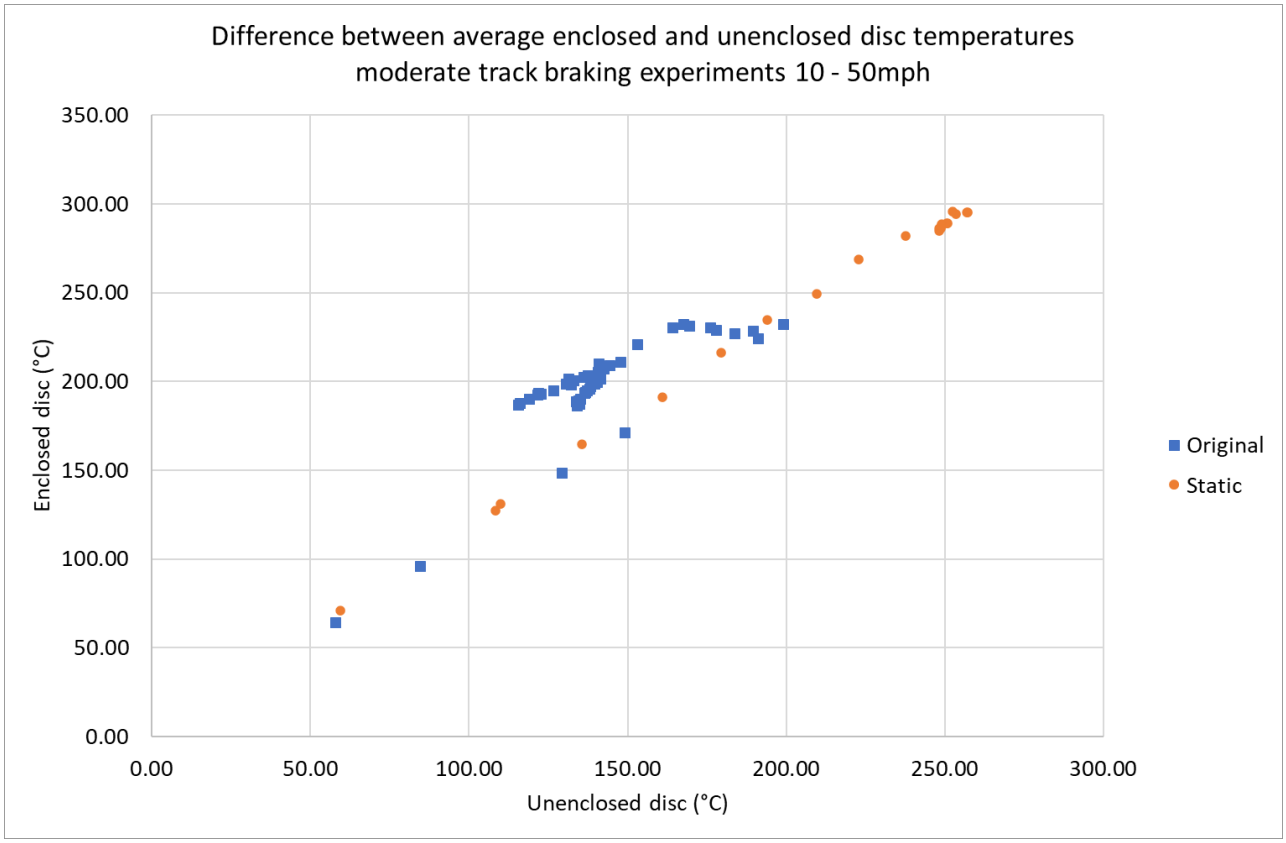

Results for the track exercise show that for the static enclosure the right-hand disc temperature increases linearly with the temperature of the left-hand disc but is ~15% higher. The right-hand disc temperature reaches a peak of ~300°C compared with a concurrent 250°C temperature from the left-hand disc. Alternatively, the original enclosure appears to have a maximum right-hand disc temperature of ~230°C compared with ~200°C at the left-hand disc. These differences may be related to the high frequency of braking events in the test track exercise, braking pressures, and driver-to-driver variances as described above, but may also be related to the structure and function of the enclosures.

Time-series evaluations of the disc temperatures from the original enclosure A and static enclosure B are shown in Error: Reference source not found and Figure 5-108 respectively. Left and right-hand disc temperatures diverge and converge on a longer time-base with enclosure A than with the static enclosure B, and the differences between the disc temperatures are greatest with enclosure A. It appears with enclosure A that the left to right differential grows with braking from higher speed and then closes as braking effort decreases from lower speeds. This may show that A has limited heat rejection, potentially due to the larger volume and less potential for external heat rejection. The differential between brake disc temperatures with enclosure B also widens with braking at higher speeds but closes up much more quickly than with enclosure A, indicating improved heat rejection.

Figure 5-107: Time-series left and right-hand disc temperatures, enclosure A

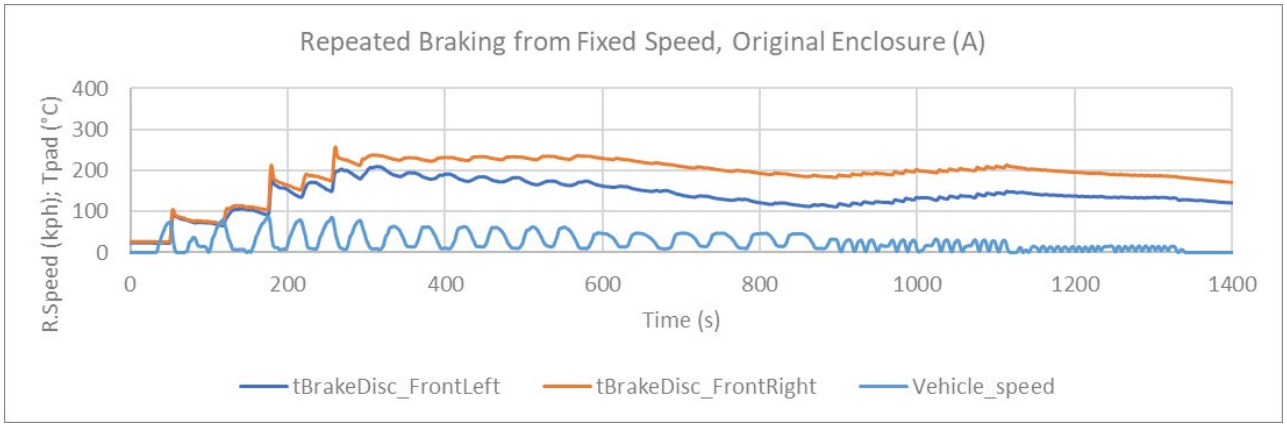

Figure 5-108: Time-series left and right-hand disc temperatures, enclosure B

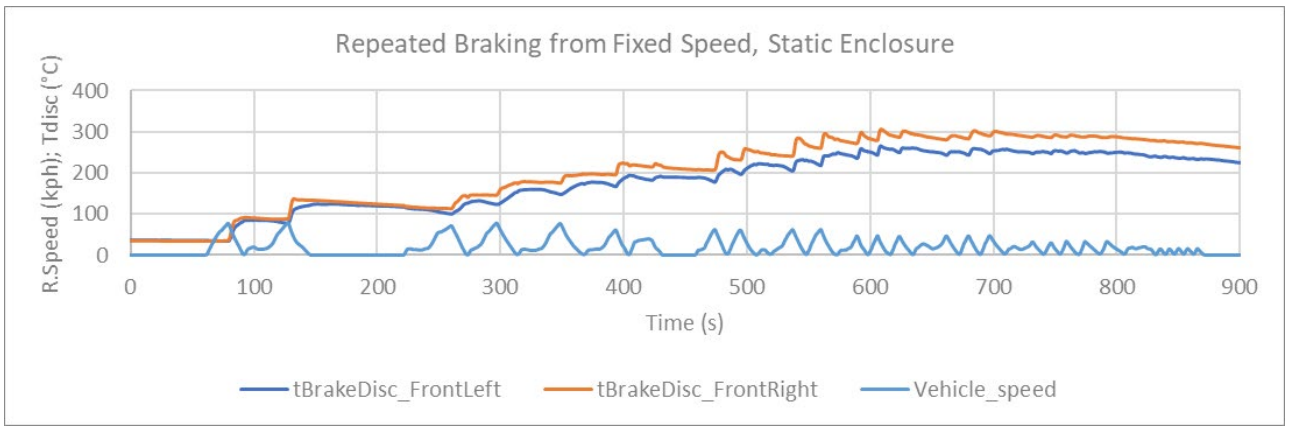

The results of these experiments illustrate the probable need for any regulatory track-based comparison of PN and PM emissions to generate highly repeatable braking events. It is likely this would need to retain the same driver and/or have a 'drivers aid' as a guide. Similarly, the design of the enclosure is likely to need to be well defined to ensure repeatable sampling.

5.4.2 Rotating enclosure C (compared to the original and static enclosures)

The following section adds the results of a third enclosure (Option C, Figure 5-4). This uses the same enclosure within the wheel as the static enclosure (Option B), but with the outer part of the enclosure rotating with the wheel as with the original enclosure (Option A), although that used the wheel itself as the enclosure. All three designs share the same fixed (non-rotating) back plate to form the rear of the enclosure, with the air inlet and sample pipes in the same location.

The testing undertaken on the static enclosure was replicated, comprising:

- 9 x PG-42 tests on the chassis dynamometer.
- 2 x Urban route tests on the roads.
- A moderate braking exercise on the test track.

Testing commenced with the PG-42 tests

5.4.2.1 PM and PN emissions from PG-42 and urban cycles

During the PG-42 cycles, brake pad and disc temperatures were recorded from both left-hand (no enclosure) and right-hand (with enclosure) front wheels. As Figure 5-109 shows, for the first of a daily sequence of three PG-42 tests from the three enclosures, different peak temperatures in the enclosure are seen for both pad and

disc although the profiles are similar, and the temperatures for the non-enclosed brake are similar in all three tests indicating those differences are due to the enclosure design. The highest peak and differential to non-enclosed wheel temperatures were observed for the original whole-wheel enclosure (A), and were lowest for the rotating 3rd enclosure (C), with the pad peaking around 30 - 50°C higher in the enclosure than for the opposite wheel, and disc temperatures around 40 - 80°C higher.

The original whole-wheel enclosure (A) has the largest volume which will reduce the rate of air exchange for the given flow rate, while the wheel rim being surrounded by a hot tyre and its air will limit heat rejection around its circumference, which together are likely to explain why this enclosure saw the highest temperature differential. The separate static (B) and rotating (C) enclosures share the same, smaller, volume leading to an improved rate of air exchange, while their aluminium thin-wall enclosure can dissipate heat to all sides. However, the rotating enclosure (C) may improve the air circulation around the brake disc and calliper for more effective cooling compared to the static (B) design, particularly at higher speeds as encountered later in the PG-42 cycle. In all designs, an increased air exchange rate (dilution air flow) is likely to reduce the temperature differential to the non-enclosed wheel, but the comparison of the otherwise identical rotating and static enclosures suggests a rotating enclosure improves cooling effect, while the separate enclosure provides better heat rejection capability than the whole-wheel approach.

Figure 5-109: PG-42 disc and pad temperatures, three enclosures

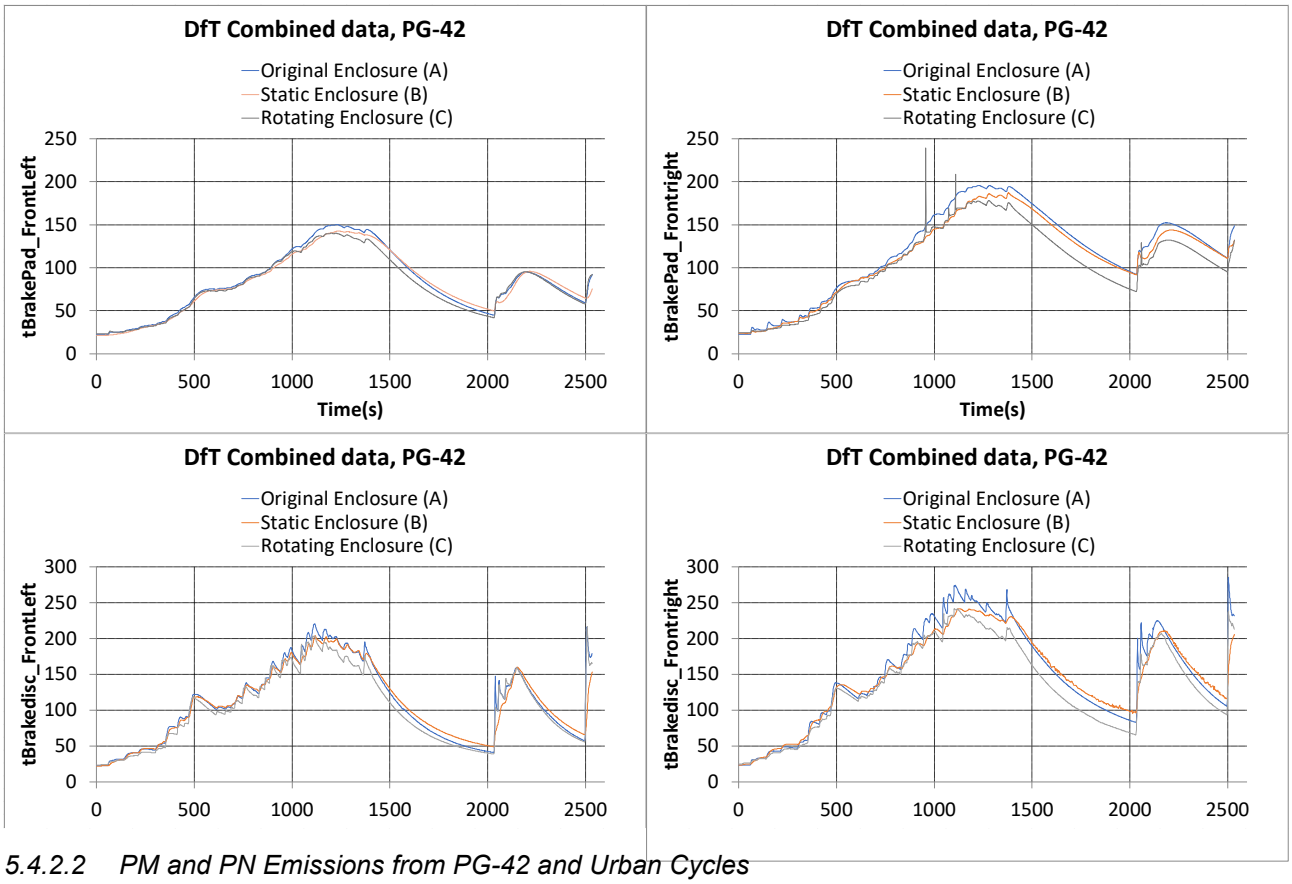

5.4.2.2 *PM and PN Emissions from PG-42 and Urban Cycles*

Comparative PN emissions collected from the 3 enclosures, during repeated PG-42 cycles, are shown in Figure 5-110, with a numerical summary presented in Table 5-16.

Note that some operational issues were experienced with the hot ELPI and no data are available from this instrument for the static enclosure.

Figure 5-110: Comparative PN & PM emissions collected from the 3 enclosures, repeated PG-42 cycles

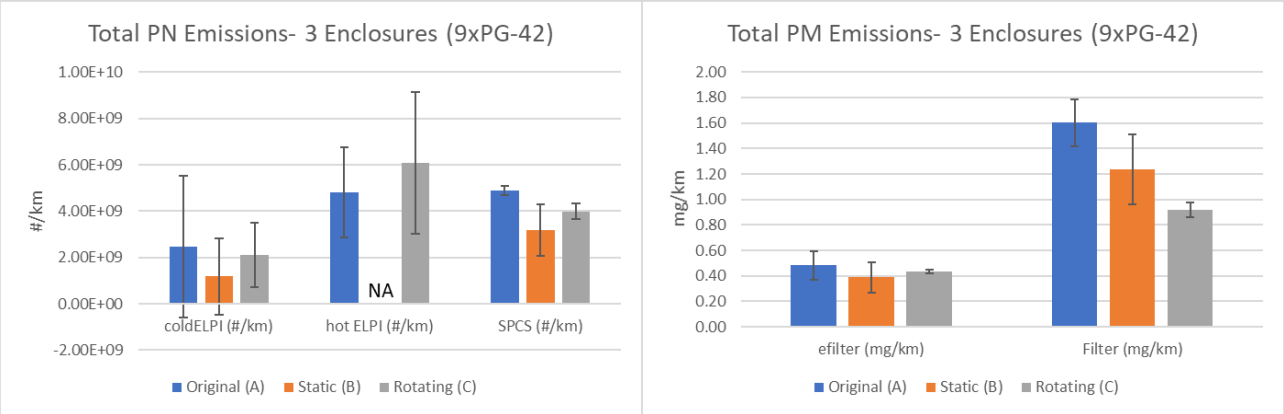

With 1-sigma error bars, PN emissions from the cold ELPI, hot ELPI and SPCS (Figure 5-110) appear to be similar between enclosures, though potentially PN emissions could be higher from the rotating enclosures than from the static enclosure. If so, higher PN from rotating enclosures could be due to the air movement in the rotating enclosures more effectively "flushing" them from around the calliper, while the static enclosure - with limited air space around the calliper – may see particle deposition in quiescent areas. Since these will be fine particles this is more apparent in the PN measurement than the mass. PM emissions from the eFilter were also similar between enclosures (Figure 5-110, right), though PM emissions from the gravimetric approach seemed to progressively reduce through Original (A) to Static (B) to Rotating (C) tests. Potentially this is related to the collection of volatiles by the glass-fibre filter media used, and this might indicate a reduction in gas phase volatile species with increased testing – a brake component conditioning effect. However, it should be noted that both the rotating enclosures' data (A and C) would be considered similar to the static enclosure's results, if not to each other.

Table 5-16: Comparative PN & PM emissions collected from the 3 enclosures, repeated PG-42 cycles

PG-42	Original Enclosure (A)			Static Enclosure (B)			Rotating Enclosure (C)		
	Average	STDEV	CoV	Average	STDEV	CoV	Average	STDEV	CoV
Cold ELPI (#/km)	2.47E+09	3.05E+09	123 %	1.18E+09	1.66E+09	141 %	2.11E+09	1.38E+09	65 %
Hot ELPI (#/km)	4.81E+09	1.95E+09	40%	N/A (malfunction)	N/A	N/A	6.08E+09	3.07E+09	50 %
SPCS (#/km)	4.91E+09	1.98E+08	4%	3.19E+09	1.12E+09	35%	3.99E+09	3.28E+08	8%
eFilter (mg/km)	0.48	0.11	23%	0.39	0.120437	31%	0.44	0.012668	3%
Filter (mg/km)	1.60	0.184	12%	1.24	0.275815	22%	0.92	0.058635	6%

Across the three enclosures the non-volatile PN measured from PG-42 tests by the SPCS was typically most repeatable of the PN measurements, with emissions in the range ~3.2 to 5 x10^9 #/km. Cold ELPI measurements were least repeatable. These results indicate both the impact of volatile particles on increased variability, but also the increased discrimination from background possible when measuring non-volatile particles.

PM (gravimetric) and eFilter emissions showed generally similar repeatability, with gravimetric PM emissions 2 to 3.5x higher than eFilter results. eFilter brake wear emissions were in the range ~0.39 to 0.48 mg/km, with gravimetric results in the range 0.92 to 1.60 mg/km.

With rotating enclosure (C), both the filter-based PM and eFilter PM measurements, plus the SPCS emissions were highly repeatable, with CoV ≤ 8% from 9 tests. Cold ELPI also showed the lowest CoV of the three enclosures (~65%). This may indicate that the enclosure design is most favourable for consistent results, but

it could also indicate that the brake system has reached a stable emissions condition for both solid and volatile particles.

Particle emissions from urban drives are shown in histogram form and tabulated in Figure 5-111 (left PN and right PM) and Table 5-17 respectively. Cold ELPI emissions appeared to reduce through the sequence of three enclosures, but the high variability with the original enclosure means that error bars overlap and emissions from the three enclosures are statistically similar, ranging from ~2.3 x10^9 #/km to ~4.7x10^9 #/km. There is no hot ELPI data available for the Static (B) enclosure, but emissions from the A (mean 5.5 x10^9 #/km) and C enclosures (4.0 x10^9 #/km) were also similar.

Figure 5-111: Comparative PN & PM emissions collected from the 3 enclosures, repeated urban cycles

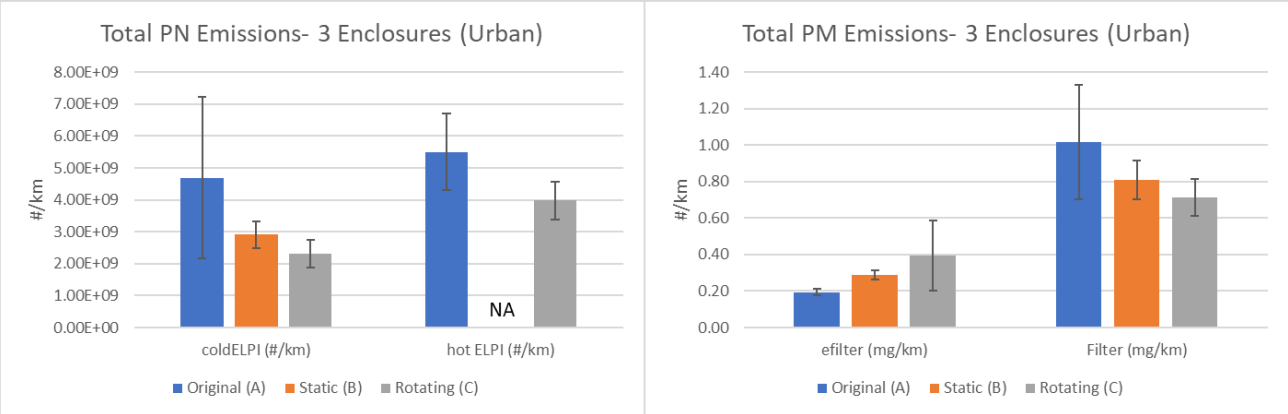

Similarly, there were only limited significant differences between mass emissions from eFilter and PM filter with different enclosures. For example, eFilter emissions from Enclosure A appeared to be lower than from the Static enclosure (B). eFilter masses ranged from 0.19 to 0.40 mg/km and PM filter masses from 0.71 to 1.0 mg/km.

If increased airflow around the calliper in rotating enclosures is a factor in higher measured PN seen in the PG-42 tests, then this effect would be diminished during urban driving where vehicle speeds are lower.

Across the three enclosures and both PG-42 and urban cycles, PN emissions were generally similar between enclosures with emissions ranging by just over a factor of 2. PM emissions varied by a similar proportion with the eFilter, and less with the gravimetric approach.

Table 5-17: Comparative PN & PM emissions collected from the 3 enclosures, repeated urban cycles

Urban	**Original (A)**			**Static (B)**			**Rotating (C)**		
	Average	STDEV	CoV	Average	STDEV	CoV	Average	STDEV	CoV
cold ELPI (#/km)	4.7E+09	2.54E+09	54 %	2.91E+09	4.25E+08	15 %	2.32E+09	4.39E+08	19 %
hot ELPI (#/km)	5.5E+09	1.21E+09	22 %	N/A (malfunction)	N/A	N/A	3.98E+09	6E+08	15 %
eFilter (mg/km)	0.194	0.017	9%	0.288	0.026	9%	0.396	0.192	48 %
Filter (mg/km)	1.016	0.315	31 %	0.809	0.104	13 %	0.712	0.102	14 %

5.4.2.3 Particle emissions from moderate track braking exercises

As described previously (Section 5.3.3.3), moderate braking exercises comprised repeated consecutive moderate braking events. With rotating enclosure (C), braking measurements were performed at approximately 50 mph/80 kph, 40 mph/64 kph, 30 mph/48 kph, 20 mph/32 kph and 10 mph/16 kph, with braking pressure ranging from lows of ~11 bar at 16 kph to a high of 32 bar at 80 kph (Figure 5-112).

Figure 5-112: Repeated moderate braking - Rotating Enclosure (C)

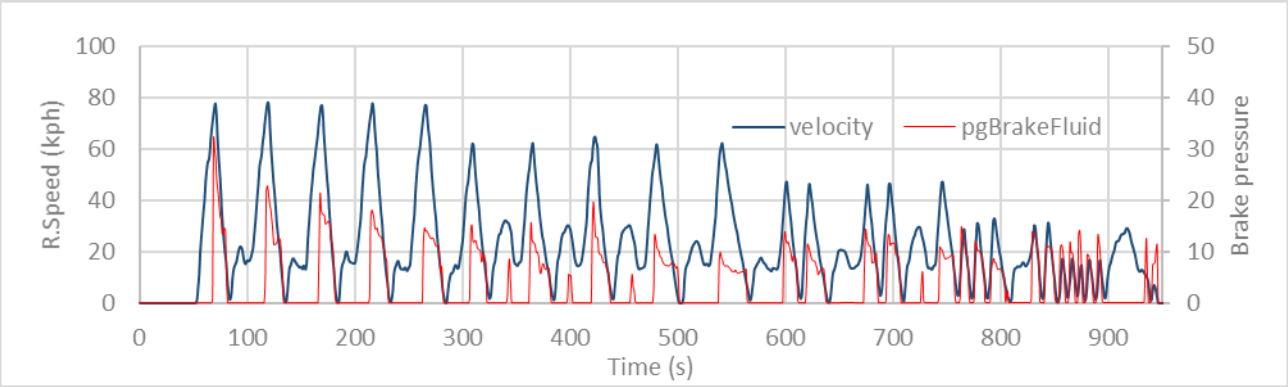

The sequence commenced at 50mph/80kph progressively reducing to 10mph/16kph.

Particle number emissions rates from the cold ELPI, at all speeds, are shown time-aligned with brake pressure and initial braking velocity in Figure 5-113. This shows that while higher speeds and braking pressures tend towards higher PN emissions, greatest emissions rates do not necessarily correspond to highest initial braking velocity and highest braking pressure combinations.

Figure 5-113: Cold ELPI PN emissions time-aligned with road speed and braking pressure, Enclosure C

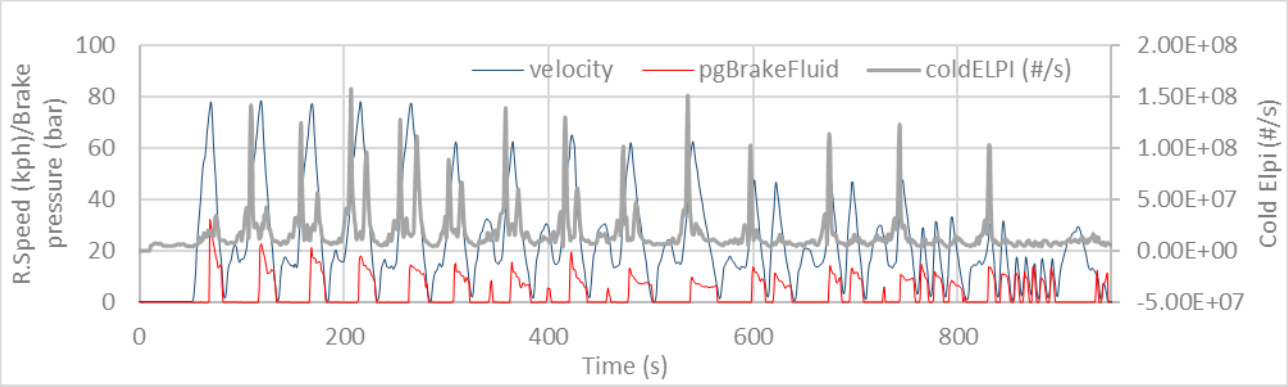

Similarly, Figure 5-114, greatest emissions rates do not correspond to highest brake disc temperatures and other factors such as the state of the disc and pad may be important.

Figure 5-114: Cold ELPI PN emissions time-aligned with road speed and disc temperature, Enclosure C

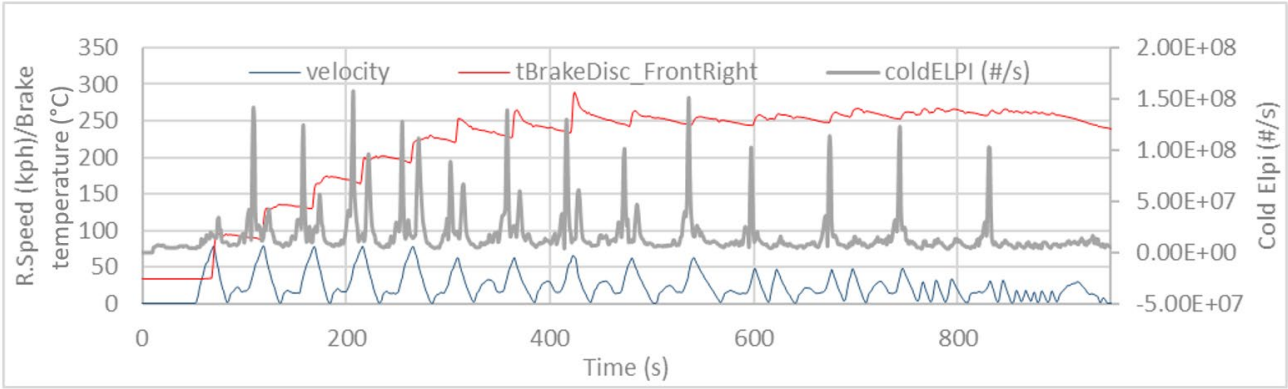

Particle emissions coincident with each single braking event at each speed, were isolated, averaged, and compared with emissions from the previous two enclosures. Data are shown for the cold ELPI and eFilter in (Figure 5-115).

Figure 5-115: Moderate track exercise PN (left) and PM (right) emissions from 3 enclosures

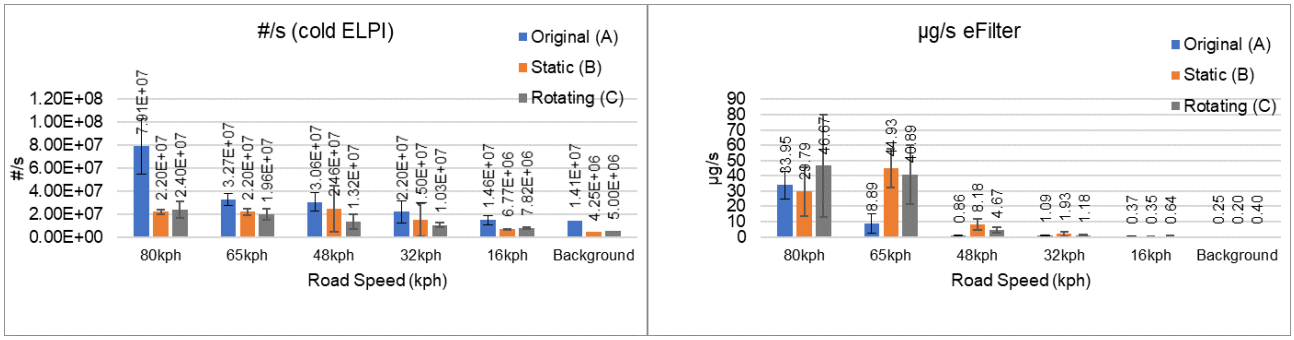

PM and PN emissions results from enclosures B and C were generally quite similar to one another, as were the temperature differences between enclosed and unenclosed brake discs (Figure 5-117), while emissions results from the original enclosure were occasionally different. This may be related to the evolution/bedding of the disc and pad over time. However, as described in Section 5.4.1.2, driver generation of braking pressures may especially impact PM emissions, and this can be seen in Figure 5-115 (right) and Figure 5-116 where lower PM emissions by eFilter correspond to lower braking pressures at both ~65kph and ~48kph. At other speeds braking pressures and PM emissions are similar between all enclosures. This phenomenon likely arises due to the dominance of non-volatile materials in the quantified brake mass (typically >90% as determined by thermogravimetry).

PN emissions were less consistent between enclosures, but these are complicated by the formation of particles through release of relatively small masses of volatile materials that can nevertheless dominate the overall number emissions. Release of volatiles may be highly dependent on small differences in local temperatures and effective dilution ratios within the enclosures. The use of non-volatile PN to quantify brake emissions would eliminate at least some of this variability.

Figure 5-116: Braking pressures from the moderate braking exercises, 3 enclosures

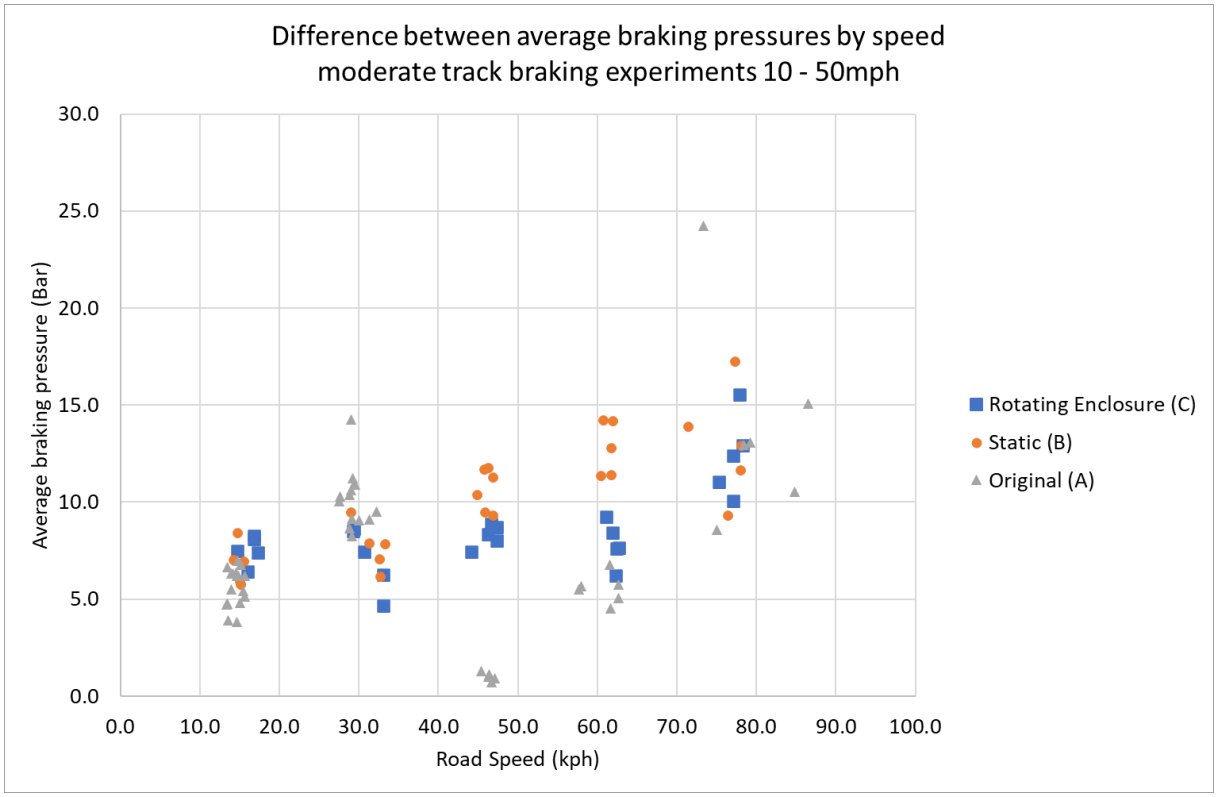

Figure 5-117: Enclosed vs. unenclosed disc temperatures, Static (B) and Rotating (C) enclosures

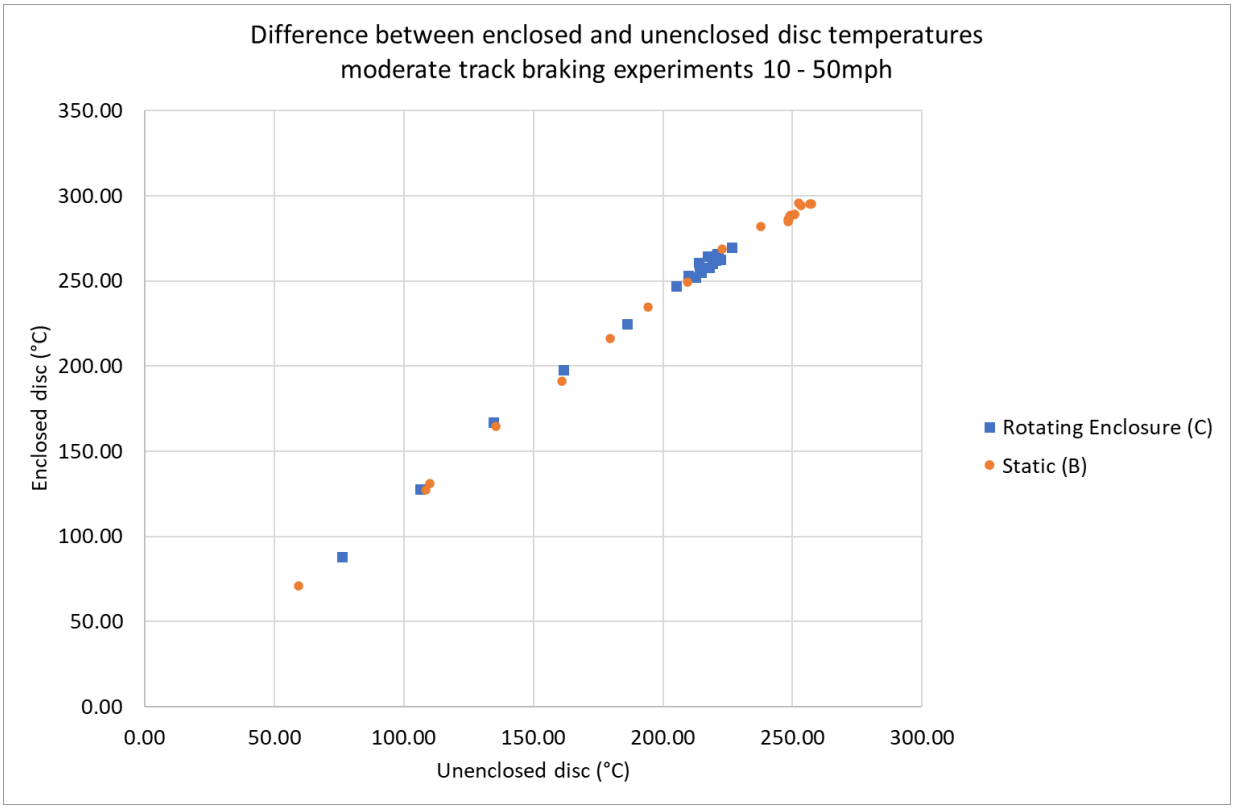

5.5 TEST RESULTS 3: AUDI A4 REAR WHEEL

Chassis dynamometer measurements of brake particle emissions were made using the Audi A4 vehicle, described in Section 5.1.1.2, from a rotating enclosure installed on the rear right-hand wheel. The rotating enclosure was very similar to the original rotating enclosure used on the Caddy (Section 5). These experiments permit the assessment of:

- Transferability of the wheel enclosure sampling approach from one vehicle to another.
- Measurement of the particle emissions using the equipment operating externally, rather than internally on the vehicle (informative for the practicality of effective measurements from multiple vehicles on the chassis dynamometer).
- Emissions from a different brake pad/disc combination to those present on the VW Caddy.

Six PG-42 cycles were driven on the chassis dynamometer, with very good repeatability of cycle distance (CoV = 0.17%) and CO_2 emissions demonstrated (CoV =2.75%), Figure 5-118. Measurements were made with hot ELPI, cold ELPI, eFilter, GF/A PM filter and SPCS. Background measurements from the enclosure (with the vehicle stationary and sampled for ~2200s, compared to the ~2537s of the PG42 cycle) were obtained for hot ELPI, cold ELPI, eFilter and GF/A PM filter. For background comparison purposes the PM filter mass obtained was scaled by a factor of 2537/2200.

Figure 5-118: Audi PG-42, distance and CO_2 repeatability (6 tests)

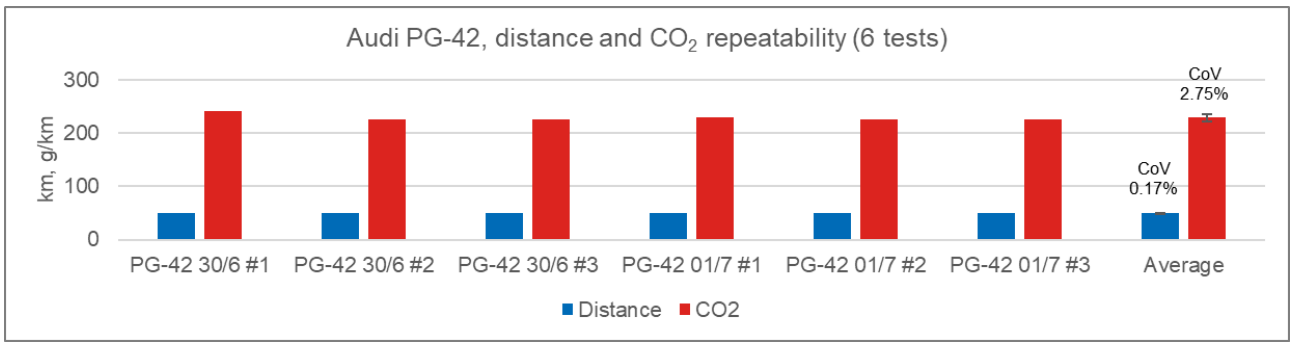

PM samples from the 6 tests were visually very similar to the filters from the VW Caddy during the PG-42 tests (for example, Figure 5-31) showing deep black particulate matter (Figure 5-119).

Figure 5-119: Three PM filters from repeated PG-42 tests, Audi A4 rear-wheel

Thermogravimetric analysis revealed slightly more non-oxidizable material (identified as remainder and most likely metal oxides), less carbon and similar levels of volatiles and water from the Audi A4 than from the VW Caddy, as shown in Figure 5-120. This may indicate slightly different brake pad bulk chemistries between the two vehicles, though further work would be required to resolve differences from test-to-test variation.

Figure 5-120: Breakdown of PM composition by thermogravimetry, VW Caddy and Audi A4 PG-42 results

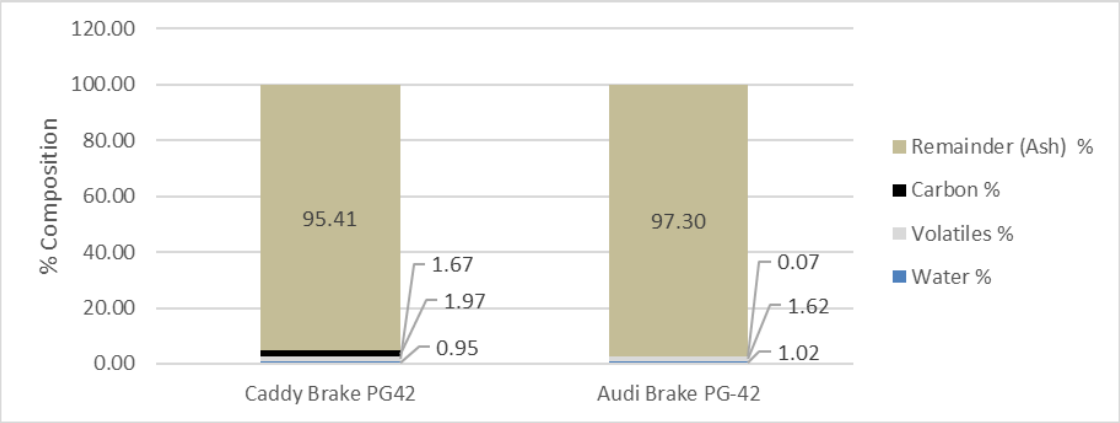

Results of particulate mass determinations are given in Figure 5-121, with gravimetric filter masses around 0.65 mg/km and eFilter mass at ~0.33 mg/km. Filter-based PM is shown uncorrected and with the background subtracted (~0.012 mg/km), while eFilter results are shown uncorrected (background ~0.009 mg/km). Repeatability of the mass methods was in the range 12 to 15%, while eFilter masses were on average 50% lower than the filter-based measurements. This is likely due to under-estimation from the eFilter due to incorrect assumptions of the particle density (based upon carbon rather than the metallic oxides) and particle size distributions present in the sample aerosol as described previously (Section 5.3.3.1.3).

Figure 5-121: PM analysis results from PG-42 Cycles, Audi A4

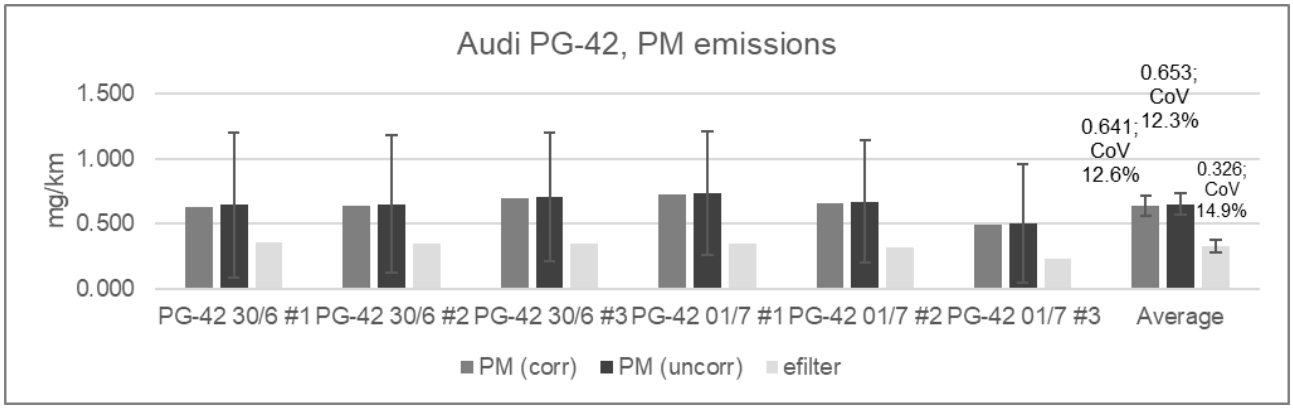

Particulate mass emissions were consistently lower than seen for the VW Caddy (Table 5-12), which showed average results for uncorrected PM at 1.602 mg/km and eFilter mass at 0.482 mg/km. Caddy repeatability was broadly similar, 7 – 23%). Lower mass emissions may be due to the lower braking forces applied to the rear brakes and the lower test inertia of the Audi A4.

PN emissions in #/km and #/s from cold ELPI, hot ELPI and SPCS from the PG-42 tests on the Audi A4 are shown in Figure 5-122.

Figure 5-122: PN emissions from cold and hot ELPIs plus SPCS from PG-42 Cycles

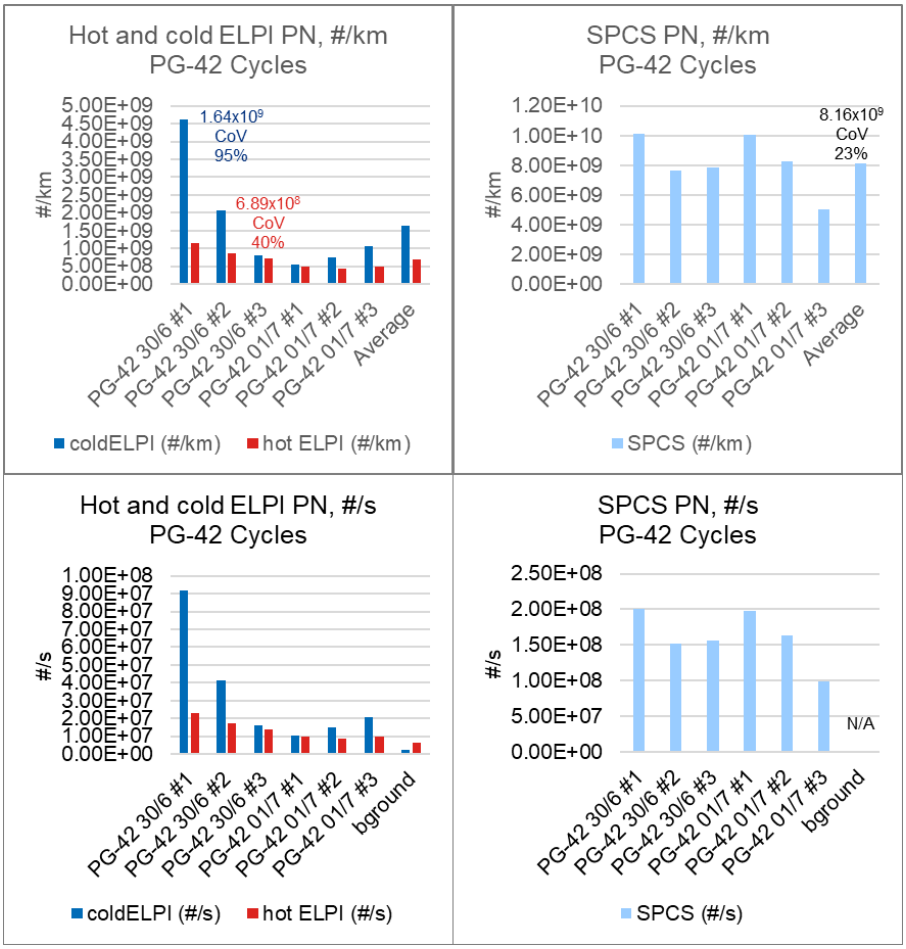

Emissions measured by the cold ELPI were lower than from the front brake on the VW Caddy (1.64 x 10^9 #/km v 2.47 x 10^9 respectively), as were emissions from the hot ELPI (4.81 x 10^9 #/km v 6.89 x 10^8 respectively). This is consistent with the reduction seen in PM. However, on the VW Caddy the PN emissions levels from the hot ELPI were higher than from the cold ELPI, believed to be due to restructuring of the particle size distribution in the hot ELPI alongside the elimination of some volatiles. Conversely, on the Audi A4, the hot ELPI emissions are lower than those from the cold ELPI, which may indicate that the materials released by the brake pad during PG-42 braking events are more volatile and thus more easily eliminated at 180°C than those from the pad on the VW Caddy. As seen with the thermogravimetric analyses, this may be an indication of different particle production from different pads deriving from different chemical compositions.

The size distributions, averaged over the 6 tests, from the two ELPIs are shown in Figure 5-123. These indicate generally reduction in PN levels across the size range, excepting a slight restructuring of the accumulation mode above 0.5µm.

Figure 5-123: Size distributions from 6 averaged PG-42 tests, cold and hot ELPIs

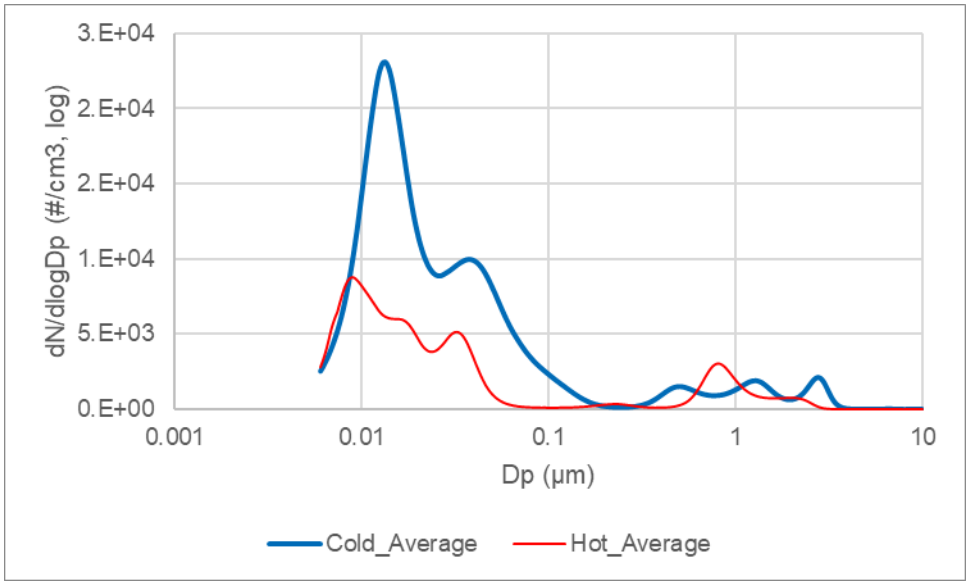

Emissions from the SPCS (~8x10^9 #/km) were higher than from the hot or cold ELPI and higher than from the VW Caddy (~5 x 10^9 #/km). This conflicts with the comparative results for the ELPIs between the VW Caddy and the Audi A4. The SPCS had just returned from a scheduled annual service and calibration prior to the Audi tests. However, there is no obvious reason for the large difference between the SPCS and ELPIs observed, excepting that the ELPIs were running much closer to their limits of detection in these tests. Both were less repeatable and less able to reproducibly indicate particle emissions peaks during the cycle.

Critically, when considering the potential of particle number counting of brake wear measurements for legislative purposes, the SPCS is consistently more repeatable (CoV = 23%) than the cold or hot ELPIs (CoV of 95% and 40% respectively). Real-time repeatability of the SPCS and hot ELPI are shown in Figure 5-124.

Figure 5-124: Real-time PN traces from PG-42 cycles, SPCS (top) and hot ELPI

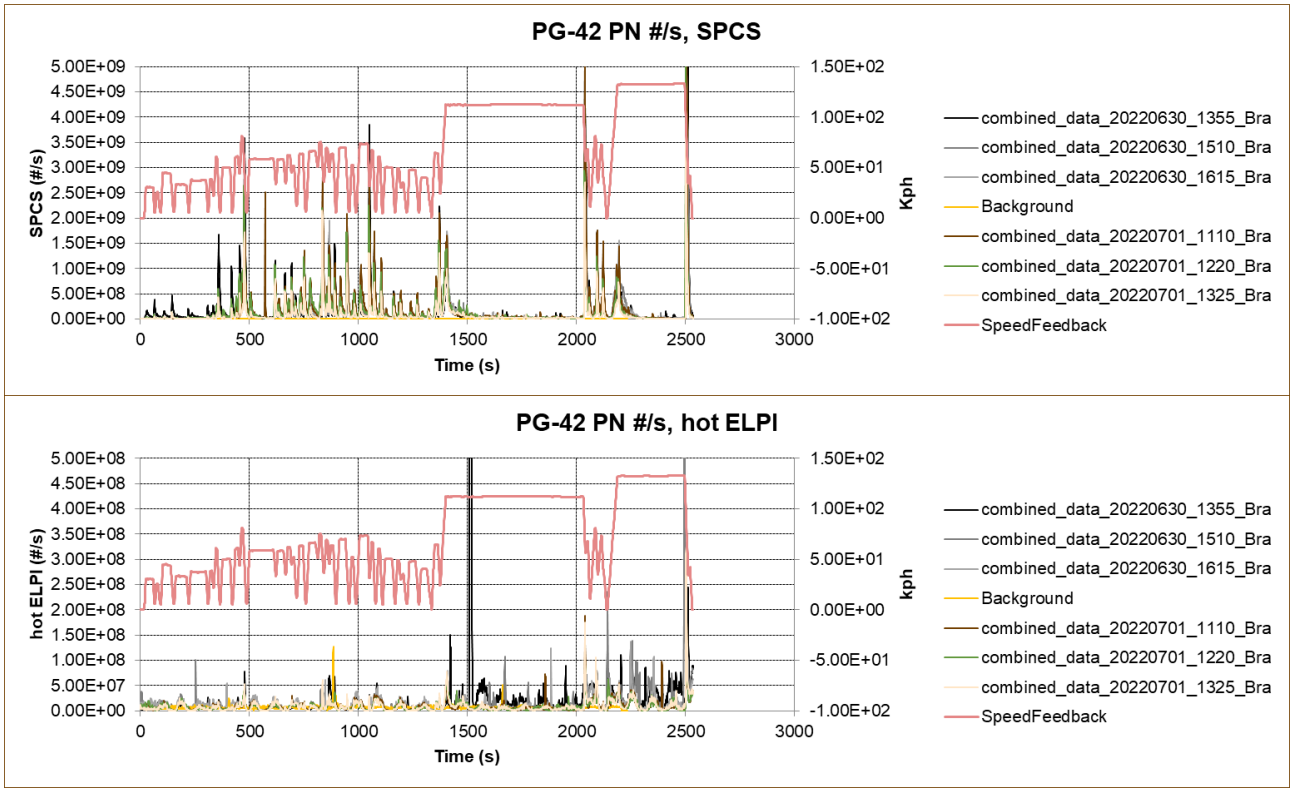

These figures indicate that while the non-volatile measurements from the SPCS appear to reflect the braking events well, the hot ELPI measurements appear less reliable. This is further indication that a regulatory particle number metric would be best focused on non-volatile particles.

5.6 OTHER INVESTIGATIONS

5.6.1 A comparison of brake emissions from this study with literature values

Brake wear particle number emissions from literature were summarised in Table 2-4. These were sampled from the brake dynamometer approach currently under development in the PMP NEPE group. The values from Table 2-4 are reproduced in Table 5-18 below, along with data from this project (in the grey-shaded columns). The first three rows indicate total particle number emissions, in this project using cold ELPI (from original enclosure, Figure 5-62) while the 4th row indicates non-volatile PN emissions, in this project using SPCS (from original enclosure, Figure 5-34).

Table 5-18: Summarised total and solid PN emissions, various cycles

	WLTP brake cycle	20 min of LACT <153°C	20 min of LACT >153°C	5 Tests average NAO	20 min of LACT total PN	3h-LACT	WLTP brake cycle	PG-42	Urban	Moderate braking	Extreme braking
Max	6.00E+09		1.30E+13								
Mean Total		1.00E+10		4.50E+10	7.00E+12	1.00E+10	6.50E+09	4.20E+09	2.50E+09	4.80E+09	5.00E+12
Min	1.50E+09		2.00E+12								
Mean solid					4.00E+09	3.50E+09	7.00E+09	5.00E+09	[-]	[-]	[-]

Results suggest that mean solid PN emissions from this study are consistent with values seen for the LACT and WLTP brake cycles, with total particles slightly lower during moderate braking. Extreme braking emissions tests from this study were likely more aggressive than the “20 min of LACT” excerpt, but again total PN emissions were lower. Dilution and sampling conditions play a key role in the formation of volatile particles, as do the measurement systems themselves (for example, comparing the hot and cold ELPI). The brake dynamometer measurement system has much higher dilution flows and different cooling capacity for the sample, this may lead to different gas to particle conversion resulting in increased or reduced volatile particle formation, while anticipated impacts on solid particle emissions would be much smaller.

As discussed in Section 2.4.3, literature PM_{10} brake system emission factors were found to be 5 ± 0.7 mg/km per brake over the WLTP-Brake cycle (all vehicles using low steel (LS) brake pads, four studies). In this study using the gravimetric filter approach, front brake emissions from the PG-42 cycle, and all three enclosures, ranged from 0.82 to 1.84 mg/km, with a mean value of 1.33 mg/km. This represents around 27% of the literature values on average. Potentially the sampling system used in this study may under-sample the larger particles leading to lower mass. Other contributory factors to the difference could be, that the relatively long distance of the PG-42 cycle (50km), and long cruises in the cycle without braking, mean that the PG-42 is a lower emitting cycle than the WLTP brake cycle; the brake pads and discs used in this study are lower emitting than used in the literature tests.

5.6.2 Estimates of tyre wear emissions and tyre sampling efficiency via sample duct

An estimate of the total material lost from a single tyre can be estimated in different ways:

1. Firstly, literature provides some assumptions (e.g., Grigoratos et al, [15]): mass loss from a tyre is ~1,000 to 1,500g over the lifetime of a tyre; typical lifetime distance driven on a tyre is 20,000km and ~10% of the mass is present in the PM10 regime. This results in PM10 emissions per km of 5 mg/km to 7.5 mg/km.
2. Assuming the density of crumb rubber (1.2 g/cm^3), initial tread depth of 8mm and end-of-life tread depth of 1.6mm, tyre tread area of ~122,000mm^2 (from Ricardo measurements) it can be calculated that total mass loss in 20,000km would be ~316g per mm of tread lost and 2022g over the vehicle lifetime. This equates to ~100mg/km total mass loss and ~10mg/km PM10 per tyre.

Both methods arrive at similar values, in the range 5-10 mg/km, but these values are substantially higher than measured by the tyre sample duct approach used in this project, where typical emissions values from the PG-42 cycle were in the range 0.03 mg/km to 0.06 mg/km measured by eFilter and gravimetry. It is clear that the tyre sample duct used as described in 5.1.3 will not collect all the emissions from the tyre, but establishing a ratio of the mass of sample collected to the total mass emissions of the tyre (the mass collection efficiency) for such an open system is a challenge.

One approach to estimating the collection efficiency is to consider the proportion of the gap between the tyre and the road that is filled by the sample duct opening, as shown in Error: Reference source not found. The duct has an opening approximately 7 mm tall in a gap between the tyre and the road of approximately 70 mm, giving a ratio of 1:10, which could be taken to be the collection efficiency if emissions are aspirated homogenously from the contact patch. However, the particulates emitted from the tyre will not be distributed evenly across this gap, a significant proportion may be entrained close to the tyre to depart later, or be released from the surface of the tyre further around its rotation, while others may be deposited onto the road surface. It should be noted that the penetration of particles through the sampling system at the typical operating condition of 350 slpm will be a little over 20% at 10µm, so the system slightly under-samples PM_{10} (Figure 4-10) which, by definition, requires a 50% efficiency at 10µm, and this would tend towards the sampling system indicating lower mass emissions. Therefore, we can assume the ratio of 1:10 or 10% is the upper bound for the collection efficiency of the sample duct.

Figure 5-125: Tyre sample duct opening to gap ratio

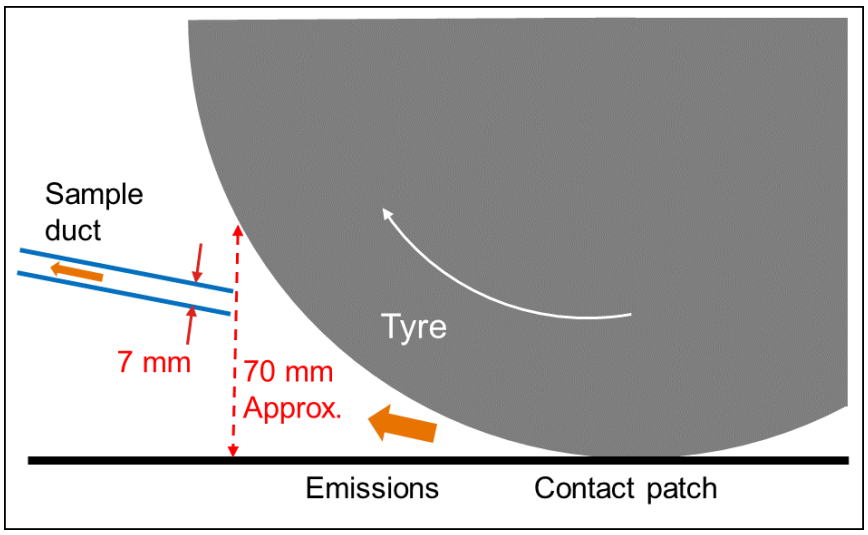

An alternative approach is to compare the ratio of the area of the sample duct opening to that of the tyre contact surface, that is the raised area of the tread that makes contact with the road. Measurements of the tyre and analysis of the tyre tread compared to measurements of the duct estimated the duct area to be approximately 1/150th of the total tyre tread area. If the whole circumference of the tyre contact surface sheds particles at the same rate during braking (rather than emissions being concentrated at the contact patch), this ratio of 1:150 or 0.67% is taken to be a lower bound for the collection efficiency of the sample duct.

The mass emitted by the tyre would be the measured mass emissions rate (e.g., mid-range of measurements) 0.045 mg/km * the duct sampling efficiency. While these estimates for the sampling efficiency between 1 in 10 and 1 in 150 covers quite a wide range, if the efficiency is assumed to be somewhere between the two, e.g.: 1 in 100, then mass emissions = 0.045*100 = 4.5 mg/km (PM10). This value is consistent with the values identified in (1) and (2) above considering that larger particles may not be aspirated (i.e., are deposited on the road surface), but further work is required to establish the validity of this estimate. Similarly, work is required to determine the collection efficiency of the scoop for particle number rather than particulate mass, as this may be significantly higher than for mass.

6. SUMMARY AND CONCLUSIONS

6.1 SPECIFIC CONCLUSIONS, BRAKE EMISSIONS

The following specific conclusions are based primarily on the experiments conducted with the original brake enclosure, and tyre emissions with the same enclosure installed.

- Backgrounds were quantified as mass (typically µg) or number per second, including from the gravimetric filter. This enables any background to be applied to a test of any duration, or distance. This approach was taken with background samples drawn from the brake enclosure and through the tyre sampling scoop, with the vehicle static
- Roadside/on-road backgrounds of PM and PN emissions can be consistent and don't appear to be related to the sample probe location employed. Cold ELPI PN backgrounds (~$2x10^8$#/s) were higher than hot ELPI backgrounds (~$5x10^7$#/s) with eFilter PM (~2.85µg/s) higher than filter-based PM (~0.5µg/s).
- PN backgrounds in the VERC chassis dyno facility were up to 10x lower than roadside backgrounds, with PM (eFilter and gravimetric) at least a factor of 4 lower.
- The PG-42 cycle demonstrated repeatable distances and CO_2 emissions when tested on the chassis dynamometer, providing a sound basis for evaluation of emissions and instrumentation
- From the original enclosure, the most repeatable metric for brake particle emissions during on-dyno PG-42 testing was non-volatile PN emissions measured using hot dilution, an evaporation tube and condensation particle counter (by the Horiba SPCS). This demonstrated a CoV of 4% from 8 tests, while gravimetric PM showed ~7%, eFilter ~23%, hot ELPI ~40%, with cold ELPI the outlier at ~123%. Individual cold ELPI braking events were difficult to resolve from the time series data, while hot ELPI and SPCS braking events were much clearer. Most braking events were also apparent in the eFilter data. Throughout testing on all enclosures, the SPCS results proved most repeatable of the particle number approaches.
- Integrated PN (cold and hot ELPI) and PM (eFilter) results from PG-42 tests appeared to differ in magnitude related to test order, this effect was not seen with the SPCS. This indicates the influence of volatile release on PN and PM emissions, potentially related to cumulative energy storage on a single day, and pad/disc evolution at the start of a test sequence with harsh braking in the PG-42 cycle. It also shows that the hot ELPI's 180°C heating capability does not exclude all volatiles and is unable to create a consistently stable measurement metric.
- Gravimetric PM filters from brake PG-42 tests were black in colour. Thermogravimetric analyses indicated that PM samples were >95% non-volatile and non-oxidizable with low levels of EC, volatiles and water also present. The non-volatile material was most likely iron oxide with other metal oxides and ceramics also potentially present.
- Number weighted particle size distributions from the hot ELPI during PG-42 tests differed from those measured with the cold ELPI, with some particles >1µm removed by the 180°C heating approach. Both cold and hot ELPI size distributions show several peaks, but these differ in both location and magnitude between the two instruments. Heating in the hot ELPI leads to restructuring of the size distribution determined by the cold ELPI so that it no longer truly represents the size distribution of emissions. The hot ELPI detects some volatiles in the sub-100nm region which appear to be created from the evaporation of large particles, and this leads to both variability in results and to higher PN emissions from the hot ELPI than the cold ELPI. Consequently, the hot ELPI integral is an unreliable metric for PN, and something like the PMP-derived non-volatile PN definition is advised. Particles in the region >0.5µm may be more repeatable, but the levels of these particles are very low and almost certainly not suitable for use in regulatory control.
- PG-42 particle number emissions from SPCS and hot ELPI were of the order $5x10^9$#/km/brake, with cold ELPI levels around 50% lower. Gravimetric PM emissions were around 1.6mg/km/brake, with eFilter emissions at ~25% of this.
- Urban cycle repeatability was generally similar to that observed for PG-42 measurements. The hot ELPI showing ~27% CoV, cold ELPI ~60% CoV, the eFilter ~5% and gravimetric PM ~30%.

- Urban cycle gravimetric PM filter analysis was consistent with the PG-42 result, showing >95% non-volatile, non-oxidizable constituents. This indicates that the brake enclosure is effectively shielding the PN and PM measurements from ingress of on-road background.
- Mass weighted particle size distributions from cold ELPI were similar from PG-42 and urban driving, with the PG-42 result substantially higher in magnitude. This is consistent with the more demanding braking conditions of the PG-42 and indicative of minimal background contribution.
- PM emissions levels from urban cycles were lower than from PG-42: gravimetric PM ~0.9mg/km/brake vs. <1.6mg/km/brake; eFilter ~0.19 mg/km/brake vs. 0.48 mg/km/brake and PN levels were similar (2 to $5x10^9$ #/km/brake from cold and hot ELPI). This is consistent with the urban drives seeing less aggressive braking than the PG-42 cycle. As with the lab PG-42 tests, hot ELPI PN were higher than cold ELPI PN due to the restructuring of the PM materials and creation of new volatile particles in the hot ELPI.
- Repeated moderate braking events on the test track revealed that both PN and PM emissions increased proportionally with kinetic energy supplied (with the velocity squared). Although braking events starting from the same speed were reasonably repeatable, there was no obvious relationship of increased PN emissions with increased pad and disc temperatures, in fact the opposite may have been observed. However, the experiment commenced with the higher speed braking events, and this may have masked any pad/disc temperature effect
- Higher braking pressures, from different drivers executing moderate braking exercises on different enclosures, appeared to lead to higher PM emissions as measured by the eFilter. This may be due to mechanical wear of primarily non-volatile components from the pad and disc.
- From the moderate braking experiment, there was a clear positive linear correlation between increasing PM and PN emissions and the product of initial braking velocity (kph) and max brake pressure (bar). This indicates a potential correlation between maximum energy loss to the brakes and highest PN emissions.
- During moderate on-track braking exercises, variation between emissions from different brake enclosures for PN was higher than for PM, probably due to the influence of small masses of evaporable materials generating highly variable large numbers of volatile particles.
- Extreme braking events suggested that very high pad/disc temperatures have the potential for continuous emissions of particles to occur. These are likely losses of volatile/semi-volatile materials that occur when the brake pad reaches ~300°C and the disc ~400°C. At this point it becomes impossible to discriminate isolated peaks of PN (ELPI) and PM (eFilter) emissions from near-by braking events. This might be possible with an evaporation tube or catalytic stripper based PN measurement.
- Between similar braking events, in the extreme braking events testing, which resulted in different brake pad and disc temperatures (pad 30°C and 175°C; disc 120°C and 350°C), similar PN emissions were observed with the ELPIs. This suggests that differences in the pad and disc temperatures between the enclosure on the right-hand wheel and normal braking system on the left will have a minimal effect on measured PN emissions, assuming pad and disc temperatures remain below ~300°C and ~400°C respectively.
- PN emissions from the cold and hot ELPI from extreme braking events increased as pad and disc temperatures increased. Emissions were 1-3 orders of magnitude higher than from the urban, PG-42 and moderate braking testing, exceeding 10^{11}#/km in the initial extreme tests and then exceeding 10^{12}#/km/brake as testing progressed. A similar effect was observed with the eFilter, where brake wear emissions reached close to 200mg/km at the end of the extreme testing, compared to <0.6mg/km/brake from the moderate track testing.
- Particle size distributions from urban, PG-42, moderate track testing and extreme track testing were generally similar in shape/profile from the hot ELPI, with overall PN dominated by the <100nm fraction. Above 0.5µm the particle size distributions likely show low volatility or solid modes, with the comparative magnitude of these from the different dyno, road or track tests consistent with overall PN emissions. This size range contributes to PM but does not have a major impact on PN. Cold ELPI particle size distributions are much less consistent between different dyno, road or track tests, probably due to volatiles being present right across the size range, though ranking of emissions from high to low was the same as seen with the hot ELPI. It's clear that to evaluate emissions of PN from the most

aggressive braking events a non-volatile PN metric is required, and to avoid the influence of volatile emissions being disregarded a mass metric should be employed in parallel.

- Three different approaches to enclosing the brake were tested. Generally, results were similar with little clear difference between them, but some measurements did support theories about their different characteristics.
    - The whole wheel being used as the enclosure (the original design) showed worse heat rejection capabilities (higher brake temperatures) than the two separate enclosures. This is thought to be due to the larger volume meaning less frequent air exchange, and the wheel rim and surrounding hot tyre providing less scope for heat dissipation than the separate enclosures. However, the use of larger wheels provided more air space around the separate enclosures within the wheel than would be the case with the standard wheels.
    - The static enclosure showed slightly worse heat rejection capabilities (higher brake temperatures) than the otherwise similar rotating enclosure at higher speeds. There was also some evidence of lower PN emissions being measured in higher-speed tests. This is thought to be due to restricted air flow around the calliper, which has tight clearance to the enclosure, compared to the rotating enclosure which promotes better air movement and mixing at higher rotational speeds (vehicle speeds).

6.2 SPECIFIC CONCLUSIONS, TYRE EMISSIONS

- Tyre wear was sampled using an open duct positioned near to the rear of the tyre, just above the road surface where materials evolved from the tyre will be flung away from the rotating surface. Unless the wheel locks, and that was not observed in this project, the entire surface of the tyre will be involved as the vehicle slows. Consequently, materials are emitted from the entire circumference of the tyre, and these may be released after a section of tyre has passed the duct entry. The duct likely only samples a fraction of the total tyre losses. This fraction has been calculated at between 1/10 and 1/150 for the duct and front tyre used in this study. If an efficiency of ~100 is assumed and multiplied by the measured emissions, a PM_{10} mg/km/tyre value of ~4.5 mg/km/tyre consistent with literature and calculated values (Section 5.6.2) is determined. However, the approach requires further work to understand and validate.
- Real-time spikes of PM (eFilter) and PN (SPCS) from on-dyno tyre wear during PG-42 cycles correspond to most braking events and braking pressure rises, indicating that tyre wear particles can be measured above any facility background levels. Hot ELPI responses were similar to the SPCS, but some additional peaks were observed. These may have been semi-volatile particle emissions eliminated by the high temperature of the SPCS (350°C) but not by the hot ELPI (180°C). Cold ELPI data does not appear to reliably show braking events, although it does show many peaks that are not well aligned with cycle braking activity.
- Tyre wear emissions repeatability was reduced in comparison to brake wear measurements. From ≥ 7 PG-42 cycle measurements, tyre PM emissions were most repeatable (eFilter ~ 18% CoV and gravimetric ~19% CoV). SPCS emissions were at 27% CoV, with hot ELPI data at 63% and cold ELPI data at 110%. Hot and cold ELPI data would be closer to instrumental limits of detection but would also detect more semi-volatile particles than the SPCS, leading to increased variability
- Collected gravimetric PM from PG-42 tyre emissions tests in the chassis dyno facility was a uniform light grey colour which could indicate low levels of uniformly dispersed black materials, such as tyre rubber. Thermogravimetric analyses revealed that the material comprised ~63% non-volatile, non-oxidizable materials, so these might be steel and other inorganic materials. The remaining 37% included ~ 2% elemental carbon, ~13% water with the other 22% being volatiles (rubber / HC). It is possible that some brake wear contributes to the filter mass but, if so, only a very small contribution would come from the same wheel since its braking system is enclosed with only a minor outward leakage of the brake aerosol.
- Hot ELPI particle size distributions from PG-42 tyre wear tests were generally lower in magnitude than from the cold ELPI across the measured size spectrum. In the size range between ~20nm and 35nm a new mode forms in the hot ELPI as volatilised larger particles condense and form new particles. Conversely, a dip appears in the hot ELPI particle size distribution at ~0.2µm, where a peak exists in the cold ELPI data. The cold ELPI size distributions were dominated by a ~10nm mode that is almost completely absent in the hot ELPI. As seen in the brakes data, the hot ELPI presents a more stable

measurement, but it is not representative of the size distribution emitted and is less stable and repeatable than the SPCS measurement.

- Mass weighted particle size distributions from cold ELPI were substantially higher from urban driving than from PG-42 tests, contrary to expectations regarding braking severity. This is consistent with background particulates dominating the urban data and indicates that measuring on-road tyre wear is very challenging, if not impossible.
- Particles from tyres emitted in the size spectrum above ~0.5µm appear to be of low volatility and thus stable and relatively repeatable, but levels are very low (dN/dlogDp is <100#/cm^3) and it would not be viable to consider this range in isolation for regulatory control of emissions
- Emissions of both PM (eFilter and gravimetric) and PN (ELPIs and SPCS) tyre particle emissions from PG-42 tests were comfortably higher than the facility background. Background corrected PM emissions (both PM methods) were ~0.03 to 0.04 mg/km/tyre, with PN emissions around 10^9 #/km/tyre or below (SPCS and hot ELPI), while cold ELPI PN levels were on average ~3x10^9 #/km/tyre, but highly variable. Chassis dyno evaluations of tyre wear emissions appears to be feasible, though sampled emissions concentrations are lower than brake emissions.
- Reducing tyre pressures from 2.9 bar to 2.0 bar, when testing PG-42 cycles for tyre emissions on the chassis dyno, increased cold ELPI PN emissions (by ~8x) and eFilter PM (> 2x) while hot ELPI and SPCS PN emissions were unaffected. The major impact of the tyre pressure change was the increase in the magnitude of particle concentrations in the nucleation mode peaking at, or below, 20nm through the release of volatile / semi-volatile materials.
- Questions remain regarding tyre wear measurements in the chassis dynamometer. These include:
    1. Background subtraction, as it is not clear what actually enters the sample scoop from the ambient when the wheel is rotating, and the tyre is emitting particles and vapours. Potentially these emissions could displace or repel the ingress of background materials.
    2. It is uncertain how much of the emitted particulate / aerosol from any braking event is sampled by the scoop. If aerosol is entrained in a sheath that surrounds the wheel, or the vast majority of particles emitted are immediately drawn into the scoop, then the amount sampled may be much larger than would be suggested by the ratio of the scoop area to the tyre surface area.
- Urban cycle tyre emissions repeatability appeared good, with PM (background corrected) at 16% CoV, PM (uncorrected) at 11%. Corrected eFilter, hot ELPI and cold ELPI showed CoV at 11%, 34% and 41% respectively. This likely reflects the repeatability of the background rather than emissions from the tyres.
- PM filters sampled during on-road urban drives were stained a dirty grey colour with speckling from large particulates originating from the background, probably road dust (as they were not present during PG-42 testing). The non-volatile (mass) fraction was ~86% compared to ~63% from the PG-42 tests. Particle size distributions showed higher levels of <100nm particles and more abundant >1µm particles compared to PG-42 tests, despite the milder braking events of the urban drive. These suggest substantial ambient contributions in these size ranges, and probably ambient particle contributions across the size spectrum.
- Subtracting background PM from the measured tyre emissions reduces the two most representative metrics to zero (cold ELPI, eFilter). This suggests that a background sampled in parallel would be necessary for real-world tyre measurements. This is unlikely for logistical and cost reasons, and it would likely still be difficult to resolve particle emissions repeatably. Hot ELPI PN was higher than background levels, but this may just have been due to reconfiguring of the cold ELPI particle size distribution and this reconfiguration may not occur in the same way for background particles as for tyre emissions. It appears to be very challenging to measure on-road urban tyre wear emissions
- A session of repeated moderate braking (braking pressures up to 50 bar) on the test track addressed speeds up to and including 50mph (80kph). Cold ELPI real-time PN emissions showed many spikes, occurring between braking events, as well as some that were coincident with braking events. Hot ELPI real-time PN spikes were primarily aligned with braking events, and were well above baseline/background, but even though braking events were repeatable in terms of speed and braking pressure, spikes of particle emissions were not observed with every braking event. The eFilter showed the same effect.

- The potentially sporadic, or periodic, nature of tyre particle emissions could make an on-track cycle-based assessment of emissions challenging, even if all emissions are above typical background levels. Though the longer the test cycle the more the effect would average out. However, the phenomenon may be related to the specific tyre formulation tested and further work could test this hypothesis.
- From moderate on-track tyre measurements, the hot ELPI showed emissions levels substantially above those of the cold ELPI, indicating reconfiguration of the size distribution from evaporation and recondensation mechanisms.
- A session of repeated aggressive braking from speeds up to 50 mph, and braking pressures up to 90 bar, initially showed no consistent relationship between cold ELPI, hot ELPI or eFilter real-time emissions and braking events, and although this improved slightly as testing progressed there was no clear evidence of particle emissions coinciding with every braking event. Where cold ELPI PN spikes were coincident with braking events, emissions levels were higher than from moderate braking. Hot ELPI PN emissions were lower from aggressive braking than from moderate braking, but this effect was due to the presence of a background of relatively large semi-volatile particles during moderate testing that were evaporated and recondensed in the hot ELPI to produce a very large mode at ~30nm. To measure tyre PN reliably a non-volatile approach such as SPCS is required to deal with reconfiguration of the size distribution as seen in the hot ELPI and to counter the presence of semi-volatiles in the ambient background.
- There was a significant increase in tyre particulate mass emissions between PG-42 testing in the laboratory (<0.07 mg/km/tyre for both gravimetric filter-based PM and eFilter) and urban testing on the road (>0.24 mg/km/tyre for eFilter, 1.6mg/km/tyre for uncorrected filter PM). This is likely due to ambient contributions observed with real-world testing that are not present in the air of the chassis dynamometer facility, as brake derived PM emissions were higher from the PG-42 than from urban drives. Nevertheless, road surfaces are more abrasive than the steel dyno roller, so some increase in tyre emissions might be anticipated. Moderate test track emissions with the eFilter were higher than urban, increasing from ~2.5mg/km/tyre - 3.2 mg/km/tyre during the exercise, while extreme braking increased from ~0.7mg/km/tyre to 3.4mg/km/tyre as that experiment progressed. The extreme testing results suggests that tyre emissions increase with more aggressive braking (in comparison with urban). Potentially adding heat energy to the tyres through repetitive braking increases semi-volatile emissions, in addition to abrasion effects. The consistently high PM emissions from moderate track testing was due to a very high background of large semi-volatile particles identified by the cold ELPI that weren't present for the extreme braking tests. Unpredictability of background is likely a major obstacle for on-road and on-track tyre wear PM measurements.
- As observed for the PM data, there was a significant increase in tyre PN emissions between PG-42 testing in the laboratory (~$3.3x10^9$#/km/tyre and ~$0.6x10^9$#/km/tyre for cold and hot ELPI respectively) and urban testing on the road (~$13.5x10^9$#/km/tyre and $18.5x10^9$#/km/tyre for cold and hot ELPI respectively). The generally higher emissions likely reflect an ambient PN contribution several times higher than the tyre-derived emissions, but the increased friction between road and tyre might also contribute. From both moderate (maximum of ~$43x10^9$ #/km/tyre) and extreme (maximum of ~$142x10^9$ #/km/tyre) braking exercises, cold ELPI PN emission were substantially higher than from urban or PG-42 operation. Hot ELPI PN was higher than cold ELPI PN from all testing except the PG-42, due to the evaporation of a few wholly or partly volatile >0.5µm particles and the creation of numerous <100nm ones. It is most likely these >0.5µm particles come from the ambient as they were not observed during the chassis dyno tests. Hot ELPI emissions from the moderate track exercise were extremely high due to high levels of these >0.5µm particles, reaching $700x10^9$#/km/tyre. Unpredictability of the background is likely a major obstacle for on-road and on-track tyre wear PN measurements, and the reconfiguring of the hot ELPI size distributions through heating at 180°C indicates that a robust method of eliminating volatiles is needed to define a repeatable particle number metric for tyres.

6.3 SPECIFIC CONCLUSIONS, SECOND VEHICLE & REAR WHEEL

- The principle of applying the brake enclosure approach to measurements on a second vehicle was proven through measurements on an Audi A4. In addition, the measurements were made from the rear wheel of the vehicle, demonstrating that the approach is valid for multiple vehicles and both front and rear wheels. Finally, the sampling system was installed on a trolley external to the test vehicle and

emissions measurements performed. This shows that chassis dyno brake (or tyre) particle emissions measurements could be performed rapidly on a range of suitably prepared vehicles.

- From repeat PG-42 cycles, non-volatile PN emissions using SPCS from the rear wheel of the Audi were higher (~$8x10^9$ #/km/brake) than from the front wheel of the VW Caddy (~$5x10^9$ #/km/brake). Higher braking forces are applied to the front wheel than to the back wheel, which potentially suggests an expectation of higher particle emissions from front wheels. However, the pads and discs on the Audi are different to those on the Caddy and difference in composition may explain the higher PN emissions. Mass emissions with both ELPI and eFilter were lower from the Audi A4 rear-wheel than seen from the Caddy front wheel, likely related to brake system compositional differences and potentially a tendency to produce fewer larger, more massive particles, with rear braking.

6.4 SPECIFIC CONCLUSIONS, THREE BRAKE ENCLOSURES

- Across the three enclosures and both PG-42 and urban cycles, PN emissions were generally similar between enclosures with emissions ranging by just over a factor of 2. SPCS emissions showed the lowest variation (PG-42 only, ~50%), which suggests that volatiles play a part in the variability observed. PM emissions varied by a similar proportion with the eFilter, and less with the gravimetric approach.

6.5 GENERAL CONCLUSIONS

- The favoured metric for PN measurement of brakes and tyres would be a non-volatile approach such as that developed by the PMP. This could be supplemented by a parallel total particle measurement addressing both volatile and non-volatile particles.
- A real-time mass metric would also be useful, in order to capture both solid and volatile particle mass, while a filter-based approach is useful to establish the actual mass, plus enable chemical analysis and visualisation of the PM materials collected.
- Mass emissions determined by the eFilter were lower than determined by the gravimetric approach and the difference between the two methods varied between tyre measurements and brake measurements. The eFilter response is dependent on both particle size distribution and the composition of the particles measured. For optimal application to brake and tyre wear measurements specific instrument calibrations would be required.
- Due to the challenges of achieving high transmission of particles >5µm, the mass measurements of an on board particle measurement system may be limited to PM2.5.
- Cold ELPI measurements are useful to help visualise size distributions but are unrepeatable. The hot ELPI data are of limited value due to the heating approach restructuring the size distributions and the resulting information not representing either the emissions at source or a stable non-volatile metric.
- Brake wear emissions quantification appears to be possible both on the chassis dyno and on-road. All particles emitted by the brake wear event are captured in the enclosure for sampling and measurement.
    - Measured brake wear PN over the PG-42 cycle using SPCS was ~$5x10^9$ #/km/brake, with urban cycle emissions similar. These are broadly consistent with literature values for non-volatile particles emitted during various cycles.
    - Measured brake wear PM was lower than literature values, at an average of ~1.33 mg/km/brake from the PG-42 cycle, compared with 5 ± 0.7 mg/km/brake from the WLTP brake cycle.
- Tyre wear detection using the scoop sampling approach appears to be possible on the chassis dyno where background contributions of volatile aerosols and resuspended materials are low.
- Measurement of tyre wear particle number and mass emissions is much more challenging on the test track and road using the scoop approach, due to background contributions. Outside the chassis dynamometer facility, it was not possible within this project to isolate tyre wear from resuspended materials (road wear and legacy brake and tyre emissions) and volatile particle emissions (from the tailpipe of nearby vehicles and from the general background aerosol).
- Even when confined to the chassis dynamometer facility, the tyre wear emissions sampling approach employed in this study requires further research and development to relate what is sampled to what is

actually emitted. It is likely that the more abundant smaller particles that may dominate particle number are more easily sampled and transmitted to the analysers, and a higher proportion may be drawn into the sampling probe, meaning that a PN-based assessment of tyre emissions will be more accurate than a PM-based assessment

- Literature values for tyre emissions, as referenced in Section 2.5.2, generally range from 1.9 – 9 mg/km/vehicle but can reach as high as 5 mg/km/tyre [26]. Emissions measurements from PG-42 cycles in the chassis dynamometer reported emissions of 0.03 to 0.06 mg/km for a single front wheel. The product of the mean of the scoop measurements (0.045 mg/km/tyre) and using an estimated sampling ratio of 1/100 produces tyre emissions rates, for PM_{10}, of ~4.5mg/km/tyre.
- No distance-based literature values were found for PN emissions from tyres, although a concentration of ~$2x10^6$ #/cm^3 during cornering has been reported (Section 2.5.2). In this study observed PN emissions rates from PG-42 cycles, when sampling from the same scoop used for mass determination, were around $3x10^9$ #/km/tyre for total particles (by cold ELPI) and ~$1x10^9$ #/km/tyre for non-volatile particles (by SPCS). As with the mass measurements, the investigation and exploration of sampling efficiency for particle number determination also requires further work.

7. RECOMMENDATIONS FOR PHASE 2

Based on the testing, analysis and results from Phase 1, the following recommendations for the system are provided for Phase 2.

7.1 SAMPLE ANALYSIS INSTRUMENTATION

The instrumentation for Phase 1 consisted of:

- A heated (“hot”) ELPI and a non-heated (“cold”) ELPI to measure non-volatile and total size particle distributions respectively, and related particle number concentration integrals.
- An eFilter for real-time particle mass concentrations of solid and volatile materials, while simultaneously collecting a gravimetric particulate filter sample.
- A Solid Particle Counting System (SPCS; in the chassis dynamometer only) for non-volatile particle number concentration measurements.

The analysis and results highlighted that the cold ELPI measurements are useful to help visualise actual emitted size distributions but are unrepeatable due to variability related to volatile emissions formation. The hot ELPI data are of limited value despite being more repeatable, since integrated PN following heating to 180°C leaves behind some volatile/semi-volatile materials as well as solid particles. The hot ELPI size distribution can show restructuring, via evaporation of volatiles from larger particles and then recondensation of some of those materials into a mode at a much smaller diameter but with much higher number concentration. Consequently, the total number reported by the hot ELPI can show higher concentrations than from the cold ELPI.

As such, it is recommended that non-volatile particle number should be measured following a more robust volatile removal mechanism, such as an evaporation tube or catalytic stripper as used in the approaches recommended by PMP. The particle size range should begin at ~10nm to align with the future brake dynamometer-based legislation We propose that a Mobile Particle Emission Counter (MPEC+)[11], equipped with a high temperature volatile particle remover and intended for PN-PEMS, is utilised for Phase 2. The MPEC is a smaller, more portable analyser than the ELPI and requires less power. A second MPEC+ would be used in parallel, without heating, to measure total particle emissions. MPEC+ systems will be configured and calibrated to a ~10nm lower cut-point.

With regards to particle mass, both solid and volatile particulate material were measured with the eFilter, and the analyser was shown to both be repeatable during Phase 1 and to clearly indicate spikes of brake and tyre

[11] Dekati® MPEC+™ for RDE applications - Dekati Ltd

emissions in response to braking events. Therefore, we recommend that for Phase 2 an eFilter is again included in the suite of instruments, to measure real-time particle mass. However, it is proposed to discuss with the instrument manufacturer the possibility of developing processing algorithms specific to brake or tyre materials, depending on what is being sampled. The eFilter also includes a gravimetric filter holder to measure gravimetric particle mass. The filter collection is useful for visual inspection of materials and PM analysis.

7.2 BRAKE WEAR MEASUREMENTS

Brake emissions quantification (mass, number, size distribution) is possible both on the chassis dynamometer and on-road using any of the three enclosures tested in Phase 1. However, where practicable, the system should be optimised to reduce the temperature differential between the enclosed and unenclosed brake pads and discs, reduce the footprint to aid packaging in smaller vehicles and enable ease of transferability between vehicles and, and to optimise the power supply and power consumption of the system.

7.3 TYRE WEAR MEASUREMENTS

The current system for tyre emissions quantification for mass is only practical on the chassis dynamometer. Particle number might be possible on the road but not with the measurement methods used so far.

For Phase 2, the recommendation is to first improve our understanding of the potential efficiency of the tyre scoop inlet for mass and number. This may be performed on a chassis dynamometer by using a visible tracer, such as a smoke pencil, to estimate the fraction of aerosol collected by the scoop.

Depending on the outcome of this test, it may prove necessary to consider a full tyre enclosure as an option to reduce the influence of background particles on tyre wear measurements enabling at least test track measurements, and to increase the fraction of emitted PM collected by the sample inlet. This approach will be explored. Alternatively, a larger sample inlet/ scoop could be considered.

8. REFERENCES

[1] T. Feißel, D. Hesse, I. K. Augsburg and I. S. Gramstat, “Measurement of Vehicle Related Non Exhaust Particle Emissions under Real Driving Conditions,” EuroBrake 2020, 2020.

[2] K. Augsburg, D. Hesse, T. Feißel and F. Wenzel, “Real driving emissions measurement of brake dust particles,” in *9th International Munich Chassis Symposium 2018*, Springer Vieweg, Wiesbaden, 2019.

[3] M. Mathissen, V. Scheer, R. Vogt and T. Benter, “Investigation on the potential generation of ultrafine particles from the tire–road interface,” *Atmospheric Environment,* vol. 45, no. 34, pp. 6172-6179, 2011.

[4] F. H. Farwick Zum Hagen, M. Mathissen, T. Grabiec, T. Hennicke, M. Rettig, J. Grochowicz, R. Vogt and T. Benter, “Study of brake wear particle emissions: impact of braking and cruising conditions,” *Environmental science & technology,* vol. 53, no. 9, pp. 5143-5150, 2019.

[5] J. Wahlström, U. Olofsson, A. Jansson and L. Olander, “Airborne Wear Particles Emissions fromCommercial Disc Brake Materials–Passenger Car Field Test,” 2008.

[6] Y. Tonegawa and S. Sasaki, “Development of Tire-Wear Particle Emission Measurements for Passenger Vehicles,” *Emission Control Science and Technology,* vol. 7, no. 1, pp. 56-62, 2021.

[7] T. Hussein, C. Johansson, H. Karlsson and H.-C. Hansson, “Factors affecting non-tailpipe aerosol particle emissions from paved roads: On-road measurements in Stockholm, Sweden,” *Atmospheric Environment,* vol. 42, no. 4, pp. 688-702, 2008.

[8] L. Chasapidis, T. Grigoratos, A. Zygogianni, A. Tsakis and A. G. Konstandopoulos, “Particle Emission Measurements for Passenger Vehicles." Emission Control Science and Technology,” *Emission Control Science and Technology,* vol. 4, no. 4, pp. 271-278, 2018.

[9] M. Mathissen, T. Grigoratos, T. Lahde and R. Vogt, “Brake wear particle emissions of a passenger car

measured on a chassis dynamometer," *Atmosphere,* vol. 10, no. 9, p. 556, 2019.

[10] G. Perricone, V. Matějka, M. Alemani, J. Wahlström and U. Olofsson, "A test stand study on the volatile emissions of a passenger car brake assembly," *Atmosphere,* vol. 10, no. 5, p. 263, 2019.

[11] A. Mamakos, K. Kolbeck, M. Arndt, T. Schröder and M. Bernhard, "Particle Emissions and Disc Temperature Profiles from a Commercial Brake System Tested on a Dynamometer under Real-World Cycles," *Atmosphere,* vol. 12, no. 3, p. 377, 2021.

[12] I. Park, H. Kim and S. Lee, "Characteristics of tire wear particles generated in a laboratory simulation of tire/road contact conditions," *Journal of Aerosol Science ,* vol. 124, pp. 30-40, 2018.

[13] M.-J. Foitzik, H.-J. Unrau, F. Gauterin, J. Dörnhöfer and T. Koch, "Investigation of ultra fine particulate matter emission of rubber tires," *Wear ,* vol. 394, pp. 87-95, 2018.

[14] M. Dall'Osto, C. D. Beddows, J. K. Gietl, O. A. Olatunbosun, X. Yang and R. M. Harrison, "Characteristics of tyre dust in polluted air: Studies by single particle mass spectrometry (ATOFMS)," *Atmospheric Environment,* vol. 94, pp. 224-230, 2014.

[15] T. Grigoratos, M. Gustafsson, O. Eriksson and G. Martini, "Experimental investigation of tread wear and particle emission from tyres with different treadwear marking," *Atmospheric Environment,* vol. 182, pp. 200-212, 2018.

[16] Å. Sjödin, M. Ferm, A. Björk, M. Rahmberg, A. Gudmundsson, E. Swietlicki, C. Johansson, M. Gustafsson and G. Blomqvist, "Wear particles from road traffic-a field, laboratory and modelling study.," IVL Swedish Environmental Research Institute Ltd., Göteborg, 2010.

[17] J. Kwak, S. Lee and S. Lee, "On-road and laboratory investigations on non-exhaust ultrafine particles from the interaction between the tire and road pavement under braking conditions," *Atmospheric Environment,* vol. 97, pp. 195-205, 2014.

[18] F. H. Farwick zum Hagen, M. Mathissen, T. Grabiec, T. Hennicke, M. Rettig, J. Grochowicz, R. Vogt and T. Benter, "On-road vehicle measurements of brake wear particle emissions," *Atmospheric Environment,* vol. 217, p. 116943, 2019.

[19] L. Bondorf, L. Köhler, T. Schripp and F. Philipps, "Towards the reduction of brake and tire emissions: The Zero Emission Drive Unit (ZEDU-1).," in *21 ETH Conference on Combustion Generated Nanoparticles*, Zurich, 2021.

[20] "The Tyre Collective," [Online]. Available: https://www.thetyrecollective.com/. [Accessed 20 August 2021].

[21] A. Piscitello, C. Bianco, A. Casasso and R. Sethi, "Non-exhaust traffic emissions: Sources, characterization, and mitigation measures," *Science of the Total Environment,* vol. 766, p. 144440, 2021.

[22] T. Grigoratos and G. Martini, "Brake wear particle emissions: a review," *Environmental Science and Pollution Research,* vol. 22, no. 4, pp. 2491-2504, 2015.

[23] D. Hesse and K. Augsburg, "Real Driving Emissions Measurement of Brake Dust," in *SAE Technical Paper*, 2019.

[24] A. Mamakos, M. Arndt, D. Hesse and K. Augsburg, "Physical characterization of brake-wear particles in a PM10 dilution tunnel," *Atmosphere,* vol. 10, no. 11, p. 639, 2019.

[25] C. Agudelo, R. T. Vedula, S. Collier and A. Stanard, "Brake Particulate Matter Emissions Measurements for Six Light-Duty Vehicles Using Inertia Dynamometer Testing," *SAE Technical Paper,* 2020.

[26] T. Grigoratos, *Personal Communication,* 2022.

APPENDICES

Appendix 1 Stakeholder meetings

Table A1: Overview of the stakeholder meetings that have taken place as part of this project

Organisation	Date of meeting	Discussion Areas
Joint Research Centre -ISPRA	19/03/21	PMP activities, relevant literature
University of Leeds	20/04/21	Brake wear studies
California Air Resource Board (CARB)	21/04/21	Brake wear PM testing study and preliminary results
The Tyre Collective	22/04/21	Ongoing activities on particle capture
IDIADA	22/04/21	Discussion of brake emissions project and exchange of ideas, future collaborations
British Tyre Manufacturer Association	28/04/21	Tyre wear testing methods
Umweltbundesamt	05/05/21	Brake dynamometer study and, real world tyre emissions study
European Tyre and Rubber Manufacturers' Association (ETRMA)	10/05/21	Relevant literature and contacts
Mann-Hummel	10/05/21	Brake dust particle filter
University of York	28/06/21	Laser-based systems to characterise non-exhaust particles
IDIADA	28/07/21	Discussion of LEON-T project scope, and tyre emissions results from DfT project

T: +44 (0) 1235 75 3000
E: enquiry@ricardo.com
W: ee.ricardo.com